Annika Groschner

Design and Synthesis of Modified SNARE Proteins with Respect to the α-SNAP/NSF Mediated Disassembly

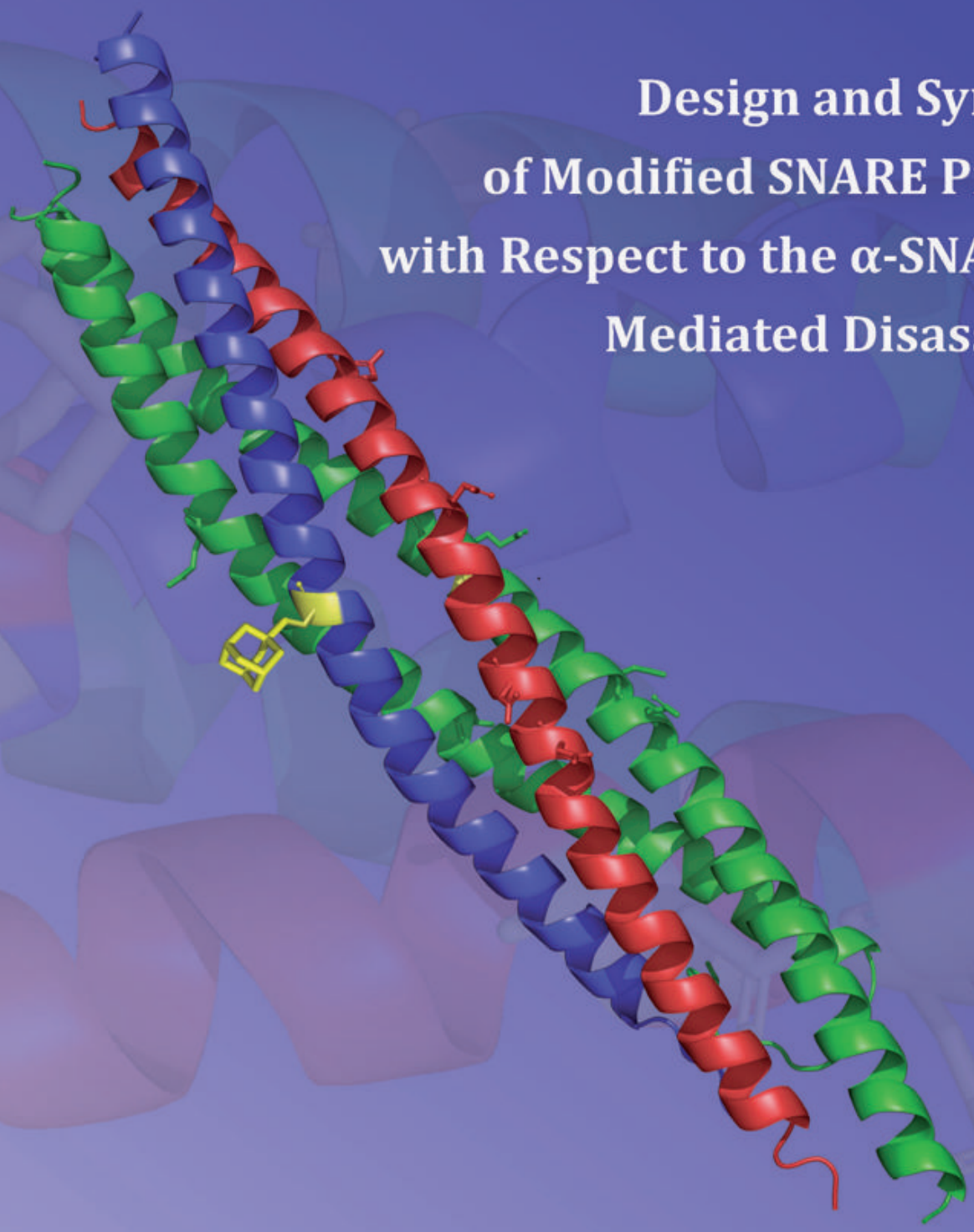

Cuvillier Verlag Göttingen
Internationaler wissenschaftlicher Fachverlag

Design and Synthesis of Modified SNARE Proteins with Respect to the α-SNAP/NSF Mediated Disassembly

Dissertation

For the award of the degree

“doctor rerum naturalium“

Division of Mathematics and Natural Sciences

of the Georg-August-Universität Göttingen

Submitted by

Annika Groschner

from Gardelegen

Göttingen 2010

Bibliografische Information der Deutschen Nationalbibliothek
Die Deutsche Nationalbibliothek verzeichnet diese Publikation in der Deutschen Nationalbibliografie; detaillierte bibliografische Daten sind im Internet über http://dnb.d-nb.de abrufbar.
1. Aufl. - Göttingen : Cuvillier, 2011
Zugl.: Göttingen, Univ., Diss., 2010

978-3-86955-662-8

Prof. Dr. ULF DIEDERICHSEN (Reviewer)

Institut für Organische und Biomolekulare Chemie, Georg-August-Universität Göttingen

Prof. Dr. REINHARD JAHN (Reviewer)

Max-Planck-Institut für biophysikalische Chemie

Prof. Dr. CLAUDIA STEINEM

Institut für Organische und Biomolekulare Chemie, Georg-August-Universität Göttingen

Date of the oral examination: 11/01/2010

Nonnenstieg 8, 37075 Göttingen
Telefon: 0551-54724-0
Telefax: 0551-54724-21
www.cuvillier.de

1. Auflage, 2011
Gedruckt auf säurefreiem Papier

978-3-86955-662-8

This work was supported by the *Deutsche Forschungsgemeinschaft* via the Collaborative Research Center 803 (SFB 803).

The work described in this doctoral thesis has been carried out under the guidance and supervision of Prof. Dr. ULF DIEDERICHSEN at the Institut für Organische und Biomolekulare Chemie of the Georg-August Universität Göttingen between January 2007 and September 2010.

I like to thank Prof. Dr. Diederichsen for the interesting and highly collaborative research topic and for his encouraging guidance, thoughtful advice, generous support and the enormous freedom of research.

Design and Synthesis of Modified SNARE Proteins with Respect to the α-SNAP/NSF Mediated Disassembly

to my family

Abstract

Soluble *N*-ethylmaleimide-sensitive attachment receptor (SNARE) proteins are the key players in membrane fusion. Localized in opposed membranes, they assemble via the SNARE motif in a stable four-helix bundle bringing the membranes close to each other and promoting membrane fusion by using the energy release during complex formation. SNARE complex assembly is regulated by several proteins. One of these, Complexin, is known to partially associate with the core complex, it may stabilize SNARE complex intermediates and unbinds upon calcium trigger. Nevertheless, the exact function of Complexin is still under discussion. After membrane fusion the recycling of free SNARE proteins is mediated by the AAA+ protein NSF in conjunction with its cofactor α-SNAP. Afterwards, the individual SNARE proteins are available for another round of membrane fusion.

To date, no effective model systems for preventing or at least decelerating the disassembly mechanism are known. Development of a potent inhibitor of the α-SNAP/NSF mediated disassembly was carried out. Therefore, the SNARE motif of Synaptobrevin, one of the SNARE proteins, was used as a model system for the investigation of defined SNARE/SNAP complex recognition sites. The full length of the SNARE motif of Synaptobrevin was obtained using solid phase peptide synthesis. Different modifications at various residues within the sequence were introduced in order to identify important interactions between α-SNAP and the SNARE complex and to prevent α-SNAP recognition.

Additionally, the regulator protein Complexin was synthesized as a β-peptide analog, also designed to inhibit the disassembly mechanism by preventing α-SNAP recognition through enhanced interaction between the β-mimic and the Synaptobrevin and Syntaxin helices. By development of the Complexin β-peptide mimic as a 14-helix, the advantages of a well-defined secondary structure with high helix propensity are obtained. Furthermore, the binding fragment of Complexin was

performed as α-peptide, extended with amino acids known to promote the α-helical propensity.

For understanding of biological systems the investigation of conformational dynamics and interactions of individual proteins is important. Therefore, in a final part, small independently folding protein domains were synthesized by solid phase peptide synthesis and labeled with respect to the development of the single molecule fluorescence spectroscopy (smFRET) technique. This method is a convenient tool of monitoring single folding and unfolding events of proteins.

Contents

Chapter 1

Outline

1.1 Intracellular Protein Transport and SNAREs

All eukaryotic cells comprise diverse compartments which are enclosed by membranes. Cellular life and differentiation depends on preserving the integrity of the cells barrier layer and its organelles constantly. However, these compartments act together by exchange of material and neurotransmitters after the transport to the specific organelle. This membrane transport is a basic requirement in order to maintain the identity of the different cell compartments and the inner organization of the cell. Work done by PALADE in 1975 led to the hypothesis that this exchange and transport between organelles is mediated by small transport vesicles.[1] After budding from the prelimanary compartment the vesicles moved to the target compartment, where they fused after overcoming of the energetic barrier between the membranes. Recognition and assembly of the membrane anchored so-called SNARE (Soluble *N*-ethylmaleimide-sensitive factor Attachment protein REceptor) proteins followed by fusion of the membranes are essential for a series of intracellular transport processes reaching from Ca^{2+}-dependent neurotransmitter release to exocytosis via the Golgi apparatus.[1]

SNAREs, the catalysts of fusion, appear in all eukaryotic organisms and their participation in various steps of intracellular transport processes was investigated in detail using various experimental assays.[2-6] The neuronal SNARE complex forms a parallel four-helical bundle, composed of the three individual proteins Syntaxin-1, Synaptobrevin-2 and SNAP-25,[7] which anchor each other at their *N*-terminal end. Via a cycle of assembly and disassembly they lead to the fusion of membranes (Figure 1).

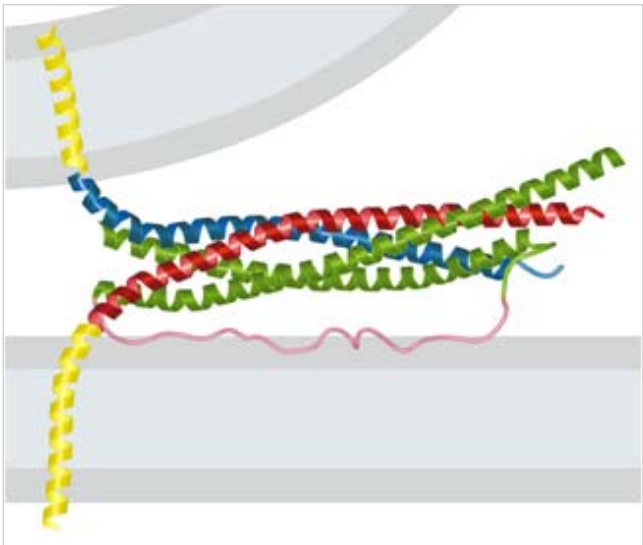

Figure 1. *Hypothetical model of the synaptic fusion complex joining two membranes. Synaptobrevin (blue) and Syntaxin 1A (red) are membrane attached via their transmembrane domains (yellow). SNAP-25 (green) is palmitoylated by a cysteine rich interhelical loop (pink) between the helices (picture from R. JAHN, MPI for Biophysical Chemistry, Göttingen).*

The assembly is regulated by special factors, such as Complexins. Meanwhile the mode of binding between Complexin (also called Synaphin) and the SNARE core complex has been investigated. An α-helical central stretch consisting of 58 amino acids was identified to bind the SNARE complex in an anti-parallel fashion.[8]

After fusion the assembled SNARE proteins form a stable complex. They are located in the same membrane and are not able to dissociate autonomously. Hence, it requires the activity of the specialized chaperone-like ATPase NSF (*N*-ethylmaleimide-sensitive factor) in conjunction with its adaptor protein α-SNAP to recover the SNARE motifs via ATP hydrolysis for further rounds of fusion.[9] NSF does not have any binding sites for SNARE complexes. Therefore, it needs its cofactor α-SNAP, which supplies high affinities for both, the SNARE motifs as well as the NSF domains. Without α-SNAP no disassembly occurs.

1.2 Investigation of Independently Folding Proteins using Single Molecule Fluorescence Spectroscopy

It is well-known how the primary nucleotide sequence information is stored in the DNA as well as the amino acid sequence in proteins. However, the complexity of their unique three-dimensional structure, a basic requirement for the specific function, has not completely been understood, yet.[10] The development of techniques that are able to monitor dynamics of folding processes, and therefore, help understanding relations between structure and function is a considerable research area. A known fact of the protein folding and unfolding is the high dimension of the structural and conformational heterogeneity to form the final structures. Therefore, investigating the structures of large ensembles of molecules in detail is difficult with classical techniques. In recent years, single molecule fluorescence spectroscopy (smFRET) experiments provide new tools for the study of biological systems, especially the conformational dynamics and interactions of individual peptides and proteins.[11] However, the method was refined within the last decade, but to be able to answer more complex dynamics it is necessary to investigate further and different folding pathways. The combination of protein design and synthesis methods as well as Molecular dynamics simulations these methods will continue to afford an important supplement to other developments. Especially the small HTH- (helix-turn-helix) and the WW motifs (named after two highly conserved tryptophans) demonstrate excellent model systems to improve our appreciation of mechanistic characteristics in protein folding (Figure 2).

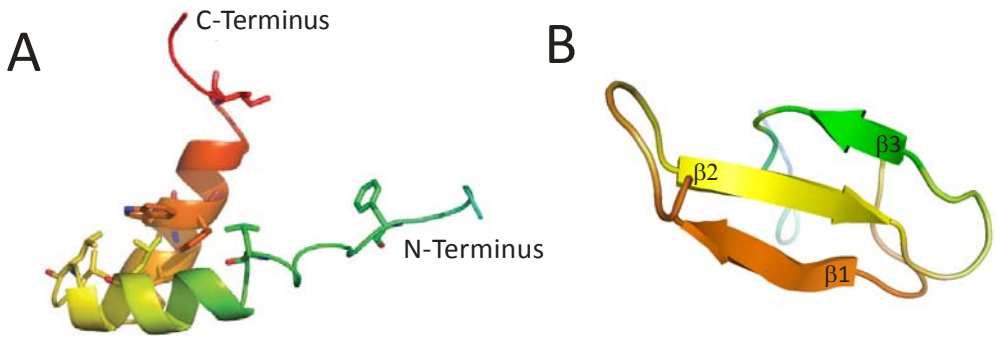

Figure 2. A *Crystal structure from the helix-turn-helix (HTH) motif of the Engrailed Homeodomain (PDB code 2P81).* ***B*** *Crystal structure of the WW domain (pdb code 1I6C).*

1.3 Motivation of this Study

Inhibition or at least deceleration of the disassembly event could help to clarify molecular mechanisms. Furthermore, no effective inhibitor for the NSF/α-SNAP mediated disassembly is known to date.

The first aim of this study is to synthesize a new class of SNARE derivatives mimicking the SNARE motif of Synaptobrevin as well as, secondly, synthesizing the recognition unit of Complexin to obtain molecules that can inhibit the α-SNAP/NSF mediated disassembly.

By replacing individual residues in the SNARE motif of Synaptobrevin by amino acids with inversed charge to the *wild type* SNARE motif or by insertion of non-native amino acid building blocks it was aspired to inhibit, or at least to weaken, the binding of α-SNAP. As mentioned before, NSF is not able to bind to SNARE complexes without its cofactor α-SNAP, therefore, if α-SNAP binding is prevented, the disassembly may be unsettled. Requirements for effective disassembly inhibitors are the capability to form stable complexes with the biological counterparts while avoiding α-SNAP binding.

Up to date, molecular details of the disassembly process are less understood. Essential structural characteristics can be identified by systematic integration of synthetic amino acid building blocks and comparison of the resulting binding properties with known parameters. It is not completely understood how the α-SNAP is capable to interact with the SNARE complex, consisting of three different proteins with different characteristics and recognition units. Solely HANSON *et al*. performed a systematic investigation to identify residues in α-SNAP interacting with the SNARE complex.[12] Based on this study, which determined several important residues in the individual SNARE proteins for α-SNAP complex recognition, a series of Synaptobrevin mimics had to be synthesized and their ability to prevent α-SNAP binding was investigated. Additionally, it is of great interest to monitor individual disassembly steps. Furthermore, with the exception of clostridial neurotoxins like botulinum and tetanus toxins, blocking the synaptic-vesicle fusion, no specific SNARE inhibitors are established.

Thus, within this work peptide synthesis and subsequent complex assembly and disassembly studies are performed. The goal of the first part contains:

i) Design and synthesis of an amino acid building block with a bulky side chain.
ii) Design and synthesis of derivatives mimicking the whole SNARE motif (residues 28-89), exhibiting exchanged charges or amino acid building blocks with bulky side chains at selected residues.
iii) SNARE complex assembly studies with the synthesized Synaptobrevin derivatives and their natural counterparts.
iv) Disassembly studies with the α-SNAP/NSF machinery.

The assembly and disassembly studies were realized in cooperation with the laboratory of Prof. R. JAHN, MPI for Biophysical Chemistry, Göttingen.

A different approach to create an effective inhibitor for the SNARE disassembly is to influence the assembly-disassembly cycle of SNARE proteins at an earlier stage. MC MAHON *et al*. reported that α-SNAP is not able to bind to the SNARE complex when Complexin is added in large excess.[13] Complexin interacts only with the Synaptobrevin and Syntaxin helices, but not with SNAP-25. The *N*-terminal part of Complexin, namely amino acids 48-70, is in close contact with the complex. The *C*-terminal end is slightly bended, probably due to its EEE-segment followed by positively charged amino acids. The structure of Complexin bound to the neuronal SNARE complex has been solved (Figure 3).[14] This leads to assumptions that they might have inhibitory properties regarding the SNARE disassembly.[13]

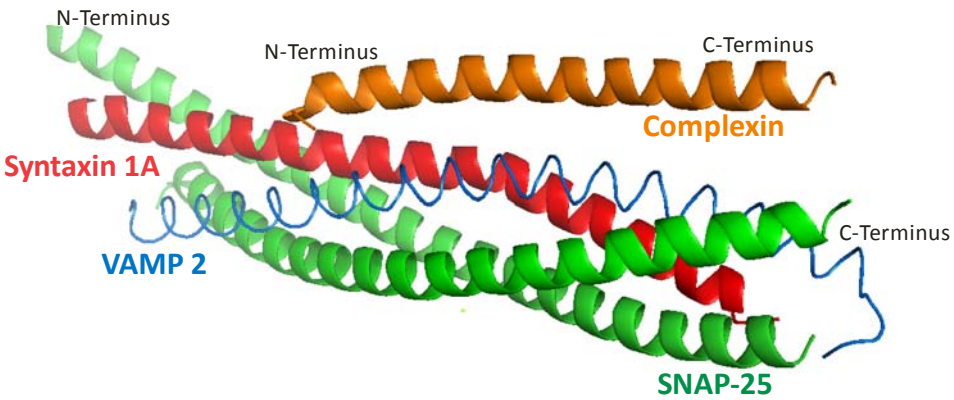

Figure 3. *Crystal structure of the Complexin/SNARE complex. Complexin binds antiparallel to the assembled SNARE complex (pdb code 1KIL).*

Synthesis of Complexin analogues with defined binding sites interacting significantly stronger with the SNARE proteins could also impede the disassembly. Introduction of additional potentially interacting amino acids and elongation of

the recognition area to the SNARE protein helices with further charges should enhance the association. Therefore, truncation of the *C*-terminal end behind the EEE-section and elongation at the *N*-terminus was intended to be realized as an α-peptide, and additionally, as a β-peptide forming a 14-helix.

The α-peptide was synthesized without changes in the sequence, whereas the sequence of the β-peptide is designed promoting a specific 14-helix by incorporation of β-amino acid building blocks. Nevertheless, regarding important side chain orientations and distances to the SNARE complex the use of β-amino acid building blocks known to induce a 14-helix, a Complexin-mimic could maintain its binding to the SNARE complex and prevent interaction with α-SNAP, and therefore, the disassembly.

Purpose of the second part:

i) Design and synthesis of Complexin analogues as α-peptides (residues 48-70), elongated at the *C*-terminal end with the AKRK-motif. Another approach is elongating the *N*-terminal end with amino acids known to stabilize the propensity building of a α-helix.
ii) Synthesis of β-amino acid building blocks.
iii) Design and synthesis of Complexin as a β-peptide.
iv) SNARE complex assembly studies with the Complexin analogues (α-peptide and β-peptide) and the individual *wild type* SNARE proteins.

In a third part the challenge is to investigate polypeptides in single molecule experiments. Hence, labeling with extrinsic fluorophores is unavoidable. For FRET measurements two (or more) chromophores are needed. Short peptides are simple systems, which can designed and synthesized with only one residue with a suitable reactive side chain.[15] With solid phase peptide synthesis natural amino acids can be individually labeled in the natural sequence by using orthogonal side chain protection groups. Applying chemical synthesis also prevents labeling of an undefined number of side chains. For some applications, such as *in vivo* imaging, the amount of labeling is not completely important, but for FRET, specificity it is absolutely essential.

The aim of this third part is to synthesize the HTH motif of the Engrailed Homeodomain (EnHD) as well as the WW domain with selected labeling of special amino acid side chains using orthogonal synthetic routes. In cooperation with Prof. J. ENDERLEIN (Department of Physics, Göttingen) this derivatives are used to study folding and unfolding experiments as well as to refine the single molecule FRET method.

For reaching this goal the following steps are necessary:

i) Design and synthesis of unlabeled and labeled HTH analogues (residues 16-59 of the full length protein (pdb code 2P81).
ii) Design and synthesis of unlabeled and labeled WW analogues.

Chapter 2

SNAREs as Mediators for Membrane Fusion

2.1 Principles of Intracellular Fusion Reactions

Membrane fusion is essential for the intracellular membrane traffic of eukaryotic cells. Next to exchange of material between different organelles or neurotransmission numerous fundamental transporting steps are important basics of life. Thereby, two separate lipid bilayers fuse when they are close together by overcoming high energy barriers and space between the membranes.[16] The merger of membranes proceeds in different transition states, from docking followed by hemifusion to opening of the fusion pore, and finally, fusion.[17,18] Specialized fusion proteins conserved in organisms from yeast to human[19,20] promote this process. Characterizing and understanding of the mode of action of these proteins is an essential research area in cell biology.

2.1.1 Structure of SNAREs and the Core Complex

In the last decades important components of the vesicular fusion machinery controlling the Ca^{2+}-regulated neurotransmitter release of Synaptic vesicles were objects of great interest and intensive studies. Next to a number of regulation proteins, essential components of this molecular machinery are the membrane bound proteins Synaptobrevin 2/VAMP 2 (vesicle-associated membrane protein), Syntaxin 1A, and SNAP-25 (synaptosome-associated protein of 25 kDa) belonging

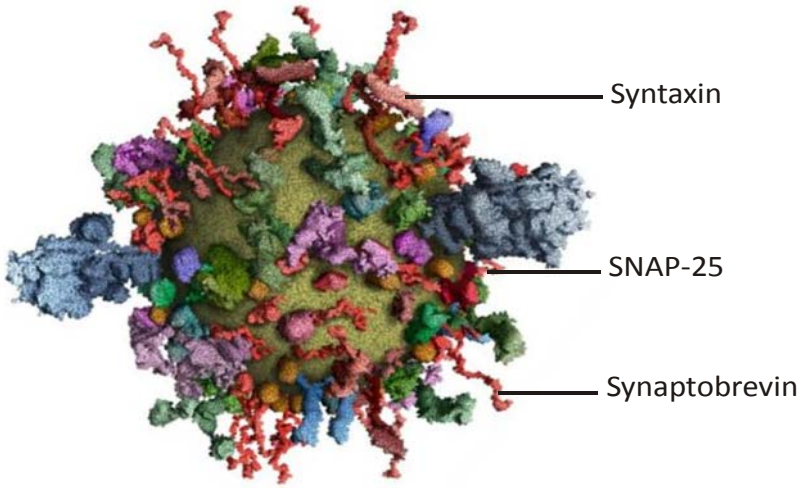

***Figure 4**. Molecular model of a synaptic vesicle with SNARE proteins (Synaptobrevin 2, red, Syntaxin, light red and SNAP-25, dark red) and other regulation proteins like Synaptotagmin (green) and energy delivering systems (V-ATPase, blue; trimeric GTPase, violet).*[21]

to the so-called SNARE (soluble *N*-ethylmaleimide-sensitive factor [NSF]-attachment protein receptor) protein family (Figure 4).

Usually, SNARE proteins are rather small (10-35 kDa), membrane proteins which are anchored via their transmembrane domain. All SNAREs contain a characteristic conserved stretch of 60 to 70 amino acids termed as 'SNARE motif' or 'core-domain'.[22-24] This SNARE motif is typically connected to a *C*-terminal transmembrane domain by a short linker. Syntaxin and Synaptobrevin each contain a single SNARE motif. SNAP-25 consists of two SNARE motifs connected by a cysteine-rich linker which is palmitoylated, and thereby, anchor SNAP-25 to the membrane.[25]

The SNARE complex contains four α-helices, two from SNAP-25 and one from Synaptobrevin and Syntaxin, respectively, which spontaneously form extremely stable complexes when combined. Complex formation is mediated by the SNARE motifs and accompanied by large conformational changes. Free SNARE motifs are unstructured in solution. The assembly reaction is accompanied by a dramatic increase of the α-helical secondary structure. The crystal structure of the coiled-coil domain was solved by SUTTON *et al.*[7] In Figure 5 A the twisted four-helical bundle is shown. All four helices are found to be orientated in a parallel manner, comparable to the coiled-coil arrangement found in viral fusion proteins. This finding was independently confirmed by site-specific labeling.[26,27] The fusion

proteins are able to help to bear numerous energetically unfavorable transition states. Most of the biophysical and structural studies were performed by using only the soluble domains of the SNAREs, cause the transmembrane domains are not necessary for the SNARE complex assembly.

On the basis of their localization and overall structure, SNAREs were initially classified into t-SNAREs (for SNAREs bound to the target membrane) and v-SNAREs (for SNAREs localized to the membrane of the trafficking vesicle).[9] Following the synaptic sample, the v-SNAREs comprised Synaptobrevin/VAMPs and their relatives. Syntaxin and SNAP-25 families were summarized into t-SNAREs. In the last decade, several additional SNARE proteins have been identified, only distantly related to the three neuronal members of the v- and t-SNARE families in some extent. Related to other helix bundles with coiled-coil structures the complex contains 16 stacked layers with mostly hydrophobic interacting side chains.

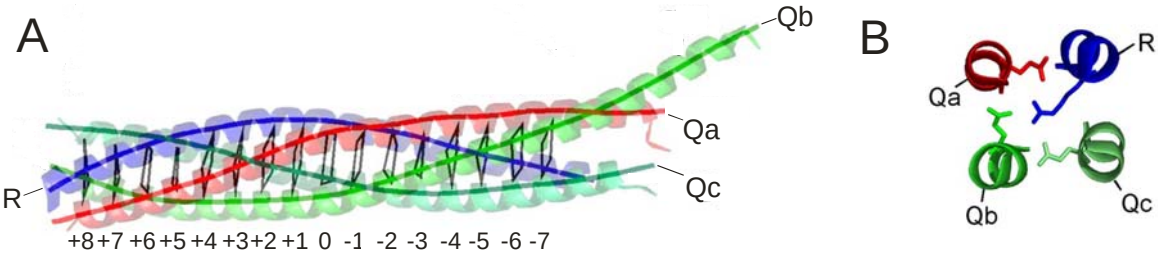

Figure 5. *SNARE core complex.* ***A*** *Crystal structure of the neuronal SNARE core complex is shown as a ribbon diagram with the hydrophobic layers (+8 until -7). This complex contains the SNARE motifs of Syntaxin-1A (Qa, red), Synaptobrevin-II (R, blue) and SNAP-25 (Qb, Qc, both green). The C-terminal ends of the helices are oriented to the left.* ***B*** *Structure of the central '0'-layer in detail. Figure modified from* KLOEPPER *et al.*[28]

Interestingly, in the center an unusual but conserved ionic layer involving all four helices is formed. This central ionic '0'-layer is built from one arginine residue contributed by the SNARE motif of Synaptobrevin and three glutamine residues of the three SNARE motifs of Syntaxin and SNAP-25, respectively (Figure 5 B). Based on this highly conserved layer of interacting amino acids in the center of the helix bundle, the subfamilies are denoted Qa-SNAREs (or Syntaxins), Qb-, and Qc-SNAREs (homologs of the *N*- and *C*-terminal SNARE motif of SNAP-25, respectively), and R-SNAREs (VAMPs).[22,29,30] The classification into Q- and R-SNAREs is preferred compared to the v- and t-SNARE terminology.

Although, SNARE core complexes generally consist of four-helix bundles, formed from one R- and three Q-SNAREs,[22,31] complexes containing only Q-SNAREs have

been observed as well. Hydrogen bonding and electrostatic interactions further stabilize the helix bundle. The complex between Syntaxin and SNAP-25, the so-called 2:1 complex, is the best characterized among them. It is also characterized by a four-helix association in which a second Syntaxin molecule replaced the R-SNARE Synaptobrevin (reviewed by FASSHAUER[32]). Although some investigations reveal indications that such complexes are required for efficient fusion, the biological impact of a helix bundle containing only Q-SNAREs is unclear so far. This energetically unfavorable composition has presumably some functional roles during SNARE complex assembly or disassembly. Mutation in the '0'-layer or other layers led to a reduced SNARE complex stability and entails damages in membrane transport.[29]

SNAREs also differ in the sequences of the *N*-terminal and *C*-terminal stretch that are adjacent to the SNARE motifs or to the membrane attachment domains. In many SNAREs, the SNARE motifs and membrane attachment domains are connected by a short linker without any individual secondary structure independently, as it is shown at the *N*-terminal proline-rich sequence of most Synaptobrevins/VAMPs. In contrast, the *N*-terminal region of Syntaxin is composed of several domains that form three-helix bundles in an antiparallel manner. These domains are conserved among Syntaxins that enable the same transporting step, but being different to those mediating different trafficking steps, while the SNARE motifs of all Syntaxins are homologous.[23] This architecture of Syntaxins indicates that their *N*-terminal domains are specific for a given transport step, whereas their SNARE motifs are more non-selective. Up to now, statements about the exact role of the *N*-terminal region remain highly speculative. Some three-helix bundles associate reversibly with the SNARE motif of the same SNARE to form a 'closed' conformation preventing the SNARE motif to build a SNARE complex.[33,34] Other SNAREs do not have this well-defined conformation, which might be an indicator that this conformation is not crucial for SNARE function.[35,36] The *N*-terminal domains might function as starting points for the binding of other proteins like SM (Sec1/Munc18-related) proteins.[3]

The ternary complex is unusually stable. The SNARE complex formation cannot be interrupted by freezing, heating up to 60 °C for 5 min or by extended storage in sample buffer.[37] Though, the energy in the core complex (or especially in about three-quarter) has been expected to be approximatly 35 k_BT (comparable to approximately 20 kcal/mol) by either AFM (atomic force microscopy) or SFA (surface-face apparatus) measurements in recent times.[38] Therefore, the affinity of the SNARE complex can be assumed to be in a low femtomolar range which

would lead to one of the most persistent protein complexes found until now. The assembly is almost irreversible under laboratory conditions, it is resistant to the detergent SDS[39] or heat[40] and not denatured by proteolysis with botulinum and tetanus[39] neurotoxins.

The first definitive indication to the function of SNARE complexes was the observation that the neuronal SNAREs (Synaptobrevin, Syntaxin 1A and SNAP-25) were targets for botulinum and tetanus neurotoxins representing bacterial proteins which are highly effective vesicle exocytosis inhibitors.[41,42]

2.1.2 Synaptobrevin - A Deeper View to One of the SNARE Proteins

Synaptobrevin, or Vesicle-Associated Membrane Protein 2 (VAMP 2), is a 18 kDa membrane protein, anchored through a *C*-terminal hydrophobic stretch of amino acids, its transmembrane domain, in the synaptic vesicle membrane. As well as Syntaxin and SNAP-25 it belongs to the SNARE protein family. Together, they form the highly stable core complex that supply the driving energy for membrane fusion.[42,43] TRIMBLE *et al*. firstly identified it as a central component of synaptic vesicles,[44] thus, ROTHMAN and coworkers termed it v-SNARE (vesicle associated SNARE).[45] It is located in the membranes of virtually all small synaptic vesicles. According to Synaptobrevins highly conserved arginine (R) residue in its central '0'-layer the VAMP family is reclassified as R-SNAREs.[29] Up to now, two isoforms of Synaptobrevin (I and II) have been identified and characterized.[46] Each SNARE protein contains at least one core domain that binds to the other SNARE proteins. The SNARE motif of Synaptobrevin includes amino acids 28-89.

Synaptobrevin is composed of four domains. After a proline-rich *N*-terminus a highly conserved hydrophobic core domain, the SNARE motif, is attached. It contains two segments (aa 37-54 and aa 55-88) with high affinity to form amphipathic helices. This is followed by the transmembrane region close to the *C*-terminal region, connected by a short linker.[47] Individual Synaptobrevin is unstructured in solution.[48,49] During SNARE complex assembly excessive structural changes reveal helical conformations in each of the SNARE proteins. Recent investigation of full length Synaptobrevin (aa 1-116) in dodecylphosphocholine (DPC) micelles with NMR shows the presence of two

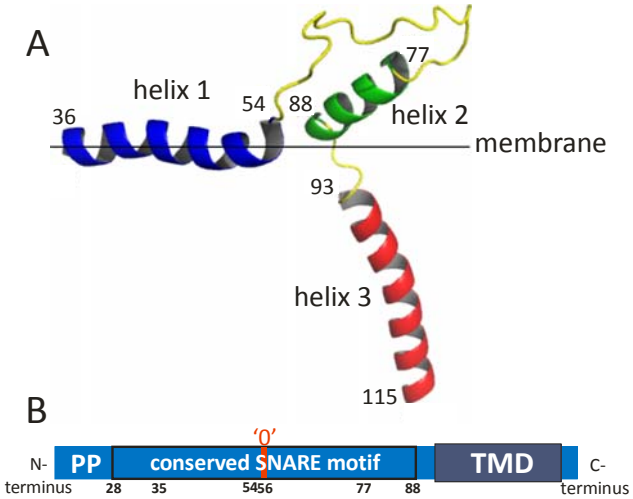

Figure 6. A *Helices 1-3 of Synaptobrevin in DPC. Structure is identified via NMR data for full length Synaptobrevin. Helix 1 and 2 are on the hydrophilic side of the boundary layer and helix 3 is on the hydrophobic side. The basically unstructured N-terminal region (aa 1-35) is not shown. Figure modified from* ELLENA *et al.*[50] ***B*** *Schematic structure of Synaptobrevin. The amino-terminal proline rich (PP) domain is attached to the SNARE motif. The '0'-layer is marked in red. The transmembrane domain (TMD) is then connected via a short linker.*

helices flanked by basically unstructured regions in its SNARE motif as well (Figure 6).[50]

The third helix in the transmembrane domain is relatively stable, whereas helix 1 and 2 are volatile. Each of these helices may achieve an important contribution for SNARE complex folding and membrane fusion. The *N*-terminal helix 1 is relatively disordered and forms probably a nucleation site, helix 2 could function as a connector between SNARE complex folding and function.

It is known that *C*-terminal, but not *N*-terminal, truncation of the SNARE complex decreases the stability as found in temperature-dependent CD and SDS melting curves,[51] just as interactions between the protein and the lipid controlled the reactivity of Synaptobrevin by its *C*-terminal region. In order to the zipper model, membrane fusion occurs after *N*-terminal recognition of the individual SNARE proteins and successive assembly of them towards the *C*-terminal membrane anchor leading to the SNARE complex. The crystal structure of the SNARE complex reveals that the individual helices were stabilized by interacting residues which are arranged in hydrophobic layers. Amino acid 84 of Synaptobrevin is the last involved residue in the *C*-terminal end (+8) of these layers (Figure 5). The sequence and structure of Synaptobrevin is highly conserved implying a conserved mechanism of exocytotic secretion in which Synaptobrevin plays a central role.

2.1.3 From *N* to *C*: The Assembly Pathway

The conclusion of *N*- to *C*-terminal assembly of the SNARE complex is supported by *in vitro* assembly studies using deletion mutants,[52-54] site-specific labeling and by the finding that a *C*-terminal Synaptobrevin peptide activates *in vitro* fusion assays, whereas *N*-terminal peptides inhibit SNARE complex formation entirely and block fusion.[5,40,55-57] The first binding event appears at the *N*-terminal end of the SNARE motifs proceeding in a 'zipper'-like manner towards the *C*-terminal membrane domains, thus, the membranes are tightly compressed together and probably giving force on the membranes, resulting in removing of the repulsion between the membranes, and afterwards, fusion of the opposed bilayer.[56,58] By site-directed mutagenesis it was developed that Synaptobrevin, Syntaxin and SNAP-25 bind to each other solely via their SNARE motifs with a 1:1:1 stoichiometry.[5,33,39,59,60] No different biophysical and biochemical properties between assembled SNARE complexes containing only the four SNARE motifs without the *N*- and *C*-terminal domains and complexes formed by the intact proteins were observed.[5]

2.1.4 The Assembly of SNARE Core Complexes

The fundamental mechanism of SNARE core complexes in membrane fusion and their remarkably biophysical stability entail extensive studies of the complex formation. From these studies, several principles can be derived. One of the key questions was how the assembly of proteins can lead to the fusion of two membranes. Even though the answer has not been conclusively found, some meanwhile well-understood basic mechanistic principles of SNARE assembly are helpful to establish different models. The 'zipper'-mechanism, one of these concepts for SNARE assembly, became widely accepted over the years (Figure 7).[61] This model implies that the individual SNARE proteins recognize each other at their *N*-terminal ends and via zippering they assemble by energy release. After association of the SNARE complex the membranes are close enough to fuse. Syntaxin and Synaptobrevin each contribute one helix to this complex and SNAP-25 two α-helices, respectively.

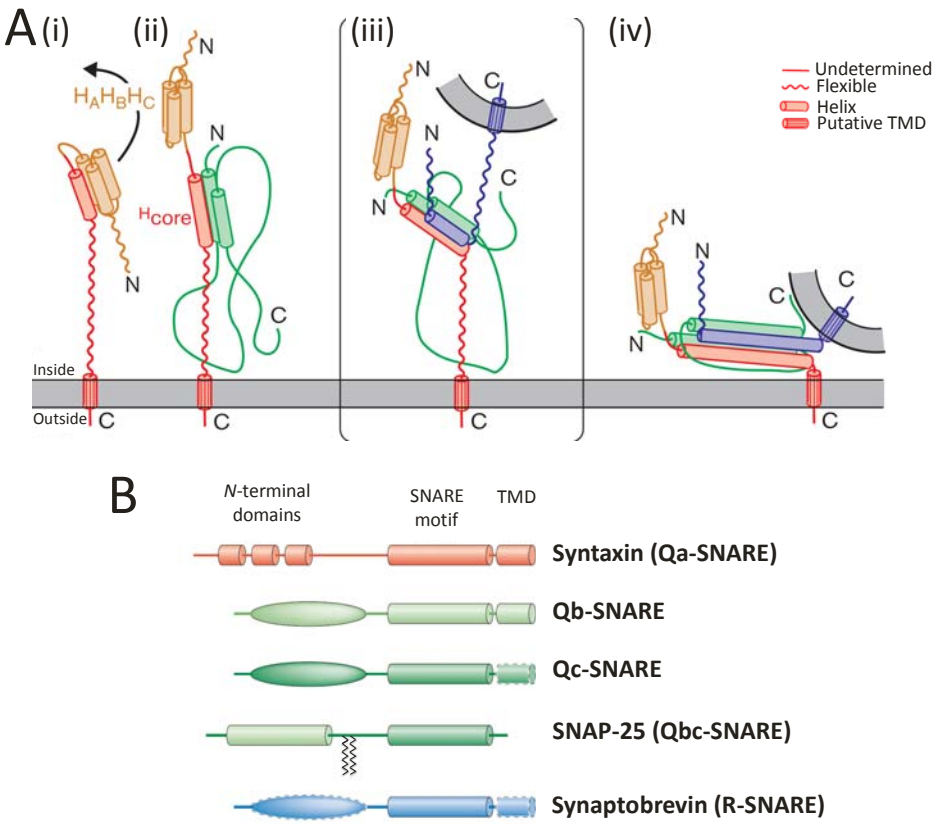

Figure 7. *Complex formation and schematic composition of individual SNARE proteins.* ***A*** *Proposed zipper model. (i) Closed state of Syntaxin (Qa-SNARE). (ii) 1:1 Complex of Qa- and Qb/c-SNARE. (iii) and (iv) formed 4-helix SNARE complex.* ***B*** *The structure of the individual SNARE proteins. The N-terminal end of Qa-SNAREs is composed of three α-helices which form three antiparallel helix bundles. The Qb-, Qc- and R-SNAREs comprise non conserved N-terminal domains, shown by an oval shape. SNAP-25 is composed of one Qb-SNARE as well as one Qc-SNARE motif. They are combined by a cysteine rich linker ('zig-zag' lines). Figure modified from* BRUNGER *(2000)*[62] *and* JAHN *and* SCHELLER.[3]

In the uncomplexed form, the groove of the t-SNARE into which the v-SNARE fits is occupied by the *N*-terminal regulatory domain of Syntaxin forming also a small antiparallel three-helix bundle ($H_AH_BH_C$ domain) (see Figure 7 A(i)). The first, energy providing step for merging the membranes is binding of Synaptobrevin with the 1:1 heterodimer resulting in SNARE complex formation (Figure 7 A(ii)). An upper limit for the subsequent binding of Synaptobrevin is given by the affinity of the 1:1 heterodimer formation. The *N*-terminal coil of Synaptobrevin binds reversibly to the *N*-terminal region of the Syntaxin-SNAP-25 heterodimer.[63] The arrangement of helices in the SNARE complex is parallel with the membrane anchors of Synaptobrevin and Syntaxin on the same side of the complex[7] giving reason for the possibility that directed assembly in a 'zipper-like' fashion, beginning at their *N*-terminal ends, brings the membranes together (Figure

7 A).[43] Alternatively, a second Syntaxin polypeptide chain can fill the groove of an open t-SNARE, and thereby, complete the four-helix bundle (2:1 complex). Assembled SNARE complexes bridging two membranes are called *trans*-SNARE complexes (see Figure 7 A(iii) and A(iv)). *Trans*-SNARE complexes are in a dynamic equilibrium between an unfixed and a more rigid connected state. Indeed, the SNARE assembly is sufficient to overcome the energetic repulsion between the membranes and entail fusion via several transition states.[64]

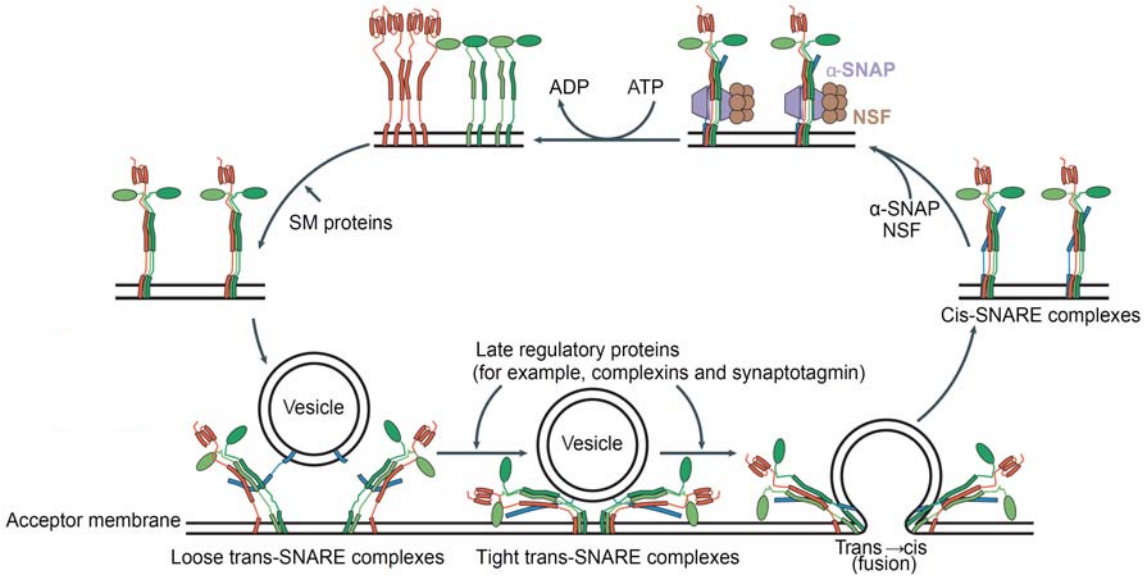

Figure 8. *The assembly-disassembly cycle of SNARE mediated fusion. At the acceptor membrane three Q-SNAREs and on the vesicle one R-SNARE were considered (red: Qa-SNARE; green: Qb- and Qc-SNARE; blue: R-SNARE) (top left). SM (Sec1/Munc18-related) proteins regulate the arrangement of the binary complex of the Qa- and Qbc-SNARE. Afterwards, the acceptor complex assembles the R-SNARE according to the proposed zippering-model. The formed so-called trans-complex brings the membranes together, whereas the conformation changes to a tight cis-configuration and fusion occurs. Afterwards, cis-complexes are dissociated by the AAA+ protein NSF and its cofactor α-SNAP via ATP-ADP hydrolysis. Figure modified from* JAHN *and* SCHELLER.[3]

The molecular character of the *trans*-complexes still remains unclear.[65] After fusion, the assembled SNARE complexes are present on the recently combined membrane, in the so-called *cis*-conformation. *Cis*-SNARE complexes are not able to induce fusion and their disassembly is decisive for the re-use of free, reactive SNARE molecules. The extreme kinetic and thermodynamic stability of *cis*-SNARE complexes means that they need to be regenerated by a specialized chaperone machinery.[37,66,67] The disassembly is mediated by the enzymatic activity of NSF, a hexameric AAA-ATPase, together with its co-factor α-SNAP. They mediate the

ATP-dependent SNARE disassembly to dissociate *cis*-SNARE complexes, opening SNAREs for productive *trans*-complex assembly and allowing the recycling of SNAREs that already have mediated membrane fusion (Figure 8). [16,68-70]

The precise amount of SNARE complexes required for membrane fusion has been conversialy discussed over the last decades. As mentioned above, corresponding to the stalk hypothesis,[16,17] an extensive activation energy of approximately 35 k_BT has to be supplied by the SNARE assembly process. Because of the remarkably stability evaluated by the Surface-Face apparatus (SFA) entails that only a small number of, maybe still only a single complex are needed to provide enough energy for membrane fusion.[38] Recently, VAN BOOGART *et al*. demonstrated evidence that a individual SNARE complex is sufficient for membrane fusion.[71] By *in vitro* experiments using Förster resonance energy transfer (FRET) measurements liposomes containing only one single SNARE molecule are able to induce membrane fusion.

As mentioned above, assembly in solution can be quite non-selective. In addition to assembling into R:Qa:Qb:Qc cognate complexes (i.e. functional *in vivo*), SNAREs can also build disordered complexes in many ways like forming homo-oligomers. For example, Syntaxin forms dimers and tetramers (Qa2 or Qa4) that are not likely to be functional *in vivo*.[72,73] SNAREs can also form hetero-oligomeric complexes that do not contain each of the R- and Q-SNARE motif types. For instance, Syntaxin and SNAP-25 associate to form a 2:1 complex (Qa2:Qb:Qc).[66] Due to a low number of side-chain interactions within the binary complexes of Synaptobrevin with Syntaxin or SNAP-25 they are relatively unstable.[7,40] More stable is the 2:1 complex of Syntaxin and SNAP-25, with only glutamines in the 'ionic' layer,[40] although this binary complex was never monitored *in vivo*. When Synaptobrevin is added, one of the Syntaxin molecules is displaced.[40,52] Interestingly, the SNARE-assembly is much more selective when they are anchored in proteoliposomes. ROTHMAN and co-workers evaluated the fusion abilities of many yeast SNARE combinations[31,74-76] to compare the assembly of liposome-anchored SNAREs with the assembly of their soluble analogues. This specificity seems to lie in the geometry of the *trans*-SNARE complexes. These *trans*-SNARE complexes are under pressure because they are anchored simultaneously in two different membranes. The amount of pressure depends on the distribution of the four SNAREs among the two membranes. In many cases, all possible topological combinations except one appear to be too highly strained to mediate proteoliposome attachment and fusion.[75] Thus, the proteoliposome

assay provides a powerful system for measuring the intrinsic physical properties of SNARE proteins.

2.1.5 Recycling of the SNARE Core Complex - NSF and SNAPs

After complex assembly, the R- and Q-SNAREs are located in the same membrane and are no longer free for further rounds of fusion. Hence, basically no spontaneous dissociation occurs. If there is no counteracting mechanism, all fusion events would come to an end when all free SNAREs were used one time. Of course, the cell could constantly dispose of the fully assembled SNARE complexes and synthesize new free SNAREs for single-use processes, but having in mind that during assembly the SNAREs undergo only structural but no degradational changes, one can assume the existence of a faster and probably more efficient solution for this problem.

Compared to the assembly reaction little is known about the molecular details of the disassembly. Due to the thermodynamically stable core complex a specialized machinery for dissociation of the SNARE complex is required. The disassembly proceeds under ATP hydrolysis, which provides the required energy. Using an *in vitro* trafficking assay developed during the early 1980s, ROTHMAN and co-workers were able to purify two soluble proteins required for reconstituting efficient transport.[77] The chaperone *N*-ethyl-maleimide sensitive factor (NSF) acts together with the soluble NSF attachment proteins (SNAPs) (no relation to SNAP-25). NSF and SNAPs are structurally and functionally conserved in evolution and act in many intracellular trafficking pathways.[67,78] Initially it was assumed that they were fundamental regulation factors of vesicular transport between Golgi compartments. This hypothesis was replaced by the now known function as SNARE complex control in almost all intracellular transport steps. The importance of NSF for the neuronal exocytosis was shown by an inactivation experiment using a temperature-sensitive NSF variant in *Drosophila*, which yielded in a concentration of assembled SNARE complexes without recycling of the individual SNARE proteins being available for further fusion cycles, and therefore, a decreased exocytosis.[79]

NSF is an important component in many vesicular transport pathways in addition to intra-Golgi transport. The sequence of NSF shows its homology to the yeast protein Sec18p, which is somehow required for transport from Endoplasmic Reticulum (ER) to Golgi.[80] Sec18p requirement has been demonstrated at every

step of the secretory pathway in yeast,[81] and is also implicated in the endocytotic pathway.[82] NSF is a hydrophilic 76 kDa protein which belongs to the AAA protein superfamily (ATPases associated with various cellular activities) identified by a highly conserved ATP binding site.[83,84] They function as molecular chaperones, meaning, via ATP hydrolysis it is able to modify the conformation of its target proteins.

The overall structure of the NSF oligomer is a hexameric ring.[56,85,86] It forms an asymmetric barrel with a central pore.[87] This ring is composed of subunits which contain three distinct domains: the substrate binding *N*-terminal domain (N-domain, aa 1-205) and two nucleotide binding domains, a D1- (aa 206-477) and D2-domain (aa 478-744) (Figure 9 A).[88] In Figure 9 B an electron micrograph of NSF is shown.[86] The catalytic activity of NSF arises from ATP hydrolysis delivered by the D1-domain, whereas the D2-domain is responsible for sustaining the hexameric ring. The D2-domain shows little ATPase activity, but it does not hydrolyze ATP.[88-90] The slow intrinsic ATPase activity of NSF is necessary for fusion. Mutation of either site seriously compromises both, ATPase activity and fusion, mutation of both sites eliminates ATPase activity and fusion. Electron microscopy (EM) studies reveal the NSF hexamer as a funnel of two rings with an ≈2.5 nm diameter pore, ≈10 nm length and ≈13 nm wide when adenosine diphosphate (ADP) occurs, corresponding to the D1- and D2-domains, respectively.[56,91] During the hydrolysis from ATP to ADP+P_i the whole NSF-hexamer undergoes a conformational change in which might use mechanical force onto the bound complex (Figure 9 C).

The D1 subdomain is an dynamic ATPase and supply the energy for NSF action, whereas the D2-domain shows a symmetrical hexagonal shaped ring.[92] Among nucleotide-binding proteins this structure containing a nucleotide-binding as well as a carboxy-terminal subdomain is unique.[92,93] In the middle of the hexamer is a hole that is negatively charged. The *N*-terminal part of the core complex has positively charges, and hence, it is assumed that they these parts can interact. The D2-domain of NSF is determined for oligomerization of the protein since mutants lacking this domain are monomeric, and when this domain is expressed by itself it readily forms oligomers.[88]

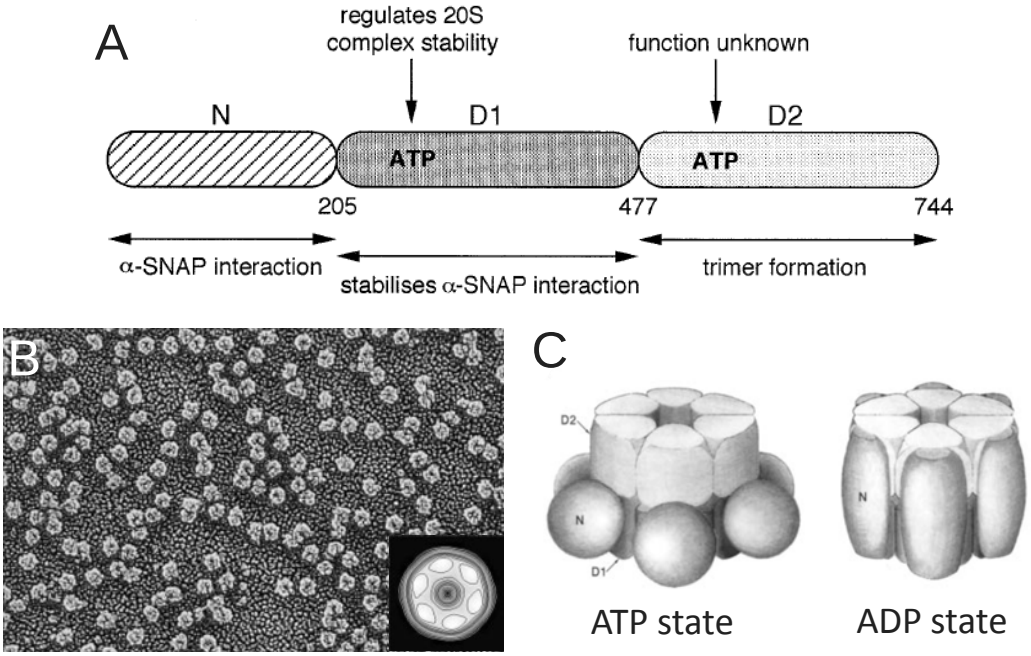

Figure 9. A *Primary structure of NSF showing the domains N, D1 and D2.* ***B*** *An electron micrograph of the hexamer of NSF.* ***C*** *Conformational changes of the N-domain at ATP-ADP hydrolysis. Figure modified from WOODMAN,*[47] *FLEMING*[85] *and HANSON.*[56]

The amino-terminal domain (N) of NSF binds the SNAP-SNARE complex and is required for disassembly. The structures of the amino-terminal domains of NSF,[94,95] of the yeast homolog Sec18p[96] and of the homologous VAT protein[1] of the archaebacterium *T. acidophilum*[97] are almost identical demonstrating the structural conservation of the family of AAA-ATPases. The amino-terminal domain contains two subdomains which form a groove between for interactions with the carboxy-terminal section of α-SNAP.[94,95] This region accommodates numerous basic residues, which are necessary to compensate the highly negatively charged *C*-terminus of α-SNAP; and has a defined size and shape compatible to interact with α-helical peptides. Electron microscope images show NSF in its ADP bound state as a symmetrical barrel that is build of the hexameric D2- and D1-domains lying upon another (Figure 10). During the catalytic cycle the conformation of NSF and its mutants changes to the ATP form. At this, the spherical N-domain surrounds the hexameric rings.[56]

SNARE complexes do not display any direct binding sites for NSF. In order to disassemble the complex, SNAPs (soluble NSF attachment proteins) are required providing high affinity binding sites for both, the enzyme as well as its substrate.[98]

[1] valosine-containing protein-like ATPase from *Thermoplasma acidophilum*

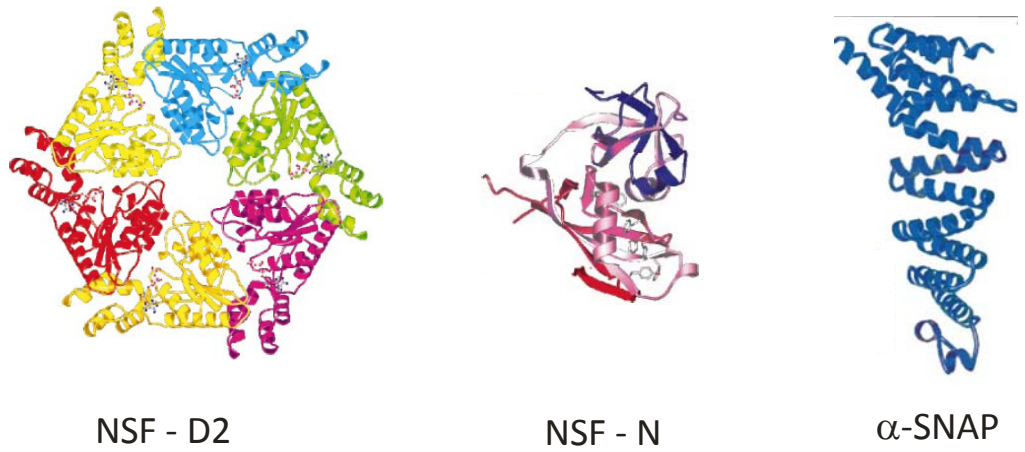

Figure 10. *Crystal structures of the subunits of NSF and α-SNAP.*[62]

Three variants of SNAPs, termed as α-, β-, and γ-SNAP, respectively were found in mammals.[99] Thereby, α-SNAP can be replaced in *in vitro* transport reactions by the brain specific β-SNAP (which is > 80 % homolog) due to their functionally equivalence.[98,100] Sec17, the yeast homolog of α-SNAP, reveals α-helical hairpins arranged in twisted sheets and a spherical carboxy-terminal domain.[101] Deletion mutagenis and *in vitro* binding experiments were carried out to identified interactions between α-SNAP (Sec17) and SNAREs, showing that the SNAP-interacting region of SNAREs were identical with the domains required for complex formation.[59,60,102] This, in conjunction with the synaptic core complex structure[7] and the monitored variety of SNAP-SNARE interactions suggests that SNAPs are able to identify general surface individualites (e.g. shape or electrostatic charge distribution) of the parallel four-helix bundle. Indeed, the four-helix bundle forms a bended groove compatible of the bending of the twisted sheet of α-SNAP. Electron microscopy and mutagenesis studies of SNAP-SNARE complexes indicate that the SNARE complex is almost full-length encased from SNAP. In a variety of homologous SNAPs numerous conserved residues likely interacting with SNAREs and/or NSF-Sec18 were predominantly positioned showing to one side of α-SNAP. These surfaces are likely to interact with. In fact, little is known about the disassembly mechanism, the number of α-SNAPs required is still under discussion. Three might be needed, but alternatively one or two are also thought to be sufficient. However, complexes between Syntaxin and Synaptobrevin (which are stabilized by SNAP-25) will closely bind two α-SNAP molecules and a supplemental SNAP binding site is generated within the ternary complex.[60,103] In any case, participation of more than three can be excluded. It is still unclear in which way one SNARE complex, one to three α-SNAPs, and six NSF

molecules (one hexamer) can rationally be put together. Only SNARE complexes serve as SNAP receptors not monomeric SNAREs. In Figure 11 a schematic assembly-disassembly cycle demonstrates how NSF and α-SNAP process the SNARE complex after fusion to recover the monomers. It has been illustrated that NSF-dependent ATP hydrolysis drives a conformational change in Syntaxin that releases α-SNAP and Synaptobrevin, which will not re-bind Syntaxin for some time, indicating that the change of conformation is long-lasting.

α-SNAP interacts with the SNARE complex and NSF, in turn, engages that the α-SNAP-SNARE complex forms a '20 S' complex, termed after the sedimentation characteristics of the whole complex. The cytosolic proteins NSF and α-SNAP are able to disassemble SNARE complexes from almost all intracellular transport steps. Detailed investigation of the SNAPs and their binding partner led to the characterization of the first SNARE complex.[9]

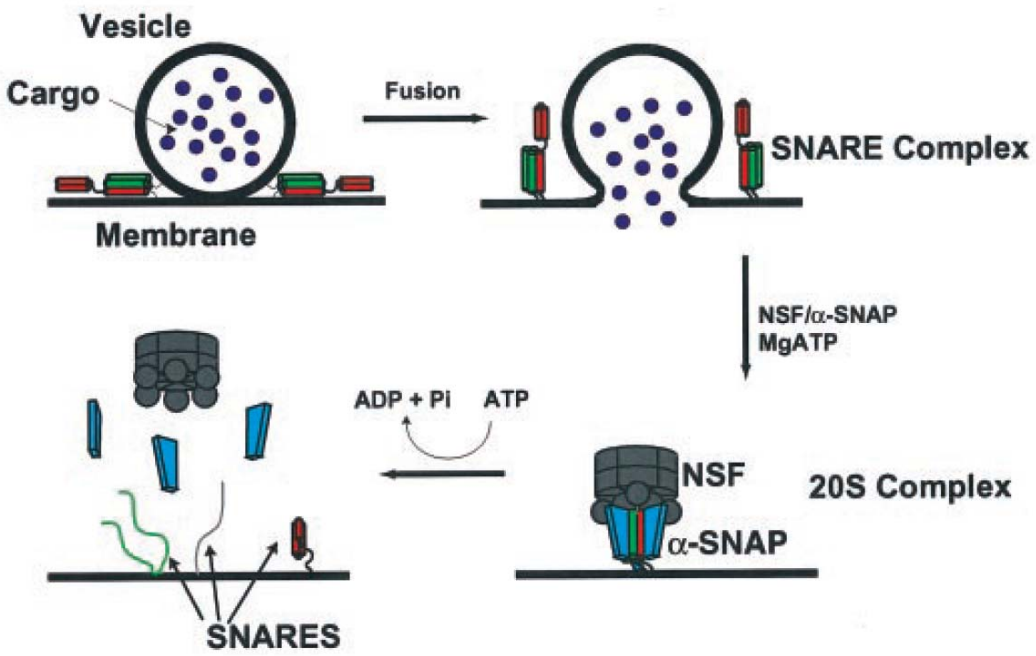

Figure 11. *After SNARE complex formation the vesicle fuse with the membrane. Afterwards, NSF and SNAP disassemble the SNARE complexes by configuration of a '20S' complex by ATP-ADP hydrolysation. SNARE proteins can form trans- (opposing membranes) as well as cis- (same membrane) complexes being binding platforms for SNAPs and NSF.*[104,105]

In Figure 12 the stepwise assembly of a '20 S' complex is illustrated. Initially, α-SNAP enclose laterally the SNARE complex with the *N*-terminus of each α-SNAP close to the membrane-proximal *C*-termini of the SNAREs.[91] This arrangement produces a surrounding which is needed for the detachment of the notably stable core complex. Interaction between α-SNAP and SNAREs along the SNARE length converts the energy generated by ATP hydrolysis via NSF. Then, the NSF double ring binds to the SNAP/SNARE complex at the *C*-terminal end of α-SNAP. Based on the length of the cone shaped tail of the '20 S' complex with 13 nm composed to the 12 nm length of the SNARE complex, the '20 S' complex can be partially placed into the hole of NSF. Though, the major fragment of NSF pluged over the SNAP/SNARE complex. An indication that the inner ring is build of the N- or D1-domains involved in SNAP and SNARE interactions is the position of the carboxyl terminus of NSF to the outer ring.

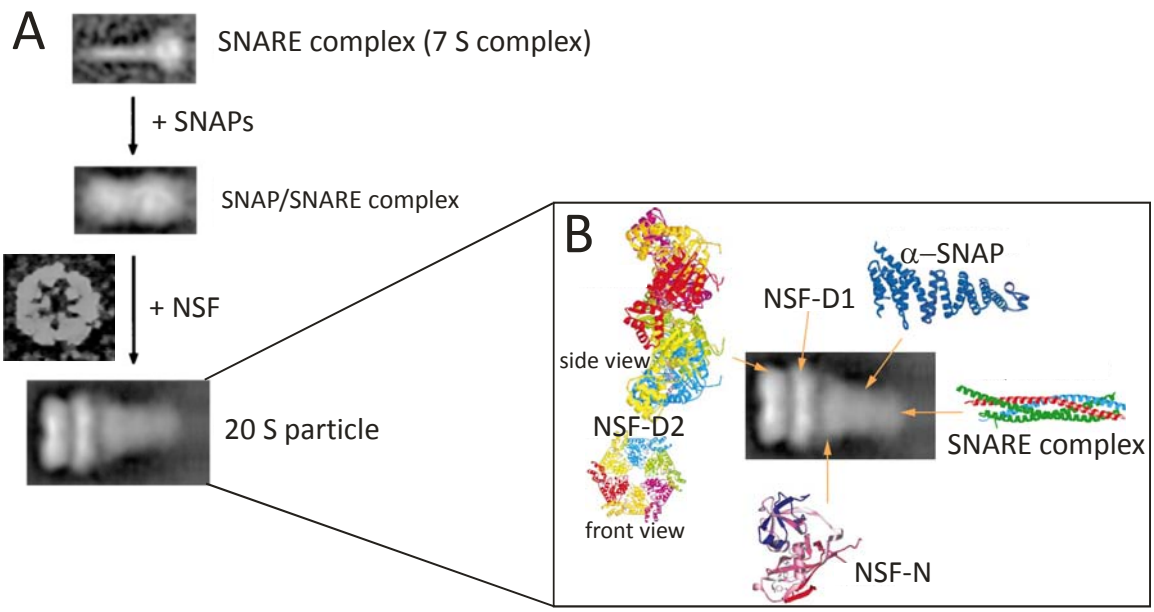

Figure 12. *Structure of the '20 S' complex.* ***A*** *Structural assembly pathway of the '20 S' complex. α-SNAP wraps the SNARE complex. Afterwards, NSF binds to the SNAP/SNARE complex at the opposing end to the SNARE transmembrane domain. The assembly pathway is shown at electron micrographs.*[91] ***B*** *Crystal structures of the individual elements of the 20 S complex in conjunction with an electron micrograph to show their exact position therein. The NSF-D2-domain forms a hexameric ring that fits to the sheath-like SNARE/α-SNAP complex. The sequences and structures of the D1- and D2-domains are identical. Therefore, they probably constitute the two rings. Figure modified from* HOHL *et al.*[91] *and* BRUNGER.[62]

The localization of the *C*-terminus of NSF to the outer ring suggests that the internal ring is build of the N- or D1-domains which are interact with the SNAP and SNARE proteins,[89,91] whereas the D2 hexamerization domain is localized at the outer ring.[92,93] Via at least two NSF binding that are distributed to the *C*- and *N*-terminal half of the α-SNAP molecule sites it is possible that α-SNAP effected some of these structural conformations.[106]

Even thirty decades after the discovery of NSF, molecular details of the α-SNAP/NSF mediated disassembly are less understood. This might be justified at the primarily hypothesis that α-SNAP and NSF functioned as regulators in the last step of membrane fusion. Various convincing investigations have disproved these assumption and display NSF as the mediator of SNARE recycling. This meanwhile approved function of NSF in conjunction with its cofactor α-SNAP to disassemble the SNARE complex is an essential step within membrane fusion mechanisms. Though, other regulation factors exist assuring stabilized SNARE complex assembly, and therefore, membrane fusion.

2.2 Complexin: Inhibitor or Stimulator of the SNARE Mediated Fusion Process?

Several proteins are interacting with and potentially regulating the SNARE complex, although their precise functions are still contendend. As already discussed, the conformation of free SNARE molecules and their availability for complex formation is partly regulated by members of the SM (Sec1/Munc) family, however, the exact role of these proteins remains unclear. Studies with SNAREs of the secretory pathway indicate that SM proteins act positively to promote SNARE assembly, perhaps allowing the transition of SNAREs to change from inactive-closed to active-open conformations. Alternative regulators of *trans*-SNARE complexes are members of the Synaptotagmin and Complexin families. Synaptotagmin is considered as the Ca^{2+}-sensor of fast synaptic vesicle exocytosis and interacts with both SNAREs and acidic phospholipids in a Ca^{2+}-dependent way. Following Ca^{2+}-binding, Synaptotagmin is thought to promote fusion, although it is still unclear to which dimension due to its binding to SNAREs.[107] Another example of a SNARE binding-protein responding to Ca^{2+}-increase in neurosecretion is the so-called Complexin (also known as Synaphin). This molecule is believed to partially associate with SNARE complexes and unbind once the calcium trigger arrives.[108] It is essential for fast kinetics of membrane fusion at synaptic contacts.[13,109]

The Complexins represent a family of small (15-16 kDa) α-helical proteins without folding similarities to any other protein family being fundamental for an efficient Ca^{2+}-evoking release of neurotransmitters and are occurring in all multicellular eukaryotes. For example, neurotransmitter release shows profound deficits when Complexin genes are deleted.[110] Point-mutations cause drastical reduction in synaptic transmission and were suggested to contribute to the symptoms of Huntington´s disease,[111] Parkinson´s disease,[112] Alzheimer´s disease,[113] fetal alcohol syndrome[114] or schizophrenia.[115-117] Complexin binds tightly to an assembled neuronal complex along the groove between Syntaxin and Synaptobrevin up to approximately layer +3 in its membrane-proximal half, in a 1:1 fashion and may stabilize *trans*-complexes,[14,109] though it binds weakly or not at all to its individual v- and t-SNARE subunits.[7,8,118,119] The Complexin structure bound to the neuronal SNARE complex has been solved.[14] An α-helical central stretch consisting of 58 amino acids was found to bind the SNARE complex in an

antiparallel manner.[8] The crystal structure of the Complexin-SNARE complex is shown in Figure 13. The structure of the arrangement between Complexin and the SNARE complex shows that Complexin forms a fifth antiparallel helix on the four-helix parallel bundle of the SNARE complex.[14] It covers about two-thirds of the *C*-terminal end of the groove between the Synaptobrevin and Syntaxin helices of the rod-shaped SNARE complex. Therefore, it may stabilize the fully assembled *trans*-SNARE complex, as its structure does not change (Figure 13). Originally Complexins have been reported to displace α-SNAP from the SNARE complex when added in excessive amounts leading to speculations that they might have inhibitory properties with respect to SNARE disassembly.[13] Notwithstanding these findings, *in vitro* assays directly monitoring SNARE disassembly do not show any negative influence of Complexin on SNARE complex disassembly.

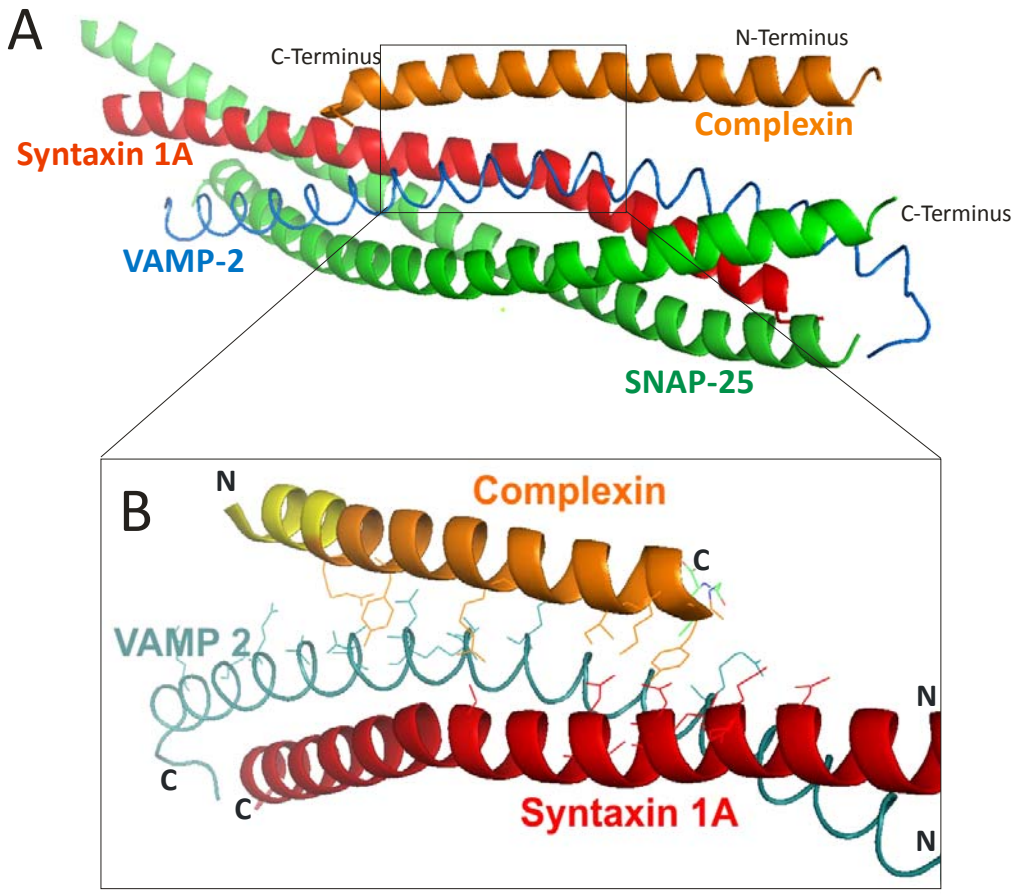

Figure 13. A *Crystal structure of Complexin bound to the SNARE complex.* ***B*** *Important side chain interactions between Complexin, Syntaxin and Synaptobrevin are shown. (Synaptobrevin-blue, Syntaxin-red, SNAP-25-green, Complexin-orange), (pdb code 1KIL).*

The question whether Complexins facilitate or inhibit SNARE mediated fusion processes is currently under discussion. If Complexin could bind analogously to the zippering SNARE monomers that drive fusion, it could potentially clamp fusion by arresting the fusion mechanism,[120] but it could also promote fusion by stabilizing a key intermediate.[14] This leads to the assumption that Complexin functions as an inhibitor of the last step of SNARE assembly. This does not exclude the possibility that the 'Complexin clamp' serves as protection against unwanted disassembly at the same time. Altogether the apparently contradictory results could, in principle, also be explained by a fine-tuning capability which might depend on a physiological Complexin concentration. Therefore, too little as well as too much Complexin would harm the balanced fusion process and might lead to similar phenotypes. Inhibitory effects of Complexin have also been detected in artificial systems such as the flipped SNARE assay[54,121] or the liposome fusion system.[122] Although Complexins themselves do not appear to bind calcium, the phenotype of the double knockout can be bypassed simply by raising extracellular calcium.[109]

Since its discovery the molecular details of SNARE complex disassembly and their scope of function as well as their regulative proteins like Complexin offered many open questions. Subsequent work has established a role for NSF in the assembly-disassembly cycle essential for cell survival. The appreciation of NSF regulation has been a key development and reflects our increased understanding of the complexity of membrane trafficking mechanisms. Anyhow, many molecular details are still unclear. For example, it is still uncertain how NSF uses ATP hydrolysis to disassemble the SNARE complexes at a molecular level.

The function of Complexin is already under discussion as well. It appears that it is a fusion clamp and is necessary for fast fusion. It helps to allow fast calcium-triggered exocytosis. Indeed, such a modulatory protein might either completely abolish or, in other cases, only decrease the disassembling activity of NSF and/or SNAPs. Insights into these methodologies may be achieved in studies directly investigating the requirements for optimal SNARE disassembly. Comparison of disassembly assays in presence or absence of assumed regulatory factors might help to give evidence on the mechanistic aspects of the disassembly reaction. Thus, many other molecules need to be identified in order to obtain a global view on any molecular detail of the assembly-disassembly pathway.

An additional approach might be to generate synthetic Complexin mimics with enhanced interactions to the SNARE complex in order to prevent α-SNAP

recognition, and therefore, the complex disassembly. As α-SNAP is not able to displace the Complexin mimic and the individual SNARE proteins were even recovered, more information regarding assumed α-SNAP binding sites and the number of required α-SNAP molecules were available.

2.3 Bioinspired Organic Chemistry

During the last decades the frontiers between chemical and biological questions have become intertwined. Therefore, chemical input is obviously a good way for understanding many biological processes like establishing new molecular systems or formation of large, stable and well-defined three-dimensional structures. Supporting the design of promising catalysts, receptors and materials for effective synthesis of artificial proteins and nucleic acids by application of synthetic oligomer building blocks will be useful. Replacing a proline residue in a turn in native ribonuclease A by 5,5-dimethyl-L-proline (**1**) increases the required *cis*-conformation of the β-turn. The protein folding as well as the stability of the resulting protein is enhanced, whereas being as active as the *wild type* RNase A (Figure 14).[123]

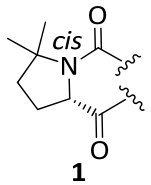

Figure 14. *5,5-Dimethyl-L-proline (**1**).*

Hence, it is important to control the characteristics of *de novo* biomimics designed for processes like signaling and molecular motors. Therefore, much effort is invested at designing and controlling β-sheet structures similarly at defining the requirements for stability.[124] Folded polymers are used in nature for almost every vital process. Nonnatural folded polymers, or foldamers have the potential for similar variety; and the design and improvement of such molecules is of current interest.

Nature suggests that biomimetic polymers are receivable targets. A lot of groups (GELLMAN,[125] NIELSEN[126]) studied homogenous, sequence specific oligomers, partially including nucleobases with PNA as DNA/RNA mimic,[127] alternative peptidic[128-130] or sugar backbones[131-133] mimicking various aspects of folding and organization of polypeptides. Other researchers are focused on conventional peptides, especially β-peptides.[125,134,135]

2.3.1 β-Peptides

β-Peptides are attractive constructs for understanding and observation of protein structures and stabilization processes at the molecular level. β-Amino acids are distinguished from α-amino acids only by introduction of a methylene group. β-Substituted amino acids as they are required for β-peptides can easily be synthesized by homologation of α-amino acids[136] or by numerous other practical routes.[137-139] Early investigations of polymeric β-peptides indicate their ability of adopting stable helical structures. They utilize the same strong H-bonding properties generating stable secondary structures at an oligomer length of only six residues.

So far, five different helical structures have been identified in the field of β-peptides: the 14-,[136,140,141] the 12-,[142] the 10-,[143] the 12/10-,[135,144] and the 8-helix (Figure 15 A).[145,146] Thus, control over preferred helical secondary structures can be achieved via reasonable selection of the substitution pattern.

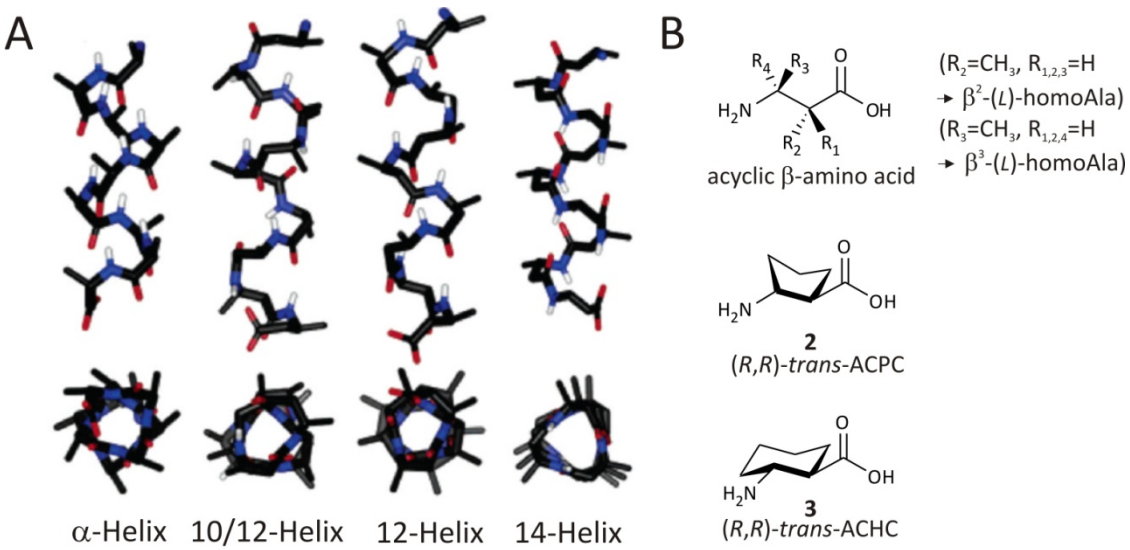

Figure 15. A *Structure of the helices formed by α-, and β-peptides. Carbon atoms are shown in black, nitrogens in blue, oxygens in red and amide hydrogens in white. Other hydrogen atoms are omitted for clarity.* ***B*** *β-Amino monomers known to promote the formation of unique helices. (top - N-terminus, bottom - C-terminus). Figure modified from* KRITZER *et al.*[147]

The helix type is largely determined by the choice of the β-amino acid monomer: cyclic ring restraints within the monomer of four, five or six atoms favor the 10-, 12- or 14-helix. Residues, which are aliphatic and monosubstituted (β^2- or β^3-

residues) exhibit the tendency to fold into 14- or 10/12-helices when arranged (Figure 15 B).

The 14-helix has emerged as the best studied of the folding structures of β-peptides.[148,149] Peptides synthesized with β^3-amino acids deduced from naturally occurring L-amino acids reveal left-handed 14-helices. By introducing salt bridges in neighboring positions on one side of the helix these helical structures can be stabilized in water, but regarding the total dipole of the helix a more adaptable route has been established.[140,141,150] Furthermore, insertion of the conformational rigid cyclic amino acid *trans*-2-aminocyclohexanecarboxylic acid (ACHC) facilitates the configuration of 14-helical structures. Between an amide proton at position *i* and a main chain carbonyl at position *i+2* in a three residue repetitive configuration resulting in 14-membered hydrogen-bonded rings, so every third residue is on top of another one on one side of the helix differing from an α-helix in many respects. In contrast to the α-helix which needs 3.6 residues per turn, the 14-helix has a slightly wider radius (2.7 Å then 2.2 Å) (Figure 16).[151,152]

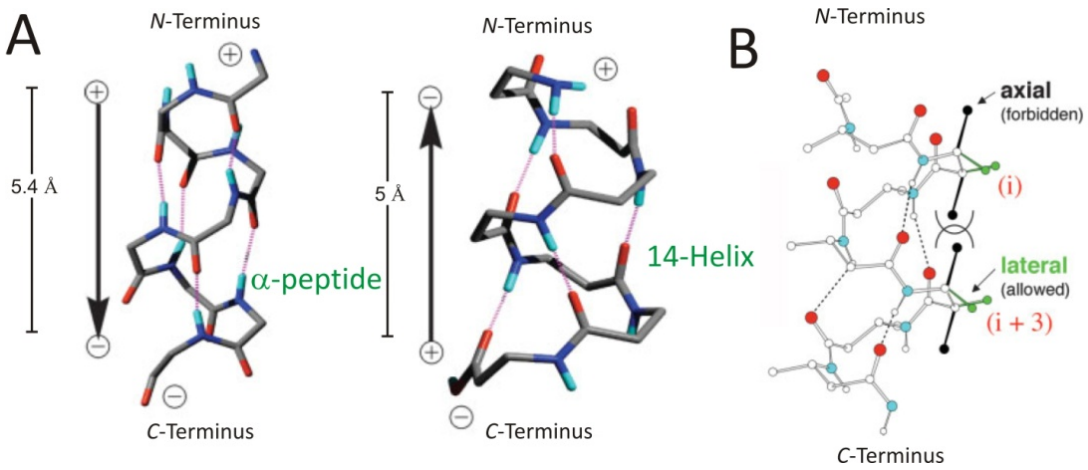

Figure 16. A *Crystal structures of an α- and 14-helix to compare the stabilizing interactions and the inversed dipole.* ***B*** *Left-handed 14-helix with lateral (allowed) substituents in the i and i+2 position. Structures modified from* SEEBACH *and co-workers.*[146]

Molecular modeling showed that for steric reasons only hydrogen, hydroxy or fluorine are allowed to substitute the tetrahedral β^3-carbon in axial positions.[153] As mentioned before, the cyclic amino acid ACHC and the integration of β^3-amino acids appear as stabilizing parts. Formation of salt bridges or covalent bonds between *i* and *i*+3 as well as the '*N*-terminal capping' promote 14-helix

formation.[140,147,154,155] In contrast, syn-configurated $\beta^{2,3}$-amino acids or disubstituted β^2- or β^3-amino acids have a destabilizing effect.

On the other hand, the 12/10-helix forms a peculiar, right-handed helix containing 12- and 10-membered hydrogen-bonded rings in alternating configuration (Figure 15). This conformation can be formed with alternating β^2- and β^3-monosubstituted residues.[144] A smaller ring size results when positions 2 and 3 of the β-amino acid are separated from the five-membered ring (ACPC, *trans*-2-amino-cyclopentanecarboxylic acid). For stabilizing the 12-helix hydrogen bonding between the amide protons at position *i* and the amide carbonyl groups at the *i+3* position is performed. The helix repeats itself every 2.5 residues. Formation of a 10-helical structure will be promoted by smaller rings such as *cis*-aminooxetane carboxylic acids.[143] Like the 10-helix, the 8-helix cannot be found in oligomers containing homologated proteinogenic amino acids. Every turn exists of approximately 2 residues.

For designing β-peptides several factors have to be considered. The chemical nature of the β-amino acids and their influence of the secondary structure were already mentioned. Other aspects, e. g. the solubility or the overall charge are also important elements. Their high stability makes β-peptides attractive compounds for proteolytic enzymatic degradation.[156-158] SEEBACH and GELLMAN analyzed hundreds of derivatives concerning their stability towards enzymes.[159-161] They observed no degradation at all after two to five days. The β-heptapeptide **4**, shown in Figure 17, designed by GELLMAN *et al.*, is entirely inert against trypsin, known to cleave peptide bonds which are close to positively charged side chains. SEEBACH *et al.* demonstrated that peptides constituted of α- and β-amino acids were partially cleaved exactly at the link between both strands by pronases (mixture of different proteinases and peptidases, isolated from *Streptomyces griseus*).[159,162]

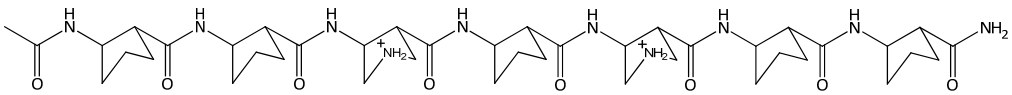

4

Figure 17. *β-Heptapeptide **4**, designed by GELLMAN et al., which is completely inert against trypsin.*

Another interesting observation is the antibacterial activity of biological active β-peptides. Due to their ability of building cationic, amphiphilic helices in presence of adequate cell membranes or vesicles they are able to interact with membranes. Based on natural occurring antibacterial peptides as Magainin, DEGRADO, GELLMAN and SEEBACH designed a series of β-peptides and analyzed them against all kinds of bacteria.[141,161-165] One of the important results was, that an amide capped *C*-terminus enhances the attraction between β-peptide and membrane. Therefore, a rigid secondary structure is not always required. Of particular impact in recent years was a mimetic of Somatostatin (**5**), synthesized by SEEBACH *et al*., acting as a substrate for the receptor human Somatostatin 1-5 ($hSSt_{1-5}$) and inhibiting the release of the human growth hormone Somatotropin found in a series of tumors like in lung, breast or brain. The peptide mimetic **7** is more stable than Somatostatin (**5**), which has a half-life time of two minutes in blood.[162,164] Binding studies of the synthesized tetramer indicate successful inhibition of the human Somatostatin 5 ($hSSt_4$) receptor (Figure 18).

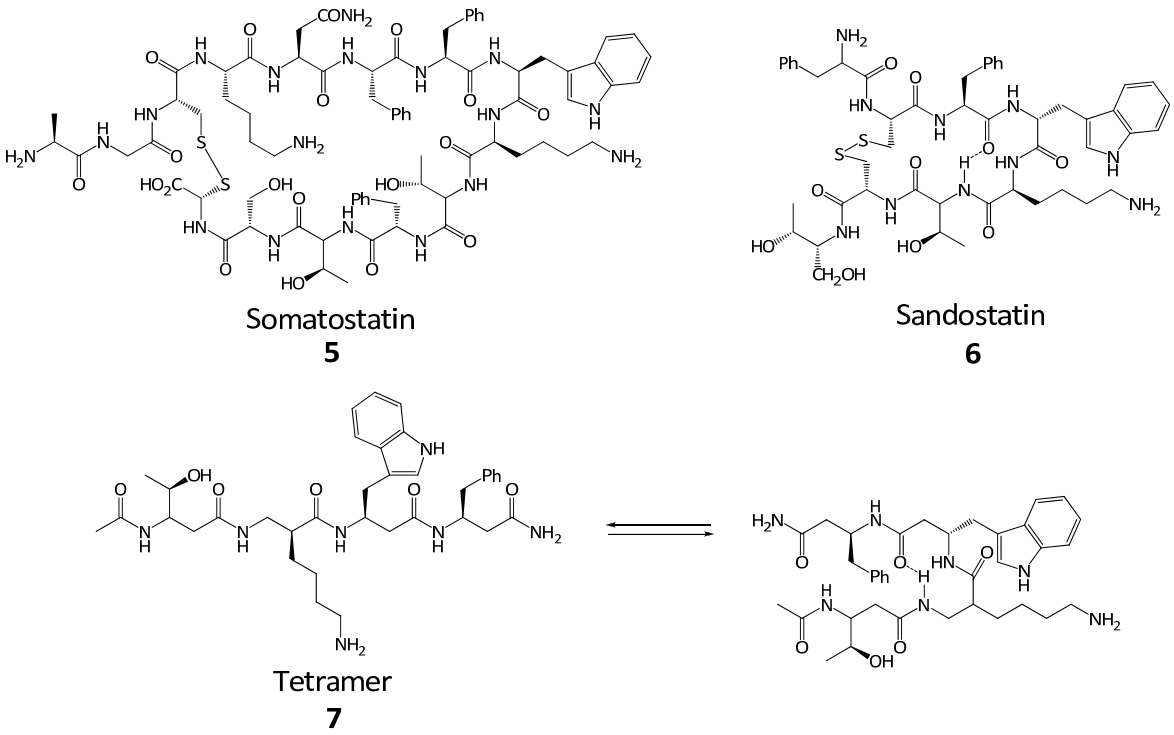

Figure 18. *The natural Somatostatin (**5**) and his mimetics. Sandostatin® (**6**) is in therapeutical use. The Tetramer **7** shows successful indications for a potent agonist of Somatostatin (**5**) in binding studies.*

As already described β-peptides with well-defined conformations similar to natural proteins were investigated in the last decades. Generating synthetic β-

peptidic oligomers with enhanced interaction compared to their corresponding α-peptides is an interesting field of peptide design.

2.3.2 Folding Processes of Single Protein Motifs - HTH and WW Motifs

Another way of understanding how proteins operate in biological processes is to study the folding and unfolding processes. Because of refined theoretical and experimental methods and their interaction the comprehension of protein folding has enhanced.[166] Common structure motifs are the helix-turn-helix (HTH) and the β-sheet. Principally, they merge into compact, globular structures, so-called domains. As mentioned above the proteins are able to change their conformation during biological processes. Thereby, protein folding is only one of numerous options of processes and the better understanding of the dynamics of the folding events has profound implications in molecular design. This requires a development of methods which are able to monitor such dynamics as well as small model systems enhancing their applications.

The helix-turn-helix motif is one of the simplest secondary structures with a specific function. At this, two α-helices are connected by a linker (turn) region.[167] DNA repair and replication proteins as well as RNA metabolism proteins or catalytic domains of diverse enzymes contain this special motif. Changes in sequence or shifting are not tolerated.[168] In solution the HTH is monomeric and folded.[168] The smallest proteins with an HTH motif are the three helix homeodomain proteins, for example the Engrailed Homeodomain (EnHD)[169] (Figure 19) from *Drosophila melanogaster* or the dimeric *Arc repressor*.[170]

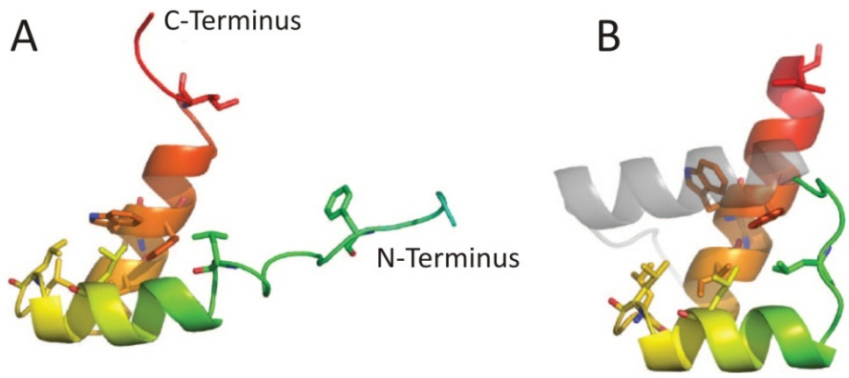

Figure 19. *Structure of the HTH motif.* ***A*** *Lowest energy structure.* ***B*** *Structure of the HTH in EnHD. (pdb code 2P81).*[168]

Homeodomains are generally composed of three helices, with helix 1 (H1, aa 10-22) and helix 2 (H2, aa 28-37) being antiparallel to each other and helix 3 (H3, aa 42-56) lying across both. They are very small (ca 6 kDa), conserved proteins. The EnHD is an ultrafast independently folding domain, it shows the fastest unfolding kinetics and is one of the fastest folding proteins known so far.[171] It has biphasic folding kinetics, meaning an intermediate is adopted in microseconds followed by a 10-fold slower refolding of the native state.[172]

Differentiation between early intermediates and denatured states at varying concentration is mostly unfeasible due to the extensive transition states and the poor stability of early folding intermediates. With high salt concentrations (2M NaCl) the fragment 16-59 of the EnHD was stabilized and had a well-defined folding transition.[168] As mentioned above, even small mutations are not tolerated by the HTH motif. The mutated L16A variant in the EnHD loses all interactions with H1. The stability decreases and the protein denatures at physiological ionic strength.[172] L16 is a highly conserved residue placed in the middle of helix 1, hence, a L16A mutation numerous local and long-range interactions with amino acids in H2 and mainly H3 were eliminated. The L16A mutant shows the best characteristics of a valid model for the denatured state of EnHD under folding conditions. The denatured state is characterized as the lowest energy non-native state under defined conditions.

The second common form of secondary structures is the β-sheet, a compact module composed of β-strands connected laterally by a turn separating each β-strand. Generally, these β-strands form a twisted, pleated sheet (see Figure 20 A). The WW domain, firstly described by BORK and SUDOL,[173] is a short, only 35 amino acids long, conserved region in a number of unrelated proteins, folding as a stable, triple-stranded β-sheet (β1-β3), with strands β1 and β2 being longer than β3. The name WW (WWP) domain is deduced from two highly conserved tryptophans (located in β1 and in β2) that are separated by 20-23 residues and of a signature proline located in the β3 loop. Usually, the *N*- and *C*-termini of the WW domain are near to each other, as it is characteristic of a modular domain. It constitutes the smallest monomeric triple-stranded antiparallel β-sheet protein domain don´t need disulfide bonds, tightly bound ions or ligands for stability.[174]

The WW domain binds to proteins with proline-motifs. A large variety of proteins containing WW domains are known. These include Dystrophin (Figure 20 B), a multidomain cytoskeletal protein; Utrophin, a Dystrophin-like protein of unknown function and vertebrate YAP protein.

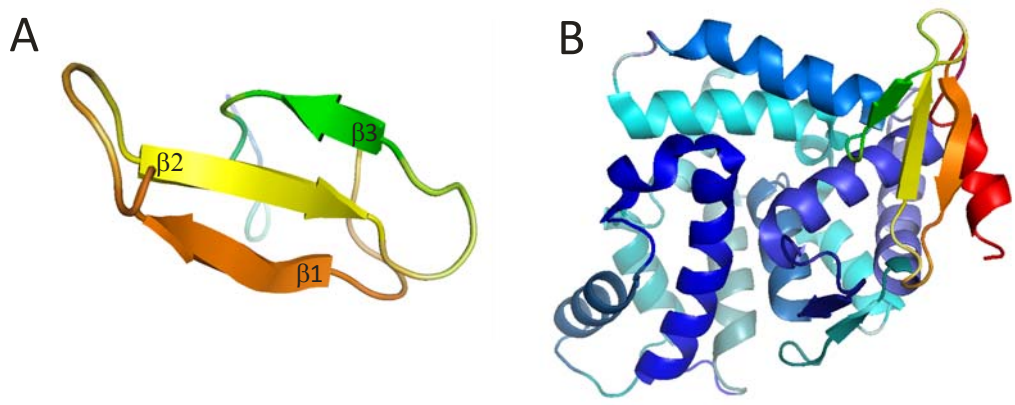

Figure 20. A *A common triple-stranded antiparallel β-sheet. Strands β1 and β2 are longer than β3 (pdb code 1I6C).* ***B*** *Crystal structure of a Dystrophin WW domain fragment in complex with a β-Dystroglycan peptide (pdb code 1EG3).*

WW domains take part in a range of cellular processes, including ubiquitin-mediated protein degradation, viral budding, RNA splicing, transcriptional co-activation, and mitotic regulation,[175] hence, WW domain-containing proteins can be found in human diseases like Liddle's syndrome, Duchenne muscular dystrophy, Huntington and Alzheimer disease.[175] It is often associated with other domains representing proteins which are involved in signal transduction. Because of their chemical and thermal denaturation reversibility in conjunction with wide-stretched unfolded transition states WW domains were found to be distinguished model systems for folding and stability studies concerning β-sheet proteins.

Due to their simple domain structure and their rapid folding and unfolding the HTH and the WW motifs are excellent candidates to test new or improved methods like Differential Scanning Calorimetry (DSC) for recording thermal unfolding events, Molecular Dynamics (MD) simulations or fluorescence dependent methods. Meanwhile, these α-peptide motifs are reviewed very well, and thus, they will allow direct comparison of new and existing data.

Molecular dynamic approaches are largely benefiting from the aspiring field of single molecule fluorescence. Calculations from MD simulations can be compared with data from single molecule experiments instead of many molecule averages. Within the last years, single molecule fluorescence spectroscopy (smFRET) experiments have increased to become a capable new method for answering questions about conformational dynamics and interactions of peptides and proteins.[11,176] For a full understanding of protein-folding mechanisms a defined distribution of the microscopic pathways connecting the folded and unfolded

states are required.[177] The ability to monitor individual folding pathways and equally internal dynamics of conformational events between proteins in the unfolded and folded state is an advantage of smFRET.

smFRET studies were carried out using the Förster resonance energy transfer (FRET), which measures the energy transfer efficiency from an excited 'donor'-fluorophore to another 'acceptor'-fluorophore. The limitation of smFRET studies are the restricted time during a single molecule is observed and studied and the photostability of the fluorescent labels. The classical smFRET setup measures photon distributions of fluorescence dye pairs. The photon distribution is used to calculate FRET efficiencies or FRET rates. Afterwards, the Förster theory is used to calculate molecular distances on the scale of tens of Ångstrom from the FRET efficiencies. The basic idea with FRET experiments for protein folding is demonstrated in Figure 21, where a donor and an acceptor dye are fixed to the termini of a protein. If the molecule was illuminated by a focused laser beam the excitation of the donor dye comes out in a rapid energy transfer to the acceptor dye, because of the close proximity of the termini in a folded protein (Figure 21 A). Thereby, the acceptor emits most of the fluorescence photons. In an unfolded protein the average distance between the donor and the acceptor dye is larger. Subsequently, the energy transfer rate is reduced and the number of released photons by the acceptor is decreased (Figure 21 B).[10]

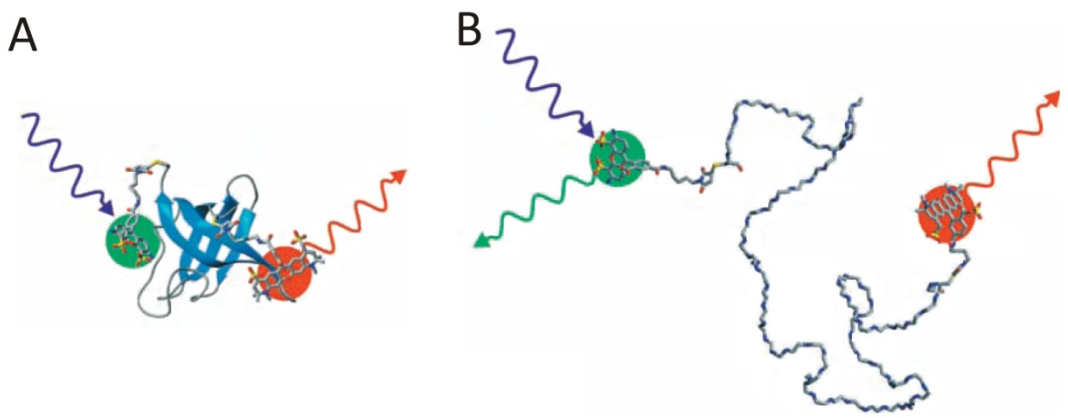

Figure 21. *Schematic structures of a folded (**A**) and unfolded (**B**) protein labeled with donor and acceptor dyes.*[10]

Due to the limited photostability of the fluorescent dyes and the common detection time of typical confocal microscopy system smFRET studies are presently restricted. New methods, enhancing the photostability of standard dyes

with new biocompatible chemical compounds (ROXS - reducing and oxidizing system)[178] or to immobilize the proteins on surfaces were recently developed.[179,180]

Encapsulation of individual proteins in liposomes is developed by HARAN and co-workers. Thereby, the whole complex is immobilized on a surface and can be screened with a confocal microscope to study with smFRET.[179] Indeed, individual encapsulated proteins and their folding pathway can be observed, however, liposomes are relatively weak, which complicates measuring of various characteristics (denaturant concentration, temperature). Furthermore, immobilizing and searching for these individual proteins by scanning is time-consuming, so the number of possible screened protein molecules is limited. An attractive option is encapsulation into nano-containers made of block copolymers, which are able to assemble themselves. These polymerosomes do not influence the folding and unfolding dynamics of the enclosed proteins, are persistent against changes in temperature, osmotic and mechanical stress and stable under harsh ambient conditions.[181,182] They are established systems to form vesicles, suitable for enclosing proteins.[183] So far, numerous proteins have been successfully studied using smFRET, e.g. the all-β cold-shock protein Csp*Tm* from *Thermotoga maritime*.[184,185]

A better understanding of relations between secondary structures and their influence regarding the functions of small self-assembling proteins can help to enhance the comprehension of bigger molecules as well as their mode of action.

Chapter 3

Synthesis of Synaptobrevin Derivatives and their Application Regarding the α-SNAP/NSF-Mediated Disassembly

3.1 Design of the Synaptobrevin Derivatives

In order to develop a potent inhibitor of the α-SNAP/NSF mediated disassembly of SNARE complexes, it is crucial to identify the most relevant interactions of α-SNAP and NSF to the core complex. Therefore, Synaptobrevin, one of the SNARE proteins, was chosen to be the scaffold for synthesizing model systems with solid phase peptide synthesis (SPPS) and to incorporate several mutations at distinct positions in order to prevent the interaction of α-SNAP with the assembled SNARE complex, and hence, the disassembly.

It is known that α-SNAP, the cofactor of NSF, binds in the middle of the complex around the '0'-layer. MARZ *et al*. identified residues in α-SNAP that interact with the SNARE complex using site directed mutagenesis.[12] During their investigation it appeared that especially mutations in charged residues show binding effects to the SNARE complex, and therefore, to its disassembly. It is clear that more than one and likely three α-SNAPs are bound to the complex. This is in agreement with early evaluations of the stoichiometry[60] and with calibrated scanning transmission electron microscopy analysis of the 20 S complex.[186]

α-SNAP binds to the SNARE complex likely via its nine *N*-terminal α-helices which are in an antiparallel orientation (Figure 22 A). The helices form a twisted sheet providing a concave and a convex surface and might be good interaction partners

for the SNARE complex. The concave site, located in front of the SNARE complex site, has a complementary conformation to the mostly acidic convex site of the SNARE complex.[12] Based on the same slightly twisted shape of the SNARE complex conserved residues therein define the assumed three potential binding sites for α-SNAP (see one of these in Figure 22 B). To develop probable interaction partners in the α-SNAP/SNARE complex charge-charge interactions between the two systems were analyzed. MARZ *et al*. identified critical binding partners in α-SNAP.[12] The majorities of them are lysines that form salt bridges in a diagonal band across the concave site of the α-SNAP twisted sheet domain (Figure 22 B). A similar twisted area of complementary acidic residues is located on the SNARE complex surface, defining three potential binding sites, which lead to the assumption that three α-SNAP proteins are necessary for disassembly. Mutation of any of these lysines in α-SNAP significantly decreases the SNARE complex binding. As mentioned before, due to binding of the α-SNAP in the middle of the SNARE complex, surrounding the ionic '0'-layer, it is not surprising that a number of α-SNAP mutations influence the binding stability, and therefore, the disassembly lying around this layer. In Synaptobrevin the three residues Asp-51, Glu-55 and Asp-65 were identified to define potential binding residues with α-SNAP (Figure 22 B).

Regarding these interactions, synthetic Synaptobrevin derivatives that are still perfectly capable of forming SNARE complexes while being modified to prevent α-SNAP/SNARE complex recognition will be selected.

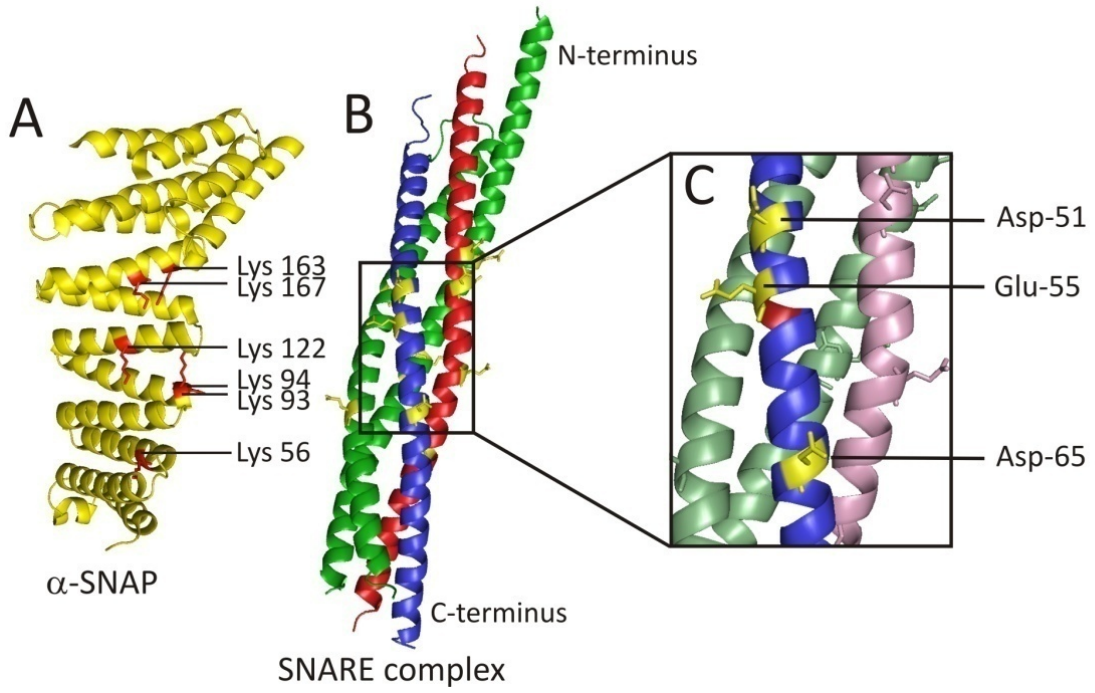

Figure 22. *Crystal structure of the α-SNAP binding site to the SNARE complex.* ***A*** *Ribbon diagram of α-SNAP showing lysine residues (red) whose mutation reduces SNARE complex binding.[12] (Pdb code 1QQE)* ***B*** *Conserved acidic residues (yellow) on the SNARE complex (blue - Synaptobrevin, red - Syntaxin, green - SNAP-25) were identified to form salt bridges with the lysines from α-SNAP.[12] (pdb code 1KIL)* ***C*** *Detailed view of the interacting residues of Synaptobrevin Asp-51, Glu-55 and Asp-65. The '0'-layer is marked in red.*

Firstly, the three residues Asp-51, Glu-55 and Asp-65, identified from Marz *et al.*,[12] which interact with the lysines in α-SNAP are selected by replacing with native amino acids such as lysines for changing the charge surface, and therefore, substituting favorable salt-bridges by repulsive charge-charge interactions. On the other hand, synthetic amino acid building blocks with bulky side chain residues, such as adamantane, should be introduced to prevent α-SNAP binding cause of steric hindrance. With respect to the '0'-layer (residue 56) further possible suitable amino acids (residues 57, 58 and 62) were functionalized. These residues are located close to the '0'-layer with the side chains outside of the complex towards α-SNAP, and hence, probably interfering α-SNAP recognition. Thus, three additional compounds were selected for synthesis (Figure 23).

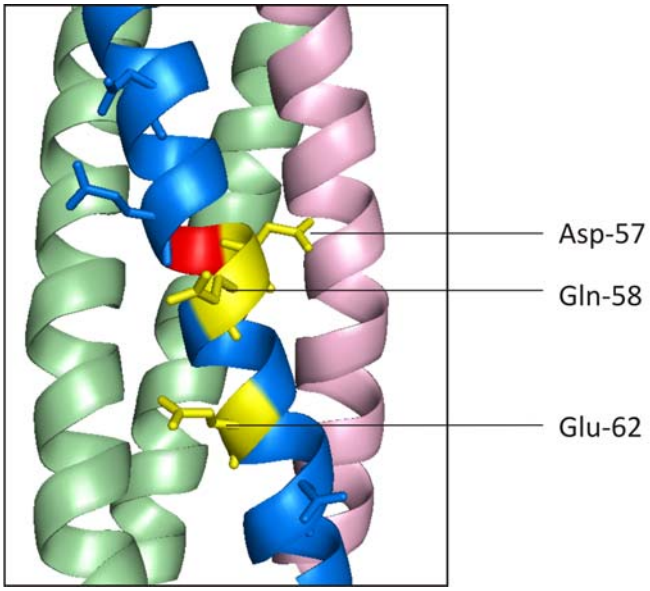

Figure 23. *Further residues (yellow), replaced with a non-natural amino acid building block for preventing disassembly on the SNARE complex (blue-Synaptobrevin, light red-Syntaxin, green-SNAP-25). The '0'-layer is marked in red.*

Secondly, almost the whole SNARE motif (aa 32-84) has to be synthesized to assure that the derivatives can recognize the other natural SNARE protein counterparts to form the SNARE complex. This includes all layers (-7 to +8). The proline rich *N*-terminal region is not necessary for SNARE complex assembly, just like the transmembrane domain and the linker in-between. Figure 24 shows the sequence of the SNARE motif of the *wild type* of neuronal Synaptobrevin (**8**).[51] Amino acids, chosen for replacement by other residues or building blocks are marked in bold.

SNRRLQQTQAQVDEVVD*IMR*VNV**D**KVL**E**R**DQ**KLS**E**LD**D**RADALQAGASQFETSAAKL **8**
28 32 40 51 55 57 58 62 65 70 80 84

Figure 24. *Sequence of the wild type Synaptobrevin motif (**8**).[51] The '0'-layer is marked in red. Residues selected for exchange are shown in bold.*

3.1.1 Synthetic Synaptobrevin Model Systems

In order to clearly distinguish between important side chain interactions of the individual residues Asp-51, Glu-55 and Asp-65 or to investigate if a cooperation of all of these three residues prevents α-SNAP binding, a series of constructs was prepared (Table 1). Firstly, the three conserved acidic residues are replaced by lysines (derivative **9**). As control of potentially different assembly properties between the expressed and the synthesized Synaptobrevin derivative the original sequence of the SNARE motif was additionally synthesized (derivative **10**) (Figure 25). Due to better complex assembly derivatives **8** and **11** with elongated sequences were also synthesized (Figure 26). The notation of the individual residues is retained avoiding confusions with previous explanations.

LQQTQAQVDEVVD*IMR*VNV**K**KVL**K**RDQKLSELD**K**RADALQAGASQFETSAAKL **9**
32 40 51 55 57 58 62 65 70 80 84

LQQTQAQVDEVVD*IMR*VNVDKVLERDQKLSELDDRADALQAGASQFETSAAKL **10**
32 40 51 55 57 58 62 65 70 80 84

Figure 25. *Sequence of Synaptobrevin derivatives **7** and **8**.[51] The '0'-layer is marked in red. Conserved acidic residues, identified to interact with α-SNAP,[12] selected for mutation with lysines in derivative **7** are shown in bold. Derivative **8** shows the synthesized original sequence of the Synaptobrevin SNARE motif.*

Further derivatives were synthesized each with a various number of introduced synthetic adamantyl amino acid building block **12**. A bulky adamantyl building block is attached at the side chain of Fmoc-Asp-O*t*Bu. The obtained Fmoc-Asp(Adam)-OH (**12**) is termed with the abbreviation 'Adam' (Figure 26).

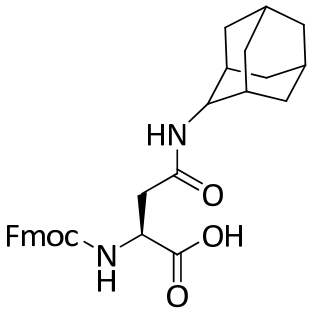

12

Figure 26. *Non-natural Fmoc-amino acid building block **12** ('Adam').*

The conserved acidic residues Asp-51, Glu-55 and Asp-65 were replaced by building block **12**. Thus, initially one of the residues each was planned for exchange obtaining derivatives **13**-**15**. Additionally, derivatives **16**-**18** with two

replaced residues at positions 51 and 55, 55 and 65 or 51 and 65, respectively, were selected to perform in order to probably identify one of the α-SNAP interaction sites to the SNARE complex capable for disassembly inhibition. Especially derivatives **17** and **18**, with exchanged Asp-51 or Asp-55, respectively, and Asp-65 address two sites of the SNARE complex regarding α-SNAP recognition, appeared as interesting constructs.[12] Furthermore, construct **19** with three introduced 'Adam'-building blocks was synthesized to provide interruption of α-SNAP binding site 1 at positions 51 and 55 of Synaptobrevin, and in addition, of site 2 at position 65.[12]

However, three more derivatives (**20**-**22**) were synthesized, each containing a single synthetic adamantane building block. For this, different residues (Asp-57, Gln-58 and Glu-62) which are located near the '0'-layer in *C*-terminal direction were exchanged. The residues were chosen with respect of their side chain direction towards α-SNAP. As control experiment of the influence of a charged or non-charged *N*-terminus the peptide **22** was acylated prior to SPPS-cleavage to obtain construct **23**.

Table 1 shows a summary of the synthesized derivatives.

No.	Sequence
9	H-[aa 32-49]-V**K**KVL**K**RDQKLSELD**K**RADAL-[71-84]-NH_2
10	H-[aa 32-49]-VDKVLERDQKLSELDDRADAL-[71-84]-NH_2
11	H-[aa 28-49]-V**K**KVL**K**RDQKLSELD**K**RADAL-[71-84]-OH
8	H-[aa 28-49]-VDKVLERDQKLSELDDRADAL-[71-84]-OH
13	H-[aa 28-49]-V**D(Adam)**KVLERDQKLSELDDRADAL-[71-84]-OH
14	H-[aa 28-49]-VDKVL**D(Adam)**RDQKLSELDDRADAL-[71-84]-OH
15	H-[aa 28-49]-VDKVLERDQKLSELD**D(Adam)**RADAL-[71-84]-OH
16	H-[aa 28-49]-V**D(Adam)**KVL**D(Adam)**RDQKLSELDDRADAL-[71-84]-OH
17	H-[aa 28-49]-VDKVL**D(Adam)**RDQKLSELD**D(Adam)**RADAL-[71-84]-OH
18	H-[aa 28-49]-V**D(Adam)**KVLERDQKLSELD**D(Adam)**RADAL-[71-84]-OH
19	H-[aa 28-49]-V**D(Adam)**KVL**D(Adam)**RDQKLSELD**D(Adam)**RADAL-[71-84]-OH
20	H-[aa 28-49]-VDKVLERD**D(Adam)**KLSELDDRADAL-[71-84]-OH
21	H-[aa 28-49]-VDKVLERDQKLS**D(Adam)**LDDRADAL-[71-84]-OH
22	H-[aa 28-49]-VDKVLER**D(Adam)**QKLSELDDRADAL-[71-84]-NH_2
23	Ac-[aa 28-49]-VDKVLER**D(Adam)**QKLSELDDRADAL-[71-84]-NH_2

Table 1. *Peptide constructs **8**-**11** and **13**-**23** synthesized for use in assembly and disassembly studies.*

3.2 Synthesis of the Synaptobrevin Constructs

The derivatives **8**-**11** and **13**-**23** of the SNARE motif of Synaptobrevin were synthesized at preloaded Wang resin and NovaSyn® TGR resin using Fmoc-solid phase peptide synthesis (SPPS) and standard Fmoc-amino acid building blocks with their acid labile side chain protecting groups as well as coupling reagents such as HOBt (4.00 eq), HBTU (3.90 eq) and DIEA (5.00 eq).

3.2.1 Synthesis of Synaptobrevin Derivatives with Lysine Mutations

Initially, the construct **9** (aa 32-84) with lysines instead of aspartate and glutamate at positions 51, 55 and 65 and derivative **10**, the original sequence (aa 32-84), were synthesized using the automated *ABI 221* peptide synthesizer and a NovaSyn® TGR resin which was manually preloaded with Fmoc-Leu-OH (Figure 25).

As derivatives **9** and **10** were found to be uncapable of complex formation (see complex assembly studies in chapter 4.3.1), constructs with an elongated SNARE motif (residues 28-84) were synthesized (derivatives **8** and **11**), apparently more suited for forming SNARE complexes with the *wild type* of Syntaxin and SNAP-25. It is crucial to use low loaded resins for peptide synthesis, therefore, instead of initially applied NovaSyn® TGR resin it was switched to Wang resin with low loading, and hence, the peptide synthesis was successful. During SPPS test cleavages were carried out routinely after every tenth amino acid in order to identify difficult sequences of the final 56 residues long peptides. Synthetic problems during SPPS appeared especially at Ile-46, Met-47 and Arg-48 and at the four last amino acids (28-32) at the end of the synthesis (Figure 27, marked in italic).

*SNRR*LQQTQAQVDEVVD*IMR*VNV**K**KVL**K**RDQKLSELD**K**RADALQAGASQFETSAAKL **11**
28 32 40 51 55 57 58 62 65 70 80 84

Figure 27. *Sequence of the derivative **11** bearing lysines at positions 51, 55 and 65.[51] The '0'-layer is marked in red. Conserved acidic residues, identified to interact with α-SNAP,[12] selected for mutation are shown in bold and amino acids detected to be difficult in Fmoc-SPPS are indicated in italic.*

The *N*-terminal part of the sequence is probably highly coiled, thus, coupling and deprotection time increases markedly. These problems were solved by employing the elongation of the coupling time, double coupling and a large excess of amino acid building blocks.

3.2.2 Synthesis of Synaptobrevin Derivatives with Adamantyl Building Block

*Synthesis of the Adamantyl Building Block **12***

In order to develop amino acid building blocks suitable to prevent α-SNAP binding to the SNARE complex adamantane derivatives appear as applicable candidates for incorporation as side chain in common amino acids. Adamantane is a cycloalkane consisting of three condensed cyclohexanes, therefore, it is very rigid and unflexible. Furthermore, a short and efficient synthetic route with reasonable coupling behavior is required. Therefore, it was decided to synthesize building block **12** as described in Scheme 1.

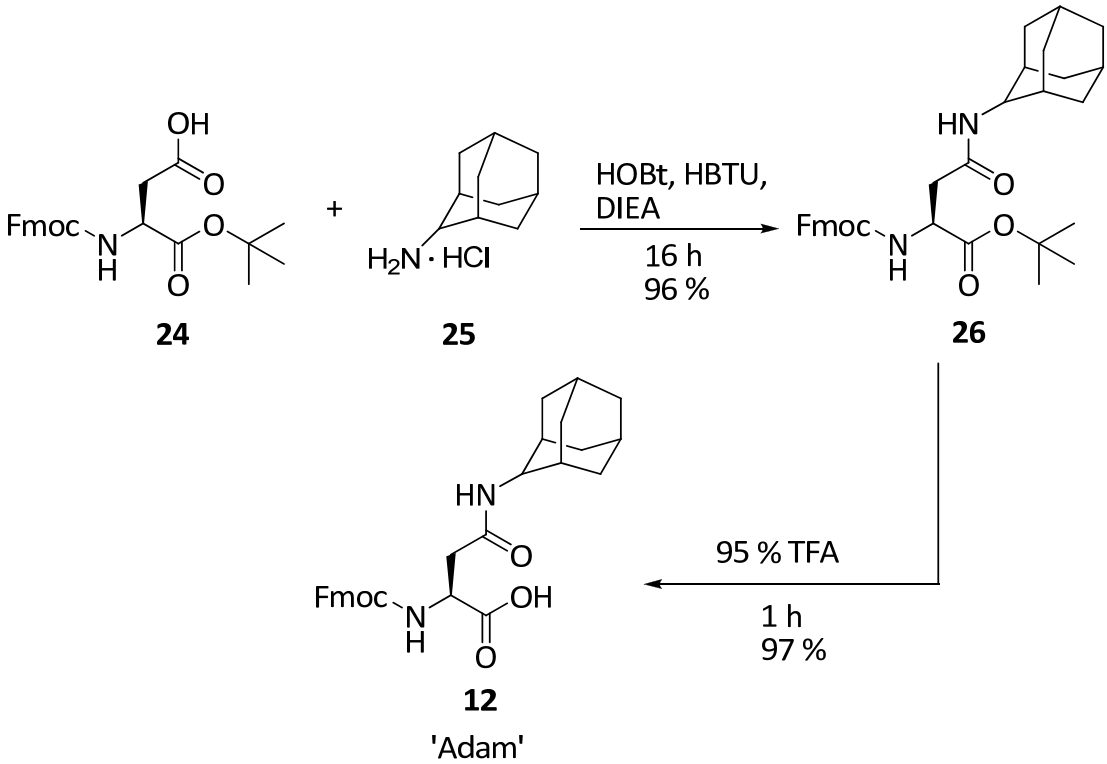

Scheme 1. *Synthesis of the Fmoc-amino acid building block **12**.*

Based on Fmoc-Asp-O*t*Bu (**24**) the required amino acid building block **12** bearing an adamantyl side chain was prepared using HOBt (1.50 eq), HBTU (1.50 eq) and DIEA (2.00 eq) in DMF, followed by treatment with 95 % TFA (Scheme 1). Fmoc-Asp(Adam)-OH (**12**) was obtained in two steps in good yields.

Synthesis of the Synaptobrevin Derivatives

According to the synthesis of derivatives **9-11**, constructs **13**-**23** were synthesized via SPPS. The peptides **13**-**21** were partially synthesized using the microwave assisted automated *Liberty®* peptide synthesizer from *CEM*. For derivative **27** (66-84) the synthesis was run on a 0.1 mmol scale with 5-fold excess of Fmoc-protected amino acids and a single 5 min coupling time (Figure 28). Afterwards, the resin was subdivided in 12.5 µmol scales. Remaining amino acids (28-65) were coupled manually. For avoiding previous coupling problems double coupling (45 min) was performed for arginine (8 eq), lysine, isoleucine, methionine, building block **12** (8 eq) and for the last 10 residues. Single coupling (1 h) was carried out for all remaining amino acids. Free *N*-termini were capped after each coupling step. Deprotection time was elongated to 15 min and was carried out twice. Constructs **22** and **23** were automatically synthesized using the *ABI 221* peptide synthesizer, only interrupted for manual coupling of Fmoc-Asp(Adam)-OH (**12**). After cleavage (TFA/H_2O/EDT/TES 94:2.5:2.5:1, 2 h) all derivatives were purified by HPLC. Due to numerous truncated sequences within the synthesis threefold purification was required.

RADALQAGASQFETSAAKL **27**
66 70 80 84

Figure 28. *Synthesized construct **27** (aa 66-84).*

Structural Investigation of the Synaptobrevin Derivatives

Unassembled SNARE proteins are usually unstructured.[40,187,188] α-Helices are formed upon SNARE complex assembly. CD spectroscopy is a convenient method for investigating structural changes of proteins, so, all synthesized Synaptobrevin derivatives **11** and **13**-**21** were analyzed regarding secondary structures. As expected, no characteristic minima at 215 and 222 nm indicating the formation of an α-helix were monitored. The CD spectra showed disordered structures of the Synaptobrevin derivatives (see Appendix).

3.3 Investigation of SNARE Complex Assembly and Disassembly Properties

In order to investigate the disassembly reaction it is necessary to assemble the species **8**-**11** and **13**-**23** into SNARE complexes with their natural counterparts Syntaxin 1A and SNAP-25. As the *N*-terminal autonomously folded region of Syntaxin 1A is not part of the core SNARE complex, a construct bearing only the SNARE motif (also referred to as the H3-domain) of Syntaxin was used for the studies. Due to availability, Syntaxin was used either with or without TMD. No difference in the quality of complex assembling was observed. For disassembly experiments the $H_AH_BH_C$ domain and the transmembrane domain of Syntaxin is also not required.[189]

3.3.1 Investigation of SNARE Complex Assembly

The assembly assay was carried out combining the accordant Synaptobrevin derivative with Syntaxin 1A and SNAP-25 in a 2:1:1 ratio, followed by incubation overnight at 4 °C.[189] Successful complex assembly was monitored using SDS (sodium dodecyl sulfate) gel electrophoresis, exploiting the fact that the ternary core complex is stable in SDS buffer, unless heated.[37]

In a first experiment, construct **11** with exchanged lysines, the synthesized original sequence **8** and the expressed *wild type* (**wt**) were analyzed regarding SNARE complex assembly. Figure 29 shows a 12 % SDS gel after coomassie staining. For the SNARE complex assembly with the *wild type* (lane 4) a band was observed at 52 kDa, whereas derivative **11** (lane 1 and 2) shows no band. In contrast, construct **8**, assembles with the other SNARE proteins (lane 3).

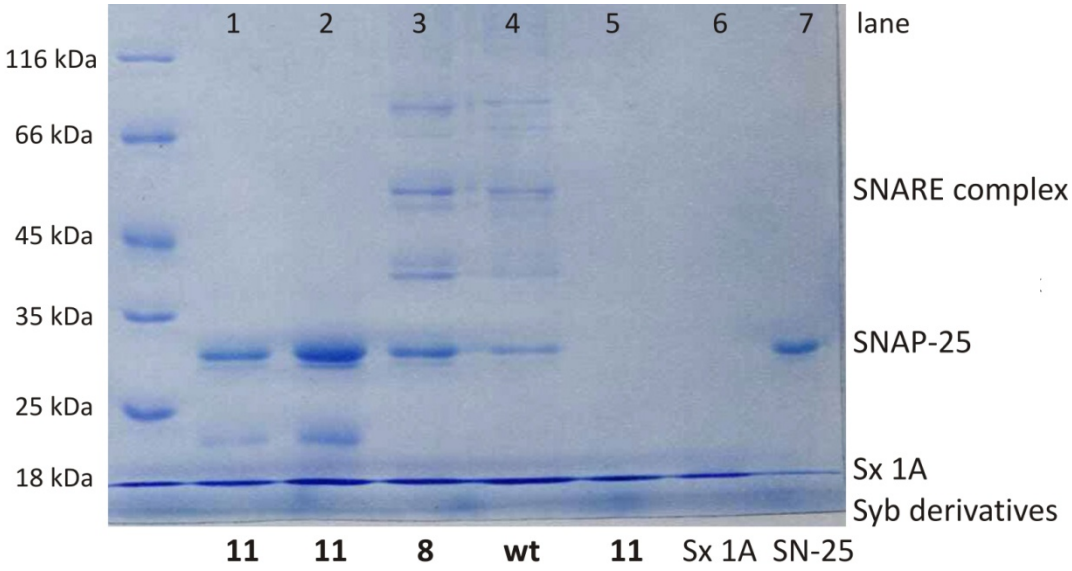

Figure 29. *Analysis of SNARE complex assembly. Derivative **11** with lysine mutations (lanes 1 and 2), the chemical synthesized original sequence **8** (lane 3) and the expressed wild type (**wt**, lane 4) were incubated with their native counterparts (Syntaxin with TMD) and monitored by SDS PAGE. Lanes 5-7 show the individual SNARE proteins.*

It could be concluded that the charge alternation of the natural sequence has a negative impact regarding SNARE complex assembly. Assumptions regarding charge-charge repulsion with the neighboring residues (arginines and lysine) followed by conformational influence on the helix as well as a changed overall charge of the protein might be responsible for hindered complex formation and explain the observations.

In a second set of experiments, all constructs containing various numbers of adamantyl-building blocks were tested regarding their ability to assemble with natural Syntaxin and SNAP-25 (Figure 30). In lane 1 the *wild type* of Synaptobrevin is shown again, whereas lanes 2-10 displayed the derivatives **13**-**21**. Derivative **13, 14** and **15** (lanes 8-10) with only one adamantyl-building block in positions 51, 55 or 62 and the derivatives **16**, **17** and **18** (lanes 5-7) with two building blocks at positions 51 and 55 (**16**), 55 and 65 (**17**) and at positions 51 and 65 (**18**) show significant SNARE complex assembly. Considerable lower amounts of SNARE complexation was monitored for construct **19** (lane 4) containing three building blocks at all of these positions. Derivatives **20** and **21** were also capable of forming SNARE complexes (Figure 30). The bands above the SNARE complex can be explained by formation of higher-ordered oligomers possibly resulting from crosslinking by the SNAP-25 linker domain.[110]

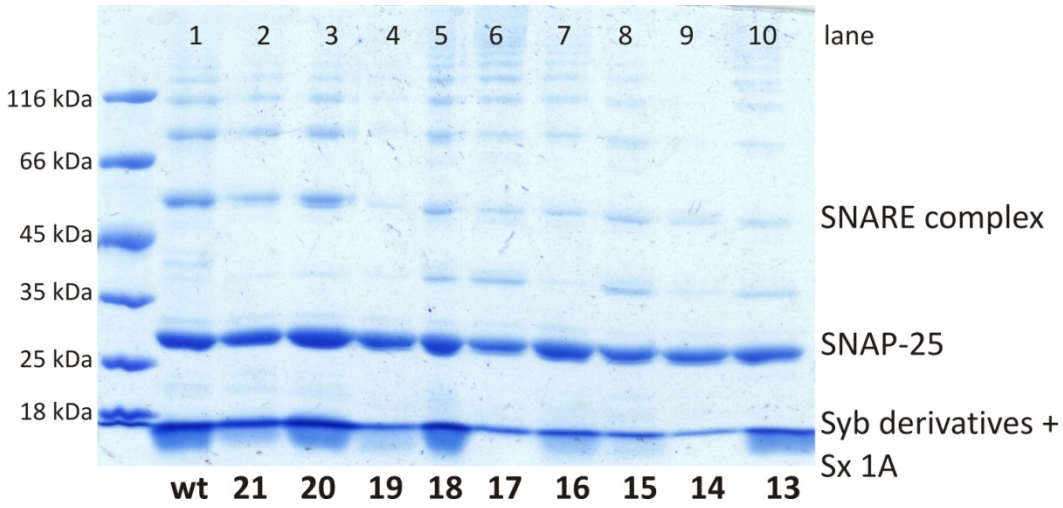

Figure 30. *Assay of the SNARE complex assembly. Synaptobrevin derivatives* ***13-21*** *and wild type (**wt**) were incubated with Syntaxin 1A (with TMD) and SNAP-25 (2:1:1 ratio) overnight at 4 °C.*[189] *Derivatives* ***18, 20*** *and* ***21*** *show the best assembling properties. Complex assembly was monitored via a 12 % SDS gel.*[190]

As already shown, Synaptobrevin constructs containing the whole SNARE motif (residues 28-84, derivatives **8** and **13**-**21**) were able to form complexes with native Syntaxin and SNAP-25. Figure 31 shows the comparison of the complex assembly with the shorter Synaptobrevin derivatives **9** and **10** (aa 32-84). Syntaxin 1A lacks the transmembrane domain (except lane 5), which apparently has no influence on complex assembly. In lanes 1 and 2 complex assembly with constructs **wt** and **22** were indicated. They are able to form complexes, whereas for constructs **9** and **10** only minimal amounts of SNARE complexation (lane 3 and 4) was detected. Lane 5 showed complex assembly of Synaptobrevin derivative **23**, SNAP-25 and Syntaxin 1A (containing an intact transmembrane domain) (Figure 31).

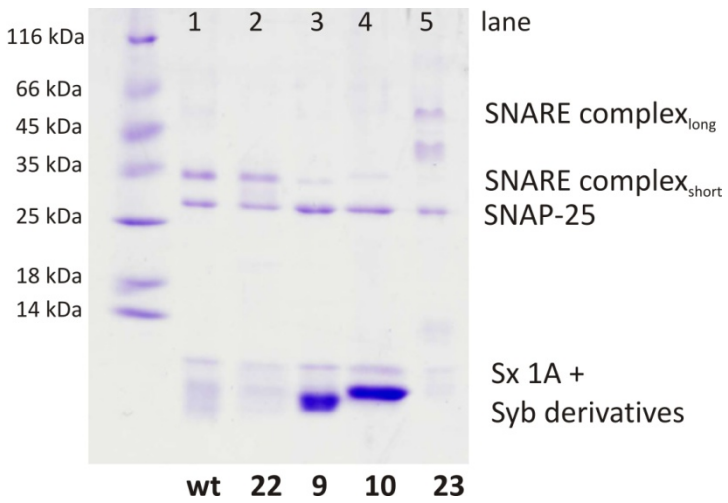

Figure 31. *Assay of the SNARE complex assembly with 'short' Synaptobrevin derivatives **7** and **8** (aa 32-84) or 'long' constructs **wt** and **24** (aa 28-84), Syntaxin 1A (without TMD, lanes 1-4) and SNAP-25 (ratio Syb:Sx:SNAP-25 2:1:1). Incubation was carried out overnight at 4 °C. **Wt** and **20** (lanes 1 and 2) inidicated successful complex formation whereas the shorter constructs **7** and **8** are not able to assemble with their native counterparts. Lane 5 shows complex assembly with Synaptobrevin construct **21**, 'long' Syntaxin 1A (with TMD) and SNAP-25 as control.*

Only the derivatives **8** and **13**-**23**, containing the full length of the SNARE motif of Synaptobrevin, were able to form SNARE complexes with their natural counterparts. Derivatives **9** and **10** lacking the first four residues indicated no SNARE complex assembly, probably due to recognition mismatches. Except derivative **11** and derivative **19** containing three mutated lysines or non-natural adamantyl building blocks, respectively, all synthesized derivatives (**8**, **13**-**18** and **20**-**23**) showed significant complexation with Syntaxin and SNAP-25 to the core complex. Interestingly, the amount of complex assembly varied for the derivatives **11**-**13**, **18** and **19** containing only one adamantyl building block. The derivatives **13**-**15** with the replaced conserved acidic residues at positions 51, 55 and 65, identified from Marz *et al*. showed lower SNARE complex assembly than the other derivatives **20** and **21**, lying close to the '0'-layer, at positions 58 and 62. This indicates a possible interaction of these conserved amino acids within the individual layer. Incorporation of a second adamantyl building block into the sequence showed no difference in the amount of SNARE complex assembly. Replacement of three residues in the Synaptobrevin SNARE motif seemed to interfere structurally and probably due to charge characteristics of the helix preventing SNARE complex assembly.

3.3.2 Investigation of SNARE Complex Disassembly Properties

The assembled SNARE complexes were subjected to a disassembly protocol in order to investigate the influence of the chemical modifications.[189] Derivatives **wt**, **14**, **15** and **18** were analyzed by time-dependent disassembly. Firstly, incubation of the *wild type* SNARE core complex with NSF and α-SNAP under disassembly conditions prior to gel electrophoresis led to a loss of intensity of the complex band after 10 min. The reaction was carried out in a HEPES/KGlu/KAc buffer (pH = 7.4). The assembled SNARE complex was incubated with α-SNAP at 4 °C for 30 min.[191] Afterwards, NSF, $MgCl_2$ and ATP were added and the reaction mixture was allowed to react for 0, 5, 10, 15, 30 and 60 min at 37 °C. The reaction was stopped each by adding SDS sample buffer. As control of the preceding disassembly reaction, lane 1 shows only the SNARE complex, without α-SNAP and NSF. Lanes 2-7 demonstrate the disassembly reaction (Figure 32). The *wild type* SNARE complex is disassembled after 10 min. The last two lanes are control experiments. EDTA for Mg^{2+}-complexation was added, therefore, the disassembly reaction was inhibited (lane 8). The last sample was heated to 95 °C for 5 min to completely dissociate all complexes into their individual components.

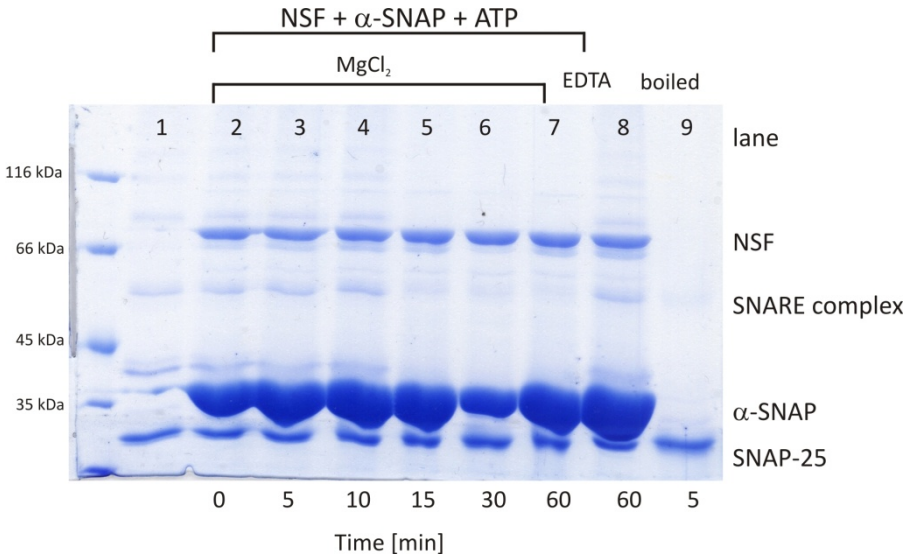

Figure 32. *NSF and α-SNAP dependent wild type (**wt**) SNARE complex disassembly. The reaction was monitored on a SDS gel. The complex, assembled with the wild type Synaptobrevin, was incubated with 5 mM $MgCl_2$, 5 mM ATP, 1 µM NSF and a 14 fold-excess of α-SNAP at 37 °C. The disassembly reaction was monitored time-dependently (lanes 2-7). As comparison the first lane shows only the assembled SNARE complex without NSF and α-SNAP, lane 9 shows the reaction with EDTA instead of $MgCl_2$ (negative control) and lane 10 shows the sample heated to 95 °C for 5 min for a completed disassembly of the complex.*

The disassembly reactions of the synthesized compounds **16**, **17** and **20** showed different results. The most pronounced effect of disassembly inhibition was observed for construct **20**, the derivative with one adamantyl-building block at position 58, which is two amino acids next to the '0'-layer in *C*-terminal direction. A decrease of reaction velocity is monitored. After 15 min the SNARE complex concentration decreases, but it is not completely disassembled (Figure 33, lane 2-7). Lanes 1, 8 and 9 displayed the comparison samples as indicated before.

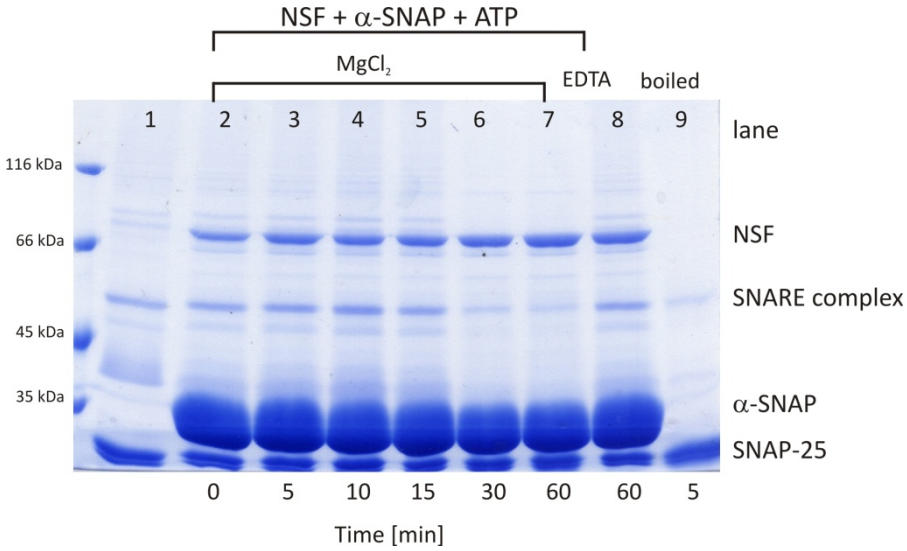

Figure 33. *NSF and α-SNAP dependent SNARE complex disassembly with construct* ***20****. The reaction was monitored on a SDS gel. The progress of the disassembly reaction was time-dependently controlled (lanes 2-7). As comparison the first lane showed only the assembled SNARE complex without NSF and α-SNAP, lane 9 demonstrated the reaction with EDTA instead of* $MgCl_2$ *(negative control) and lane 10 displayed the sample heated to 95 °C for 5 min for completed disassembly of the complex.*

The SNARE complexes associated with compounds **16** and **17** are more readily disassembled. The one including the Synaptobrevin derivative **16** is disassembled after 10 min (Figure 34 A). In the case of derivative **17** the individual SNARE proteins are recovered after 15 min (Figure 34 B). Both comprise two adamantyl-building blocks at positions 51 and 55 (derivative **16**) and at positions 55 and 65 (derivative **17**).

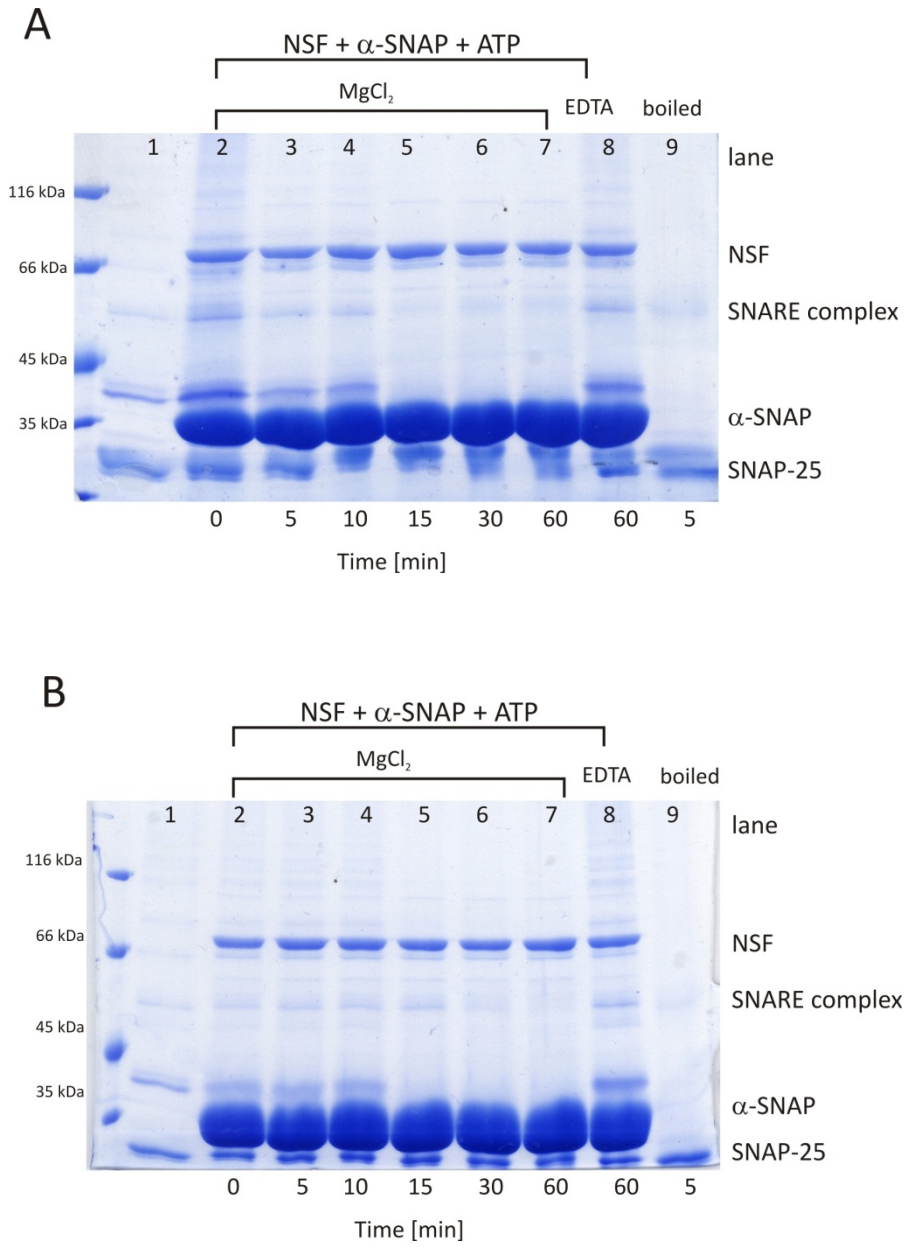

Figure 34. *NSF and α-SNAP dependent SNARE complex disassembly with constructs **16** (**A**) and **17** (**B**). The reaction was monitored on a SDS gel. The complex assembled with Synaptobrevin derivatives **16** and **17** was incubated with 5 mM $MgCl_2$, 5 mM ATP, 1 µM NSF and a 14-fold excess of α-SNAP at 37 °C. The disassembly reaction was time-dependently monitored (lanes 2-7). As comparison the first lane showed only the assembled SNARE complex without NSF and α-SNAP, lane 9 demonstrated the reaction with EDTA instead of $MgCl_2$ (negative control) and lane 10 displayed the sample heated to 95 °C for 5 min for completed disassembly of the complex.*

Figure 35 showed a detailed view of the important bands for better evaluation of the time-dependent disassembly assay between the derivatives **wt**, **16**, **17** and **20** (Table 2). Firstly, lane 1 shows complex formation of the **wt** and the derivatives **16**, **17** and **20** with Syntaxin and SNAP-25 compared to the other lines. Lanes 2-7

illustrated time-dependent disassembly. Comparison of the several gels clearly indicated an assembled SNARE complex with construct **20** after 15 min, when the *wild type* (**wt**) and complex **16** were already dissociated. In this case, a light band was still observed. The complex, assembled with derivative **17** seemed to have a longer stability than the *wild type*, but complex formation was relatively poor.

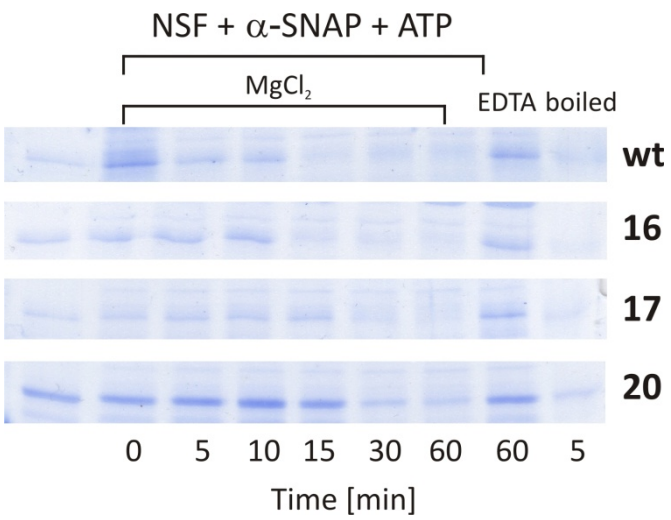

Figure 35. *Detailed view of the important bands from the time-dependent disassembly assays described before (Figures 32-34).*

No.	Sequence
wt	H-[aa 30-49]-VDKVLERDQKLSELDDRADAL-[71-84]-OH
16	H-[aa 28-49]-V**D(Adam)**KVL**D(Adam)**RDQKLSELDDRADAL-[71-84]-OH
17	H-[aa 28-49]-VDKVL**D(Adam)**RDQKLSELD**D(Adam)**RADAL-[71-84]-OH
20	H-[aa 28-49]-VDKVLERD**D(Adam)**KLSELDDRADAL-[71-84]-OH

Table 2. *Wild type Synaptobrevin (**wt**) and synthesized peptide constructs (**16, 17** and **20**) investigated in disassembly studies.*

With derivative **20** a potent inhibitor of the α-SNAP recognition to the SNARE complex was synthesized. By preventing α-SNAP binding to the SNARE complex NSF was not capable to regenerate the individual SNARE proteins. Building block **12** was incorporated at residue 58, located two amino acids next to the '0'-layer in the *C*-terminal direction. The side chain is directed outside the SNARE complex towards the α-SNAP, though, it was not part of the derivative series (**13**-**19**) designed regarding the conserved acidic residues, identified by MARZ *et al.*[12] With derivative **20** associated in the SNARE complex, probably differentiation between the three SNARE/SNAP interaction sites is possible. As described before,

the assembled SNARE complex defined three potential binding sites for α-SNAPs but it is not clear if one of these sites is more preferable than the others. The adamantyl building block **12** introduced at position 58 addressed only one α-SNAP recognition site and was capable of decreasing the disassembly reaction.

Both derivatives **16** and **17**, each containing two adamantyl building blocks, were uncapable of preventing α-SNAP recognition, and therefore, complex disassembly. One of the adamantyl building blocks in derivative **17** was incorporated at position 55, one residue next to the '0'-layer in the *N*-terminal direction. SNARE complex formation as well as disassembly containing this derivative **17** did not seem to be bothered from this mutation. Additionally, this derivative addressed two putative binding sites for α-SNAP within the SNARE complex, and therefore, probably two α-SNAP molecules.

Thus, it is necessary to investigate the other two SNARE proteins, too. SNARE protein derivatives, derived from both, Syntaxin and SNAP-25 should answer the question if one of the individual proteins have more influence than the other two or if they all were needed for interaction with α-SNAP. Investigation from the α-SNAP-side was done by MARZ *et al*. by mutation of various basic and acidic residues, identifying important interaction partners.[12] A second approach might be exchanging of the adamantyl residue optionally by fluorophor dyes to investigate direct interactions by FRET measurements.

Quantifying the efficiency of assembly and disassembly monitoring with different fluorescence spectroscopy methods like FRET spectroscopy and fluorescence anisotropy is important. Then, evaluation of the inhibition ability of the individual Synaptobrevin constructs which are identified to decelerate the disassembly reaction is more precise. Therefore, fluorescence labeled derivatives are required. The SNARE motif of *wild type* Synaptobrevin as well as its derivatives contains no cysteines, so it is not possible to label them afterwards using common maleimide chemistry. Attachment of succinimidyl ester-conjugated dyes requires orthogonal side chain protection groups at lysines or resin bound peptides.

3.4 Conclusion

The aim of this study was to synthesize SNARE protein constructs which are able to inhibit the α-SNAP/NSF mediated disassembly process. The SNARE motif of Synaptobrevin was chosen as model system since its recognition is essential for the interaction with α-SNAP. Several derivatives were synthesized, either containing various mutations according conserved acidic residues, known to affect the α-SNAP binding or involve a non-natural building block near the '0'-layer. Mutation of the '0'-layer prevents SNARE complex assembly, therefore, this residue was not exchanged.

Synaptobrevin constructs **9** and **10** lacking the first four amino acids at the *N*-terminal end of the SNARE motif (32-84) were uncapable of forming SNARE complexes with the expressed *wild types* Syntaxin and SNAP-25. Elongated derivatives (except construct **19**, containing three adamantyl building blocks) were able to form SNARE complexes with their natural counterparts. Disassembly studies carried out with freshly expressed NSF from the JAHN laboratory indicated derivative **20** as the scaffold for developing a potent inhibitor of the α-SNAP/NSF mediated disassembly. The assembled SNARE complex has three binding sites for α-SNAP. In Figure 36 A the binding sites were illustrated. The identified conserved residues within the individual SNARE proteins were color-coded regarding the corresponding binding α-SNAP (Figure 36 B). An axial view through the '0'-layer (black) of the SNARE complex is shown in Figure 36 C. So far, it is unclear if one of these sites is preferable. With the synthesis of derivative **20** a possible model system for differentiation between these sites was developed. As each α-SNAP interacts with three SNAREs might explain why no complete inhibition was observed. The binding of α-SNAP to the remaining two SNARE proteins Syntaxin and SNAP-25 might be sufficient for disassembly, even if the reaction is slower than for the *wild type* SNARE complex.

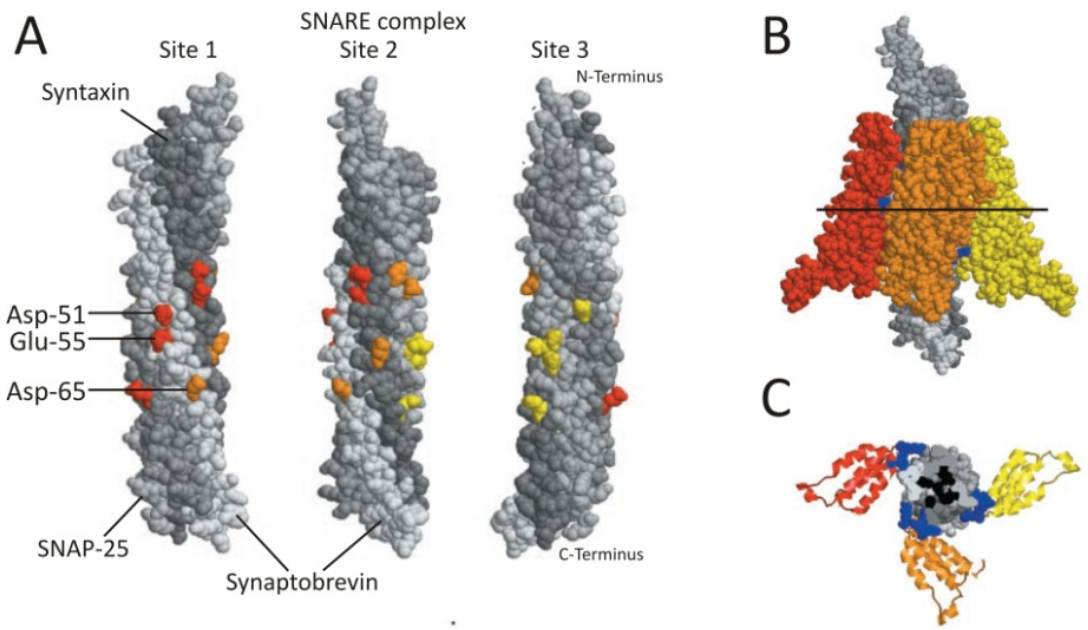

Figure 36. A *Ribbon diagram of the SNARE complex, showing the three supposed binding sites for α-SNAP. The residues were color-coded regarding the corresponding α-SNAP.* ***B*** *Model of the SNARE complex surrounded by three α-SNAPs.* ***C*** *Axial view of the SNARE complex through the '0'-layer (black), basic residues in α-SNAPs, identified to reduce the SNARE complex/α-SNAP recognition are coloured blue. Figure modified from MARZ et al.*[12]

Chapter 4

Design and Synthesis of Peptide Mimics of Complexin

Complexins, small (15-16 kDa), highly charged proteins were known to regulate fusion processes.[13,192-194] They tightly bind to the assembled SNARE complex around the ionic '0'-layer in an antiparallel manner, but not to individual SNARE proteins,[13,14,195] except to the binary complexes like Syntaxin and SNAP-25.[196] Complexin is composed of four domains. The *N*-terminal domain is unstructured (residues 1-26) followed by an accessory helix (aa 29-47) which adopts an α-helical conformation without any binding sites to the SNARE complex.[8,195] The central helical region interacting with the Synaptobrevin and Syntaxin helices of the SNARE complex includes residues 48-70. The *C*-terminal end is also unstructured.[14,120] Initially, Complexins were reported to displace α-SNAP from the SNARE complex when added in excessive amounts, and therefore, have inhibitory properties regarding the disassembly mechanism, but further investigations using knock-out mice[108,109,197] and overexpression assays[117,198] give contradictory results. All these biochemical studies *in vitro* and *in vivo* observed negative impact of exocytosis, even if Complexin lacks or is abundant. Other studies monitored no difference in disassembly inhibition at all, even with or without Complexin, except when very low amounts of α-SNAP were used.[189] This leads to new discussions about the function of Complexin. Several studies identified Complexins acting as so-called fusion clamps binding to the partially zippered *trans*-state in the preliminary fusion state. They might stabilize the transition state, recruiting Synaptotagmin 1, and mediate fast synaptic vesicle exocytosis upon calcium triggering.[54,108,122,199] Concluding these findings, it has been shown that simultaneous binding of Complexin and Synaptotagmin does not

occur.[200] Therefore, the molecular function of Complexins remains unclear to date.[201]

4.1 Complexin as a β-Peptide

4.1.1 Design of a β-Peptide Analog of Complexin

It has been reported that α-SNAP displaces Complexin after fusion, thus, enforcing the disassembly reaction. Designing a Complexin mimic which binds tighter to the SNARE complex might prevent α-SNAP interaction, and therefore, disassembly of the core complex. The most essential interactions were identified almost ten years ago.[14] Based on the crystal structure of the Complexin/SNARE complex, solved by SUTTON *et al*. in 1998,[7] a slightly twisted, central α-helix that binds to the center of the groove between Synaptobrevin and Syntaxin 1 over a length of at least 30 Å was identified, while the *N*-terminus exhibited no direct contacts with the four-helix bundle (Figure 37 A).[14,120]

The core Complexin fragment interacting with the SNARE complex is formed by residues Arg-48 to Tyr-70. Figure 37 shows the crystal structure as well as an overview of the important interactions between the Synaptobrevin, Syntaxin and Complexin helices. The closest contact to the core complex is formed between layer +3 and +1. At layer +3 Asp-218 from Syntaxin forms a salt bridge to Lys-69 from Complexin and a hydrogen bond between Asp-214 and Tyr-70 can be observed (Figure 37 B). Furthermore, a number of polar interactions at the ionic '0'-layer like Arg-63 and Arg-59 from Complexin form salt bridges to Asp-57 from Synaptobrevin (Figure 37 C). Beyond the '0'-layer strong interactions of Tyr-52 as well as Arg-48 from Complexin with Asp-65 and Asp-68, respectively, from the Synaptobrevin helix are developed by hydrogen bonds (Figure 37 C). This overall number of hydrophobic and polar interactions allows the formation of a stable five-helix complex. A side view of the contacting residues between the recognition units of Synaptobrevin, Syntaxin and Complexin is shown in Figure 37 D. Its deplacement by α-SNAP could be prevented by enhancing the binding of Complexin to the SNARE complex. Mimicking the α-helical recognition unit with a β-peptide providing a well-defined 14-helix and elongation of the helix at their *C*-terminal end with a -AKRK motif should enhance the affinity. This sequence extends the Complexin analog by one turn and it is assumed to interact with the Synaptobrevin and Syntaxin helices.

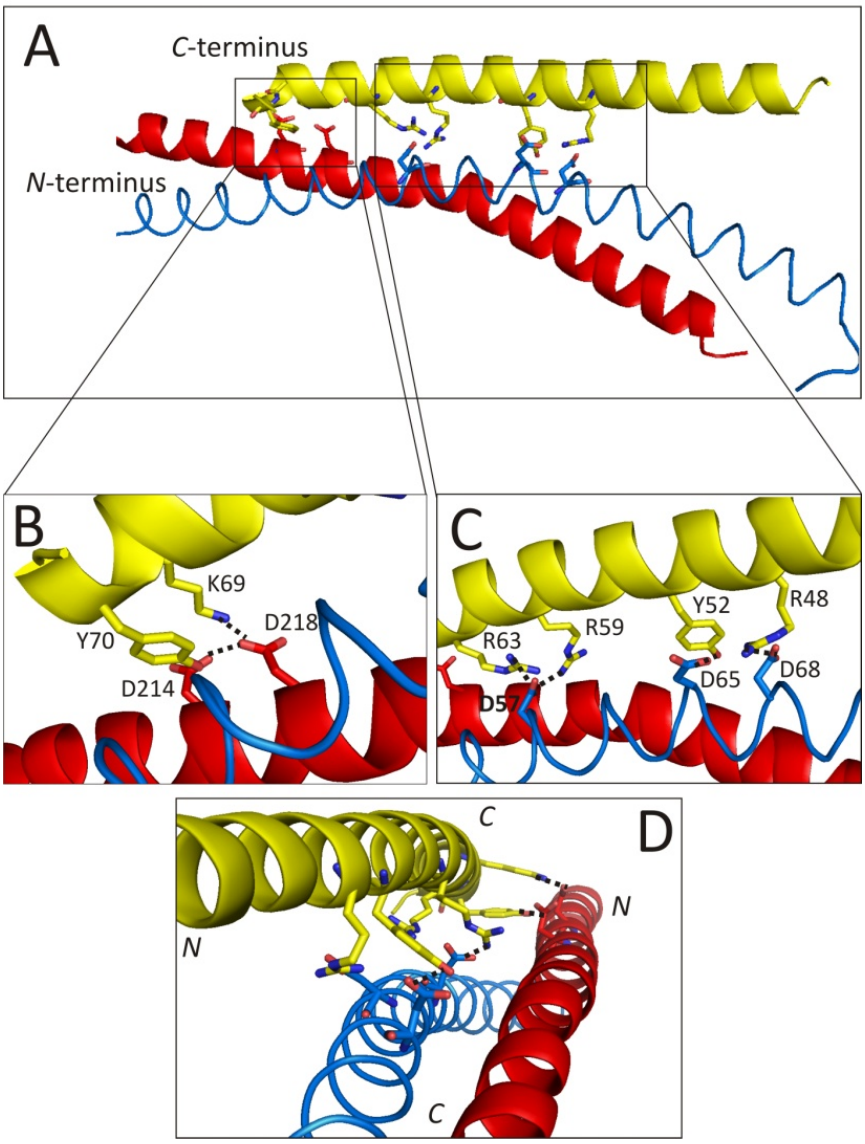

Figure 37. *Detailed view of the Complexin-Synaptobrevin-Syntaxin interactions.* ***A*** *Crystal structure of the Complexin/SNARE complex (yellow-Complexin, blue-Synaptobrevin, red-Syntaxin).* ***B*** *Closeup interactions between Complexin-Syntaxin (Y70-D214; K69-D218).* ***C*** *Closeup interactions of Complexin-Synaptobrevin (R63-D57; R59-D57; Y52-D65, R48-D68).* ***D*** *Side view of the Complexin-Synaptobrevin-Syntaxin interactions. (pdb code 1KIL)*

β-peptides received growing interest especially with respect to the formation and biological activity of well-defined secondary structures.[202] Replacement of the binding fragment of Complexin (residues 48 to 70) by a 14-helical β-peptide mimic could enhance the interactions between the derivative and the SNARE proteins Synaptobrevin and Syntaxin, and therefore, prevent displacing it by α-SNAP.

The first approach of designing the β-peptide analog of Complexin (**28**) comprises almost the whole natural sequence of the α-peptide **29** (Figure 38). Essential amino acids for the recognition to the SNARE complex are shown in bold. Regarding the identified interactions between the three helices the β^3-homoarginine (β^3-hArg), β^3-homotyrosine (β^3-hTyr) and β^3-homolysine (β^3-hLys) were chosen to provide the potential salt bridges. Thus, the Arg-48 and the Tyr-52 at the *N*-terminal end of Complexin were selected to be the starting point for the β-mimic design. Both interact with aspartate residues (65 and 68) at the Synaptobrevin helix (Figure 37 C). The residues were arranged in *i* and *i+3* positions for having the residues at the same side. The next important interacting residue is Arg-59 of the natural Complexin. This β^3-homoarginine building block was also introduced at the same side of the peptide in order to interact with Asp-57 of Synaptobrevin. Both, Lys-69 and Tyr-70 of the Complexin α-helix interact with the Syntaxin helix of the SNARE complex. It was decided to introduce only β^3-hLys at this position, due to the β-helical turn and the resulting distances between β^3-hTyr to the corresponding D-214 of Syntaxin. The β-peptide building blocks between the interacting residues in this first approach were also not varied in order to other required polar interactions and hydrogen-bonds known to be not so important for the recognition, but being probably also essential. Furthermore, it was decided to elongate the derivative **28** by an -AKRK motif at the *C*-terminal end. At this part Complexin interacts only with the Syntaxin helix and in position Sx-210 a glutamate could constitute a possible additional binding partner. Some residues of the natural sequence were omitted regarding the wide overall length of the peptide.

β-peptide	**R** KA **Y** AKM EA**R**NVMRQ **I**AD**K**A***KRK***	**28**
α-peptide	**R**KAK**Y**AKMEAE**R**EVMRQG**I**RD**K**	**29**
	48 52 59 66 69	

Figure 38. *Designed β-peptide sequence **28** and the corresponding natural α-peptide sequence **29** of Complexin. Essential interactions are marked in bold, the elongated motif at the C-terminal end is shown in italic.*

4.1.2 Synthesis of Complexin as a β-Peptide

Synthesis of Boc-β^3-Amino Acids

As mentioned before β-peptides are an important class of synthetic foldamers also providing helical secondary structures. β-Amino acids differ from α-amino acids as they bear an extra methylene group between C2 and the carboxyl carbon atom. They can be classified with respect to the positioning and stereochemistry of the side chain substituent as β^2- (**31**), β^3- (**32**) or β^2/β^3- (**33**) amino acids (Figure 39). β-Peptides, solely consisting of β^3-configuration have been shown to prefer 14-helical structures. They are able to adopt stable helical structures in solution containing as few as six residues whereas α-peptides usually require 15-20 residues for a well-defined helical structure with significant propensity.[203]

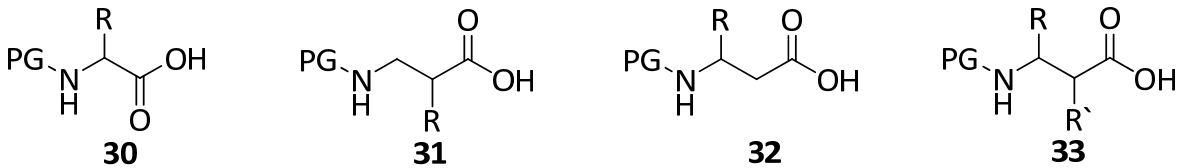

Figure 39. *Structures of α- (**30**), β^2- (**31**) β^3- (**32**) and $\beta^{2,3}$- (**33**) amino acids.*

In the last decade several methods for the synthesis of enantiomerically pure β^3-amino acids were developed.[204,205] They are important building blocks for the preparation of β-lactam antibiotics or macrolides showing interesting pharmacological properties.[135,206-211] Starting materials for almost all syntheses are α-amino acids, because they are inexpensive, enantiomerically pure and commercially available. The most popular method for the synthesis of β^3-amino acids or their derivatives is the ARNDT-EISTERT homologation (Scheme 2).[204,205] Thereby, the activated α-amino acids were converted into the corresponding α-diazoketones by treatment with diazomethane. Subsequent WOLFF-rearrangement yielded the desired β^3-amino acid building blocks.[139,212,213]

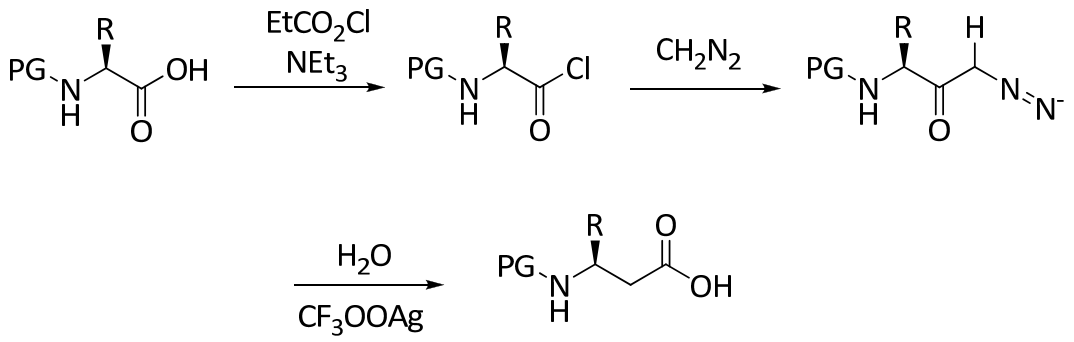

Scheme 2. *ARNDT-EISTERT homologation leading to the diazoketone followed by a WOLFF-rearrangement (PG - protecting group).*

By using this method the required β-amino acid building blocks were synthesized (Scheme 3). Hereby, the α-amino acid was transformed at -20 °C into the diazoketone using isobutyl chloroformiate, triethylamine and diazomethane. Afterwards, the diazoketone was converted into the β-amino acid building block using silver salts. The syntheses of most of the building blocks (**52**-**60**) are well-known and frequently carried out in the lab.

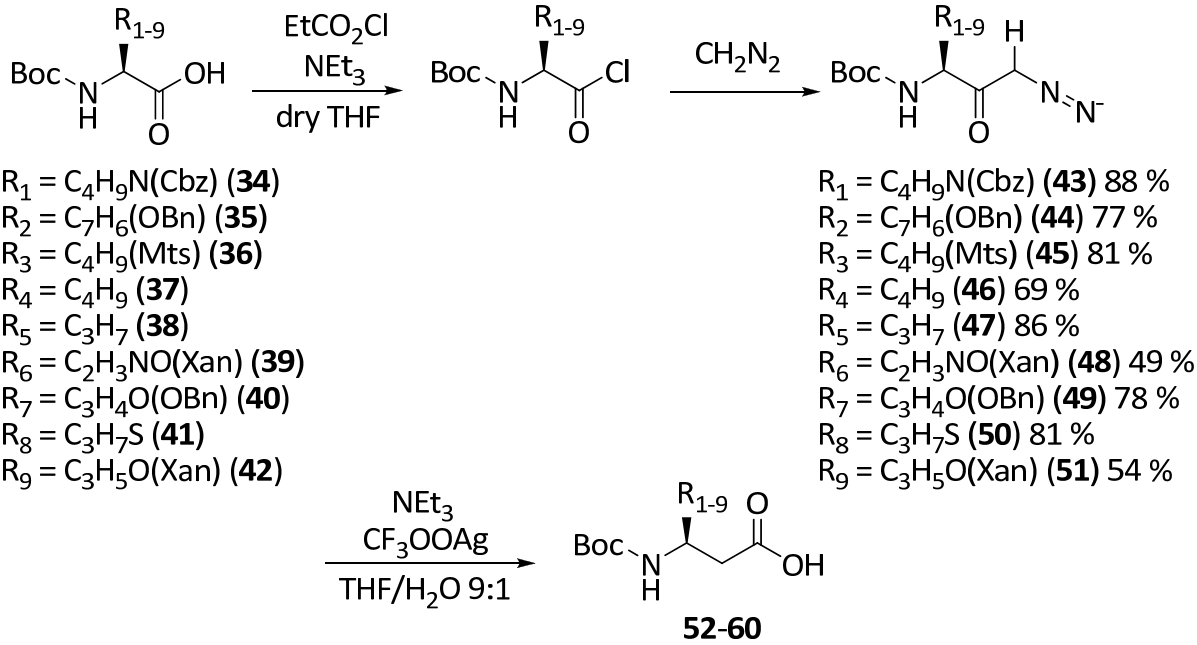

Scheme 3. *ARNDT-EISTERT homologation of α-amino acids **34**-**42** to diazoketones **43**-**51**, and further WOLFF-rearrangement yielding β^3-amino acid building blocks **52**-**60** required for the synthesis of β-peptide **28**.*

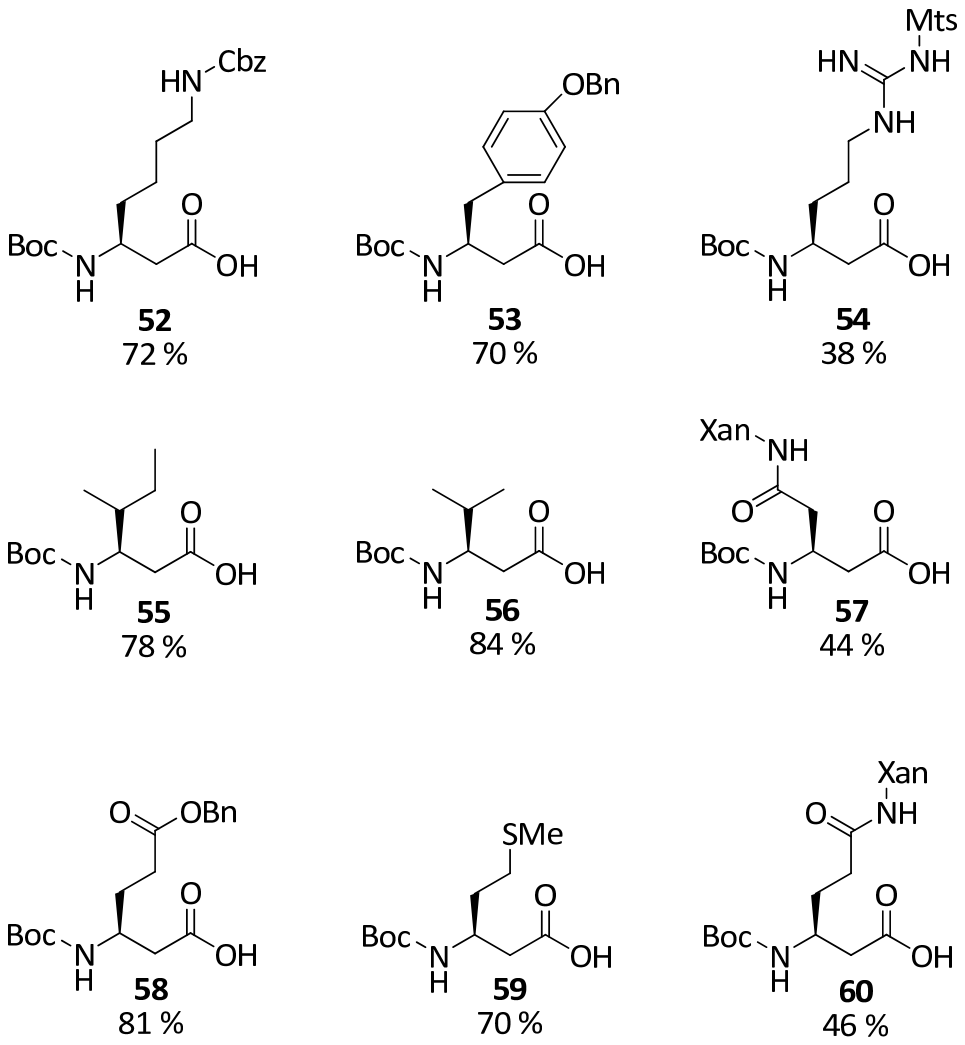

Scheme 4. *β^3-Amino acid building blocks **52**-**60** (expanded view) required for the synthesis of β-peptide **28**.*

Nevertheless, β^3-hArg(Mts)-OH (**54**), β^3-hAsn(Xan)-OH (**57**) and β^3-hGln(Xan)-OH (**60**) made some difficulties. The yield of β^3-hArg (**54**) was always low (25-38 %).[214,215] Modified reaction time, heat or different solvents did not enhance the results. Scheme 2 illustrates the synthesis of diazoketones **43**-**51**, followed by WOLFF-rearrangement, yielding β^3-amino acid building blocks **52**-**60** (Scheme 4).

Synthesis of the β-Peptide using SPPS

The synthesized β-amino acid building blocks **52**-**60** were used for solid phase peptide synthesis. Initially, the standard Boc-protocol was applied, starting at a MBHA-PS resin (0.15 mmol). The resin was manually preloaded with β^3-hLys(Cbz)-OH (**52**). The *N*-terminal protecting group was then cleaved with TFA/*m*-cresol

(95:5) for 5 min. Each coupling step was carried out with the β-amino acid (5.00 eq) preactivated with HATU (5.00 eq), HOAt (5.00 eq) and DIEA (10.0 eq) at 50 °C for 2 h. β^3-hArg(Mts)-OH (**54**) was coupled twice (Scheme 5).

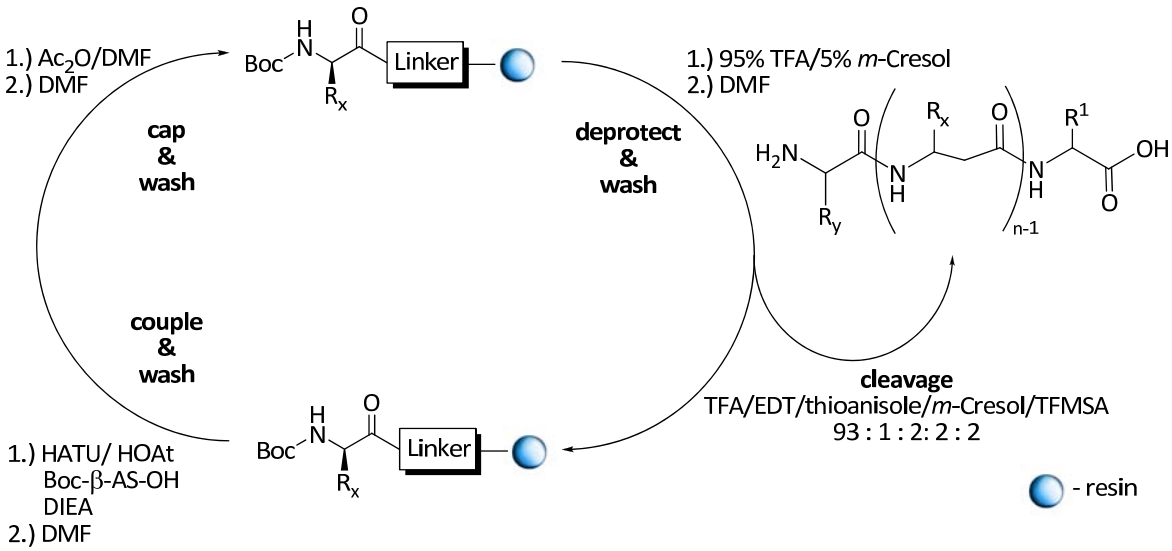

Scheme 5. *General scheme of standard Boc solid phase peptide synthesis.*

The synthesis of β-peptide **28** via the described coupling conditions was not successful. Different approaches utilizing microwave assisted peptide synthesis, varying equivalents of the building blocks, different heating conditions, enhanced coupling time and using different coupling reagents were carried out,[216,217] but the required β-peptide **28** was not obtained. Mostly shorter peptides, truncated after β^3-hArg(Mts)-OH and β^3-hMet-OH were obtained.

Synthesis of Fmoc-β^3-Amino Acids

Due to better monitoring of the individual coupling steps, the synthesis strategy was turned to Fmoc-SPPS. Via the Kaiser test examining of difficult coupling steps is possible.[218] Based on coupling efficiency for β-amino acid building blocks it is not the common synthesis strategy for β-peptides in our lab. Only the first four required building blocks were synthesized (Figure 40). Fmoc-β^3-amino acid building blocks **69**-**72** were generated with ARNDT-EISTERT homologation, followed by WOLFF-rearrangement. Due to the basic labile Fmoc-protecting group, the

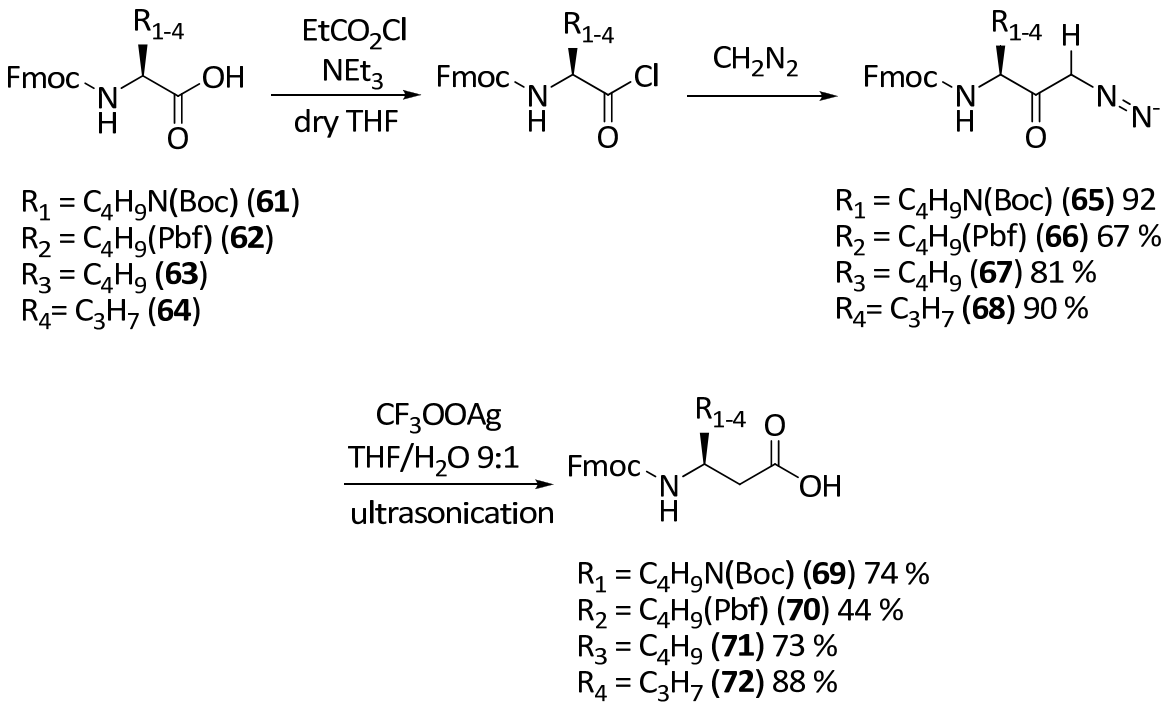

Scheme 6. *Synthesized Fmoc-β-amino acid building blocks (**69-72**) required for synthesis of β-peptide **28**.*

triethylamine in the last step was omitted and the reaction was ultrasonicated (Scheme 6).[215,219]

Fmoc-SPPS was carried out by using the Fmoc-strategy as described in Chapter 3, with the exception of longer reaction times (2-5 h) and higher temperatures (50-75 °C). Similarly to the described Boc-strategy the synthesis was performed either with or without microwave assistance.[216,217] For excluding synthetic problems at the first step in the synthesis a preloaded resin with Fmoc-β^3-hAla-OH was used. Though, as well, no successful peptide coupling was observed.

For this reason, the sequence of the β-peptide was reconsidered for simplification. The various β-amino acids might complicate the synthesis and it is unclear which effect they have regarding the 14-helix propensity. As it is known that β^3-hVal-OH promotes a 14-helix all non-interacting residues were exchanged by this building block to design the new sequence for the Complexin mimic **73** (Figure 40).[203,220-222]

β-peptide	**R** VV **Y** V E V V **R** V V **R**VVV**I**VV**K**A***KRK***	**73**
α-peptide	**R**KAK**Y**AKMEAE**R**EVM**R**QG **I**RE**K**	**29**

Figure 40. *Designed β-peptide sequence **73** and the corresponding natural α-peptide sequence **29** of Complexin. Essential interactions are marked in bold and the elongated motif at the C-terminal end in italic.*

The Boc-protocol was chosen for synthesis of β-peptide **73**. Though, for each coupling step the reaction temperature was increased to 90 °C, the reaction time decreased to 1 h and for all β-amino acid building blocks double coupling with fresh preactivated reaction mixture was applied. β^3-hArg(Mts)-OH (**54**) was coupled threefold. With this procedure, β-peptide **73** was successfully synthesized (Figure 41). Cleavage from the resin was carried out by using TFA/TMSOTf/*m*-cresol (5.75:1.6:1) at 0 °C for 2 h, followed by precipitation with cold diethylether and purification by HPLC.

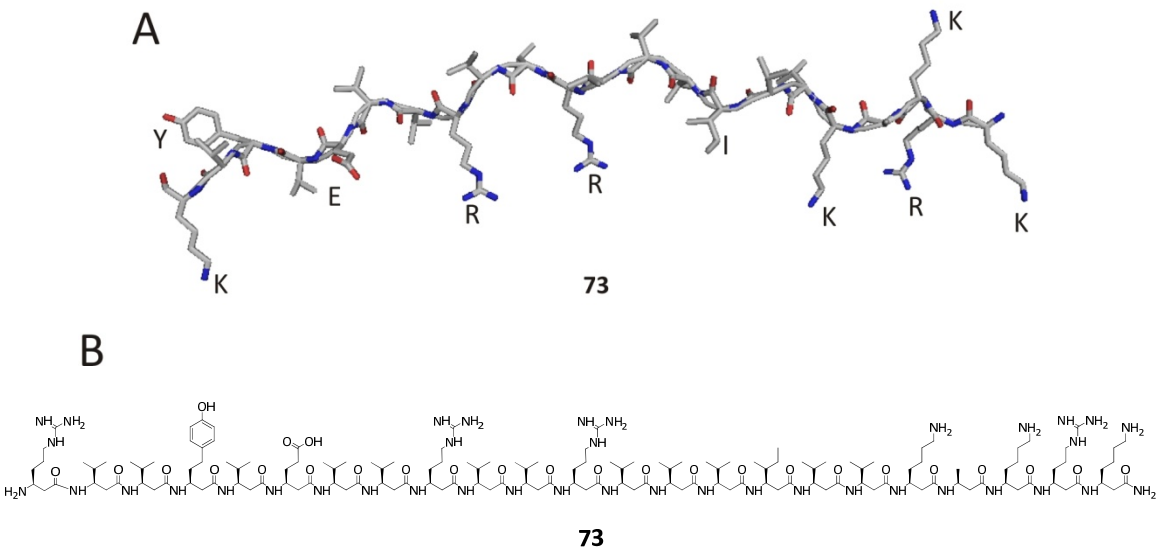

Figure 41. *Synthesized Complexin mimic **73** as a β-peptide. **A** Assumed helix secondary structure of peptide **73**, essential interactions are indicated. **B** Sequence of peptide **73**.*

4.1.3 Characterization of the Helix Conformation

Structural properties of the derivative **73** were analyzed via Circular Dichroism (CD) spectroscopy.[152] It represents a standard method studying conformations of α- and β-peptides.[223,224] The measurements were carried out by using trifluorethanole (TFE) as well as Tris·HCl buffer (10 mM, pH = 7.4) with a peptide concentration of 1.5 µM (Figure 42). The spectrum showed a negative cotton effect at 215 nm representing a right-handed 14-helical structure. As it is commonly known, TFE promotes the formation of the 14-helix, so there is a distinct better helix propensity than in Tris·HCl buffer.[215]

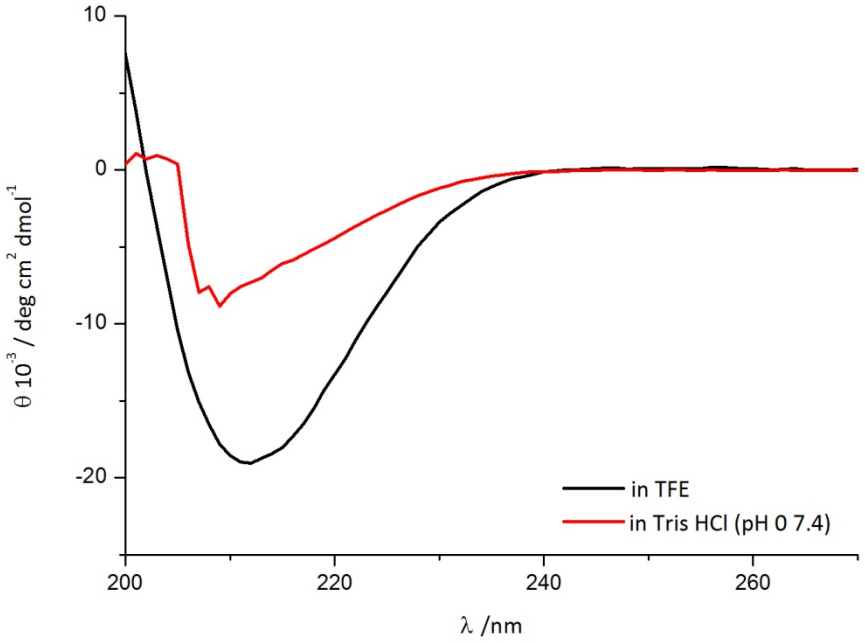

Figure 42. *CD spectrum of β-Complexin derivative **73**, 1.5 µM in TFE (black line) and in 10 mM Tris·HCl buffer (pH = 7.4) (red line). The spectrum was standardized with buffer, concentration of the sample (5.0 µM), length of cell and number of amino acids.*

4.1.4 Investigation of Complex Formation with the SNARE Complex

As mentioned before, Complexin only binds to the assembled SNARE complex, not to the individual SNARE proteins. Therefore, pre-assembled SNARE complexes with Synaptobrevin (aa 30-84), Syntaxin (H3-domain) and full-length SNAP-25 in standard SNARE buffer were employed for the investigation of complex formation. The Complexin derivative **45** was added in five fold excess.[14] The mixture was incubated at 4 °C for 24 h and putative Complexin/SNARE complex formation analyzed by SDS PAGE (Figure 43). As control lane 1 only shows the assembled SNARE complex, the assumed complex formation was controlled in lane 2 and 3 of the SDS gel. As the bands were not shifted, compared with the control experiment, it could be concluded that a thermodynamical stable complex was not formed.

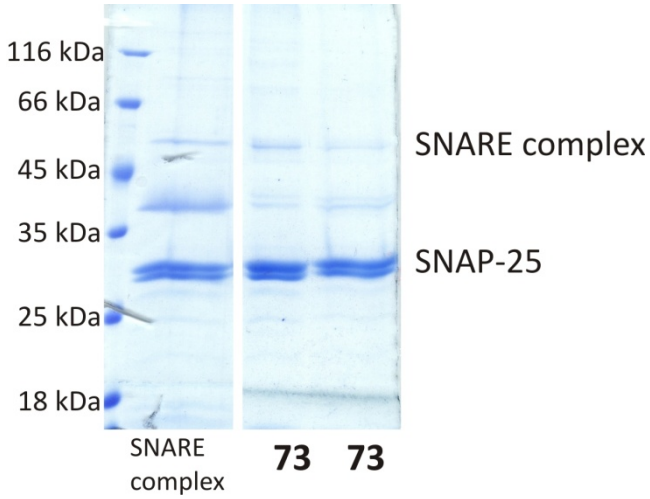

Figure 43. *Assay of the Complexin/SNARE complex assembly. Complexin derivative* ***73*** *was incubated with the assembled SNARE complex in a 5:1 ratio overnight at 4 °C. Lane 1 showed the SNARE complex. Lanes 2 and 3 indicated no complex formation of the SNARE complex with Complexin derivative* ***73****.*

As derivative **73** did not seem to be capable to assemble with the SNARE complex it was assumed that more interacting residues are required for successful complex formation. Probably as a result of the less pronounced 14-helix-arrangement of the β-peptide **73** no required hydrophobic and polar interactions with the Synaptobrevin and Syntaxin helices were developed. Thus, support by more rigid building blocks such as ACHC seems to be required.

4.2 Extension of the Complexin Helix

The influence of elongation at the *N*-terminal as well as the *C*-terminal end of the binding fragment of the natural Complexin helix regarding the α-helical conformation was investigated assisted by M. QUAST during her bachelor thesis.

The formation of an α-helical conformation depends on the amino acid sequence, based on different residues which stabilize the helix. Experimental data suggest alanine as the amino acid promoting the highest α-helix propensity.[225-229] Helix-forming propensities of the remaining amino acids were calculated by SCHIFFER *et al*. and compared with alanine.[225,226,228,229] Valine, isoleucine, lysine and glutamine were known to enhance the α-helix propensity,[228] whereas the rigid ring structure of proline and flexible conformation of glycine breaks the helix. Furthermore, the helix may be stabilized by positioning oppositely charged residues at positions *i* and *i+4*.

4.2.1 Design of Elongated Complexin Derivatives

The scaffold for the derivatives comprises the central helix region of Complexin known to interact with the Synaptobrevin and Syntaxin helix of the SNARE complex. This region includes residues 48 to 70. As a control of the influence of the attached residues it was decided to synthesize derivative **74**. Alanine is known to promote an α-helical conformation. For enhancing the propensity to form an α-helix five alanine residues were attached at the *N*-terminal part (derivative **75**). Furthermore, a Complexin derivative **76** with two valine residues, one isoleucine and two alanine residues was synthesized. Finally, extension of the *C*-terminus was performed in derivative **77**, regarding the -KRK motif which was also introduced in β-peptide **73**. Enhanced SNARE complex/derivative formation as well as identification of additional interacting residues in the groove was addressed. The *C*-terminal end was elongated to introduce more interacting residues in the groove between Syntaxin and Synaptobrevin and increase the binding with the Complexin helix (Figure 44).

RKAKYAKMEAEREVMRQGIRDKY	**74**
AAAAARKAKYAKMEAEREVMRQGIRDKY	**75**
AIVAVRKAKYAKMEAEREVMRQGIRDKY	**76**
RKAKYAKMEAEREVMRQGIRDKY**RGIKRK**	**77**

Figure 44. *Binding Complexin fragment **74** and the designed corresponding putative α-helical derivatives **75**-**77** of Complexin. Additional residues are marked in bold.*

4.2.2 Synthesis of Elongated Complexin Derivatives

Derivatives **74** and **77** were synthesized using Fmoc strategy at the automated microwave (MW)-assisted *Liberty* peptide synthesizer starting from preloaded Fmoc-Tyr(*t*Bu)-Wang resin and from Fmoc-Lys(Boc)-Wang resin, respectively. The Fmoc-amino acid building blocks with their acid labile side chain protecting groups were coupled using coupling reagents such as HOBt (4.00 eq), HBTU (3.90 eq) and DIEA (5.00 eq). Afterwards, the resin with the attached fully protected derivative **74** was divided in aliquots and a sample of each was cleaved from the resin with TFA/EDT/H_2O/TES (94:2.5:2.5:1), precipitated with cold diethylether and purified by HPLC. Resin bound peptide **74** was elongated by SPPS manually with Fmoc-Ala-OH, Fmoc-Val-OH and Fmoc-Ile-OH to obtain Complexin derivatives **75** and **76** after cleavage and HPLC.

4.2.3 Investigation of the Secondary Structure

In order to analyze the secondary structure of the synthesized peptides **74**-**77** CD spectra were measured (Figure 45). All of the investigated derivatives **74**-**77** show a characteristic spectrum of a right-handed α-helix with minima at 215 and 220 nm. Derivative **74** only comprising the natural binding fragment reveals the best α-helix propensity, whereas derivative **75** with five alanine amino acids attached at the *N*-terminus as well as derivative **76** with introduced valines and isoleucines showed a slightly less, but comparable α-helix formation. Extended derivative **77** with the -KRK motif at the *C*-terminal end indicates the α-helix with the lowest propensity.

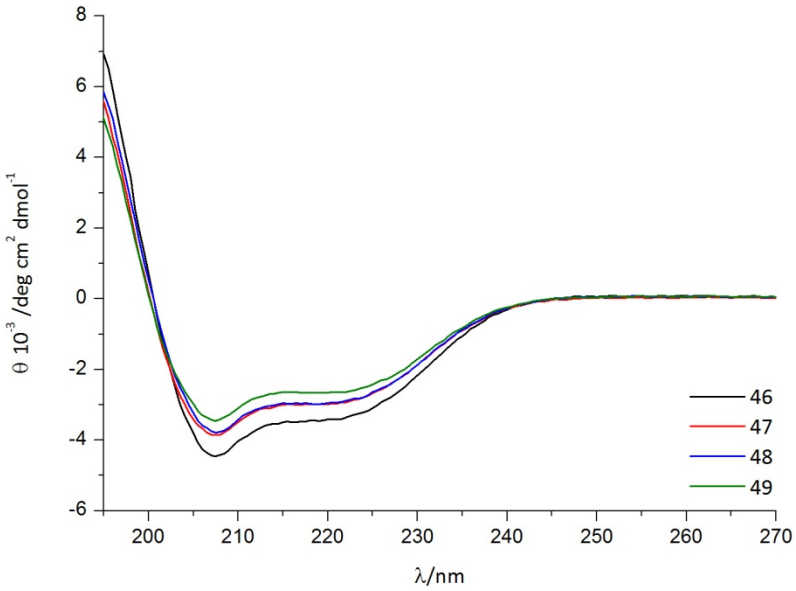

Figure 45. *CD spectra of the synthesized Complexin derivatives **74**-**77** in TFE. All spectra were standardized with solvent, concentration of the sample (6.0 µM), length of cell and number of amino acids.*

The CD spectra illustrating the structure of derivative **74** illustrated the different results as found by Xue *et al.*[230] Even without the additional α-helix (residues 29-47) the binding fragment of Complexin (residues 48-70) which is equivalent to peptide **74** revealed an α-helical structure.[230] Attaching of amino acids known to promote an α-helical propensity such as alanine or valine did not lead to an enhanced α-helix formation.

4.2.4 Investigation of the SNARE Complex/Complexin Assembly

As Complexin derivatives **74**-**77** were found to develop α-helical structures, assembly with the SNARE complex was carried out. Therefore, Complexin derivatives **74**-**77** were added in a 1:5 ratio to preassembled SNARE complexes (SNARE complex:derivatives) and allowed to interact overnight at 4 °C. Assembling was then checked by SDS PAGE (Figure 46).

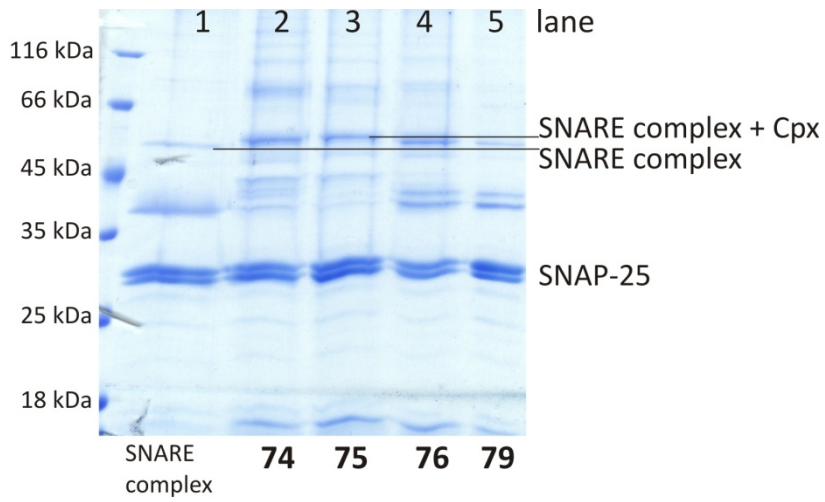

Figure 46. *Assay of the SNARE complex/Complexin derivatives **74**-**77** assembly. Complexin derivatives **74**-**77** were incubated with the previously assembled SNARE complex in five-fold excess overnight at 4 °C. As control lane 1 showed the SNARE complex without any derivatives. Lanes 2 and 3 indicated interaction of the derivatives **74** and **75** with the SNARE complex, observed by a slightly shift of the bands. In lane 4 and 5 the band shift was lower than observed in lane 2 and 3.*

Though, the Complexin derivatives have only a small molecular weight of 2 kDa first indications for complex formation was monitored with a SDS PAGE assay. It appears that the bands in lane 2 and 3 are slightly shifted compared with the SNARE complex in lane 1. This could indicate interactions of the SNARE complex and Complexin derivative **74**, the natural fragment and **75** which is extended at the *N*-terminus with five alanines, but further experiments for exact evidence are required. Derivative **76** with attached valines and isoleucine at the *C*-terminal end did not seem to bind to the SNARE complex (Figure 46, lane 4). However, an intensive band monitored stabilization of the SNARE complex. In lane 5 the intensity of the SNARE complex is very low. At this, the *C*-terminal end was extended with a -KRK motif. No band shift and intensively SNARE complex formation was displayed. For clarity, fluorescence measurements such as FRET fluorescence anisotropy experiments will be required. Labeling of the Complexin

derivates and of one of the SNARE proteins, associated in the complex could show explicite results.

These observations indicated that probably no residues were addressed in the groove between Synaptobrevin and Syntaxin, for interacting with the elongated Complexin derivative **77**, though, there is a glutamate at position 210 which is directed to the Complexin side. Probably the helix of the derivative **77** is slightly kinked or there is too much space between the Complexin and the Syntaxin helix. Formation of an α-helix is required for side chain interaction within the groove between Syntaxin and Synaptobrevin with the derivatives **74**-**77**. Therefore, extension of the Complexin helix with five alanines appears as the best derivative (**75**) in this experimental series. Furthermore, no increased binding with the SNARE complex was observed with *C*-terminal elongation of the Complexin fragment 48-70. This indicates no interaction partner for hydrophobic interactions, interesting for the design of the β-Complexin mimic.

4.3 Conclusion

The overall structure of a β-peptide 14-helix differs from that of the α-helix in many respects. As the α-helix has a slightly smaller radius and a longer rise for a given chain length than the β-helix it is not possible to transfer a sequence one to one with respect to binding properties. Furthermore, the α-helix has a 3.6-residue repeat, whereas the side chains of a 14-helix are stacked at every three residues,[135,159,160] remaining in well-defined structures with amino acid side chains of every third residue which are directly on top of one another along one face of the helix. Due to this, designing of a β-peptide that is able to bind with known binding partners of an α-helix requires exact identification of the addressed interaction partners.

The aim of this part was to design and synthesize Complexin mimics which are able to bind closely at the preassembled SNARE complex and might inhibit the α-SNAP/NSF-mediated disassembly by occupying one of the three assumed required binding sites for α-SNAP. Therefore, the binding fragment of the natural Complexin sequence (residues 48-70) was synthesized, initially, as a β-peptide derivative regarding important hydrophobic and polar interactions between Complexin and the two SNARE proteins, Synaptobrevin and Syntaxin by using the benefit of a 14-helix enhancing the interactions of their well-defined and rigid secondary structure.

Numerous β-amino acid building blocks (**52**-**60** and **69**-**72**) were synthesized via ARNDT-EISTERT-homologation followed by WOLFF-rearrangement. Boc- as well as Fmoc-solid phase peptide synthesis was carried out to obtain the β-peptide derivative of Complexin. Because of synthetic problems due to the high diversity of β-amino acid building blocks with low coupling efficiencies and for promotion of a 14-helical propensity of the target peptide the primarily designed peptide sequence was altered. Except for the known interacting residues all remaining amino acids were exchanged by β^3-hVal-OH which promotes the required 14-helix. The resulting β-peptide **73** was successfully synthesized by Boc-strategy. Investigation of the secondary structure by CD spectroscopy indicated a 14-helical β-peptide. The assembly assay regarding complex formation of the preassembled SNARE complex with the β-mimic of Complexin showed no results. No band shift indicating a five-helix-complex was observed.

In a second approach, the α-helical binding fragment of Complexin was elongated with various α-amino acid building blocks known to promote an α-helical propensity for investigation of their influence in SNARE complex binding. Hence, four α-peptides (**74**-**77**) were synthesized with additional amino acids attached at the *N*- and at the *C*-terminal end, respectively. All derivatives **74**-**77** show formation of an α-helix (Figure 45), whereas derivative **74** that recreated the natural sequence of the binding fragment of Complexin (residues 48 to 70) to the SNARE complex demonstrated the best α-helical propensity. Nevertheless, it appears that derivatives **74** and **75** were able to bind to the SNARE complex, whereas the band intensity in the SDS gel especially for derivative **77** with the *C*-terminal elongation indicated no interactions. For clearness, further experiments using FRET and fluorescence anisotropy techniques have to be arranged. Though, attaching of fluorescent label is required.

As a control for the β-peptide derivative of Complexin the *C*-terminal elongation in the α-peptide **77** was introduced enhancing binding interactions. Though, the results indicated that the additional residues address any amino acids in the considered Syntaxin fragment (residues 204-211).

Regarding the capability of Complexin inhibiting the α-SNAP/NSF mediated disassembly by preventing α-SNAP interaction many investigations were performed in the last decade. [8,13,189,195,198,200,231] Opposing results, led to various interpretations of the mechanism.[189] Measurements of binding affinities of Complexin (less than 10 mM) with the SNARE complex suggested that its interactions are more stable than those of α-SNAP to the SNARE complex.[195]

Overexpression of Complexin as well as small amounts might influence the balanced fusion process, and therefore, similar results are observed.[189,198] Comparison of all these investigations led to the assumption that the quantity of disassembly inhibition highly depends on the Complexin as well as the α-SNAP concentration. Complexin binds only to one of the three assumed binding sites of the corresponding interaction model for α-SNAP described by MARZ *et al*.[12] Whereas α-SNAP develops numerous hydrophobic interactions with each of the assembled SNARE proteins, Complexin was simply detected in the groove between Syntaxin and Synaptobrevin. This observation did not exclude that the other sites are unaffected by Complexin binding but no additional interactions were detected so far. It addressed the same side of the SNARE complex as derivative **20** in chapter 3 which demonstrated indications for being a good inhibitor regarding α-SNAP recognition. Further experiments for confirming these observations are required.

Chapter 5

Design and Synthesis of Independently Folding Protein Domains

5.1 The HTH Motif as Model System for smFRET Studies

The functionality of proteins highly depends on their three dimensional structure. The HTH (helix-turn-helix) motif is a small domain of 44 residues comprising two α-helices connected by a short turn. It is well-suited to serve as a model system for the development of single molecular fluorescence spectroscopy (smFRET) method. Via an experimentally well-characterized transition state it folds in microseconds. By using the FRET technique, which is a convenient tool for distance measurements in biomolecules, it is possible to evaluate the space between two residues within one protein or between different molecules, and hence, monitoring of conformational changes is feasible. Here, with this tool and labeling of key residues with advanced fluorescent dyes the smFRET technique should be developed. Investigation with FRET requires a donor and an acceptor dye. In collaboration with the group of Prof. J. ENDERLEIN, Department of Physics, Göttingen smFRET studies were carried out on the chemically synthesized and labeled HTH EnHD (Engrailed homeodomain) motif.

5.1.1 Design of the HTH EnHD Motif

In order to generate a construct that closely resembles the natural folding kinetics of the HTH motif of the Engrailed homeodomain, only the fragment comprising residues 16-59 of the full length protein lacking the *N*-terminus and

half of helix I, was investigated. It is known that this fragment exhibits the properties expected from a 'self-folding domain', such as diverse secondary structure elements, measurable folding events and resistance against thermal unfolding.[232] Regarding the Förster radius (56 Å) the Alexa fluorescent dyes were placed at positions 28 and 52 (Figure 47). The residues at these positions are a glutamate (28) and a lysine (52), so, successive labeling was possible using the orthogonal side chain protection strategy. Due to limited understanding how residue replacements within the sequence influence the secondary structure in this structural domain no changes were allowed. Glutamate and lysine were positioned close to each other at the end of the respective helices in the folded state, and therefore, served as good candidates for labeling.

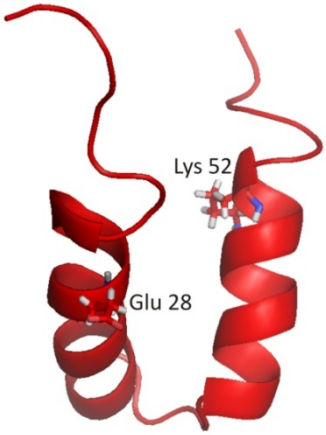

Figure 47. *The HTH EnHD motif with key residues chosen for labeling (Glu-28 and Lys-52).*

Originally, the HTH EnHD protein is a three helix bundle, but for measurements of folding kinetics the first helix is not required. MAYOR *et al*. found that a L16A mutation decreases the stability of the native state resulting in ten-fold slower folding processes. This mutant is capable forming the HTH motif without interactions with helix I.[171,172,233,234] Therefore, a fragment containing the turn and helices II and III (**78**, residues 16-59) was synthesized (Figure 48).

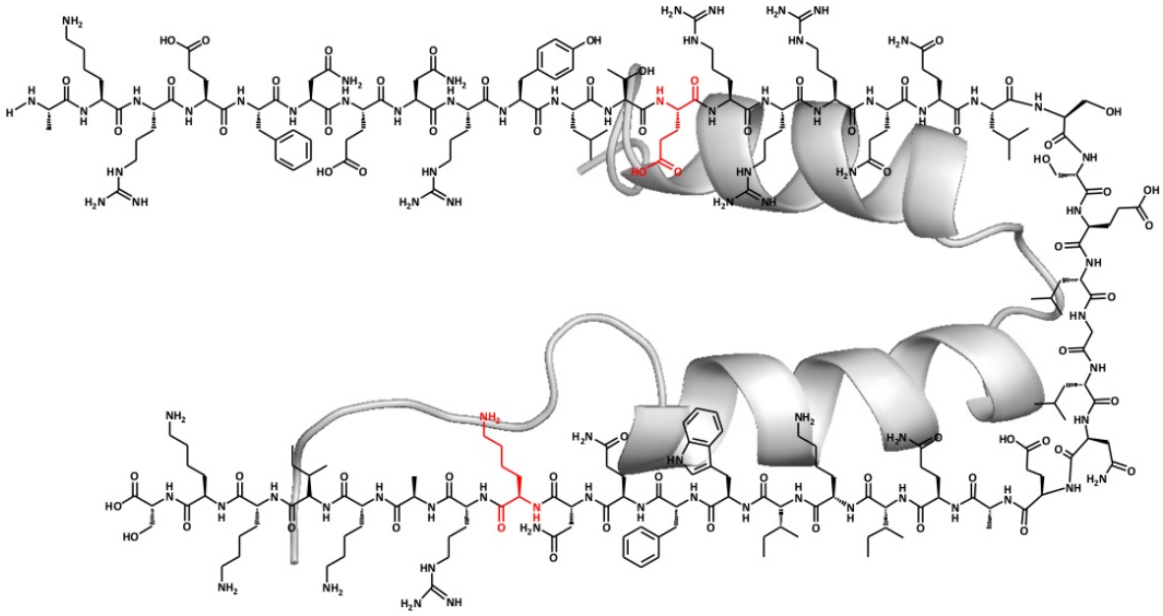

78

Figure 48. *Sequence of the HTH EnHD motif, helix II, turn and helix III. Key residues Glu-28 and Lys-52 were marked in red.*

The selection of fluorescence dyes was crucial for the intended experiments. The utilized dyes should tolerate minimal structural disturbances while displaying high photostability, quantum yields and stability of peptide synthesis conditions. Furthermore, convenient and site-specific coupling at the peptide as well as an available acceptor and donor pair compatible with the distance between the residues was required. The Alexa Fluor dyes are very high photostable conjugates.[235,236] Additionally, they are available with various substitutions for easy attaching at different side chains and fulfilling almost all listed requirements. Solely, the big extent of the dyes compared with the length of the protein as well as charge-charge interactions could be problematic. For control experiments also single-labeled HTH derivatives were synthesized. The donor/acceptor pair selected for this work is the Alexa 488 (**79**)/647 (**80**) dye (Figure 49).

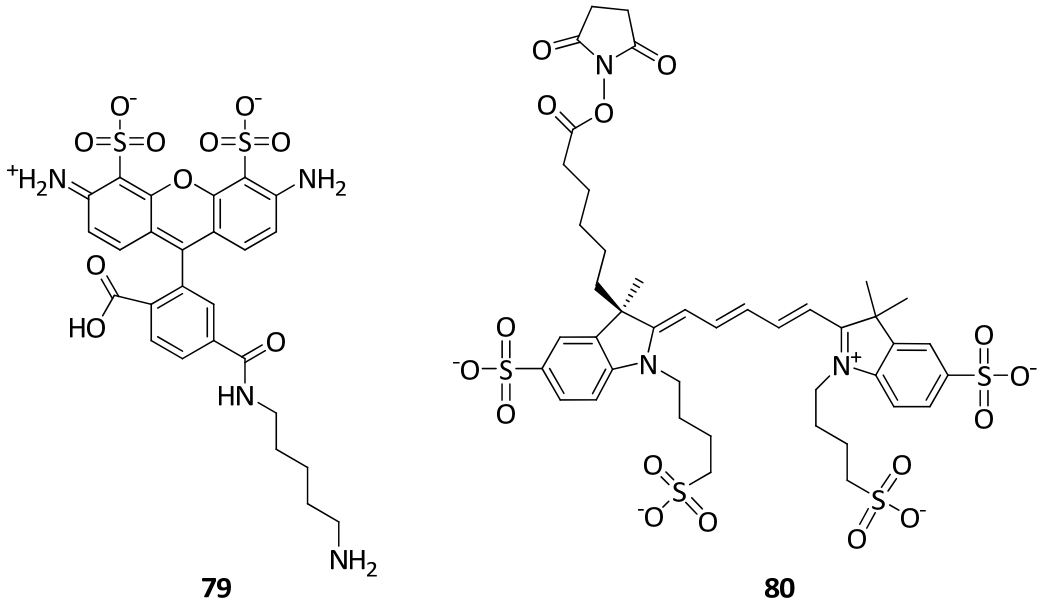

Figure 49. *Alexa 488 dye (**79**) and Alexa 647 dye (**80**), both with linker.*

For investigating the impact of the fluorescent dyes regarding structural capacities, four different peptides were synthesized. As control the first derivative **78** contained no label. Derivative **81** was labeled with the single dye **79** at the glutamate (residue 28). The lysine at position 52 was substituted with the single dye **80** yielding derivative **82**. Finally, the double labeled derivative **83** was synthesized (Figure 50). The notation of the individual residues is retained avoiding confusions with previous explanations.

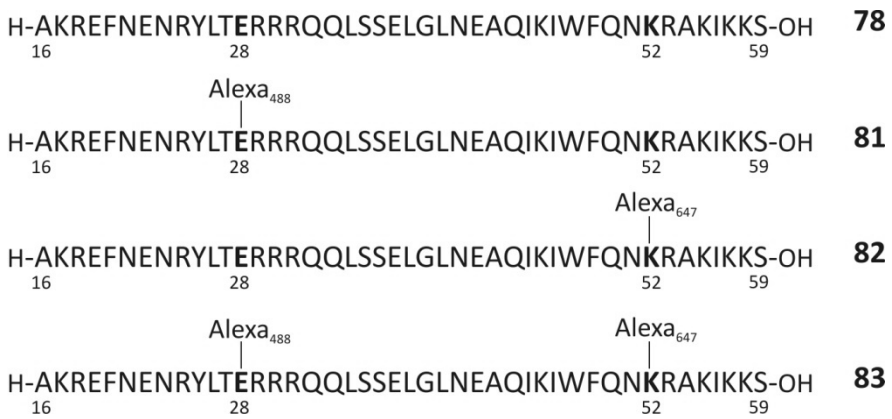

Figure 50. *Sequences of the HTH derivatives **78**, **81**-**82**.*

The Alexa dyes are available with the required substitutions. Therefore, Alexa 488 (**79**) was used as a cadaverine sodium salt, capable for coupling at the carboxylic

acid function of glutamate. After preactivation of the resin bound peptide with PyBOP (3.90 eq) and DIEA (10.0 eq) the Alexa 488 dye (**79**) was added. Oppositionally, Alexa 647 (**80**) was attached as succinimidyl ester at the amine function of the lysine.

Derivatives **81**, **82** and **83** were synthesized via Fmoc-SPPS. For site-specific labeling the orthogonally side chain protection strategy for the SPPS was chosen. The glutamate was protected with the OAll-group, the lysine with an Alloc-protecting group, respectively. Both were removable with a palladium catalyst and a methylene borane complex. Regarding synthesis of construct **84** a triple-orthogonal strategy was performed. The protecting group of the lysine was changed to the Mts-group. Finally, the secondary structure of the synthesized derivatives **78** and **81**-**83** were analyzed with CD spectroscopy.

5.1.2 Synthesis of the HTH Motif

The derivatives **78** and **81**-**83** were synthesized with the Fmoc-protocol using the automated microwave (MW) assisted *Liberty* peptide synthesizer, starting from preloaded Fmoc-Ser(*t*Bu)-Wang resin and Fmoc-Cys(Trt)-Wang resin, respectively. With the exception of Fmoc-Lys(Alloc)-OH, Fmoc-Lys(Mts)-OH and Fmoc-Glu(OAll)-OH, Fmoc amino acid building blocks with their standard acid labile side chain protecting groups as well as coupling reagents such as HOBt (4.00 eq), HBTU (3.90 eq) and DIEA (5.00 eq) were selected. Initially, derivatives **78** and **82** were synthesized (Scheme 7). For orthogonal side chain deprotection the Fmoc-Lys(Alloc)-OH building block was incorporated at position 52. Boc-Ala-OH was *N*-terminal integrated being stable against the basic Alloc-deprotection conditions. The Alloc-protecting group of Lys-52 was then removed with $Pd(PPh_3)_4$ (0.10 eq) and $Me_2NH{\cdot}BH_3$ (40.0 eq) in 4 h under inert atmosphere, whereas the remaining residues were still protected. After side chain deprotection of Lys(Alloc) the resin was sampled. Derivative **78** was obtained by cleavage from resin using TFA/TES/H_2O (95:2.5:2.5) over a period of 2 h, precipitation with cold MTBE and purification via HPLC. For the labeling reaction the resin bound peptide (2.5 µM) was allowed to react with the Alexa 647 succinimidyl ester (**80**) (1.00 mg, 3.00 eq), preactivated with DIEA (10.0 eq) for 2 d under the exclusion of light. Afterwards, the resin was thoroughly washed with DMF and DCM and dried under reduced pressure. Finally, the single-labeled peptide **82** was cleaved from the resin using TFA/TES/H_2O (95:2.5:2.5) in 2 h under light-exclusion, precipitated with cold MTBE and purified by analytical HPLC (Scheme 7).

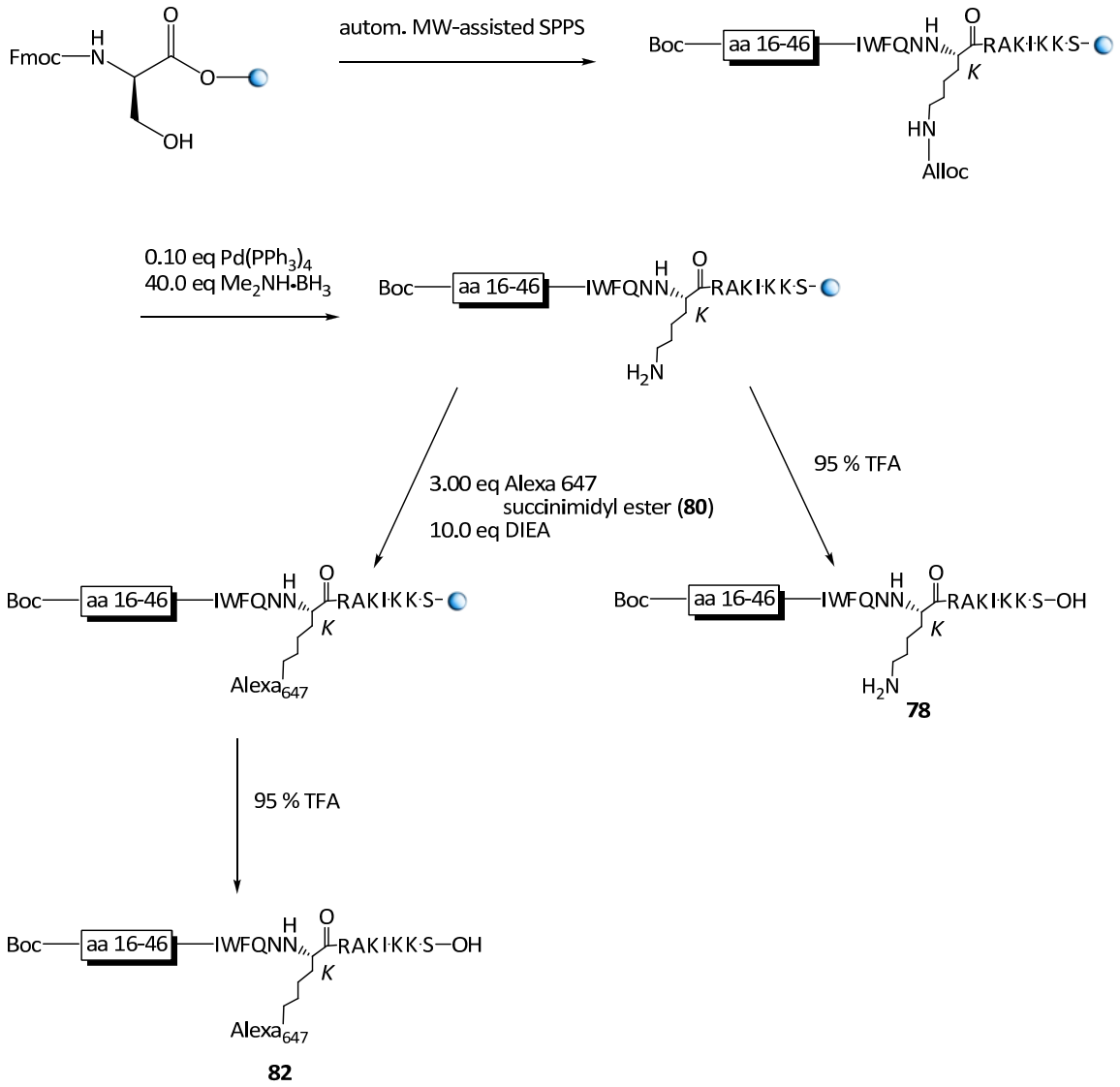

Scheme 7. *Synthesis of derivatives **78** and **82**. After automated microwave (MW) assisted SPPS the resin was treated with $Pd(PPh_3)_4$ and $Me_2NH{\cdot}BH_3$ in DMF under inert atmosphere for 4 h. Afterwards, the resin was separated into two fractions. Derivative **78** was obtained by cleaving from the resin with TFA/TES/H_2O (95:2.5:2.5) over a period of 2 h. Labeling of derivative **82** was carried out using 3.00 eq of the fluorescent dye Alexa 647 succinimidyl ester and preactivation with 10.0 eq DIEA. The mixture was allowed to react for 2 d under light-exclusion. Afterwards, the resin was cleaved by TFA/TES/H_2O (95:2.5:2.5) obtaining the labeled derivative **82**.*

Derivative **81**, single-labeled with Alexa 488 (**2**) was obtained, using the same steps as described for derivatives **78** and **82** (Scheme 8). A side-chain OAll-Glu building block was incorporated at position 28. After peptide synthesis using the automated MW-assisted peptide synthesizer the resin was treated with $Pd(PPh_3)_4$ (0.10 eq) and $Me_2NH{\cdot}BH_3$ (40.0 eq) in 4 h under inert atmosphere to remove the

OAll-side chain protection of Glu-28. The other residues remain fully protected. The carboxylic acid function of Glu-28 (3.00 eq) in the resin bound peptide was preactivated with PyBOP (3.90 eq) and DIEA (10.0 eq) in a DMF/H_2O (9:1) solution and added to the Alexa 488 cadaverine sodium salt (**79**) within 2 d under exclusion of light. Cleavage with TFA/TES/H_2O (95:2.5:2.5), precipitation with cold MTBE and purification by analytical HPLC yielded derivative **81** (Scheme 8).

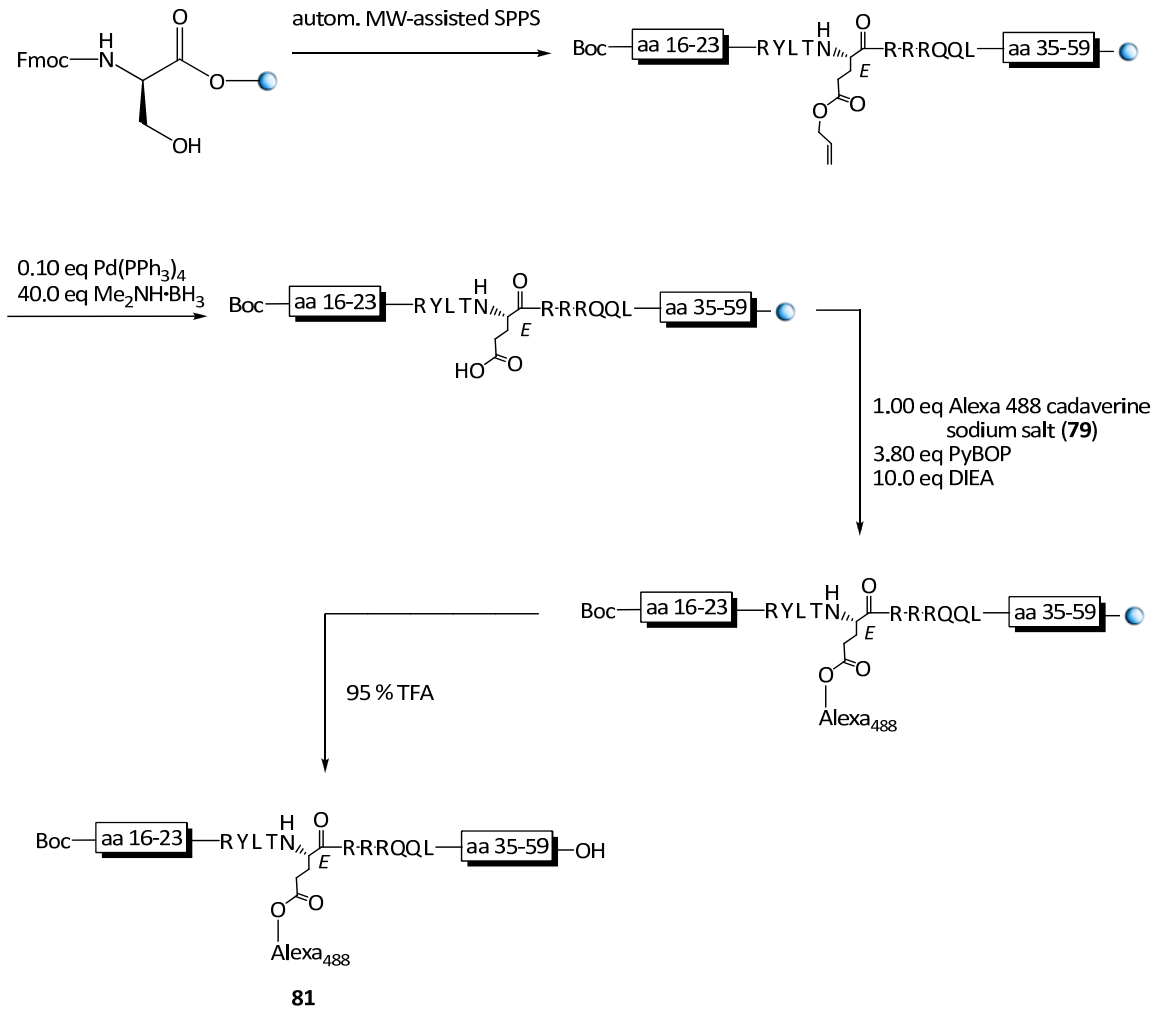

Scheme 8. *Synthesis of derivative **81**. After automated microwave (MW) assisted SPPS the resin was treated with $Pd(PPh_3)_4$ and $Me_2NH{\cdot}BH_3$ in DMF under inert atmosphere for 4 h. Then, labeling was carried out using 3.00 eq of the fluorescent dye Alexa 488 cadaverine sodium salt (**79**). The mixture was allowed to react for 2 d under light-exclusion. Afterwards, the resin was cleaved from the resin by TFA/TES/H_2O (95:2.5:2.5) obtaing the labeled derivative **81**.*

According to the synthesized constructs **81** and **82** the synthesis of the double-labeled derivative **83** was performed. For a stepwise attaching of the two

fluorophor dyes, a triple-orthogonal protecting group strategy was chosen. The peptide was coupled via Fmoc-synthesis.

The glutamate at position 28 was protected with the OAll-group as well as the lysine at position 52 with the Mtt-protecting group. Initially, after successful peptide synthesis the glutamate was deprotected using $Pd(PPh_3)_4$ (0.10 eq) and $Me_2NH{\cdot}BH_3$ (40.0 eq). Then the Alexa 488 fluorescent dye (**79**) was attached and the Mtt-protecting group was selectively removed under mild acidic conditions (Scheme 8). The coupling of the Alexa 647 dye (**79**) was carried out under the same conditions as for derivative **82** (Scheme 7). Though, after cleavage (TFA/TES/H_2O 95:2.5:2.5) only construct **81** labeled with a single dye was observed (Scheme 9). To exclude that the huge Mtt-protecting group at the lysine interfered with the attached dye the coupling strategy was altered. Therefore, initial Mtt-deprotection, followed by coupling of Alexa 647 (**80**) was carried out. Afterwards, the OAll-protecting group of the glutamate was removed and the Alexa 488 dye attached. However, only the single-labeled peptide **82** was obtained.

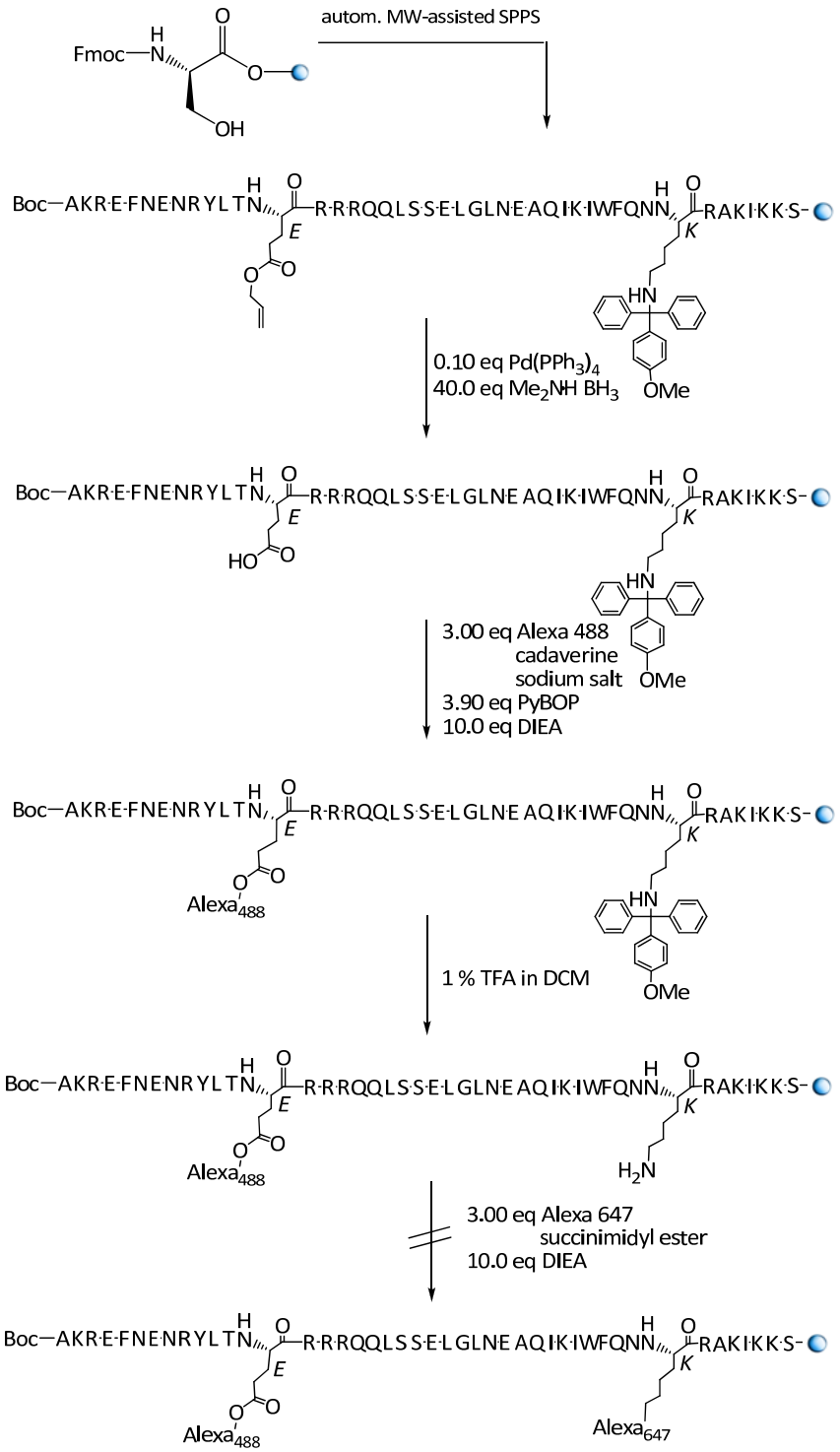

Scheme 9. *Planned synthesis of derivative* ***83****. After SPPS, OAll-deprotection, labeling of resin bound peptide with Alexa 488 cadaverine sodium salt (****79****) and removal of the Mtt-protecting group of the lysine at position 52 with 1 % TFA in DCM the resin was treated with preactivated Alexa 647 dye for 2 d. Only derivative* ***81*** *was obtained.*

As these methods were found to be incapable of forming the double-labeled peptide **83** it could be assumed that the helices of the HTH motif are too close to each other, and in contrast the fluorophors were too big, therefore, it was not possible to attach both of the dyes at these positions (28 and 52) due to its steric hindrance. Additionally, both dyes were negatively charged.

Regarding these observations a new labeling strategy was chosen. The fluorophors were attached to the termini of the peptide in order to get more space for both dyes. Therefore, new HTH derivatives with an additional cysteine residue at the *C*- and *N*-terminus, respectively, were synthesized (Figure 51). Thereby, the fluorescent dyes should be attached as maleimides in buffer, a common technique for peptide and protein labeling. The first strategy was to synthesize derivative **84** with only one cysteine at the *C*-terminal end by the Fmoc strategy as described before starting with preloaded Fmoc-Cys(Trt)-Wang resin. No special side chain protecting groups were introduced. After resin sampling peptide **84** was successfully labeled with the Alexa 488 succinimidyl ester at the *N*-terminal end obtaining construct **8** (conditions already described in Scheme 7). The remaining resin bound peptide was elongated with a cysteine residue (**9**). With regard to possible racemization of cysteines at basic conditions the coupling conditions were modified.[237] Fmoc-Cys(Trt)-OH was activated using HOBt (3.90 eq), HBTU (4.00 eq) and *sym*-collidine (5.00 eq) in DCM. It is known that the racemization occurs only in limited amounts with this activation reagent.[238]

H-AKREFNENRYLTERRRQQLSSELGLNEAQIKIWFQNKRAKIKKS**C**-OH **84**
16 28 52 59

Alexa$_{488}$-AKREFNENRYLTERRRQQLSSELGLNEAQIKIWFQNKRAKIKKS**C**-OH **85**
16 28 52 59

H-**C**AKREFNENRYLTERRRQQLSSELGLNEAQIKIWFQNKRAKIKKS**C**-OH **86**
16 28 52 59

Figure 51. *Sequences of the HTH EnHD motif with cysteines attached at the C-terminus (derivative **84**) or at both terminal ends (derivative **86**), respectively. For derivative **85** construct **84** was labeled with the Alexa 488 dye (**79**).*

Peptides **78**, **81** and **82** as well as the derivatives **84**-**86** were submitted to the group of Prof. J. ENDERLEIN, Department of Physics, Göttingen, for labeling and investigation of folding events.

5.1.3 Investigation of Structural Characteristics of the HTH Motif

In order to analyze the secondary structure of the synthesized peptides (**78** and **85**) CD spectra were carried out. Initially, the α-helix conformation of the unlabeled HTH derivative **78** was controlled at different temperatures by Dr. Qui VAN, group of Prof. J. ENDERLEIN, Department of Physics, Göttingen (Figure 52). As expected, minima at 215 and 222 nm were monitored, indicating the formation of an α-helix. At increased temperature the helix propensity decreased.

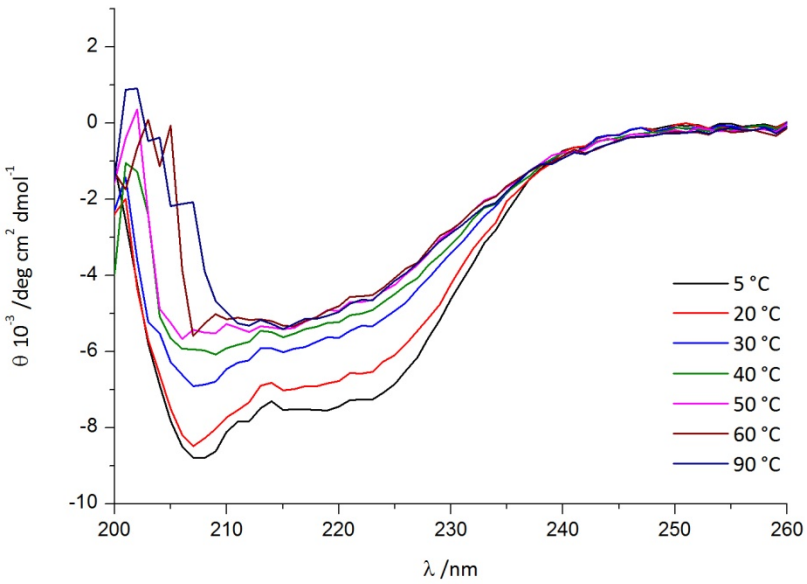

Figure 52. *CD spectra of the unlabeled HTH derivative **1** at different temperatures. Measurements were carried out by Dr. Qui Van, Department of Physics, Göttingen.*

Additionally, CD spectra of the unlabled peptide **78**, compared with the single-labeled derivative **85** in PBS buffer at 20 °C were accomplished (Figure 53). No influence induced by the introduced fluorescent dye **79** was observed.

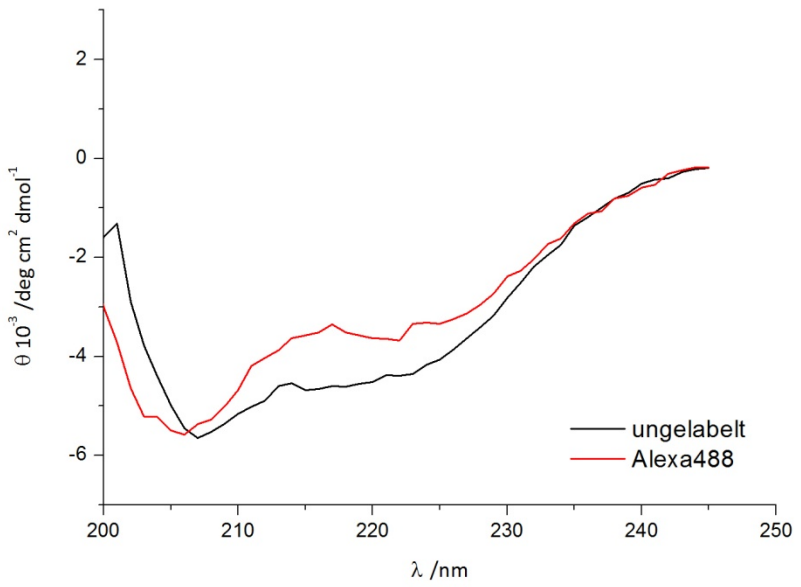

Figure 53. *CD spectra of the unlabeled HTH derivative* ***78*** *and single-labeled derivative* ***85*** *at 20 °C in PBS buffer. Measurements were performed by Dr. Qui Van and Phillip* KROEHN*, Department of Physics, Göttingen.*

5.2 The WW Domain

The WW motif is also an ultrafast folding protein domain.[239] The domain is arranged as a compact module composed essentially of a three-stranded β-sheet, and can therefore, serve as an excellent model system for additional interesting information of folding pathways and kinetics.

5.2.1 Design of the WW Motif

The fragment of the WW motif required for folding dynamics comprises 36 residues of the typically 38-44 amino acids length single-domain protein. Also, to complete experimental data and for comparison with known α-helix folding pathways investigation of the WW domain with FRET experiments will be performed by Philipp KROEHN in the group of Prof. J. ENDERLEIN, Department of Physics, Göttingen. Site-specific labeled derivatives of the WW motif are required. Hence, three derivatives **87**-**89** were synthesized. Based on the experiences with the synthesis of the HTH derivatives only the *C*- and *N*-terminal attached cysteine derivatives **87**-**89** were synthesized (Figure 54).

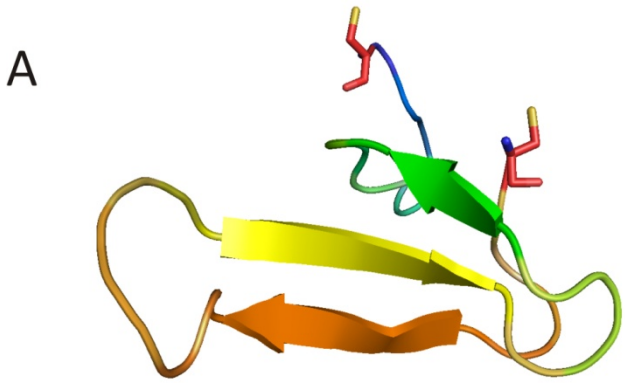

B

H-VPLPAGWEMAKTSSGQRYFLNHIDQTTTWQDPRKAM**C**-OH **87**
1 36

Atto$_{488}$-VPLPAGWEMAKTSSGQRYFLNHIDQTTTWQDPRKAM**C**-OH **88**
1 36

H-**C**VPLPAGWEMAKTSSGQRYFLNHIDQTTTWQDPRKAM**C**-OH **89**
1 36

Figure 54. A *WW motif with attached cysteines (red) at the C- and N-terminal end.* ***B*** *Sequences of the WW motif with cysteines attached at the C-terminus (derivative* ***87****), and at both terminal ends for derivative* ***89****.*

The same coupling and labeling conditions as described for derivative **82** were realized. The fluorescent dyes were changed to Atto dyes because of enhanced photostability, less charge and lower price. The chemical structure of Atto 488 (**90**) is shown in Figure 55.

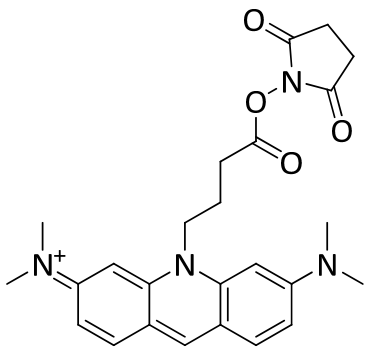

90

Figure 55. *Structure of the Atto 488 fluorescent dye (****90****).*

5.2.2 Synthesis of the WW Motif

The WW domain derivatives **87** and **89** were synthesized using the standard SPPS Fmoc-protocol as already described for derivative **78**. Starting with preloaded Fmoc-Cys(Trt)-Wang resin the synthesis was accomplished via the automated MW-assisted *Liberty* peptide synthesizer with standard Fmoc-amino acid building blocks and protected with its standard side chain protecting groups. The labeling strategy for obtaining derivative **88** was the same as for the HTH motif, the Atto 488 dye as succinimidyl ester was added to the resin bound peptide with a free amine at Lys-52. The resin, not used for the labeling reaction, was treated with Fmoc-Cys(Trt)-OH for elongation of the sequence. The amino acid building block was activated with HOBt (3.90 eq), HBTU (4.00 eq) and *sym*-collidine (5.00 eq). Double coupling at the *N*-terminal end of derivative **89** was carried out.[238] Derivatives **87**-**89** were cleaved from the resin using TFA/EDT/H_2O/TES (94:2.5:2.5:1) and purified by HPLC.

After purification the peptides **87**-**89** were submitted to the group of Prof. J. ENDERLEIN, Department of Physics, Göttingen, whereas the acceptor dye will be attached via the maleimide function.

5.3 Conclusion

Synthesis of small ultrafast folding proteins and site-specific labeling of key residues within the peptide and at the termini, respectively, was performed. Numerous derivatives **78**, **81**, **82**, **84**-**86**, either from the HTH EnHD domain, a protein with an α-helical substructure as well as from the WW domain (**87**-**89**) containing a three-stranded antiparallel β-sheet were synthesized. Though, only attachment of a single fluorescent dye was feasible. Several approaches to generate double-labeled constructs were investigated, but it is assumed that charge-charge interaction of the fluorescent dyes were impeding each other for coupling. After coupling of the first dye an anion was generated, whereupon the second dye, comprising also numerous negative charges, was electrostaticly repulsed. Test reactions with inversed deprotection-labeling strategy produced only single-labeled proteins, therefore, both fluorescent dyes were individually coupled. Interferences from resin loading could also be excluded. Synthesis of the HTH derivatives was carried out on a chlorotrityl-resin, followed by cleavage with HFIP in DCM yielded the fully protected peptide. These double-labeling experiments were also performed with no results.

Combining experimental data with computer simulation is required for understanding folding pathways at the molecular level. Therefore, additional Molecular Dynamics (MD) simulations are applied in the group of Prof. H. GRUBMÜLLER, MPI for biophysical Chemistry, Göttingen. For calculations of folding dynamics of the double-labeled HTH motif Timo GRAEN started to develop a suitable smFRET-MD simulation program during his bachelor thesis (Figure 56).[240]

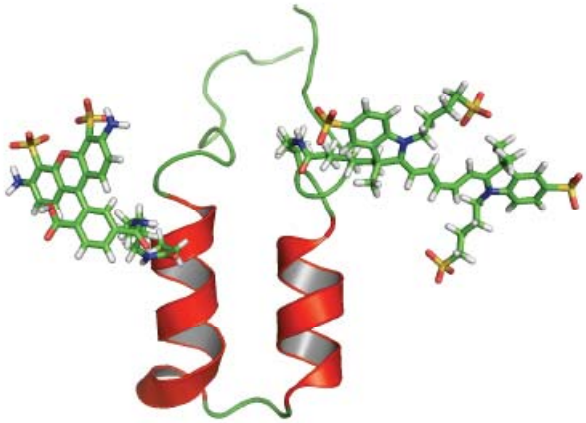

Figure 56. *The HTH motif with Alexa 488 (left) and Alexa 647 (right). Picture from Timo GRAEN, Group of Prof. H. GRUBMÜLLER, MPI for biophysical Chemistry, Göttingen, bachelor thesis.*

Chapter 6

Summary

6.1 Inhibition of the α-SNAP/NSF Mediated SNARE Complex Disassembly

Fusion of vesicles with the cell membrane is a basic requirement for exocytosis, and therefore, of neurotransmitter release. Work done by PALADE and coworkers in 1975 triggered the hypothesis that they are crucial intermediates of these communication pathways.[1] These vesicles exchange material by opening the pore after docking to the target membrane. Firstly, they bud from the starting compartment and moved to the target compartment, where they dock and fuse. Decisive processes are mediated by specific soluble and membrane-resident proteins and are highly regulated. Fusion with acceptor compartments requires the function of SNAREs, which are present on two opposed membranes. These membrane associated proteins are able to form thermodynamically stable complexes that merge the opposed membranes, finally resulting in membrane fusion.[2-4] The neuronal SNARE complex forms a parallel four-helix bundle between the three proteins Syntaxin-1, Synaptobrevin-2 and SNAP-25.[7] After fusion, the SNARE proteins are recovered for further rounds of fusion.[9] This disassembly process depends on the ATPase NSF and its cofactor α-SNAP. Little is known about exact mechanistical properties of the disassembly. It is commonly believed that α-SNAP binds to the lateral side of the SNARE complex surrounding the '0'-layer. NSF binds to the SNARE-SNAP complex at the end opposite to the SNARE membrane anchors and via ATP-ADP hydrolysis the individual SNARE complexes are recycled.[91] Without α-SNAP no disassembly occurs.

Inhibition or at least deceleration of the disassembly event could help to clarify molecular mechanisms. In order to generate such an inhibitor, the SNARE motif of Synaptobrevin, one of the SNARE proteins, was chosen as scaffold. By introducing amino acid building blocks with an exchanged charge regarding the natural ones or with a bulky side chain, interaction of the α-SNAP molecules might be prevented. For this purpose, numerous derivatives with individual replaced residues were synthesized by Fmoc solid phase peptide synthesis. Initially, selected acidic amino acids (Asp-51, Glu-55 and Asp-65), which were identified to promote important interactions within the α-SNAP-SNARE complex recognition,[12] were mutated by basic lysines. In another approach, an amino acid building block with a voluminous side chain was incorporated in the SNARE motif of Synaptobrevin in order to prevent α-SNAP recognition due to sterical reasons. Residues in the sequence which are located near the '0'-layer and directed towards the α-SNAP were exchanged by the non-natural adamantyl building block, containing a voluminous adamantyl side chain. Several peptides with various numbers of the synthetic bulky amino acid building block were synthesized. Asp-51, Glu-55 and Asp-65 as well as each Asp-57, Gln-58 and Glu-62, located next to the '0'-layer, were exchanged. Except for derivative **11** with introduced lysines, all peptides were successfully assembled with their natural counterparts Syntaxin and SNAP-25 leading to SNARE complexes. Peptides missing terminal amino acids, comprising only residues 32-84 were also not capable of forming SNARE complexes. The assembled SNARE complexes containing the synthesized derivatives **16**, **17** and **20** were analyzed in NSF mediated disassembly assays regarding their capability of preventing α-SNAP recognition, and therefore, inhibition of the recycling of the individual SNARE proteins. Derivative **20** containing an adamantyl building block at position 58 was found to inhibit the α-SNAP/NSF mediated disassembly compared with the SNARE complex including the *wild type* Synaptobrevin. These findings may result in the conclusion that probably one of the three SNARE/SNAP interaction sites was identified being decisive over the other. Whether mutations of α-SNAP primary influence interactions to one, two, or each of the SNARE complex sites or whether the mutations impair only one decisive site, and thereby, disrupt cooperative bindings is not investigated to date.

Complexins are regulation factors responsible for assembling the SNARE complex. Nevertheless, the exact role of Complexin is controversially discussed. Several studies indicate that Complexins might inhibit the disassembly progress by

replacing α-SNAP.[13] Meanwhile, the association mode of Complexin and the SNARE core complex has been investigated.[7] An α-helical central stretch consisting of 22 amino acids (residues 48 to 70) was identified to bind the SNARE complex in an antiparallel fashion. It interacts only to the assembled SNARE complex in the groove between the Synaptobrevin and the Syntaxin helices.[8]

The β-peptide mimic of Complexin could benefit from the well-defined and rigid structure of the typical β-peptidic 14-helical structure. Five important amino acid residues were identified to interact with the SNARE proteins. With respect to the three arginines, two tyrosines and one lysine, and by using β^3-homovaline building blocks known to promote a 14-helix a β-Complexin-mimic was synthesized. Investigation of the secondary structure by CD spectroscopy confirmed the 14-helical secondary structure. Nevertheless, the assembly assay with the preassembled SNARE complex indicated no formation of a SNARE/Complexin mimic complex. Further experiments such as FRET and fluorescence anisotropy could clarify the preliminary results. Additionally, introduction of rigid ACHC β-amino acid building blocks would enhance the 14-helical formation.

Furthermore, several Complexin derivates comprising the SNARE complex binding fragment were synthesized. These peptides were designed for stabilizing the SNARE complex binding properties of the Complexin fragment by enhancing the α-helical propensity. Therefore, the binding fragment of Complexin (residues 48-70) was elongated with α-amino acids, known to promote the α-helical propensity. Though, all of these peptides were capable of forming an α-helical structure. Data from SDS gel assays appear two derivatives could actually be recognized and bound the SNARE complex, thereby, providing a Complexin mimic/SNARE complex adduct, but further experiments for clarity are required.

6.2 Synthesis of Independently Folding Domains for Investigation of Folding Dynamics using smFRET

Single-molecule fluorescence methods provide new tools for the study of biological systems, especially the conformational dynamics and interactions of peptides and proteins.[11] Full comprehension of protein-folding mechanisms assumes specified characterization of microscopic pathways connecting the folded and unfolded states.[177] One of the benefits of smFRET is its capability to monitor single folding and unfolding events as well as interior structural

occurences among conformers in the folded and unfolded state by using the important Förster resonance energy transfer (FRET).[177] The method was refined within the last decade, but in order to be able to elucidate more complex dynamics it is necessary to investigate further and also different folding pathways.

Therefore, small independently and ultrafast folding domains were synthesized and labeled with potent fluorescent dyes. The HTH EnHD motif and the WW domain (named after its two highly conserved thyrosine residues) were chosen as applicable model systems containing α-helical- and β-sheet-structures.

Numerous derivatives of the HTH motif and the WW domain were synthesized and labeled at different residues. Initially, orthogonally protected HTH derivatives were synthesized and labeled with the required Alexa fluorescent dyes. Investigation of some of these derivatives by CD spectroscopy displayed no influence of the bulky fluorophores regarding secondary structures. Additionally, the whole sequence of the WW domain was generated.

Chapter 7

Experimental Part

7. 1 Materials and Characterization

Solvents were the highest grade available. Dry solvents like DMF and THF were purchased from *Fluka* (Taufkirchen, Germany) and were stored over molecular sieves (4 Å). Acetonitrile and Methanol (HPLC grade) were obtained from *Acros Organics* (Geel, Belgium), *Fisher Scientific* (Nidderau, Germany) or *VWR* (Fontenay-sous-Bois, France). All technical solvents, used for flash chromatography were distilled prior to use. Ultra pure water was obtained using the water purification unit *Simplicity* (*Millipore*, Bedford, UK).

Reagents were of analytical grade and used as supplied. All Chemicals were purchased from *ABCR* (Karlsruhe, Germany), *Acros Organics* (Geel, Belgium), *Alfa Aesar* (Karlsruhe, Germany), *Biorad* (Richmond, USA), *Carl Roth GmbH* (Karlsruhe, Germany), *Fluka* (Taufkirchen, Germany), *Merck* (Darmstadt, Germany), *Lancaster* (Karlsruhe, Germany), *Sigma-Aldrich* (Taufkirchen, Germany) and *VWR* (Fontenay-sous-Bois, France). Amino acid derivatives as well as coupling reagents and resins for the solid phase synthesis were purchased from *Bachem* (Bubendorf, Switzerland), *GL Biochem* (Shanghai, China), *IRIS Biotech* (Marktredwitz, Germany), *Merck* (Darmstadt, Germany) and *NovaBiochem* (Darmstadt, Germany). Fluorescent labels were purchased from *Invitrogen* (Darmstadt, Germany) and *Atto-Tech GmbH* (Siegen, Germany).

Protein Constructs were expressed and purified according known to literature[5,241-243] and were obtained from the laboratory of Prof. Reinhard JAHN (MPI for Biophysical Chemistry, Göttingen, Germany). The neuronal SNARE

proteins used in this study were Syntaxin 1A (H3 domain, residues 180-262 (without transmembrane domain), residues 183-288 (with transmembrane domain)), SNAP-25 (cysteine-less variant, residues 1-206) and Synaptobrevin 2 (residues 1-96 (without transmembrane domain), residues 30-89 (only SNARE motif). The α-SNAP and the AAA ATPase NSF (Chinese hamster ovary, residues 1-744 in pET28a (His tag)) were obtained from the JAHN group, too. Antibodys for Western Blotting were purchased from *Synaptic Systems* (Göttingen, Germany).

Reactions under inert atmosphere (argon or nitrogen) were performed in heat dried glass equipment.

Flash chromatography (FC) was performed using *Merck* silica gel 60 (40-63 µm) at 0.5-1.5 bar pressure. The used solvent mixtures are stated below.

Thin layer chromatography (TLC) was carried out using *Merck* coated aluminum sheets of silica gel F_{254}. Substances were detected under UV at 254 nm and/or by treatment with 3.00 % ninhydrine in ethanol followed by heating.

High performance liquid chromatography (HPLC) was performed using different devices. A *Pharmacia Äkta basic* system (*GE Healthcare*, London, UK) with a pump type *P-900*, variable wavelength detector *UV-900* using a linear gradient of A (0.1 % TFA in H_2O) to B (0.1 % TFA in acetonitrile:H_2O 8:2) and a *Jasco* system (Groß-Umstadt, Germany) with two pumps *PU-2080Plus*, a programmable UV detector *UV-875* and an online degasser *PG-208053* using a linear gradient of A (0.1 % TFA in H_2O) to B (0.1 % TFA in acetonitrile) were used to purify the synthesized peptides. A micro HPLC system (*Jasco*, Groß-Umstadt, Germany) equipped with two pumps *PU2080Plus*, a diode array multi wavelength detector *MD2010Plus*, a column thermostat *CO-2060Plus* and an autosampler unit *AS-2055Plus* using a linear gradient of A (0.1 % TFA in H_2O) to B (0.1 % TFA in acetonitrile) was used to analyze the purity of the peptides and building blocks.
Peptides and proteins were purified and analyzed using the following columns and flow rates: i) *YMC-Pack* column ODS-A, RP-C18, 250x4.6 mm, 4 µm, 80 Å, with a flow of 1 mL min^{-1}, ii) *Jasco Reprosil* 100 ODS-A column, RP-C18, 250x4.6 mm, 5 µm, 100 Å, with a flow of 1 mL min^{-1}, iii) *Phenomenex Jupiter* RP-C18, 250x4.6 mm, 5 µm, 300 Å, with a flow of 1 mL min^{-1}, iv) Sephadex™ 300/10 GL, with a flow of 0.2 mL min^{-1}, v) *Phenomenex Jupiter* RP-C18, 250x10 mm, 5 µm, 300 Å, with a flow of 3 mL min^{-1}, vi) *Jasco Reprosil* 100 ODS-A column, RP-C18, 250x10 mm, 5 µm, 100 Å, with a flow of 1 mL min^{-1}, vii) *YMC-Pack* column ODS-A, RP-C18, 250x20 mm, 4 µm, 80 Å, with a flow of 10 mL min^{-1}.

The UV-absorption was detected at 215, 254 and 280 nm for regular peptides and protein constructs. If the derivatives were labeled with Alexa 488, Alexa 647, Atto 488 or/and Atto 647 the UV-absorptions were recorded at 488 or 647 nm instead of the detection at 254 and/or 280 nm.

Lyophilization of peptides or building blocks from aqueous solutions and mixtures containing small amounts of acetonitrile was carried out using a *Christ Alpha 2-4 lyophilizer* equipped with a high vacuum pump. A *Christ RVC-2-18* centrifuge, connected to the lyophilization unit was used for small amounts.

Electrospray ionization mass spectra (ESI-MS) were obtained from a *Finnigan* instrument (type *LGC* or *TSQ 7000*). High resolution spectra were performed on a *Bruker* spectrometer (type *Apex-Q IV 7T*).

^{1}H- and ^{13}C nuclear magnetic resonance spectra (NMR) were recorded with a *Varian Unity 300* spectrometer or a *Varian Inova 600* spectrometer. Chemical shifts (δ) were denoted in parts per million (ppm) downfield of TMS. Abbreviations for signals are: s (singlet), d (doublet), t (triplet), q (quartet), m (multiplet), bs (broad singlet). Coupling constants are given in Hz.

Circular dichroism spectroscopy (CD) was performed on a *Jasco-810* spectropolarimeter (Groß-Umstadt, Germany) equipped with a *Jasco PTC432S* temperature controller. The sample cell was flushed with nitrogen. All measurements were carried out in a 10 mM Tris·HCl buffer (pH = 7.5). The peptide concentrations were adjusted to 10 µM. The spectra were recorded at 20 °C in a wavelength range of 350-195 nm with 1.0 bandwidth, using the 'continuous mode', 1.0 s response, a scan speed of 50 nm min^{-1} and an average of five spectra. The spectra were background-corrected against the buffer.

UV-spectroscopy (UV) were performed with a *Jasco V-550* UV spectrometer (Gross-Umstadt, Germany).

Concentrations of the peptide constructs **8**-**11** and **13**-**23** were determined using UV-absorption at 595 nm with the BRADFORD protein assay.[244] A series of protein standard concentrations (0, 1, 2, 3, 4 and 6 µg mL^{-1}) using BSA (*bovine serum albumin*) were prepared. Also a dilution series of the unknown sample were prepared. All samples were filled up with distilled water to a volume of 200 µL and afterwards with 800 µL of the Bradford reagent. After 5 min each of the samples was measured at 595 nm by UV spectroscopy. Each standard concentration was measured twice and the unknown samples threefold. With the calibration curve of the standard samples the concentrations of the unknown

samples could be calculated. The concentration of the complexin derivatives **73-77** were determined using UV-absorption at 280 nm. Therefore the absorption of the tyrosine residue (ε_{280nm} = 1280 L mol^{-1} cm^{-1}) was recorded. Concentrations were calculated using *Lambert-Beer´s* law.

SDS polyacrylamide gel electrophoresis (SDS-PAGE) was carried out using the protocol reported by U. K. LAEMMLI.[190] A stock solution of 30 % (*w/v*) acrylamide and 0.8 % (*w/v*) bisacrylamide was prepared. Seperating gels with 12 % and 16 % (*w/v*) acrylamide (1.5 M Tris-HCl, pH = 8.8, 0.4 % (*w/v*) SDS) and stacking gels (5.0 % (*w/v*)) acrylamide, 0.5 M Tris-HCl, pH = 6.8, 0.4 % (*w/v*) SDS were used. The electrophoresis was performed at 150 V for approximately 1 h.[245]

Coomassie staining was performed using staining solutions A-C (A: Coomassie® brilliant blue R 250 (500 mg), water (650 mL), isopropanol (250 mL), acetic acid (100 mL), B: Coomassie® brilliant blue R 250 (50.0 mg), water (800 mL), isopropanol (100 mL), acetic acid (100 mL), C: Coomassie® brilliant blue R 250 (20.0 mg), water (900 mL), acetic acid (100 mL) and microwave heating for approximately 30 s. After slightly agitation for 5 min in each case the gels were destained with solution D (10 % (*v/v*) acetic acid in water).[246]

Colloidal staining for sensitive staining of protein gels was performed using the Staining Kit purchased at *Invitrogen* (Darmstadt, Germany). First the gel was agitated in a fixing solution (20 mL ultrapure water, 25 mL methanol and 5 mL acetic acid) for 10 min. Afterwards, the gel was washed twice with water. Then, the staining solution (27.5 mL deionized water, 10 mL methanol, 10 mL Stainer A) was allowed to react with the gel by gentle agitation before 2.5 mL Stainer B was added. The gel was shaked in the staining solution for 4 h. Afterwards, the solution was decanted and the gel was washed with ultrapure water, until the background was clear.[247]

Semi dry Western blotting was carried out by transferring the proteins to a nitrocellulose membrane after gel electrophoresis. Therefore, the gel and the membrane were sandwiched between blotting papers (GB003, *Schleicher* & *Schuell*, Dassel, Germany), soaked with transfer buffer (25.0 mM Tris-HCl, pH = 8.3, 193 mM glycine, 20 % (*v/v*) methanol, 0.1 % SDS), before the transfer was performed at a constant voltage of 50 mA for 1 h. Afterwards, the membrane was washed twice with blocking solution (5.0 % (*w/v*)) dry milk powder, 0.1 % Tween 20 in PBS) each for 10 min while agitation. After washing, the primary antibody (Cell Line 71.1, for SN-25), which was diluted 1000 times in blocking solution, was added to the membrane and 2 h slightly agitated. After the

incubation time, the membrane was washed three times with the blocking solution to remove unspecifically bound antibodys. Afterwards, the secondary antibody (2000 times diluted) was added to the membrane and was allowed to incubate overnight at 4 °C. Finally the membrane was washed twice with PBS buffer. The membrane was treated with horseradish peroxidase, which emits luminescence after the addition of chemoluminescence reagent (*Perkin Elmer*, Waltham, USA) to visualize the proteins. The luminescence was detected using the luminescent image analyzer.

7.2 General Procedures

General β^3-amino acid building block synthesis was performed in two steps:

GP 1: The diazo ketone synthesis
Under inert atmosphere the *N*-Boc-protected amino acid (1.00 eq) was dissolved in dry THF. At -20 °C triethylamine (1.10 eq) and isobutylchloroformiate (1.10 eq) were added to the solution. After 30 min at 0 °C the reaction vessel was protected against sunlight and cooled to -15 °C. A solution of diazomethane in diethyl ether (0.3-0.4 M, 2.00 eq) was added. The mixture was allowed to warm up to room temperature and then stirred for 5 h. Excess diazomethane was destroyed by addition of a small amount of glacial acetic acid. After aqueous workup by extraction with satd. $NaHCO_3$, NH_4Cl and NaCl solutions, the organic solution was separated and dried over Na_2SO_4. After the solvent was evaporated, the residue was purificated via chromatography silica gel to afford the pure diazo ketone.

GP 2: The β^3-amino acid synthesis
The diazo ketone (1.00 eq) was dissolved in THF/water (60.0 mL, 9:1) with exclusion of light. At -20 °C silver benzoate (0.11 eq), dissolved in triethylamine (3.00 eq) was added. The mixture was allowed to warm to room temperature and stirred for 3-12 h till complete conversion. For Fmoc-building blocks, the triethylamine was omitted and the reaction was carried out by sonication. The solvent was removed under reduced pressure and the residue was taken up in diethyl ether. The organic phase was extracted with $NaHCO_3$ (3 x 30.0 mL). After this the aqueous phase was carefully adjusted to pH = 2 with 2 M HCl. After extraction of the aqueous phase with ethyl acetate and evaporation of the solvent and chromatography on silica gel, the β^3-amino acid was isolated.

Resin loading with the first amino acid was required if the pre-loaded resin was not purchasable. According to the required *C*-terminal end of the peptides or the used SPPS protocol different resins were loaded. If possible (Fmoc-SPPS), the loading density was estimated via UV-analysis of the Fmoc-dibenzofulven deprotection product at 304 nm (see below). All resins were loaded according to known literature.[248] For loading of *NovaSyn®TGR resin* or *MBHA polystyrene resin* the dry resins were transferred in an acid/base resistant syringe, equipped with a polyethylene frit and initially swollen in DCM (1 h) and afterwards in NMP or DMF (1 h). The required amino acid building block (5.00 eq), HOBt (5.00 eq) and HBTU (5.00 eq) were dissolved in a minimum of DMF. After addition of DIC

(5.00 eq), the reaction mixture was preactivated for 2-3 min. Afterwards, the mixture was transferred to the syringe and agitated for 2 h. Then the resin was washed threefold with NMP, twice with DCM and threefold with NMP again. For loading of *Wang resin* the dry resin was transferred in a dry flask and flushed with argon. The resin was swollen in dry DCM (1 h). The required amino acid (5.00 eq) was dissolved in dry DCM in a separate flask. MeIm (3.75 eq) and MSNT (5.00 eq) were added and stirred until MSNT was dissolved. The reaction mixture was transferred into the flask with the swollen resin and agitated gently at room temperature for 1 h. Afterwards, the resin was transferred into a syringe as described above and washed with DCM (2 x) and NMP (3 x). If necessary, the loading procedure was repeated. After resin loading the remaining free amine functions were capped applying Ac_2O (20 % (*v/v*)) and DIEA (5.0 % (*v/v*)) in NMP for 2 x 10 min. The resins were dried over KOH under reduced pressure.

Estimation of level of first residue attachment was performed via UV-absorbtion measurements.[248] Therefore 5.00 mg of the resin were deprotected with 2.00 mL of DBU in NMP by gentle agitation for 1 h. Afterwards the deprotection solution was transferred into another flask and filled with acetonitrile up to 10.0 mL. The solution was further diluted with acetonitrile (1:12.5) and transferred to an UV precision cell. The absorbtion of the cleaved Fmoc-dibenzofulven species was detected at 304 nm (ε_{304} = 7624 L mol^{-1} cm^{-1}) and corrected against the reference.[249] The resin loading was calculated using *Lambert-Beer´s* law.

General automated SPPS was realized on different peptide synthesizers. Firstly, an automated *ABI 221* peptide synthesizer (*Applied Biosystems*, Norwalk, USA) was used. The standard Fmoc-protocol FastMoc 0.1MonΩPrevPeak, including capping and non-conditional double couplings for particular amino acids was selected using the 0.1 mmol scale. The Fmoc-protecting group was removed by treatment with piperidine (20 % in NMP, *v/v*). The efficiency of the Fmoc-deprotection was automatically monitored via a conductivity cell and was repeated if necessary. Each coupling step was carried out by activation of 5.00 eq of the required Fmoc-protected amino acid with 3.90 eq of HBTU, 4.00 eq HOBt and 10.0 eq of DIEA (0.5 M). Alternatively, the *Liberty®*12-Channel automated Peptide Synthesizer from *CEM* (Kamp-Lintfort, Germany), equipped with a *Discover* microwave (MW) reaction cavity (*CEM*) was used for automated peptide synthesis. Standard Fmoc-amino acid building blocks containing standard side chain protection groups, reagents, protocols and procedures were used for

deprotection (20 % piperidine in NMP), coupling steps (HBTU, HOBt, DIEA, NMP) and capping (Ac_2O/DIEA/NMP 1:1:8).
Special side chain protected Fmoc-amino acid building blocks used were Fmoc-Lys(Mtt)-OH, which was deprotected with 1% TFA in DCM for 1 h and Fmoc-Lys(Alloc)-OH and Fmoc-Glu(OAll)-OH, which were deprotected using $Pd(PPH_3)_4$ (0.1 eq) and $MeNH{\cdot}BH_3$ (40 eq) in DMF under inert atmosphere for 4 h.
Double couplings were usually performed for Arg-, Ile-, Phe-, Trp- and Tyr-residues.

General manual SPPS was carried out in polypropylene fritted syringes in 12.5-50 µmol scales. The resins initially were swollen in DCM (1 h) and afterwards in NMP or DMF (1 h). According to the *N*-terminal protection group the conditions for removal were adapted. The Fmoc-protection group was removed using 20 % piperidine in NMP (*v/v*, 2 x 10 min), whereas the *N*-terminal Boc-group was deprotected with a mixture of TFA:*m*-cresol (95:5 (*v/v*), 3 x 3 min). After filtration, the resins were washed with NMP or DMF (5 x), DCM (5 x) and NMP or DMF (5 x). The coupling step was carried out by dissolving the amino acid building block (5.00 eq), HBTU (5.00 eq) and HOBt (5.00 eq) respectively HATU and HOAt (each 5.00 eq) for the Boc-SPPS protocol, in a minimum of NMP or DMF. As activator base DIEA (10 eq) was added. After incubation time of 2-3 min the reaction mixture was transferred into the syringe containing the resin. Standard coupling time for α-amino acid building blocks was 30 min at room temperature. The Boc-β-amino acid building blocks were allowed to react for 1 h at 90 °C. Double couplings were usually performed for Arg-, Ile- and Phe-residues, as well as for all α-amino acid building blocks used in the synthesis of the SNARE derivatives (**13-23**) after amino acid 45, combined with a reaction time of 45 min. All Boc-β-amino acid building blocks were double coupled, too. Because of the possibility of racemisation of Fmoc-Cys(Trt)-OH the activator base was exchanged to *sym*-collidine (5.00 eq) and the reaction was carried out in DCM.[250] After coupling, the resin was filtrated and washed with NMP or DMF (5 x), DCM (3 x) and NMP or DMF (5 x) and the free amino groups were capped (DMF/DIEA/Ac_2O (8:1:1)). After coupling of the last amino acid the resin was washed with NMP or DMF (3 x), DCM (3 x) and NMP or DCM (3 x) and dried over KOH under reduced pressure.

General Cleavage from the resin was carried out regarding the performed SPPS protocol.
Peptides, synthesized according standard Fmoc-protocol were cleaved by standard TFA cleavage (TFA/EDT/H_2O/TES 94:2.5:2.5:1 (*v/v/v/v*)) using moderate

scavengers. The cleavage was usually carried out for 2 h at room temperature. Afterwards the resin was filtered and washed with TFA (3 x).
The β-peptides, synthesized via Boc-SPPS were cleaved using TMSOTf cleavage. For the cleavage the resin was transferred in a small flask and cooled at 0 °C. The cleavage mixture TFA/TMSOTf/*m*-cresol (5.75:1.6/1), cooled as well, was added to the resin and afterwards was agitated gently at 0 °C for 2 h.[248] Afterwards the resin was filtered and washed with TFA (3 x).

General Post-Cleavage Work-Up was performed by removing TFA under reduced pressure. The crude peptide was isolated by precipitation from cold MTBE (−15 to −20 °C). The resulting suspension was centrifuged at -20 °C. The supernatant was discarded and the remaining pellet was washed twice with MTBE and dried over KOH under reduced pressure. The crude peptide was dissolved in water/acetonitrile and filtered before this peptide solution was purified by preparative RP-HPLC.

Assembly of the SNARE complexes was performed using Syntaxin (H3 domain), SNAP-25, and Synaptobrevin (or its derivatives) in a 1:1:2 ratio. They were incubated overnight at 4 °C. Successful complex formation was verified by SDS PAGE and Coomassie Blue staining.

The Complexin/SNARE complex was prepared by addition of 5.00 eq of the complexin derivatives **73** and **74**-**77** to the preassembled SNARE complex followed by an overnight incubation. Complex formation was checked by nondenaturing PAGE.[14]

Disassembly of the minimal core complex was carried out by addition of equal amounts of NSF and a 14-fold excess of α-SNAP, 2 mM $MgCl_2$ and 5 mM ATP to the SNARE complex.[189] The disassembly reaction was performed in a buffer, containing 50 mM HEPES, pH = 7.4, 120 mM KGlu and 20 mM KAc for 5, 10, 15, 30 and 60 min at 37 °C and subsequent stopped by adding SDS sample buffer. As a negative control on the one hand the ATPase activity of NSF was abolished by replacing $MgCl_2$ with 10 mM EDTA, on the other hand the SNARE complex was heated to 97 °C for 5 min. All samples were analyzed by SDS-PAGE and Coomassie Blue or Colloidal staining or Western Blotting.

Peptide labeling was carried out with different fluorophors (Alexa 647 succinimidyl esters, Alexa 488 cadaverine, Atto 647- and Atto 488 NHS-ester) on solid phase at the fully-protected peptide only providing one free amino-functionality or in case of the Alexa 488 cadaverine the free carboxy-functionality

of the glutamic acid. Therefore, amino acid building blocks with orthogonally protected side chains were introduced, the exact description of the deprotection conditions are described for the respective peptides, below.
For fluorophor labeling the succinimidyl esters (3.00 eq), were dissolved in a minimum of dry DMF and activated with PyBOP® (3.90 eq) and DIEA (10 eq). This reaction mixture was transferred to the preswollen resin (1.00 eq) and allowed to react for 2 d while gently agitation under exclusion from light. Afterwards the resin was filtered, washed with DMF (5 x) and DCM (5 x) and dried over KOH under reduced pressure prior to cleavage.

7.3 Building Block Synthesis

7.3.1 Synthesis of the *N*-Fmoc-adamantyl-amino acid building block

(**26**) (*S*)-(*tert*-Butoxycarbonyl)-2-(9-fluorenylmethyloxycarbonyl)-4-(1-adamantylamino)-oxobutane

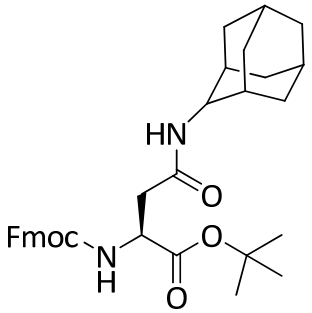

26

$C_{33}H_{40}N_2O_5$ [544.70]

N-Fmoc-Asp-O*t*Bu (**24**) (0.67 g, 1.62 mmol, 1.50 eq), HOBt (0.22 mg, 1.62 mmol, 1.50 eq) and HBTU (0.61 mg, 1.62 mmol, 1.50 eq) were dissolved in a minimum of DMF (3.5 mL) and activated with DIEA (0.09 mL, 0.53 mmol, 2.00 eq). The reaction mixture was stirred for 3 min, before 1-adamantylaminohydrochloride (**25**) (0.20 mg, 1.08 mmol, 1.00 eq) in DMF (1.50 mL) was added and allowed to react overnight. Afterwards, the solvent was removed under reduced pressure and the residue was dissolved in ethyl acetate. The organic layer was washed with 0.1 M HCl solution (3 x 10.0 mL), saturated aqueous NaCl solution (10.0 mL), 0.5 M aqueous $NaHCO_3$ solution (3 x 10.0 mL) and saturated aqueous NaCl solution (10.0 mL), then, dried over Na_2SO_4. The solvent was removed under reduced pressure. The residue was purified by flash chromatography (eluent: ethyl acetate/pentane 1:1) to furnish **26** as a light brown foam (0.57 mg, 1.04 mmol, 96 %).

Analytical data: **TLC** (ethyl acetate/pentane 1:1) R_f = 0.69. **^{1}H-NMR** (300 MHz, $CDCl_3$, rt) δ = 1.42 (bs, 11 H, adamantyl-CH, *t*-Bu), 1.61 (bs, 5 H, adamantyl-CH), 1.95 (bs, 9 H, adamantyl-CH, adamantyl-CH_2), 2.52-2.79 (m, 2 H, β-H_2), 4.18-4.41 (m, 2 H, Fmoc-CH, α-H), 7.24-7.58 (m, 6 H, Fmoc-CH), 7.76 (d, $^3J_{H,H}$ = 7.1 Hz, 2 H, Fmoc-CH), 8.00 (bs, 2 H, NH). **ESI-MS** (m/z): 545.51 $[M+H]^+$. **HRMS** (ESI): 545.30100 $[M+H]^+$ (calcd. for $C_{33}H_{41}N_2O_5$: 545.29372), 567.28294 $[M+Na]^+$ (calcd. for $C_{33}H_{40}N_2O_5Na$: 567.28349).

(**12**) (*S*)-2-(9-Fluorenylmethyloxycarbonyl)-4-(1-adamantylamino)-4-oxobutanoic acid

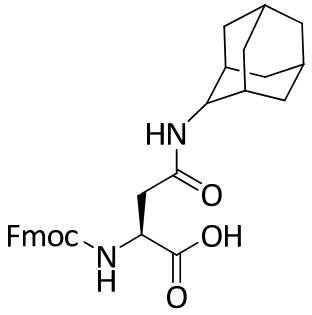

12

$C_{29}H_{32}N_2O_5$ [488.59]

26 (0.57 mg, 1.04 mmol) was stirred in TFA (95%, 2.00 mL) for 1 h. Afterwards, the TFA was removed under reduced pressure. The residue was dissolved in ethyl acetate. The organic layer was washed with 0.1 M HCl solution (3 x 10.0 mL), saturated aqueous NaCl solution (10.0 mL), 0.5 M $NaHCO_3$ solution (3 x 10.0 mL) and saturated aqueous NaCl-solution (10.0 mL) and dried over Na_2SO_4. The organic layer was then removed under reduced pressure. The residue was purified by flash chromatography (eluent: DCM/methanol 9:1) to furnish **12** as a white foam (0.54 mg, 1.11 mmol, 97 %).

Analytical data: **TLC** (DCM/methanol 9:1) R_f = 0.27. **^{1}H-NMR** (300 MHz, $CDCl_3$, rt) δ = 1.61 (bs, 11 H, adamantyl-CH), 1.95 (bs, 5 H, adamantyl-CH), 2.06 (bs, 9 H, adamantyl-CH, adamantyl-CH_2), 2.63-2.88 (m, 2 H, β-H_2), 4.16-4.46 (m, 2 H, Fmoc-CH, α-H), 7.22-7.58 (m, 6 H, Fmoc-CH), 7.74 (d, $^3J_{H,H}$ = 7.2 Hz, 2 H, Fmoc-CH), 8.80 (bs, 2 H, NH). **ESI-MS** (m/z): 489.51 $[M+H]^+$, 511.65 $[M+Na]^+$. **HR-MS** (ESI): 489.23840 $[M+H]^+$ (calcd. for $C_{29}H_{33}N_2O_5$: 489.23112), 511.22034 $[M+Na]^+$ (calcd. for $C_{29}H_{32}N_2O_5Na$: 511.22089).

7.3.2 Synthesis of the *N*-Boc-β^3-amino acid building blocks

(**43**) (*S*)-7-(Benzyloxycarbonylamino)-3-(*tert*-butoxycarbonylamino)-1-diazoheptane-2-one

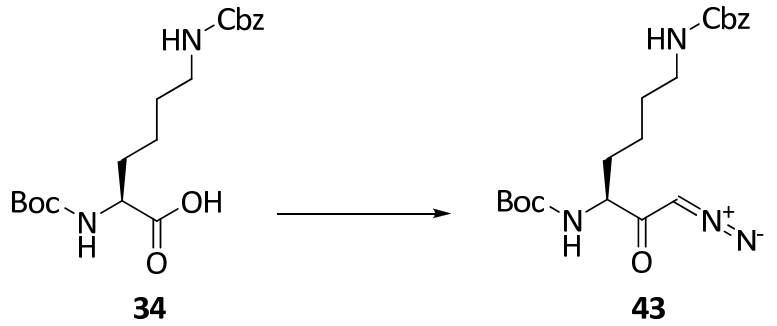

34 $C_{19}H_{28}N_2O_6$ [380.44]

43 $C_{20}H_{28}N_4O_5$ [404.47]

Starting with *N*-Boc-Lys-(Z)-OH (**34**) (3.00 g, 7.89 mmol, 1.00 eq) the synthesis was executed according to the general procedure described in **GP 1**. The crude residue was purified using flash chromatography on silica gel (ethyl acetate/pentane 2:3) to yield the pure product (2.81 g, 6.96 mmol, 88 %) as a yellow solid.

Analytical data: **TLC** (ethyl acetate/pentane 2:3) R_f = 0.54. **^{1}H-NMR** (300 MHz, $CDCl_3$, rt): δ = 1.40-1.59 (m, 11 H, *t*-Bu, δ-H_2), 1.60-1.86 (m, 2 H, β-H_2), 3.13-3.27 (dt, $^3J_{H,H}$ = 6.1 Hz, $^3J_{H,H}$ = 6.3 Hz, 2 H, ε-H_2), 4.00-4.17 (m, 1 H, α-H), 4.98-5.16 (m, 1 H, Cbz-NH), 5.10 (s, 2 H, Cbz-CH), 5.16 (d, $^3J_{H,H}$ = 7.8 Hz, 1 H, Boc-NH), 5.45 (bs, 1 H, CHN_2), 7.30-7.41 (m, 5 H, Ph) ppm. **ESI-MS** *m/z* (%): 427.1 (99) $[M+Na]^+$, 830.8 (100) $[2M+Na]^+$.

(**52**) (*S*)-7-(Benzyloxycarbonylamino)-3-(*tert*-butoxycarbonylamino)-heptanoic acid

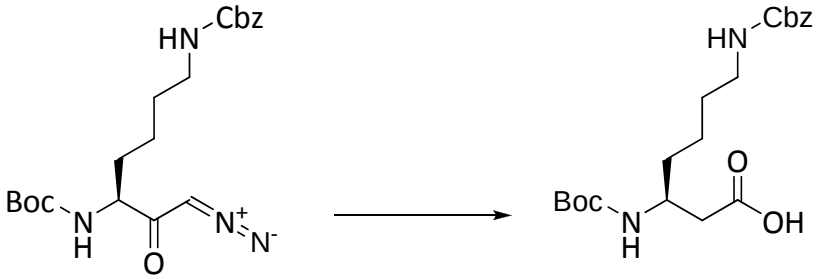

43 $C_{20}H_{28}N_4O_5$ [404.47] **52** $C_{20}H_{30}N_2O_6$ [394.47]

Starting with **43** (2.81 g, 6.96 mmol, 1.00 eq) the synthesis was executed according to the general procedure described in **GP 2**. The crude residue was purified using flash chromatography on silica gel (DCM/MeOH 2:3) to yield the pure product (1.87 g, 4.88 mmol, 72 %) as a white solid.

Analytical data: **TLC** (DCM/MeOH 2:3) R_f = 0.41. **^{1}H-NMR** (300 MHz, $CDCl_3$, rt): δ = 1.28-1.61 (m, 15 H, *t*-Bu, γ-H_2, δ-H_2, ε-H_2), 2.42-2.60 (m, 2 H, α-H_2), 3.10-3.24 (m, 2 H, ζ-H_2), 3.72-3.96 (m, 1 H, β-H), 4.90-5.01 (m, 1 H, Cbz-NH), 5.07 (s, 2 H, Cbz-CH_2), 5.93 (bs, 1 H, Boc-NH), 7.27-7.41 (m, 5 H, Ph) ppm. **ESI-MS** *m/z* (%): 417.2 (84) $[M+Na]^+$, 811.0 (100) $[2M+Na]^+$.

(**44**) (*S*)-3-(*tert*-Butoxycarbonylamino)-4-phenyloxy-benzyl-1-diazobutan-2-one

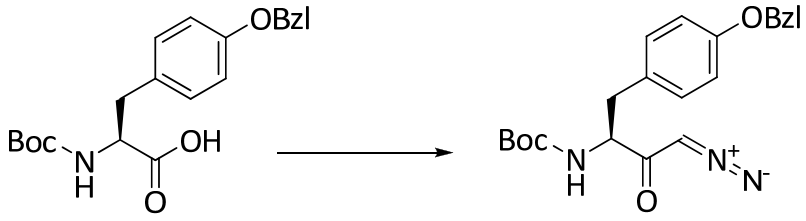

35 $C_{21}H_{25}NO_5$ [371.43]

44 $C_{22}H_{27}N_3O_4$ [395.45]

Starting with *N*-Boc-Tyr-(Bzl)-OH (**35**) (2.50 g, 6.74 mmol, 1.00 eq) the synthesis was executed according to the general procedure described in **GP 1**. The crude residue was purified using flash chromatography on silica gel (ethyl acetate/pentane 2:3) to yield the pure product (2.05 g, 5.18 mmol, 77 %) as a yellow solid.

Analytical data: **TLC** (ethyl acetate/pentane 2:3) R_f = 0.79. **^{1}H-NMR** (300 MHz, $CDCl_3$, rt): δ = 1.39 (s, 9 H, *t*-Bu), 2.96 (d, $^3J_{H,H}$ = 6.3 Hz, 2 H, β-H_2), 4.33-4.38 (m, 1 H, α-H), 5.10 (s, 2 H, CH_2-Ph), 5.16 (s, 1 H, NH), 6.78-6.86 (m, 2 H, *o*-H^{Tyr}), 7.05-7.12 (m, 2 H, *m*-H^{Tyr}), 7.44-7.65 (m, 5 H, Ph) ppm. **ESI-MS** *m/z* (%): 418.1 (70) $[M+Na]^+$, 812.8 (100) $[2M+Na]^+$.

(**53**) (*S*)-3-(*tert*-Butoxycarbonylamino)-4-phenyloxy-benzyl-butanoic acid

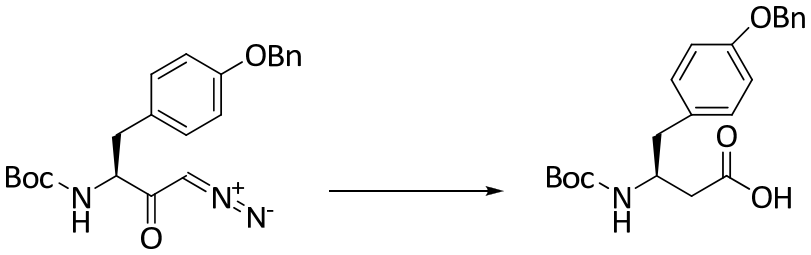

44 $C_{22}H_{27}N_3O_4$ [395.45]

53 $C_{22}H_{27}NO_5$ [385.45]

Starting with **44** (2.05 g, 5.18 mmol, 1.00 eq) the synthesis was executed according to the general procedure described in **GP 2**. The crude residue was purified using flash chromatography on silica gel (DCM/MeOH 9:1) to yield the pure product (1.87 g, 4.88 mmol, 70 %) as a white solid.

Analytical data: **TLC** (DCM/MeOH 1:1) R_f = 0.25. **^{1}H-NMR** (300 MHz, $CDCl_3$, rt): δ = 1.32 (s, 9 H, *t*-Bu), 2.30-2.34 (m, 2 H, γ-H_2), 2.65 (d, $^3J_{H,H}$ = 6.8 Hz, 2 H, α-H), 3.84-3.90 (m, 1 H, β-H), 5.06 (s, 2 H, CH_2Ph), 6.63 (d, $^3J_{H,H}$ = 7.8 Hz, 1 H, NH), 6.91-6.93 (m, 2 H, *m*-H^{Tyr}), 7.07-7.10 (m, 2 H, *o*-H^{Tyr}), 7.35-7.43 (m, 5 H, Ph) ppm. **ESI-MS** (*m*/*z*): 408.1 (84) $[M+Na]^+$, 793.0 (100) $[2M+Na]^+$.

(**47**) (*S*)-3-(*tert*-Butoxycarbonylamino)-4-methyl-1-diazo-pentan-1-one

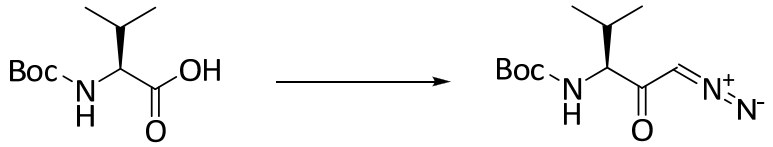

38 $C_{11}H_{19}NO_4$ [217.13]

47 $C_{12}H_{21}N_3O_3$ [241.28]

Starting with *N*-Boc-Val-OH (**38**) (3.00 g, 13.8 mmol, 1.00 eq) the synthesis was executed according to the general procedure described in **GP 1**. The crude residue was purified using flash chromatography on silica gel (ethyl acetate/pentane 2:3) to yield the pure product (2.94 g, 11.9 mmol, 86 %) as a yellow solid.

Analytical data: **TLC** (ethyl acetate/pentane 2:3) R_f = 0.69. **^{1}H-NMR** (300 MHz, $CDCl_3$, rt): δ = 0.86 (d, $^3J_{H,H}$ = 6.6 Hz, 3 H, CH_3), 0.96 (d, $^3J_{H,H}$ = 6.6 Hz, 3 H, CH_3), 1.41 (s, 9 H, *t*-Bu), 2.06-2.13 (m, 2 H, β-H), 3.96-4.10 (m, 1 H, α-H), 5.12 (s, 1 H, NH), 5.39 (s, 1 H, C*H*N_2) ppm. **ESI-MS**: (*m*/*z*): 278.4 (89) $[M+Na]^+$, 533.3 (100) $[2M+Na]^+$.

(**56**) (*S*)-3-(*tert*-Butoxycarbonylamino)-4-methyl-pentanoic acid

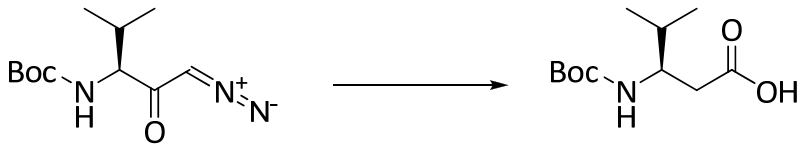

47 $C_{12}H_{21}N_3O_3$ [241.28] → **56** $C_{12}H_{21}NO_4$ [231.13]

Starting with **47** (2.94 g, 11.9 mmol, 1.00 eq) the synthesis was executed according to the general procedure described in **GP 2**. The crude residue was purified using flash chromatography on silica gel (DCM/MeOH 9:1) to yield the pure product (2.13 g, 9.23 mmol, 84 %) as a white solid.

Analytical data: **TLC** (DCM/MeOH 9:1) R_f = 0.56. **^{1}H-NMR** (300 MHz, $CDCl_3$, rt): δ = 0.94 (d, $^3J_{H,H}$ = 6.8 Hz, 6 H, 2 x CH_3), 1.44 (s, 9 H, *t*-Bu), 1.85 (m, 1 H, γ-H), 2.50-2.60 (m, 2 H, β-H), 3.69-3.82 (m, 1 H, α-H), 4.89 (d, $^3J_{H,H}$ = 8.4 Hz, 1 H, NH) ppm. **ESI-MS** (*m*/*z*): 254.1 (20) $[M+Na]^+$, 230.0 (68) $[2M-H]^-$.

(**46**) (*S*)-3-(*tert*-Butoxycarbonylamino)-4-methyl-1-diazo-hexan-1-one

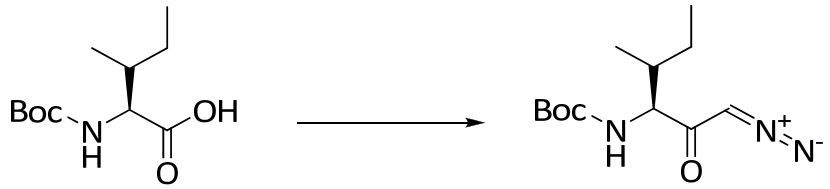

37 $C_{11}H_{21}NO_4$ [231.28] **46** $C_{12}H_{23}N_3O_3$ [255.16]

Starting with *N*-Boc-Ile-OH (**37**) (3.00 g, 13.0 mmol, 1.00 eq) the synthesis was executed according to the general procedure described in **GP 1**. The crude residue was purified using flash chromatography on silica gel (ethyl acetate/pentane 2:3) to yield the pure product (2.30 g, 8.95 mmol, 69 %) as a yellow solid.

Analytical data: **TLC** (ethyl acetate/pentane 2:3) R_f = 0.47. **^{1}H-NMR** (300 MHz, $CDCl_3$, rt): δ = 0.90 (t, $^3J_{H,H}$ = 7.6 Hz, 3 H, CH_3), 0.93 (d, $^3J_{H,H}$ = 7.1 Hz, 3 H, CH_3), 1.23 (s, 9 H, *t*-Bu), 1.25-1.31 (m, 2 H, $C\underline{H}_2CH_3$), 2.01-2.06 (m, 2 H, β-H), 4.05-4.19 (m, 1 H, α-H), 5.22 (s, 1 H, NH), 5.49 (s, 1 H, CHN_2) ppm. **ESI-MS** (*m/z*): 254.1 (20) $[M+Na]^+$, 230.0 (68) $[2M-H]^-$.

(**55**) (*S*)-3-(*tert*-Butoxycarbonylamino)-4-methyl-hexanoic acid

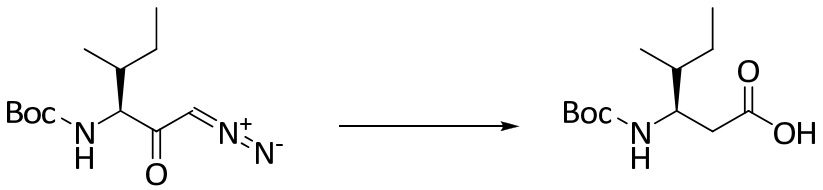

46 $C_{12}H_{23}N_3O_3$ [255.16] **55** $C_{12}H_{23}NO_4$ [245.28]

Starting with **46** (2.30 g, 8.95 mmol, 1.00 eq) the synthesis was executed according to the general procedure described in **GP 2**. The crude residue was purified using flash chromatography on silica gel (DCM/MeOH 9:1) to yield the pure product (2.13 g, 9.23 mmol, 78 %) as a white solid.

Analytical data: **TLC** (ethyl acetate/pentane 9:1) R_f = 0.47. **^{1}H-NMR** (300 MHz, $CDCl_3$, rt): δ = 0.81 (t, $^3J_{H,H}$ = 7.5 Hz, 3 H, $CH_2C\underline{H}_3$), 0.91 (d, $^3J_{H,H}$ = 7.1 Hz, 3 H, CH_3), 1.41 (s, 9 H, *t*-Bu), 1.50-1.59 (m, 2 H, $C\underline{H}_2CH_3$), 2.41-2.51 (m, 2 H, α-H), 3.78-3.84 (m, 1 H, β-H), 4.96 (d, $^3J_{H,H}$ = 8.4 Hz, 1 H, NH), 10.7 (s, 1 H, OH) ppm. **ESI-MS** (*m/z*): 268.1 (50) $[M+Na]^+$, 513.3 (40) $[2M+Na]^+$, 244.2 (100) $[M-H]^-$, 489.4 (20) $[2M-H]^-$.

(**49**) (*S*)-3-(*tert*-Butoxycarbonylamino)-6-(benzyloxy)-2,6-dioxo-1-diazo-heptan-1-one

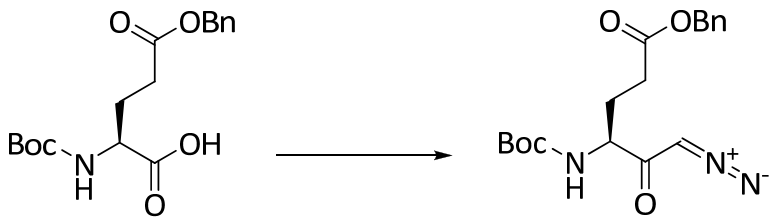

40 $C_{17}H_{23}NO_6$ [337.37] **49** $C_{18}H_{23}N_3O_5$ [361.39]

Starting with *N*-Boc-Glu-(OBzl)-OH (**40**) (4.00 g, 12.9 mmol, 1.00 eq) the synthesis was executed according to the general procedure described in **GP 1**. The crude residue was purified using flash chromatography on silica gel (ethyl acetate/pentane 1:1) to yield the pure product (3.65 g, 10.1 mmol, 78 %) as a yellow solid.

Analytical data: **TLC** (ethyl acetate/pentane 1:1) R_f = 0.43. **^{1}H-NMR** (300 MHz, $CDCl_3$, rt): δ = 1.40 (s, 9 H, *t*-Bu), 1.83-1.87 (m, 2 H, γ-H_2), 3.02 (d, $^3J_{H,H}$ = 6.6 Hz, 2 H, β-H), 4.41 -4.47 (m, 1 H, α-H), 5.07 (s, 2 H, CH_2Ph), 5.15 (s, 1 H, NH), 7.21-7.38 (m, 5 H, Ph) ppm.

(**58**) (*S*)-3-(*tert*-Butoxycarbonylamino)-6-(benzyloxy)-2,6-dioxo-heptanoic acid

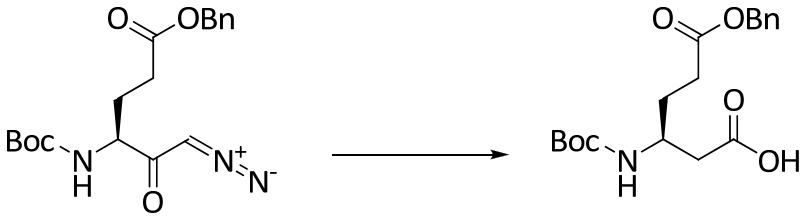

49 $C_{18}H_{23}N_3O_5$ [361.39] → **58** $C_{18}H_{25}NO_6$ [351.36]

Starting with **49** (3.65 g, 10.1 mmol, 1.00 eq) the synthesis was executed according to the general procedure described in **GP 2**. The crude residue was purified using flash chromatography on silica gel (DCM/MeOH 9:1) to yield the pure product (2.89 g, 8.23 mmol, 81 %) as a white solid.

Analytical data: **TLC** (DCM/MeOH 9:1) R_f = 0.35. **^{1}H-NMR** (300 MHz, $CDCl_3$, rt): δ = 1.41 (s, 9 H, *t*-Bu), 1.81-1.89 (m, 2 H, γ-H_2), 2.39-2.42 (m, 2 H, δ-H_2), 2.58 (dt, $^3J_{H,H}$ = 6.8 Hz, 2 H, α-H), 3.84-3.92 (m, 1 H, β-H), 5.06 (s, 3 H, CH_2Ph, NH), 7.27-7.38 (m, 5 H, Ph) ppm. **ESI-MS** (*m*/*z*): 374.2 (100) $[M+Na]^+$, 725.3 (75) $[2M+Na]^+$, 1076.5 $[3M+Na]^+$.

(**51**) (*S*)-3-(*tert*-Butoxycarbonylamino)-2,5-dioxo-5-(9*H*-xanthene-9-ylamino)-1-diazo-hexan-1-one

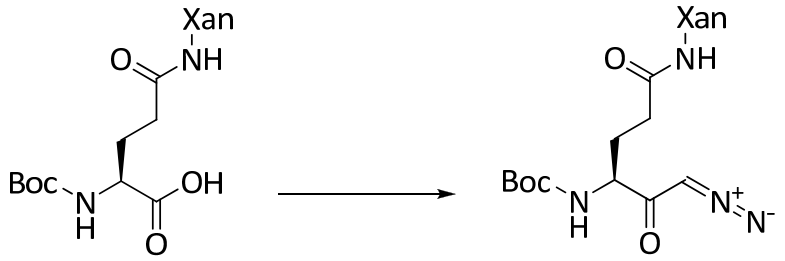

42 $C_{23}H_{26}N_2O_6$ [426.18]

51 $C_{24}H_{28}N_4O_5$ [450.49]

Starting with *N*-Boc-Gln-(Xan)-OH (**42**) (1.00 g, 2.34 mmol, 1.00 eq) the synthesis was executed according to the general procedure described in **GP 1**. The crude residue was purified using flash chromatography on silica gel (ethyl acetate/pentane 2:3) to yield the pure product (0.91 g, 2.03 mmol, 54 %) as a yellow solid.

Analytical data: **TLC** (ethyl acetate/pentane 2:3) R_f = 0.23. **^{1}H-NMR** (300 MHz, $CDCl_3$, rt): δ = 1.42 (s, 9 H, *t*-Bu), 1.76-1.82 (m, 2 H, γ-H_2), 3.12 (dt, $^3J_{H,H}$ = 6.4 Hz, 2 H, β-H_2), 4.30-4.36 (m, 1 H, α-H), 4.98 (s, 1 H, NH), 6.14 (s, 1 H, Xan-CH), 7.08-7.14 (m, 4 H, Ph), 7.20-7.27 (m, 2 H, Ph), 7.41-7.46 (m, 2 H, Ph) ppm. **ESI-MS** (*m*/*z*): 473.2 (94) $[M+Na]^+$, 923.4 (100) $[2M+Na]^+$, 449.2 (34) $[M-H]^-$, 899.5 (100) $[2M-H]^-$.

(**60**) (*S*)-3-(*tert*-Butoxycarbonylamino)-2,5-dioxo-5-(9*H*-xanthene-9-ylamino)-hexanoic acid

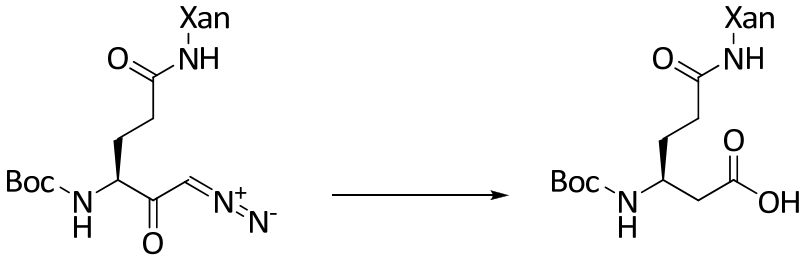

51 $C_{24}H_{28}N_4O_5$ [450.49] **60** $C_{24}H_{28}N_2O_6$ [440.51]

Starting with **51** (0.91 g, 2.03 mmol, 1.00 eq) the synthesis was executed according to the general procedure described in **GP 2**. The crude residue was purified using flash chromatography on silica gel (DCM/MeOH 9:1) to yield the pure product (0.73 g, 1.67 mmol, 46 %) as a white solid.

Analytical data: **TLC** (DCM/MeOH 9:1) R_f = 0.78. **^{1}H-NMR** (300 MHz, $CDCl_3$, rt): δ = 1.34 (s, 9 H, *t*-Bu), 1.74-1.83 (m, 2 H, δ-H_2), 2.19-2.26 (m, 2 H, γ-H), 2.58 (d, $^3J_{H,H}$ = 6.8 Hz, 2 H, α-H), 3.62-3.68 (m, 1 H, β-H), 5.38-5.66 (m, 2 H, NH), 6.12 (s, 1 H, Xan-CH), 7.01-7.08 (m, 4 H, Ph), 7.22-7.27 (m, 2 H, Ph), 7.36-7.44 (m, 2 H, Ph) ppm. **ESI-MS** (*m/z*): 463.2 (100) $[M+Na]^+$, 903.4 (82) $[2M+Na]^+$, 1343.6 $[3M+Na]^+$.

(**48**) (*S*)-3-(*tert*-Butoxycarbonylamino)-2,5-dioxo-5-(9*H*-xanthene-9-ylamino)-1-diazo-pentan-1-one

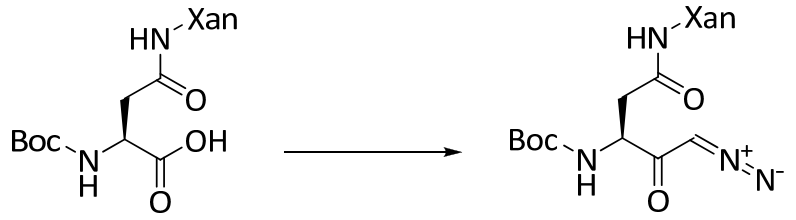

39 $C_{22}H_{24}N_2O_6$ [412.44] **48** $C_{23}H_{24}N_4O_5$ [436.46]

Starting with *N*-Boc-Asn-(Xan)-OH (**39**) (3.00 g, 7.27 mmol, 1.00 eq) the synthesis was executed according to the general procedure described in **GP 1**. The crude residue was purified using flash chromatography on silica gel (ethyl acetate/pentane 2:3) to yield the pure product (2.84 g, 6.51 mmol, 49 %) as a yellow solid.

Analytical data: **TLC** (ethyl acetate/pentane 2:3) R_f = 0.76. **^{1}H-NMR** (300 MHz, $CDCl_3$, rt): δ = 1.38 (s, 9 H, *t*-Bu), 3.22 (d, $^3J_{H,H}$ = 6.3 Hz, 2 H, β-H), 4.20-4.29 (m, 1 H, α-H), 4.88 (s, 2 H, 2 x NH), 6.37 (s, 1 H, Xan-CH), 7.09-7.14 (m, 4 H, Ph), 7.22-7.28 (m, 2 H, Ph), 7.38-7.47 (m, 2 H, Ph) ppm.

(**57**) (*S*)-3-(*tert*-Butoxycarbonylamino)-2,5-dioxo-5-(9*H*-xanthene-9-ylamino)-pentanoic acid

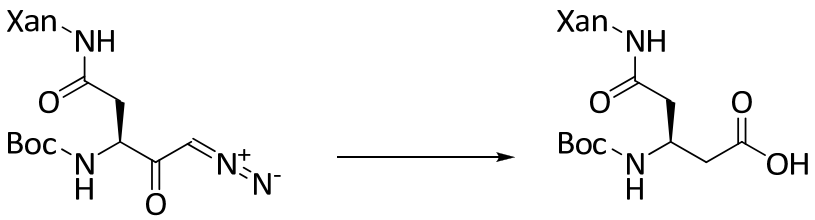

48 $C_{23}H_{24}N_4O_5$ [436.46] **57** $C_{23}H_{26}N_2O_6$ [426.52]

Starting with **48** (2.84 g, 6.49 mmol, 1.00 eq) the synthesis was executed according to the general procedure described in **GP 2**. The crude residue was purified using flash chromatography on silica gel (DCM/MeOH 9:1) to yield the pure product (2.17 g, 5.11 mmol, 44 %) as a white solid.

Analytical data: **TLC** (DCM/MeOH 9:1) R_f = 0.67. **^{1}H-NMR** (300 MHz, $CDCl_3$, rt): δ = 1.42 (s, 9 H, *t*-Bu), 2.62 (m, 2 H, γ-H), 3.24 (d, $^3J_{H,H}$ = 6.4 Hz, 2 H, α-H), 4.21-4.35 (m, 1 H, β-H), 5.38-5.66 (s, 2 H, 2 x NH), 6.38 (s, 1 H, Xan-CH), 7.01-7.08 (m, 4 H, Ph), 7.22-7.27 (m, 2 H, Ph), 7.36-7.44 (m, 2 H, Ph) ppm. **ESI-MS** (*m/z*): 449.2 (100) $[M+Na]^+$, 875.4 (30) $[2M+Na]^+$, 425.2 (50) $[M-H]^-$, 851.4 (100) $[2M-H]^-$.

(**45**) (*S*)-3-(*tert*-Butoxycarbonylamino)-6-*N*`-[(2,4,6-trimethylphenyl)sulfonyl]-6-[(aminoiminomethyl)-amino]-1-diazohexan-2-one

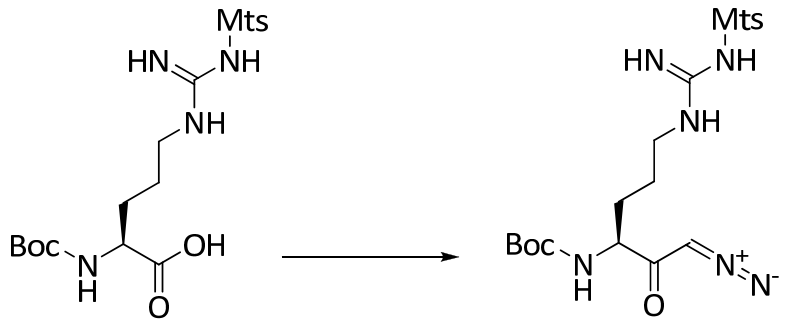

36 $C_{20}H_{32}N_4O_6S$ [456.56] **45** $C_{21}H_{32}N_6O_5S$ [480.58]

Starting with *N*-Boc-Arg-(Mts)-OH (**36**) (3.00 g, 6.55 mmol, 1.00 eq) the synthesis was executed according to the general procedure described in **GP 1**. The crude residue was purified using flash chromatography on silica gel (ethyl acetate/pentane 3:2) to yield the pure product (2.55 g, 5.29 mmol, 81 %) as a yellow solid.

Analytical data: **TLC** (ethyl acetate/pentane 3:2) R_f = 0.32. **^{1}H-NMR** (300 MHz, $CDCl_3$, rt): δ = 1.43 (s, 9 H, *t*-Bu), 1.43-1.88 (m, 4 H, β-H, γ-H), 2.22 (s, 3 H, CH_3), 2.63 (s, 6 H, 2 x CH_3), 2.62-2.70 (m, 2 H, δ-H), 4.31-4.40 (m, 1 H, α-H), 5.18-5.21 (m, 1 H, NH), 6.90 (s, 2 H, CHN_2) ppm. **ESI-MS** (*m/z*): 503.2 (100) $[M+Na]^+$, 983.4 (50) $[2M+Na]^+$, 479.2 $[M-H]^-$, 959.5 $[2M-H]^-$.

(**54**) (*S*)-3-(*tert*-Butoxycarbonylamino)-6-*N*`-[(2,4,6-trimethylphenyl)sulfonyl]-6-[(aminoiminomethyl)-amino]-hexanoic acid

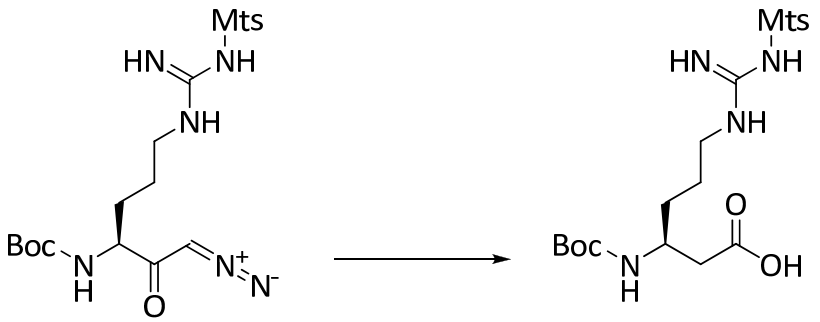

45 $C_{21}H_{32}N_6O_5S$ [480.58]

54 $C_{21}H_{34}N_4O_6S$ [470.58]

Starting with **45** (2.55 g, 5.29 mmol, 1.00 eq) the synthesis was executed according to the general procedure described in **GP 2**. The crude residue was purified using flash chromatography on silica gel (DCM/MeOH 9:1) to yield the pure product (0.96 g, 2.03 mmol, 38 %) as a white solid.

Analytical data: **TLC** (DCM/MeOH 9:1) R_f = 0.70. **^{1}H-NMR** (300 MHz, $CDCl_3$, rt): δ = 1.40 (s, 9 H, *t*-Bu), 1.48-1.67 (m, 4 H, γ-H, δ-H), 2.21 (s, 3 H, CH_3), 2.62 (s, 6 H, 2 x CH_3), 2.70-2.89 (m, 4 H, α-H, ε-H), 4.55 (m, 2 H, β-H), 6.12 (s, 2 H, 2 x NH) ppm. **ESI-MS** (*m/z*): 493.2 (100) $[M+Na]^+$, 469.2 (100) $[M-H]^-$, 939.5 (100) $[2M-H]^-$.

(**50**) (*S*)-3-(*tert*-Butoxycarbonylamino)-5-(methylsulfanyl)-1-diazopentan-2-one

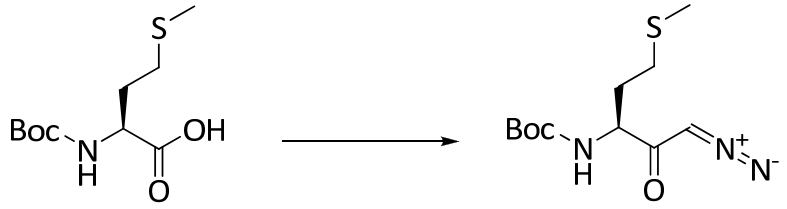

41 $C_{10}H_{19}NO_4S$ [249.33] **50** $C_{11}H_{19}N_3O_3S$ [273.35]

Starting with *N*-Boc-Met-OH (**41**) (2.00 g, 8.03 mmol, 1.00 eq) the synthesis was executed according to the general procedure described in **GP 1**. The crude residue was purified using flash chromatography on silica gel (ethyl acetate/pentane 2:3) to yield the pure product (1.79 g, 6.51 mmol, 81 %) as a yellow solid.

Analytical data: **TLC** (ethyl acetate/pentane 2:3) R_f = 0.68. **^{1}H-NMR** (300 MHz, $CDCl_3$, rt): δ = 1.41 (s, 9 H, *t*-Bu), 1.98-2.08 (m, 2 H, β-H), 2.19 (s, 3 H, SCH_3), 2.72 (m, 2 H, γ-H), 4.35-4.43 (m, 1 H, α-H), 5.86 (s, 1 H, NH) ppm.

(**59**) (*S*)-3-(*tert*-Butoxycarbonylamino)-5-(methylsulfanyl)-pentanoic acid

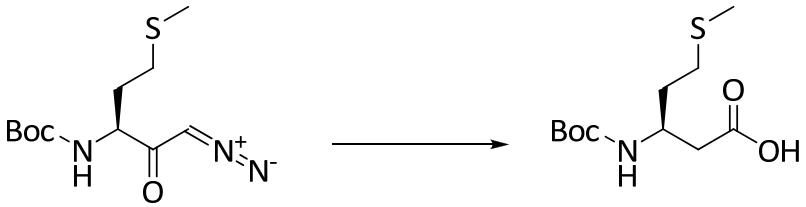

50 $C_{11}H_{19}N_3O_3S$ [273.35] **59** $C_{11}H_{21}NO_4S$ [263.35]

Starting with **50** (1.79 g, 6.51 mmol, 1.00 eq) the synthesis was executed according to the general procedure described in **GP 2**. The crude residue was purified using flash chromatography on silica gel (DCM/MeOH 9:1) to yield the pure product (1.09 g, 4.14 mmol, 64 %) as a white solid.

Analytical data: **TLC** (DCM/MeOH 9:1) R_f = 0.54. **^{1}H-NMR** (300 MHz, $CDCl_3$, rt): δ = 1.40 (s, 9 H, *t*-Bu), 1.61-1.80 (m, 2 H, γ-H_2), 2.18 (s, 3 H, SCH_3), 2.40-2.58 (m, 4 H, α-H, δ-H), 3.63-3.73 (m, 1 H, β-H), 4.86 (s, 1 H, NH) ppm. **ESI-MS** (*m/z*): 286.0 (100) $[M+Na]^+$, 549.1 (30) $[2M+Na]^+$, 262.0 (60) $[M-H]^-$, 524.0 (100) $[2M-H]^-$.

7.3.3 Synthesis of the *N*-Fmoc-β^3-amino acid building blocks

(**65**) (*S*)-7-(*tert*-Butoxycarbonylamino)-3-(9-fluorenylmethyloxycarbonyl)-1-diazoheptane-2-one

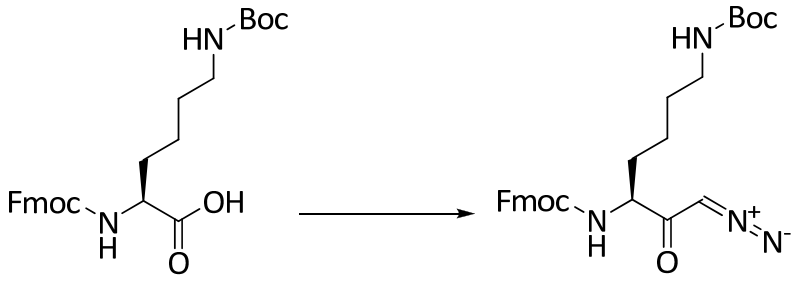

61 $C_{26}H_{32}N_2O_6$ [468.54] **65** $C_{27}H_{32}N_4O_5$ [492.57]

Starting with *N*-Fmoc-Lys-(Boc)-OH (**61**) (8.00 g, 17.1 mmol, 1.00 eq) the synthesis was executed according to the general procedure described in **GP 1**. The crude residue was purified using flash chromatography on silica gel (ethyl acetate/pentane 2:3) to yield the pure product (7.75 g, 15.7 mmol, 92 %) as a yellow solid.

Analytical data: **TLC** (ethyl acetate/pentane 2:3) R_f = 0.67. **^{1}H-NMR** (300 MHz, $CDCl_3$, rt): δ = 1.25-1.56 (m, 13 H, *t*-Bu, β-H_2, δ-H_2), 3.14 (ddt, $^3J_{H,H}$ = 6.4 Hz, $^3J_{H,H}$ = 6.3 Hz, 2 H, ε-H_2), 4.13-4.21 (m, 1 H, α-H), 4.89-5.10 (m, 1 H, Fmoc-CH), 5.23 (d, $^3J_{H,H}$ = 7.3 Hz, 1 H, Boc-NH), 6.64 (t, $^3J_{H,H}$ = 6.3 Hz, 1 H, Fmoc-NH), 7.24-7.58 (m, 8 H, Fmoc-CH) ppm. **ESI-MS** *m/z* (%): 515.1 (69) $[M+Na]^+$, 1008.14 (100) $[2M+Na]^+$.

(**69**) (*S*)-7-(*tert*-Butoxycarbonylamino)-3-(9-fluorenylmethyloxycarbonyl)-heptanoic acid

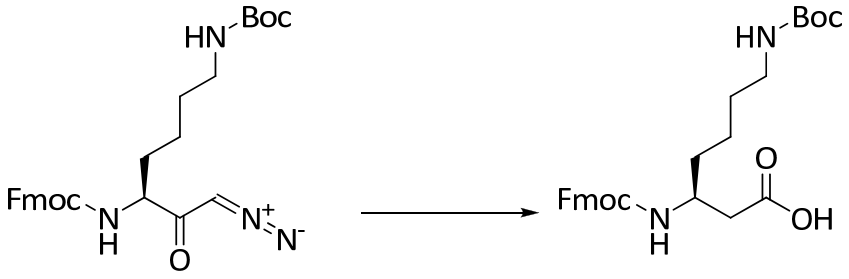

65 $C_{27}H_{32}N_4O_5$ [492.57] → **69** $C_{27}H_{34}N_2O_6$ [482.57]

Starting with **65** (7.75 g, 15.7 mmol, 1.00 eq) the synthesis was executed according to the general procedure described in **GP 2**. The reaction mixture was sonicated. The crude residue was purified using flash chromatography on silica gel (DCM/MeOH 2:3) to yield the pure product (5.61 g, 11.6 mmol, 74 %) as a white solid.

Analytical data: **TLC** (DCM/MeOH 2:3) R_f = 0.36. **^{1}H-NMR** (300 MHz, $CDCl_3$, rt): δ = 1.32-1.59 (m, 15 H, *t*-Bu, γ-H_2, δ-H_2, ε-H_2), 2.52-2.66 (m, 2 H, α-H), 3.05-3.22 (m, 2 H, ζ-H), 3.72-3.96 (m, 1 H, β-H), 4.91-5.04 (m, 1 H, Fmoc-CH), 5.93 (d, $^3J_{H,H}$ = 8.1 Hz, 1 H, Boc-NH), 6.54 (m, 1 H, Fmoc-NH), 7.37-7.58 (m, 8 H, Fmoc-CH) ppm. **ESI-MS**: *m/z* (%): 505.6 (69) $[M+Na]^+$, 987.4 (100) $[2M+Na]^+$.

(**68**) (*S*)-3-(9-Fluorenylmethyloxycarbonyl)-4-methyl-1-diazo-pentan-1-one

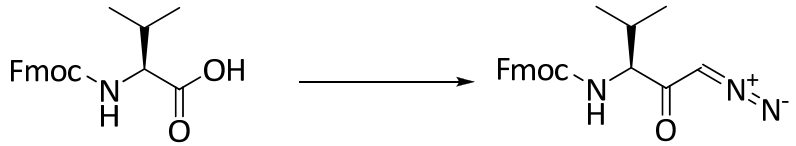

64 $C_{20}H_{21}NO_4$ [339.39] → **68** $C_{21}H_{21}N_3O_3$ [363.41]

Starting with *N*-Fmoc-Val-OH (**64**) (5.00 g, 17.0 mmol, 1.00 eq) the synthesis was executed according to the general procedure described in **GP 1**. The crude residue was purified using flash chromatography on silica gel (ethyl acetate/pentane 2:3) to yield the pure product (5.56 g, 15.3 mmol, 90 %) as a yellow solid.

Analytical data: **TLC** (ethyl acetate/pentane 2:3) R_f = 0.76. **^{1}H-NMR** (300 MHz, $CDCl_3$, rt): δ = 0.91 (d, $^3J_{H,H}$ = 6.5 Hz, 3 H, CH_3), 0.98 (d, $^3J_{H,H}$ = 6.5 Hz, 3 H, CH_3), 2.06 (d, $^3J_{H,H}$ = 6.6 Hz, 2 H, β-H), 3.93-4.01 (m, 1 H, α-H), 4.96-5.07 (m, 1 H, Fmoc-CH), 5.41 (s, 1 H, CHN_2), 7.21-7.45 (m, 8 H, Fmoc-CH), 8.01 (bs, 1 H, NH) ppm. **ESI-MS**: (*m*/*z*): 386.1 (87) $[M+Na]^+$, 749.8 (100) $[2M+Na]^+$.

(**72**) (*S*)-3-(9-Fluorenylmethyloxycarbonyl)-4-methyl-pentanoic acid

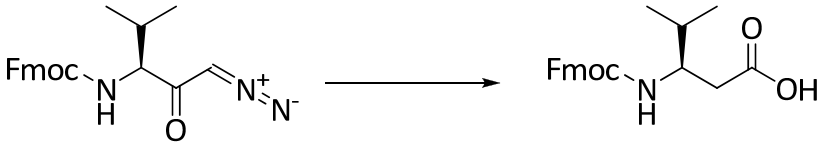

68 $C_{21}H_{21}N_3O_3$ [363.41] → **72** $C_{21}H_{23}NO_4$ [353.49]

Starting with **68** (5.56 g, 15.3 mmol, 1.00 eq) the synthesis was executed according to the general procedure described in **GP 2**. The reaction mixture was sonicated. The crude residue was purified using flash chromatography on silica gel (DCM/MeOH 9:1) to yield the pure product (4.89 g, 13.5 mmol, 88 %) as a white solid.

Analytical data: **TLC** (DCM/MeOH 9:1) R_f = 0.34. **^{1}H-NMR** (300 MHz, $CDCl_3$, rt): δ = 0.91 (d, $^3J_{H,H}$ = 6.8 Hz, 6 H, 2 x CH_3), 1.89-2.02 (m, 1 H, γ-H), 2.45-2.53 (m, 2 H, β-H), 3.71-3.82 (m, 1 H, α-H), 4.53-4.67 (m, 1 H, Fmoc-CH), 7.26-7.50 (m, 8 H, Fmoc-CH), 7.96 (bs, 1 H, NH) ppm. **ESI-MS**: (*m/z*): 386.2 (45) $[M+Na]^+$, 749.2 (89) $[2M+Na]^+$.

(**67**) (*S*)-3-(9-Fluorenylmethyloxycarbonyl)-4-methyl-1-diazo-hexan-1-one

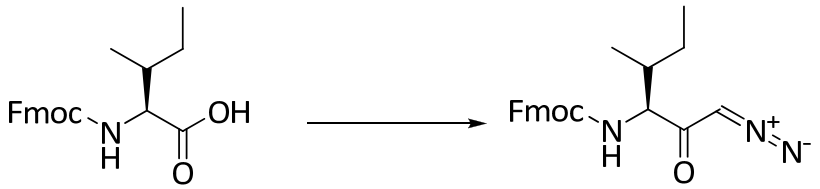

63 $C_{21}H_{23}NO_4$ [353.39] **67** $C_{22}H_{23}N_3O_3$ [377.41]

Starting with *N*-Fmoc-Ile-OH (**63**) (3.00 g, 8.84 mmol, 1.00 eq) the synthesis was executed according to the general procedure described in **GP 1**. The crude residue was purified using flash chromatography on silica gel (ethyl acetate/pentane 2:3) to yield the pure product (2.60 g, 7.16 mmol, 81 %) as a yellow solid.

Analytical data: **TLC** (ethyl acetate/pentane 2:3) R_f = 0.67. **^{1}H-NMR** (300 MHz, $CDCl_3$, rt): δ = 0.92 (t, $^3J_{H,H}$ = 7.4 Hz, 3 H, $CH_2C\underline{H}_3$) 0.94 (d, $^3J_{H,H}$ = 7.1 Hz, 3 H, CH_3), 1.45 (m, 2 H, $C\underline{H}_2CH_3$), 2.61 (d, $^3J_{H,H}$ = 6.5 Hz, 2 H, β-H), 4.05-4.19 (m, 1 H, α-H), 5.13-5.45 (m, 1 H, Fmoc-CH), 5.49 (s, 1 H, CHN_2), 7.43-7.69 (m, 8 H, Fmoc-CH), 8.04 (bs, 1 H, NH) ppm. **ESI-MS**: (*m/z*): 254.1 (20) $[M+Na]^+$, 230.0 (68) $[2M-H]^-$.

(**71**) (*S*)-3-(9-Fluorenylmethyloxycarbonyl)-4-methyl-hexanoic acid

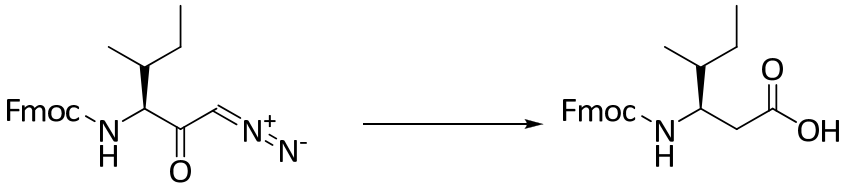

67 $C_{22}H_{23}N_3O_3$ [377.41] → **71** $C_{22}H_{25}NO_4$ [367.41]

Starting with **67** (2.60 g, 7.16 mmol, 1.00 eq) the synthesis was executed according to the general procedure described in **GP 2**. The reaction mixture was sonicated. The crude residue was purified using flash chromatography on silica gel (DCM/MeOH 9:1) to yield the pure product (1.90 g, 5.23 mmol, 73 %) as a white solid.

Analytical data: **TLC** (ethyl acetate/pentane 9:1) R_f = 0.47. **^{1}H-NMR** (300 MHz, $CDCl_3$, rt): δ = 0.95 (t, $^3J_{H,H}$ = 7.5 Hz, 3 H, C$\underline{H}_2$CH$_3$), 0.99 (d, $^3J_{H,H}$ = 7.4 Hz, 3 H, CH$_3$), 1.31 (m, 2 H, C$\underline{H}_2$CH$_3$), 2.25-2.58 (m, 4 H, α-H, γ-H), 4.09-4.21 (m, 1 H, β-H), 5.31-5.49 (m, 1 H, Fmoc-CH$_2$), 7.42-7.73 (m, 8 H, Fmoc-CH$_2$), 8.10 (bs, 1 H, NH) ppm. **ESI-MS**: (*m/z*): 386.1 (54) [M+Na]$^+$, 749.2 (68) [2M+Na]$^+$.

(**66**) (*S*)-3-(9-Fluorenylmethyloxycarbonyl)-6-*N*`-[(2,4,6-trimethylphenyl)sulfonyl]-6-[(aminoiminomethyl)-amino]-1-diazohexan-2-one

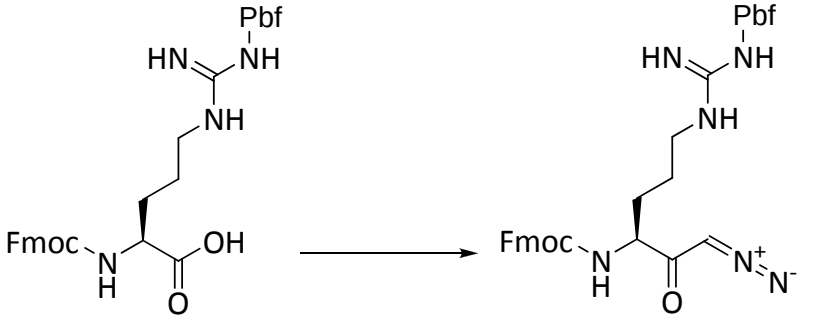

62 $C_{34}H_{40}N_4O_7S$ [648.26]

66 $C_{35}H_{42}N_6O_6S$ [672.27]

Starting with *N*-Fmoc-Arg-(Pbf)-OH (**62**) (5.00 g, 7.70 mmol, 1.00 eq) the synthesis was executed according to the general procedure described in **GP 1**. The crude residue was purified using flash chromatography on silica gel (ethyl acetate/pentane 3:2) to yield the pure product (3.47 g, 5.16 mmol, 67 %) as a yellow solid.

Analytical data: **TLC** (ethyl acetate/pentane 3:2) R_f = 0.52. **^{1}H-NMR** (300 MHz, $CDCl_3$, rt): δ = 1.30 (s, 6 H, 2 x CH_3), 1.50-1.71 (m, 4 H, β-H, γ-H,), 2.18 (s, 3 H, CH_3), 2.34 (s, 6 H, 2 x CH_3), 2.46-2.79 (m, 2 H, δ-H), 4.35-4.43 (m, 1 H, α-H), 4.64 (m, 2 H, CH_2^{Pbf}), 4.87-4.98 (m, 1 H, Fmoc-CH), 5.50 (s, 1 H, CHN_2), 7.42-7.59 (m, 8 H, Fmoc-CH), 8.04 (bs, 1 H, NH) ppm. **ESI-MS**: *m/z* (%): 695.3 (100) $[M+Na]^+$.

(**70**) (*S*)-3-(9-Fluorenylmethyloxycarbonyl)-6-*N*`-[(2,4,6-trimethylphenyl)sulfonyl]-6-[(aminoiminomethyl)-amino]-hexanoic acid

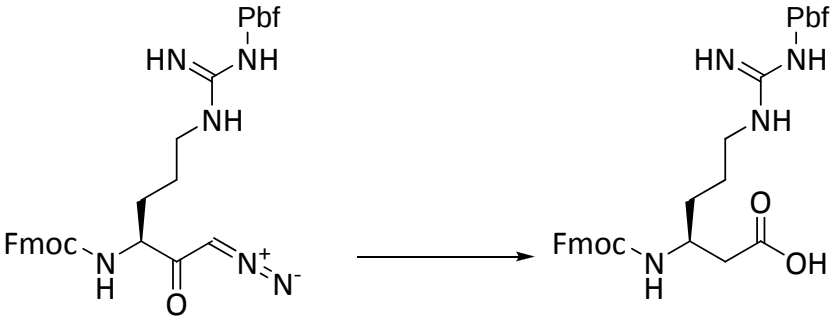

66 $C_{35}H_{42}N_6O_6S$ [672.27]

70 $C_{35}H_{42}N_6O_6S$ [662.28]

Starting with **66** (3.47 g, 5.16 mmol, 1.00 eq) the synthesis was executed according to the general procedure described in **GP 2**. The reaction mixture was sonicated. The crude residue was purified using flash chromatography on silica gel (DCM/MeOH 9:1) to yield the pure product (1.53 g, 2.27 mmol, 44 %) as a light yellow solid.

Analytical data: **TLC** (DCM/MeOH 9:1) R_f = 0.23. **^{1}H-NMR** (300 MHz, $CDCl_3$, rt): δ = 1.31 (s, 6 H, 2 x CH_3), 1.48-1.57 (m, 4 H, γ-H, δ-H), 2.20 (s, 3 H, CH_3), 2.41 (s, 6 H, 2 x CH_3), 2.46-2.79 (m, 2 H, α-H, ε-H), 4.10-4.21 (m, 1 H, β-H), 4.64 (m, 2 H, CH_2^{Pbf}), 4.87-4.98 (m, 1 H, Fmoc-CH), 6.15 (s, 2 H, 2 x NH), 7.22-7.40 (m, 8 H, Fmoc-CH) ppm. **ESI-MS**: *m/z* (%): 493.2 (100) $[M+Na]^+$, 469.2 (100) $[M-H]^-$, 939.5 (100) $[2M-H]^-$.

7.4 Synthesis of the Linear Peptides

Linear peptides were mostly automatically synthesized either at the *ABI 221* (**8**-**11**, **22**, **23**) or at the *CEM Liberty* (**27**, **74-77**, **78**, **84**, **86**, **87**, **89**) synthesizer. Peptide **27** were partially synthesized at the *CEM Liberty* (aa 1-18) and afterwards finished manually (see General Procedures). The peptides synthesized following the Fmoc-standard protocol (**8**-**11**, **13**-**23**, **74-78** and **81-89**) were attached at *Wang* or *NovaSyn® TGR* resins. The peptide, synthesized following the Boc-standard protocol, was attached at *MBHA* resins.

7.4.1 Synaptobrevin derivatives

H—LQQTQAQVDEVVDI·MRVNVKKVLKRDQKLSELDKRADALQAGASQFETSAAKL—NH
[$C_{256}H_{437}N_{77}O_{83}S$, 5953.47] (**9**)

Yield: 1.5 mg, 1.9 %. **HPLC** (*YMC-Pack* preperative column ODS-A, RP-18, 250x20, 4 µm, 80 Å, gradient: 30-80 % in 30 min): t_R = 21.97 min. **ESI-MS**: (*m*/*z*): 851.33 $[M+7H]^{7+}$, 993.21 $[M+6H]^{6+}$, 1191.65 $[M+5H]^{5+}$, 5954.23 $[M+H]^{+}$. **HR-MS** (ESI): 851.03674 $[M+7H]^{7+}$ (calcd. $C_{256}H_{443}N_{77}O_{83}S$ $[M+7H]^{7+}$: 851.03465), 992.70831 $[M+7H]^{7+}$ (calcd. $C_{256}H_{442}N_{77}O_{83}S$ $[M+6H]^{6+}$: 992.70842).

H—LQQTQAQVDEVVDI·MRVNVDKVLERDQKLSELDDRADALQAGASQFETSAAKL—NH
[$C_{252}H_{419}N_{73}O_{89}S$, 5927.47] (**10**)

Yield: 5.5 mg, 4.3 %. **HPLC** (*YMC-Pack* analytical column ODS-A, RP-18, 250x4.6, 4 µm, 80 Å, gradient: 40-80 % in 30 min): t_R = 15.07 min. **ESI-MS**: (*m*/*z*): 989.02 $[M+6H]^{6+}$, 1187.02 $[M+5H]^{5+}$, 5928.05 $[M+H]^{+}$. **HR-MS** (ESI): 1087.73852 $[M+6H]^{6+}$ (calcd. $C_{268}H_{456}N_{84}O_{95}S$ $[M+6H]^{6+}$: 1086.73911).

Adam
|
H—SNRRLQQAQVDEVVDI·MRVNVDKVLERDDKLSDLDDRADALQAGASQFETSAAKL—NH
[$C_{277}H_{463}N_{85}O_{94}S$, 6520.57] (**22**)

HPLC (*YMC-Pack* analytical column ODS-A, RP-18, 250x4.6, 4 µm, 80 Å, gradient: 5-100 % in 30 min): t_R = 21.45 min. **ESI-MS**: (*m/z*): 932.50 $[M+7H]^{7+}$, 1087.58 $[M+6H]^{6+}$, 6521.42 $[M+H]^{+}$.

Adam
|
Ac—SNRRLQQAQVDEVVDI·MRVNVDKVLERDDKLSDLDDRADALQAGASQFETSAAKL—NH
[$C_{279}H_{465}N_{85}O_{95}S$, 6562.75] (**23**)

HPLC (*YMC-Pack* preperative column ODS-A, RP-18, 250x20, 4 µm, 80 Å, gradient: 10-100 % in 30 min): t_R = 20.92min. **ESI-MS**: (*m/z*): 1313.09 $[M+5H]^{5+}$, 1641.37 $[M+4H]^{4+}$, 6563.44 $[M+H]^{+}$.

H—SNRRLQQAQVDEVVDI·MRVNVDKVLERDQKLSELDDRADALQAGASQFETSAAKL—OH

[$C_{268}H_{450}N_{84}O_{95}S$, 6401.14] (**8**)

Yield: 1.3 mg, 1.8 %. **HPLC** (*YMC-Pack* preperative column ODS-A, RP-18, 250x20, 4 µm, 80 Å, gradient: 30-80 % in 30 min): t_R = 19.22 min. **ESI-MS**: (*m/z*): 954.79 $[M+7H+Na]^{8+}$, 1087.74 $[M+6H]^{6+}$, 6402.30 $[M+H]^{+}$. **HR-MS** (ESI): 1087.73852 $[M+6H]^{6+}$ (calcd. $C_{268}H_{456}N_{84}O_{95}S$ $[M+6H]^{6+}$: 1086.73911).

H—SNRRLQQAQVDEVVDI·MRVNVKKVLKRDQKLSELDKRADALQAGASQFETSAAKL—OH

[$C_{273}H_{469}N_{87}O_{89}S$, 6426.38] (**11**)

Yield: 1.5 mg, 2.0 %. **HPLC** (*Jasco* Reprosil-Pack semipreperative column ODS-A, RP-18, 250x10, 4 µm, 80 Å, gradient: 25-80 % in 30 min): t_R = 20.58 min. **ESI-MS**: (*m/z*): 1069.33 $[M+6H]^{6+}$, 6427.33 $[M+H]^{+}$. **HR-MS** (ESI): 1069.45234 $[M+6H]^{6+}$ (calcd. $C_{273}H_{475}N_{87}O_{89}S$ $[M+6H]^{6+}$: 1069.45312).

Adam
H—SNRRLQQAQVDEVVDI·MRVNVDKVLERDQKLSELDDRADALQAGASQFETSAAKL—OH
[$C_{278}H_{465}N_{85}O_{94}S$, 6534.38] (**13**)

Yield: 1.7 mg, 2.1 %. **HPLC** (*YMC-Pack* analytical column ODS-A, RP-18, 250x4.6, 4 µm, 80 Å, gradient: 30-80 % in 30 min): t_R = 16.67 min. **ESI-MS**: (*m/z*): 956.94 $[M+7H+Na]^{8+}$, 6535.48 $[M+H]^{+}$. **HR-MS** (ESI): 1089.46961 $[M+6H]^{6+}$ (calcd. $C_{278}H_{471}N_{85}O_{94}S$ $[M+6H]^{6+}$: 1089.46867).

Adam
H—SNRRLQQAQVDEVVDI·MRVNVDKVLDRDQKLSELDDRADALQAGASQFETSAAKL—OH
[$C_{277}H_{463}N_{85}O_{94}S$, 6520.36] (**14**)

Yield: 3.0 mg, 2.7 %. **HPLC** *YMC-Pack* analytical column ODS-A, RP-18, 250x4.6, 4 µm, 80 Å, gradient: 30-80 % in 30 min): t_R = 15.27 min. **ESI-MS**: (*m/z*): 954.79 $[M+7H+Na]^{8+}$, 1087.74 $[M+6H]^{6+}$, 6421.43 $[M+H]^{+}$. **HR-MS** (ESI): 1086.73852 $[M+6H]^{6+}$ (calcd. $C_{277}H_{469}N_{85}O_{94}S$ $[M+6H]^{6+}$: 1086.73911).

Adam
H—SNRRLQQAQVDEVVDI·MRVNVDKVLERDQKLSELDDRADALQAGASQFETSAAKL—OH
[$C_{278}H_{465}N_{85}O_{94}S$, 6534.38] (**15**)

Yield: 1.9 mg, 2.2 %. **HPLC** (*YMC-Pack* analytical column ODS-A, RP-18, 250x4.6, 4 µm, 80 Å, gradient: 30-80 % in 30 min): t_R = 16.39 min. **ESI-MS**: (*m/z*): 956.94 $[M+7H+Na]^{8+}$, 1089.92 $[M+6H]^{6+}$, 1307.69 $[M+5H]^{5+}$, 6435.48 $[M+H]^{+}$. **HR-MS** (ESI): 1089.92478 $[M+6H]^{6+}$ (calcd. $C_{278}H_{471}N_{85}O_{94}S$ $[M+6H]^{6+}$: 1089.92424).

Adam Adam
H—SNRRLQQAQVDEVVDI·MRVNVDKVLDRDQKLSELDDRADALQAGASQFETSAAKL—OH
[$C_{287}H_{478}N_{86}O_{93}S$, 6653.59] (**16**)

Yield: 3.1 mg, 2.9 %. **HPLC** (*YMC-Pack* analytical column ODS-A, RP-18, 250x4.6, 4 µm, 80 Å, gradient: 30-80 % in 30 min): t_R = 19.52 min. **ESI-MS**: (*m/z*): 951.52 $[M+7H]^{7+}$, 1109.93 $[M+6H]^{6+}$, 6654.56.43 $[M+H]^{+}$, 6675.49 $[M+Na]^{+}$. **HR-MS** (ESI): 1108.34757 $[M+6H]^{6+}$ (calcd. $C_{287}H_{484}N_{86}O_{93}S$ $[M+6H]^{6+}$: 1108.34113).

Adam Adam

H—SNRRLQQAQVDEVVDI·MRVNVDKVLDRDQKLSELDDRADALQAGASQFETSAAKL—OH

[$C_{287}H_{478}N_{86}O_{93}S$, 6653.59] (**17**)

Yield: 2.3 mg, 2.4 %. **HPLC** (*YMC-Pack* analytical column ODS-A, RP-18, 250x4.6, 4 µm, 80 Å, gradient: 30-80 % in 30 min): t_R = 17.69 min. **ESI-MS**: (*m/z*): 951.52 $[M+7H]^{7+}$, 1109.93 $[M+6H]^{6+}$, 6654.56 $[M+H]^{+}$, 6675.49 $[M+Na]^{+}$. **HR-MS** (ESI): 950.51285 $[M+7H]^{7+}$ (calcd. $C_{287}H_{478}N_{85}O_{94}S$ $[M+7H]^{7+}$: 950.51889), 1108.87922 $[M+6H]^{6+}$ (calcd. $C_{287}H_{477}N_{85}O_{94}S$ $[M+6H]^{6+}$: 1108.87381).

Adam Adam

H—SNRRLQQAQVDEVVDI·MRVNVDKVLERDQKLSELDDRADALQAGASQFETSAAKL—OH

[$C_{288}H_{480}N_{86}O_{93}S$, 6667.62] (**18**)

Yield: 1.0 mg, 1.4 %. **HPLC** (*YMC-Pack* analytical column ODS-A, RP-18, 250x4.6, 4 µm, 80 Å, gradient: 30-80 % in 30 min): t_R = 19.04 min. **ESI-MS**: (*m/z*): 6668.59 $[M+H]^{+}$. **HR-MS** (ESI): 1111.48894 $[M+6H]^{6+}$ (calcd. $C_{288}H_{486}N_{86}O_{93}S$ $[M+6H]^{6+}$: 1111.48232), 1333.71863 $[M+5H]^{5+}$ (calcd. $C_{288}H_{485}N_{86}O_{93}S$ $[M+5H]^{6+}$: 1333.73375).

Adam Adam Adam

H—SNRRLQQAQVDEVVDI·MRVNVDKVLDRDQKLSELDDRADALQAGASQFETSAAKL—OH

[$C_{297}H_{493}N_{87}O_{92}S$, 6786.83] (**19**)

Yield: 1.0 mg, 1.4 %. **HPLC** (*YMC-Pack* analytical column ODS-A, RP-18, 250x4.6, 4 µm, 80 Å, gradient: 30-80 % in 30 min): t_R = 19.96 min. **ESI-MS**: (*m/z*): 969.65 $[M+7H]^{7+}$, 1131.15 $[M+6H]^{6+}$, 6787.69 $[M+H]^{+}$. **HR-MS** (ESI): 1131.13475 $[M+6H]^{6+}$ (calcd. $C_{297}H_{499}N_{87}O_{92}S$ $[M+6H]^{6+}$: 1131.14264).

Adam

H—SNRRLQQAQVDEVVDI·MRVNVDKVLERDDKLSELDDRADALQAGASQFETSAAKL—OH

[$C_{278}H_{466}N_{84}O_{95}S$, 6522.38] (**20**)

Yield: 1.2 mg, 1.5 %. **HPLC** (*YMC-Pack* analytical column ODS-A, RP-18, 250x4.6, 4 µm, 80 Å, gradient: 30-80 % in 30 min): t_R = 17.72 min. **ESI-MS**: (*m/z*): 954.79 $[M+7H+Na]^{8+}$, 1087.74 $[M+6H]^{6+}$, 6787.69 $[M+H]^{+}$. **HR-MS** (ESI): 1086.74525 $[M+6H]^{6+}$ (calcd. $C_{277}H_{463}N_{85}O_{94}S$ $[M+6H]^{6+}$: 1086.753464).

Adam

H—SNRRLQQAQVDEVVDI·MRVNVDKVLERDQKLSDLDDRADALQAGASQFETSAAKL—OH
[$C_{278}H_{467}N_{85}O_{94}S$, 6536.40] (**21**)

Yield: 2.1 mg, 2.3 %. **HPLC** (*YMC-Pack* analytical column ODS-A, RP-18, 250x4.6, 4 µm, 80 Å, gradient: 30-80 % in 30 min): t_R = 17.72 min. **ESI-MS**: (*m/z*): 6537.69 $[M+H]^+$. **HR-MS** (ESI): 1089.42157 $[M+6H]^{6+}$ (calcd. $C_{277}H_{463}N_{85}O_{94}S$ $[M+6H]^{6+}$: 1089.42464).

7.4.2 Complexin derivatives

7.4.2.1 Mimic of Complexin as α-peptide

H—RKAKYAKMEAEREVMRQGI·RDKY—OH

[$C_{122}H_{206}N_{40}O_{35}S_2$, 2857.32] (**74**)

Yield: 1.5 mg, 2.0 %. **HPLC** (*YMC-Pack* analytical column ODS-A, RP-18, 250x4.6, 4 µm, 80 Å, gradient: 20-50 % in 30 min): t_R = 12.62 min. **ESI-MS** (m/z): 2856.51 $[M-H]^-$. **HR-MS** (ESI): 715.13307 $[M+4H]^{4+}$ (calcd. $C_{122}H_{210}N_{40}O_{35}S_2$ $[M+4H]^{4+}$: 714.88254), 953.17478 $[M+3H]^{3+}$ (calcd. $C_{122}H_{209}N_{40}O_{35}S_2$ $[M+3H]^{3+}$: 952.84097).

H—AAAAARKAKYAKMEAEREVMRQGI·RDKY—OH

[$C_{137}H_{231}N_{45}O_{40}S_2$, 3212.71] (**75**)

Yield: 1.9 mg, 1.6 %. **HPLC** (*YMC-Pack* analytical column ODS-A, RP-18, 250x4.6, 4 µm, 80 Å, gradient: 15-35 % in 30 min): t_R = 23.42 min. **ESI-MS** (m/z): 3211.69 $[M-H]^-$. **HR-MS** (ESI): 643.34526 $[M+5H]^{5+}$ (calcd. $C_{137}H_{236}N_{45}O_{40}S_2$ $[M+5H]^{5+}$: 643.14460), 803.92954 $[M+4H]^{4+}$ (calcd. $C_{137}H_{235}N_{45}O_{40}S_2$ $[M+4H]^{4+}$: 803.67894).

H—A·I·VAVRKAKYAKMEAEREVMRQGI·RDKY—OH

[$C_{144}H_{245}N_{45}O_{40}S_2$, 3310.89] (**76**)

Yield: 2.3 mg, 2.2 %. **HPLC** (*YMC-Pack* analytical column ODS-A, RP-18, 250x4.6, 4 µm, 80 Å, gradient: 15-40 % in 30 min): t_R=22.82 min. **ESI-MS** (m/z): 3311.81 $[M+H]^+$. **HR-MS** (ESI): 662.96723 $[M+5H]^{5+}$ (calcd. $C_{144}H_{250}N_{45}O_{40}S_2$ $[M+5H]^{5+}$ 662.76651).

H—RKAKYAKMEAEREVMRQGI·RDKYGI·RKR—OH

[$C_{154}H_{268}N_{54}O_{41}S_2$, 3596.24] (**77**)

HPLC (*YMC-Pack* analytical column ODS-A, RP-18, 250x4.6, 4 µm, 80 Å, gradient: 10-40 % in 30 min): t_R = 22.47 min. **ESI-MS** (m/z): 3311.81 $[M+H]^+$. **HR-MS** (ESI): 720.20766 $[M+5H]^{5+}$ (calcd. $C_{154}H_{273}N_{54}O_{41}S_2$ $[M+5H]^{5+}$: 719.80703), 900.00765 $[M+4H]^{4+}$ (calcd. $C_{154}H_{272}N_{54}O_{41}S_2$ $[M+4H]^{4+}$: 899.50696), 953.17478 $[M+3H]^{3+}$ (calcd. $C_{154}H_{271}N_{54}O_{41}S_2$ $[M+3H]^{3+}$: 952.84097).

7.4.2.2 Mimic of Complexin as a β-peptide

H-β^3hArg-β^3hVal-β^3hVal-β^3hTyr-β^3hVal-β^3hGlu-β^3hVal-β^3hVal-β^3hArg-β^3hVal-β^3hVal-β^3hArg-β^3hVal-β^3hVal-β^3hVal-β^3hJle-β^3hVal-β^3hVal-β^3hLys-β^3hAla-β^3hLys-β^3hArg-β^3hLys-NH_2 (**73**)

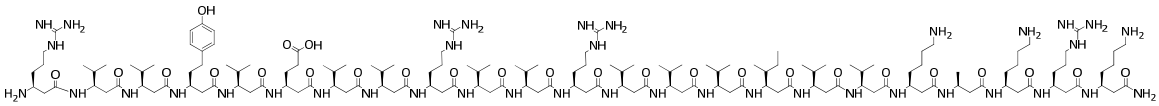

73
$C_{143}H_{264}N_{38}O_{25}$ [2901.04]

Oligomer **73** was synthesized using the MBHA-PS resin (28.0 mg, 20 µmol), which was loaded with Boc-β^3-HLys-OH (**52**) according to the loading protocol, described above. The peptide synthesis was performed manually according the standard Boc-SPPS protocol. After the final coupling the peptide was cleaved from the resin according the cleavage protocol and purified by semi-preparative HPLC followed by lyophilization to afford oligomer **73** as a white solid.

HPLC (*YMC-Pack* analytical column ODS-A, RP-18, 250x4.6, 4 µm, 80 Å, gradient: 30-100 % in 30 min): t_R = 28.99 min. **ESI-MS**: (m/z): 2902.07 $[M+H]^+$.

7.4.3 HTH EnHD derivatives

H—AKREFNENRYLTERRRQQLSSELGLNEAQI·KIWFQNKRAKI·KKS—OH

[$C_{180}H_{291}N_{55}O_{47}$, 5407.25] (**78**)

HPLC (*YMC-Pack* analytical column ODS-A, RP-18, 250x4.6, 4 µm, 80 Å, gradient: 25-50 % in 30 min): t_R = 17.50 min. **ESI-MS**: (*m/z*): 902.17 $[M+6H]^{6+}$, 5408.98 $[M+H]^{+}$. **HR-MS** (ESI): 901.99943 $[M+6H]^{6+}$ (calcd. for $C_{180}H_{297}N_{55}O_{47}$ $[M+6H]^{6+}$: 901.99944).

OAll
|
H—AKREFNENRYLTERRRQQLSSELGLNEAQI·KIWFQNKRAKI·KKS—OH

[$C_{244}H_{403}N_{77}O_{70}$, 5547.31] (**91**)

Oligomer **91** was synthesized using preloaded Fmoc-Ser(Trt)-Wang resin (0.1 mmol) automatically according the standard Fmoc-SPPS-protocol. Except Fmoc-Glu(OAll)-OH at position 13 (underlined) standard Fmoc-amino acids with standard side chain protection groups were used.

HPLC (*YMC-Pack* analytical column ODS-A, RP-18, 250x4.6, 4 µm, 80 Å, gradient: 25-50 % in 30 min): t_R = 12.54 min. **ESI-MS**: (*m/z*): 1109.05 $[M+5H]^{5+}$, 5548.04 $[M+H]^{+}$. **HR-MS** (ESI): 924.67313 $[M+6H]^{6+}$ (calcd. for $C_{180}H_{297}N_{55}O_{47}$ $[M+6H]^{6+}$: 924.67246).

$Alexa_{488}$
|
H—AKREFNENRYLTERRRQQLSSELGLNEAQI·KIWFQNKRAKI·KKS—OH

[$C_{263}H_{414}N_{81}O_{77}S_2$, 6006.86] (**81**)

Oligomer **81** was synthesized using preloaded Fmoc-Ser(Trt)-Wang resin (0.1 mmol) automatically according the standard Fmoc-SPPS-protocol. Except Fmoc-Glu(OAll)-OH at position 13 (underlined) standard Fmoc-amino acids with standard side chain protection groups were used. After synthesis, the full protected resin was treated with $Pd(PPH_3)_4$ (0.1 eq) and $MeNH{\cdot}BH_3$ (40 eq) in DMF under inert atmosphere for 4 h. Afterwards, the Alexa 488 cadaverine dye (1 mg, 3 eq) was attached after activation using Pybop (3.9 eq) and DIEA (10 eq) in DMF by agitation for 2 d under exclusion of light. Then, the resin was thoroughly washed (DMF, DCM) and dried under reduced pressure. Cleavage and purifying was carried out using the standard cleavage and purification protocols described above.

HPLC (*YMC-Pack* analytical column ODS-A, RP-18, 250x4.6, 4 µm, 80 Å, gradient: 5-30 % in 30 min): t_R = 11.68 min.

Alloc
H—AKREFNENRYLTERRRQQLSSELGLNEAQI·KI·WFQNKRAKI·KKS—OH

[$C_{256}H_{405}N_{77}O_{72}$, 5713.32] (**92**)

Oligomer **92** was synthesized using preloaded Fmoc-Ser(Trt)-Wang resin (0.1 mmol) automatically according the standard Fmoc-SPPS-protocol. Except Fmoc-Lys(Alloc)-OH at position 37 (underlined) standard Fmoc-amino acids with standard side chain protection groups were used.

HPLC (*YMC-Pack* semi-preperative column ODS-A, RP-18, 250x10, 4 µm, 80 Å, gradient: 5-30 % in 30 min): t_R = 13.34 min. **ESI-MS**: (*m/z*): 715.14 $[M+8H]^{8+}$, 953.18 $[M+6H]^{6+}$, 5714.07 $[M+H]^{+}$. **HR-MS** (ESI): 816.72723 $[M+7H]^{7+}$ (calcd. for $C_{180}H_{297}N_{55}O_{47}$ $[M+7H]^{7+}$: 816.72745).

Alexa$_{647}$
H—AKREFNENRYLTERRRQQLSSELGLNEAQI·KI·WFQNKRAKI·KKS—OH

[$C_{275}H_{442}N_{80}O_{81}S_4$, 6293.33] (**82**)

Oligomer **82** was synthesized using preloaded Fmoc-Ser(Trt)-Wang resin (0.1 mmol) automatically according the standard Fmoc-SPPS-protocol. Except Fmoc-Lys(Alloc)-OH at position 37 (underlined) standard Fmoc-amino acids with standard side chain protection groups were used. After synthesis, the full protected resin was treated with $Pd(PPH_3)_4$ (0.1 eq) and $MeNH{\cdot}BH_3$ (40 eq) in DMF under inert atmosphere for 4 h. Afterwards, the Alexa 647 succinimidyl ester dye (1 mg, 3 eq) was attached after activation using Pybop (3.9 eq) and DIEA (10 eq) in DMF by agitation for 2 d under exclusion of light. Then, the resin was thoroughly washed (DMF, DCM) and dried under reduced pressure. Cleavage and purifying was carried out using the standard cleavage and purification protocols described above.

HPLC (*YMC-Pack* analytical column ODS-A, RP-18, 250x4.6, 4 µm, 80 Å, gradient: 20-80% in 30 min): t_R = 17.73 min.

OAll Mtt

H—AKREFNENRYLTERRRQQLSSELGLNEAQI·KI·WFQNKRAKI·KKS—OH

[$C_{260}H_{412}N_{78}O_{68}$, 5718.66] (**93**)

Oligomer **93** was synthesized using preloaded Fmoc-Ser(Trt)-Wang resin (0.1 mmol) automatically according the standard Fmoc-SPPS-protocol. Except Fmoc-Glu(OAll)-OH at position 13 and Fmoc-Lys(Mtt)-OH at position 37 (underlined) standard Fmoc-amino acids with standard side chain protection groups were used.

HPLC (*YMC-Pack* semi-preperative column ODS-A, RP-18, 250x10, 4 µm, 80 Å, gradient: 50-80 % in 30 min): t_R = 23.22 min. **ESI-MS**: (*m/z*): 816.94 $[M+7H]^{7+}$, 953.16 $[M+6H]^{6+}$, 5719.34 $[M+H]^{+}$.

H—AKREFNENRYLTERRRQQSSELGLNEAQI·KIWFQNKRAKI·KKSC—OH

[$C_{242}H_{403}N_{79}O_{69}S$, 5560.39] (**84**)

HPLC (*YMC-Pack* semi-preperative column ODS-A, RP-18, 250x10, 4 µm, 80 Å, gradient: 10-50 % in 30 min): t_R = 21.23 min. **ESI-MS**: (*m/z*): 6661.09 $[M+H]^{+}$. **HR-MS** (ESI): 901.99943 $[M+6H]^{6+}$ (calcd. for $C_{180}H_{297}N_{55}O_{47}$ $[M+6H]^{6+}$: 901.99944).

H—CAKREFNENRYLTERRRQQSSELGLNEAQI·KIWFQNKRAKI·KKSC—OH

[$C_{245}H_{407}N_{79}O_{70}S_2$, 5664.52] (**86**)

HPLC (*YMC-Pack* semi-preperative column ODS-A, RP-18, 250x10, 4 µm, 80 Å, gradient: 20-65 % in 30 min): t_R = 14.43 min. **ESI-MS**: (*m/z*): 5663.11 $[M+H]^{+}$.

$Atto_{488}$—AKREFNENRYLTERRRQQSSELGLNEAQI·KIWFQNKRAKI·KKSC—OH

[$C_{261}H_{421}N_{81}O_{70}S$, 5845.26] (**85**)

HPLC (*YMC-Pack* analytical column ODS-A, RP-18, 250x4.6, 4 µm, 80 Å, gradient: 35-60 % in 30 min): t_R = 12.78 min. **ESI-MS**: (*m/z*): 767.53 $[M+8H]^{8+}$, 876.89 $[M+7H]^{7+}$, 1022.87 $[M+6H]^{6+}$, 6132.19 $[M+2TFA+FA+Na]^{+}$.

7.4.4 WW domain derivatives

H—VPLPAGWEMAKTSSGQRYFLNHI·DQTTTWQDPRKAMC—OH

[$C_{188}H_{287}N_{53}O_{55}S_3$, 4265.88] (**87**)

HPLC (*YMC-Pack* semi-preperative column ODS-A, RP-18, 250x10, 4 µm, 80 Å, gradient: 10-40 % in 30 min): t_R = 12.43 min. **ESI-MS**: (*m/z*): 4265.07 $[M+H]^+$. **HR-MS** (ESI): 1066.52104 $[M+4H]^{4+}$ (calcd. for $C_{188}H_{291}N_{53}O_{55}S_3$ $[M+4H]^{4+}$: 1066.51292).

$Atto_{488}$—VPLPAGWEMAKTSSGQRYFLNHI·DQTTTWQDPRKAMC—OH

[$C_{209}H_{312}N_{56}O_{56}S_3$, 4889.25] (**88**)

HPLC (*YMC-Pack* preperative column ODS-A, RP-18, 250x20, 4 µm, 80 Å, gradient: 30-80 % in 30 min): t_R = 14.62 min. **ESI-MS** *m/z*: 1222.83 $[M+4H]^{4+}$, 4890.26 $[M+H]^+$. **HR-MS** (ESI): 920.45209 $[M+5H]^{5+}$ (calcd. for $C_{209}H_{317}N_{56}O_{56}S_3$ $[M+5H]^{5+}$: 920.45138).

H—CVPLPAGWEMAKTSSGQRYFLNHI·DQTTTWQDPRKAMC—OH

[$C_{191}H_{290}N_{54}O_{56}S_4$, 4418.03] (**89**)

HPLC (YMC-Pack column ODS-A, RP-18, 250x10, 4 µm, 80 Å, gradient: 30-80 % in 30 min): t_R = 19.22 min. **ESI-MS**: (*m/z*): 4418.20 $[M+H]^+$. **HR-MS** (ESI): 1091.98714 $[M+H]^+$ (calcd. for $C_{191}H_{295}N_{54}O_{56}S_4$ $[M+H]^+$: 1091.98929).

Appendix

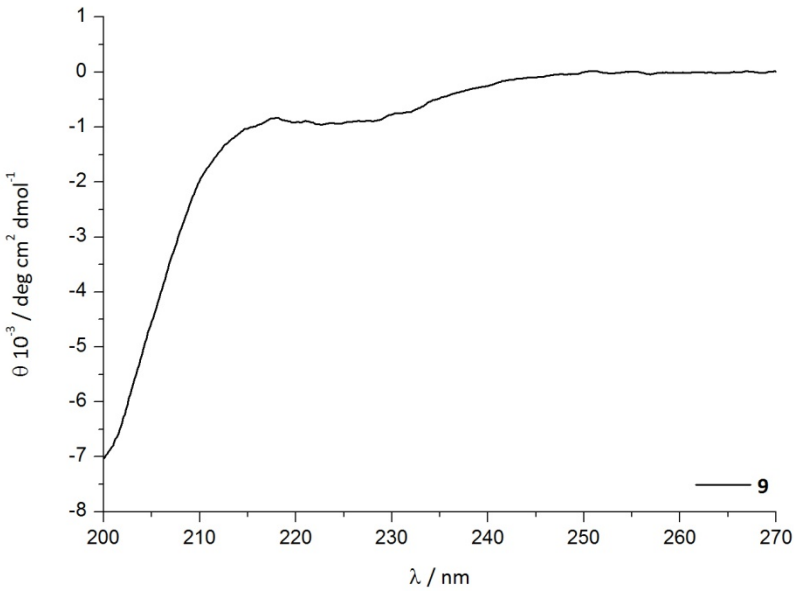

Figure 57. *CD spectra of Synaptobrevin constructs* ***9****, 5 μM in Tris·HCl buffer (10 mM, pH = 7.4). All spectra were standardized with solvent, concentration of the sample (6.0 μM), length of cell and number of amino acids.*

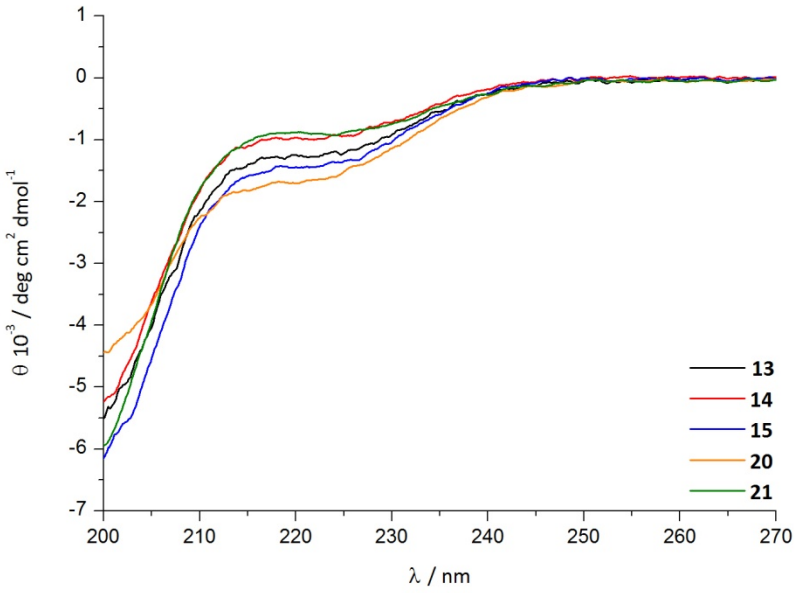

Figure 58. *CD spectra of Synaptobrevin constructs* ***13-15, 20*** *and* ***21****, 5 μM in Tris·HCl buffer (10 mM, pH = 7.4). All spectra were standardized with solvent, concentration of the sample (6.0 μM), length of cell and number of amino acids.*

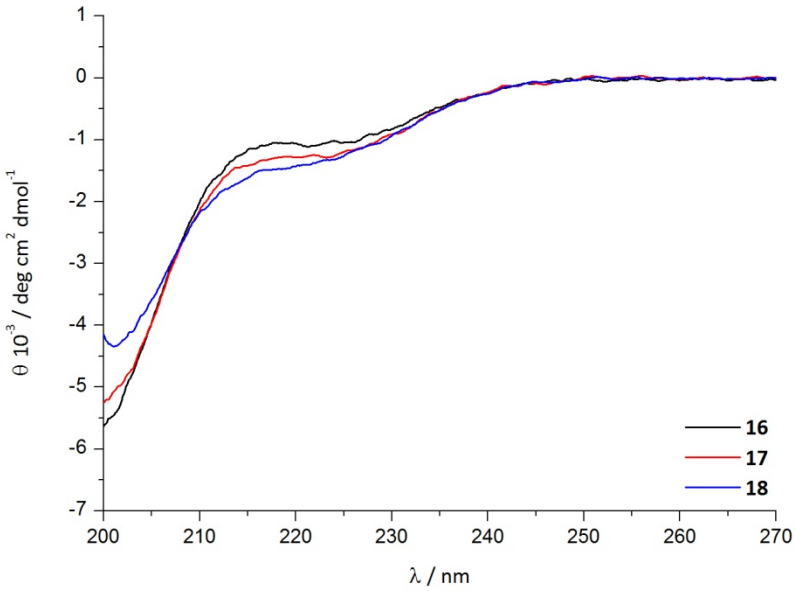

Figure 59. *CD spectra of Synaptobrevin constructs* ***16-18****, 5 μM in Tris·HCl buffer (10 mM, pH = 7.4). All spectra were standardized with solvent, concentration of the sample (6.0 μM), length of cell and number of amino acids.*

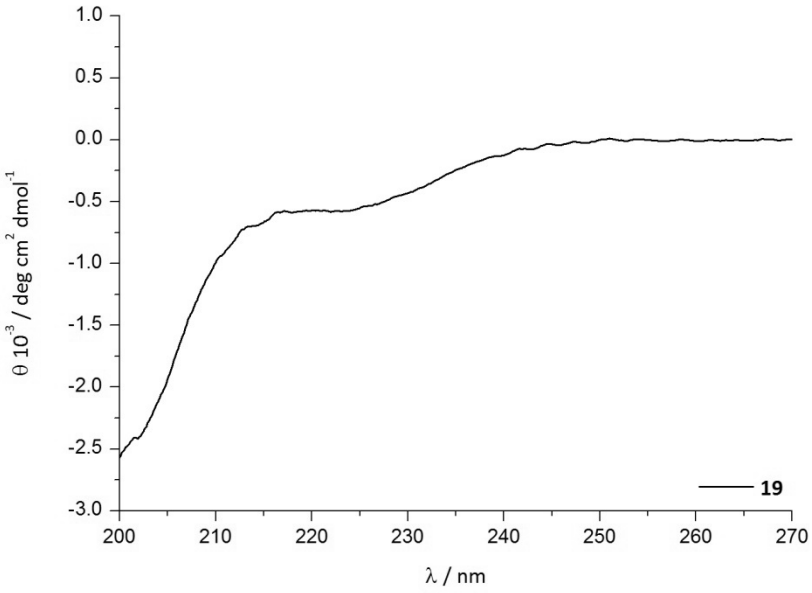

Figure 60. *CD spectra of Synaptobrevin constructs* ***19****, 5 μM in Tris·HCl buffer (10 mM, pH = 7.4). All spectra were standardized with solvent, concentration of the sample (6.0 μM), length of cell and number of amino acids.*

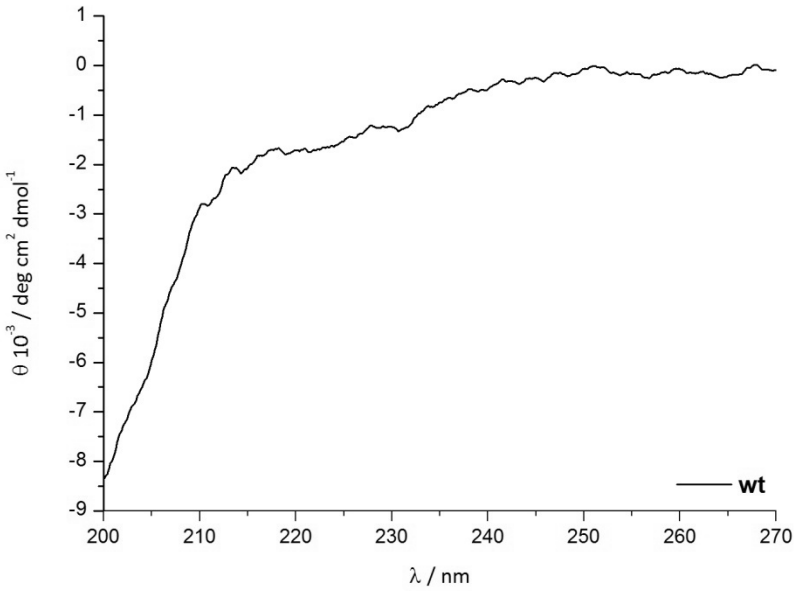

Figure 61. *CD spectra of Synaptobrevin constructs* ***wt****, 5 μM in Tris·HCl buffer (10 mM, pH = 7.4). All spectra were standardized with solvent, concentration of the sample (6.0 μM), length of cell and number of amino acids.*

Abbreviations

Å	angstrom (10^{-8} cm)
Aa	amino acids
AAA	ATPases associated with cellular activities
ACN	acetonitrile
AcOH	acetic acid
AFM	atomic force microscopy
aq.	aqueous
Bn	benzyl
Boc	*tert*-butyloxycarbonyl
c	concentration
°C	degree Celsius
calc.	calculated
CD	circular dichroism
δ	chemical shift
DCM	dichlormethane
DIC	*N*,*N*´-Diisopropylcarbodiimide
DIEA	(ethyl)diisopropylamine
DMF	dimethyl formamide
EDT	1,2-ethandithiole
EnHD	Engrailed homeodomain
equiv.	equivalent
ESI	electrosprayionisation
ER	endoplasmic reticulum
Et	ethyl
EtOAc	ethyl acetate
Fig.	figure
Fmoc	9-fluorenylmethyloxycarbonyl
h	hours
HATU	O-(7-azabenzotriazol-1-yl)-*N*,*N*,*N*',*N*'-tetramethyluronium hexafluorophosphate

HBTU	*O*-(1*H*-benzotriazol-1-yl)-1,1,3,3-tetramethyluroniumhexafluorophosphat
HTH	helix-turn-helix
HOAt	7-aza-1-hydroxybenzotriazol
HOBt	1-hydroxybenzotriazol
HPLC	high performance liquid chromatography
HR	high resolution
hSST	human Somatostatin
Hz	hertz
ITC	isothermal titration calorimetry
J	coupling constant
M	molar
m	multiplett
M	molecular weight
MBHA	4-methylbenzhydrylamin
MD	molecular dynamics
MeIm	*N*-methylimidazole
min	minutes
MS	mass spectrometry
MSNT	1-(mesitylene-2-sulfonyl)-3-nitro-1,2,4-triazole
MTBE	methyl-*tert*-butylether
Mts	mesitylene-2-sulfonyl
Mtt	methyltrityl
MW	microwave
m/*z*	ratio of mass to charge
N	normal
NMR	nuclear magnetic resonance
NSF	*N*-ethylmaleimide-sensitive factor
OAll	allyl ester
OBzl	benzyloxy
Pbf	2,2,4,6,7-pentamethyldihydrobenzofurane-5-sulfonyl
Ph	phenyl
ppm	parts per million
PyBOP®	benzotriazole-1-yl-oxy-tris-pyrrolidino-phosphonium hexafluorophosphate
R_f	retention factor
RP	reverse phase
RT	room temperature
S	Svedberg units
s	second
SDS	sodium dodecyl sulfate
SFA	surface-face apparatus
α-SNAP	α-soluble NSF-attachment protein

SNAP-25	synaptosome-associated protein of 25 kDa
SPPS	solid phase peptide synthesis
SNARE	SNAP receptor
sym-collidine	2,4,6-collidine
*t*Bu	*tert*-butyl
tert	tertiary
TFA	trifluoroacetic acid
TFE	trifluorethanole
TFMSA	trifluoromethanesulfonic acid
THF	tetrahydrofuran
TLC	thin layer chromatography
TMS	trimethylsilyl
TMSOTf	trimethylsilyl triflate
Tris	tris(hydroxymethyl)-aminomethane
t_R	retention time
Trt	trityl
VAMP	vesicle-associated membrane protein
v/v	volume to volume
w/v	weight to volume
Xan	xanthyl

References

[1] G. Palade, *Science* **1975**, *189*, 347-358.

[2] R. Jahn, T. Lang, T. C. Südhof, *Cell* **2003**, *112*, 519-533.

[3] R. Jahn, R. H. Scheller, *Nature Reviews - Molecular Cell Biology* **2006**, *7*, 631-643.

[4] S. R. Pfeffer, *Nature Cell Biology* **1999**, *1*, E17-E22.

[5] D. Fasshauer, W. K. Eliason, A. T. Brunger, R. Jahn, *Biochemistry* **1998**, *37*, 10354-10362.

[6] J. S. Bonifacino, B. S. Glick, *Cell,* **2004**, *116*, 153-166.

[7] R. B. Sutton, D. Fasshauer, R. Jahn, A. T. Brunger, *Nature* **1998**, *398*, 347-353.

[8] S. Pabst, M. Margittai, D. Vainius, R. Langen, R. Jahn, D. Fasshauer, *Journal of Biological Chemistry* **2002**, *277*, 7838-7848.

[9] T. H. Söllner, M. K. Bennett, S. W. Whiteheart, R. H. Scheller, J. E. Rothman, *Cell* **1993**, *75*, 409-418.

[10] B. Schuler, *ChemPhysChem* **2005**, *6*, 1206-1220.

[11] C. K. Johnson, K. D. Osborn, M. W. Allen, B. D. Slaughter, *Physiology* **2005**, *20*, 10-14.

[12] K. E. Marz, J. M. Lauer, P. I. Hanson, *Journal of Biological Chemistry* **2003**, *278*, 27000-27008.

[13] H. T. McMahon, M. Missler, C. Li, T. C. Südhof, *Cell* **1995**, *83*, 111-119.

[14] X. Chen, D. R. Tomchick, E. Kovrigin, D. Arac, M. Machius, T. C. Südhof, J. Rizo, *Neuron* **2002**, *33*, 397-409.

[15] B. Schuler, E. A. Lipman, W. A. Eaton, *Nature* **2002**, *419*, 743-747.

[16] R. Jahn, T. C. Südhof, *Annu. Rev. Biochem.* **1999**, *68*, 863-911.

[17] M. M. Kozlov, V. S. Markin, *Biofizika* **1983**, *28*, 242-247.

[18] S. L. Leikin, M. M. Kozlov, L. V. Chernomordik, V. S. Markin, Y. A. Chizmadzhev, *Journal of Theoretical Biology* **1987**, *129*, 411-425.

[19] S. Ferro-Novick, R. Jahn, *Nature* **1994**, *370*, 191-193.

[20] M. K. Bennett, R. H. Scheller, *Proc. Natl. Acad. Sci. USA* **1993**, *90*, 2559-2563.

[21] S. Takamori, M. Holt, K. Stenius, E. A. Lemke, M. Gronborg, D. Riedel, H. Urlaub, S. Schenck, B. Brügger, P. Ringler, S. A. Müller, B. Rammner, F. Gräter, J. S. Hub, B. L. De Groot, G. Mieskes, Y. Moriyama, J. Klingauf, H. Grubmüller, J. E. Heuser, F. Wieland, R. Jahn, *Cell* **2006**, *127*, 831-846.

[22] J. B. Bock, H. T. Matern, A. A. Peden, R. H. Scheller, *Nature* **2001**, *409*, 839-841.

[23] T. Weimbs, S. H. Low, S. J. Chapin, K. E. Mostov, P. Bucher, K. Hofmann, *Proc. Natl. Acad. Sci. USA* **1997**, *94*, 3046-3051.

[24] D. M. Terrian, M. K. White, *European Journal of Cell Biology* **1997**, *73*, 198-204.

[25] D. T. Hess, T. M. Slater, M. C. Wilson, J. H. P. Skene, *Journal of Neuroscience* **1992**, *12*, 4634-4641.

[26] L. Katz, P. I. Hanson, R. Jahn, *The EMBO Journal* **1998**, *17*, 6200-6209.

[27] M. A. Poirier, W. Xiao, J. C. Macosko, C. Chan, Y. K. Shin, M. K. Bennett, *Nature Structural Biology* **1998**, *5*, 765-769.

[28] T. H. Kloepper, C. N. Kienle, D. Fasshauer, *Molecular Biology of the Cell* **2007**, *18*, 3463-3471.

[29] D. Fasshauer, R. B. Sutton, A. T. Brunger, R. Jahn, *Proc. Natl. Acad. Sci. USA* **1998**, *95*, 15781-15786.

[30] T. Weimbs, K. E. Mostov, S. H. Low, K. Hofmann, *Trends in Cell Biology* **1998**, *8*, 260-262.

[31] J. A. McNew, T. Weber, F. Parlati, R. J. Johnston, T. J. Melia, T. H. Söllner, J. E. Rothman, *Journal of Cell Biology* **2000**, *150*, 105-117.

[32] D. Fasshauer, *Biochemical and Biophysical Acta* **2003**, *1641*, 87-97.

[33] N. Calakos, M. K. Bennett, K. E. Peterson, R. H. Scheller, *Science* **1994**, *263*, 1146-1149.

[34] I. Dulubova, S. Sugita, S. Hill, m. Hosaka, I. Fernandez, T. C. Südhof, J. Rizo, *The EMBO Journal* **1999**, *18*, 4372-4382.

[35] L. E. P. Dietrich, C. Boeddinghaus, T. J. LaGrassa, C. Ungermann, *Biochimica et Biophysica Acta* **2003**, *18* 111-119

[36] V. Rossi, D. K. Banfield, M. Vacca, L. E. P. Dietrich, C. Ungermann, M. D´Esposito, T. Galli, F. Filippini, *Trends in Biochemical Sciences* **2004**, *29*, 682-688.

[37] D. Fasshauer, W. Antonin, V. Subrananiam, R. Jahn, *Nature Structural Biology* **2002**, *9*, 144-151.

[38] F. Li, F. Pincet, E. Perez, W. S. Eng, T. J. Melia, J. E. Rothman, D. Tareste, *Nature Structural & Molecular Biology* **2007**, *14*, 890-896.

[39] T. Hayashi, H. T. McMahon, S. Yamasaki, T. Binz, Y. Hata, *The EMBO Journal* **1994**, *13*, 5051-5061.

[40] D. Fasshauer, H. Otto, W. K. Eliason, R. Jahn, A. T. Brünger, *Journal of Biological Chemistry* **1997**, *272*, 28036-28041.

[41] G. Schiavo, B. Poulain, O. Rossetto, F. Benfenati, L. Tauc, C. Montecucco, *The EMBO Journal* **1992**, *11*, 3577-3583.

[42] T. C. Südhof, P. De Camilli, H. Niemann, R. Jahn, *Cell* **1993**, *75*, 1-4.

[43] P. Hanson, J. E. Heuser, R. Jahn, *Current Opinion in Neurobiology* **1997**, *7*, 310-315.

[44] W. S. Trimble, D. W. Cowan, R. H. Scheller, *Proc. Natl. Acad. Sci. USA* **1988**, *85*, 4538-4542.

[45] J. E. Rothman, *Nature* **1994**, *372*, 55-63.

[46] T. C. Südhof, M. Baumert, M. S. Perin, R. Jahn, *Neuron* **1989**, *2*, 1475-1481.

[47] P. G. Woodman, *Biochimica et Biophysica Acta* **1997**, *1357*, 155-172.

[48] D. Fasshauer, D. Bruns, B. Shen, R. Jahn, A. T. Brunger, *Journal of Biological Chemistry* **1997**, *272*, 4582-4590.

[49] J. W. Hazzard, T. C. Südhof, J. Rizo, *Journal of Biomolekular NMR* **1999**, *14*, 203-207.

[50] J. F. Ellena, B. Liang, M. Wiktor, A. Stein, D. S. Cafiso, R. Jahn, L. K. Tamm, *Proc. Natl. Acad. Sci. USA* **2009**, *106*, 20306-20311.

[51] J. A. Ernst, A. T. Brunger, *Journal of Biological Chemistry* **2003**, *278*, 8630-8636.

[52] D. Fasshauer, M. Margittai, *Journal of Biological Chemistry* **2004**, *279*, 7613-7621.

[53] J. B. Soerensen, K. Wiederhold, E. M. Müller, I. Milosevic, G. Nagy, *The EMBO Journal* **2006**, *25*, 955-966.

[54] C. G. Giraudo, W. S. Eng, T. J. Melia Jr., J. E. Rothman, *Science* **2006**, *313*, 676-680.

[55] A. V. Pobbati, A. Stein, D. Fasshauer, *Science* **2006**, *313*, 673-676.

[56] P. I. Hanson, R. Roth, H. Morisaki, R. Jahn, J. E. Heuser, *Cell* **1997**, *90*, 523-535.

[57] R. C. Lin, R. H. Scheller, *Neuron* **1997**, *19*, 1087-1094.

[58] T. Lang, *Journal of Physiology* **2007**, *585.3* 693-698.

[59] Y. Kee, R. C. Lin, S. C. Hsu, R. H. Scheller, *Neuron* **1995**, *14*, 991-998.

[60] T. Hayashi, S. Yamasaki, S. Nauenburg, T. Binz, H. Niemann, *The EMBO Journal* **1995**, *14*, 3217-3225.

[61] A. M. Walther, K. Wiederhold, D. Bruns, D. Fasshauer, J. B. Soerensen, *Journal of Cell Biology* **2010**, *188*, 401-413.

[62] A. T. Brunger, *Current Opinion in Neurobiology* **2000**, *10*, 293-302.

[63] K. Wiederhold, D. Fasshauer, *Journal of Biological Chemistry* **2009**, *284*, 13143-13152.

[64] R. Jahn, *Annals New York Acadamy of Sciences* **2004**, *1014*, 170-178.

[65] K. M. S. Misura, A. P. May, W. I. Weis, *Current Opinion in Structural Biology* **2000**, *10*, 662-671.

[66] D. Fasshauer, H. Otto, W. K. Eliason, R. Jahn, A. T. Brünger, *Journal of Biological Chemistry* **1997**, *272*, 28036–28041.

[67] M. R. Block, B. S. Glick, C. A. Wilcox, F. T. Wieland, J. E. Rothman, *Proc. Natl. Acad. Sci. USA* **1988**, *85*, 7852-7856.

[68] Y. A. Chen, R. H. Scheller, *Nat. Rev. Mol. Cell Biol.* **2001**, *2*, 98-106.

[69] J. Rizo, T. C. Südhof, *Nature Reviews Neuroscience* **2002**, *3*, 641-653.
[70] A. P. May, S. W. Whiteheart, W. I. Weis, *Journal of Biological Chemistry* **2001**, *276*, 21991-21994.
[71] G. van den Boogart, M. G. Holt, G. Bunt, D. Riedel, F. S. Wouters, R. Jahn, *Nature Structural & Molecular Biology* **2010**, *17*, 358-364.
[72] K. M. Misura, R. H. Scheller, W. I. Weis, *Journal of Biological Chemistry* **2001**, *276*, 13273-13282.
[73] J. C. Lerman, J. Robblee, R. Fairman, F. M. Hughson, *Biochemistry* **2000**, *39*, 8470-8479.
[74] R. Fukuda, J. A. McNew, T. Weber, F. Parlati, T. Engel, W. Nickel, J. E. Rothman, T. H. Söllner, *Nature* **2000**, *407*, 198-202.
[75] F. Parlati, J. A. McNew, R. Fukuda, R. Miller, T. H. Söllner, J. E. Rothman, *Nature* **2000**, *407*, 194-198.
[76] F. Parlati, O. Varlamov, K. Paz, J. A. McNew, D. Hurtado, *Proc. Natl. Acad. Sci. USA* **2002**, *99*, 5424-5429.
[77] W. E. Balch, W. G. Dunphy, W. A. Braell, J. E. Rothman, *Cell* **1984**, *39*, 405-416.
[78] D. O. Clary, I. C. Griff, J. E. Rothman, *Cell* **1990**, *61*, 709-721.
[79] J. T. Littleton, E. R. Chapman, R. Kreber, M. B. Garment, S. D. Carlson, B. Ganetzky, *Neuron* **1998**, *21*, 401-413.
[80] C. J. M. Beckers, M. R. Block, B. S. Glick, J. E. Rothman, W. E. Balch, *Nature* **1989**, *339*, 397-398.
[81] T. R. Graham, S. D. Emr, *Journal of Cell Biology* **1991**, *114*, 207-218.
[82] H. Reizman, *Cell* **1985**, *40*, 1001-1009.
[83] S. M. Patel, M. Latterich, *Trends in Cell Biology* **1998**, *8*, 65-71.
[84] S. W. Whiteheart, T. Schraw, E. Matveeva, *International Review of Cytology* **2001**, *207*, 71-112.
[85] K. G. Fleming, T. M. Hohl, R. C. Yu, S. A. Müller, B. Wolpensinger, A. Engel, H. Engelhardt, A. T. Brunger, T. H. Söllner, P. I. Hanson, *Journal of Biological Chemistry* **1998**, *273*, 15675-15681.
[86] R. D. Vale, *Journal of Cell Biology* **2000**, *150*, F13-F19.
[87] S. W. Whiteheart, E. W. Kubalek, *Trends in Cell Biology* **1995**, *5*, 64-68.
[88] S. W. Whiteheart, K. Rossnagel, S. A. Buhrow, M. Brunner, R. Jaenicke, J. E. Rothman, *Journal of Cell Biology* **1994**, *126*, 945-954.
[89] E. E. Nagiec, A. Bernstein, S. W. Whiteheart, *Journal of Biological Chemistry* **1995**, *270*, 29182-29188.
[90] M. Sumida, R.-M. Hong, M. Tayaga, *Journal of Biological Chemistry* **1994**, *269*, 20636-20641.
[91] T. M. Hohl, F. Parlati, C. Wimmer, J. E. Rothman, T. H. Söllner, H. Engelhardt, *Molecular Cell* **1998**, *2*, 539-548.
[92] R. C. Yu, P. I. Hanson, R. Jahn, A. T. Brunger, *Nature Structural Biology* **1998**, *5*, 803-811.

[93] C. U. Lenzen, D. Steinmann, S. W. Whiteheart, W. I. Weis, *Cell* **1998**, *94*, 525-536.
[94] R. C. Yu, R. Jahn, A. T. Brunger, *Molecular Cell* **1999**, *4*, 97-107.
[95] A. P. May, K. M. S. Misura, S. W. Whiteheart, W. I. Weis, *Nature Cell Biology* **1999**, *1*, 175-182.
[96] S. M. Babor, D. Fass, *Proc. Natl. Acad. Sci. USA* **1999**, *96*, 14759-14764.
[97] M. Coles, T. Diercks, J. Liermann, A. Groger, B. Rockel, W. Baumeister, K. K. Koretke, A. Lupas, J. Peters, H. Kessler, *Current Biology* **1999**, *9*, 1158-1168.
[98] D. W. Wilson, S. W. Whiteheart, M. Wiedmann, M. Brunner, J. E. Rothman, *Journal of Cell Biology* **1992**, *117*, 531-538.
[99] S. W. Whiteheart, I. C. Griff, M. Brunner, D. O. Clary, T. Mayer, S. A. Buhrow, J. E. Rothman, *Nature* **1993**, *362*, 353-355.
[100] S. W. Whiteheart, M. Brunner, D. W. Wilson, M. Wiedmann, J. E. Rothman, *Journal of Biological Chemistry* **1992**, *267*, 12239-12243.
[101] L. M. Rice, A. T. Brunger, *Molecular Cell* **1999**, *4*, 85-95.
[102] P. I. Hanson, H. Otto, N. Barton, R. Jahn, *Journal of Biological Chemistry* **1995**, *270*, 16955-16961.
[103] H. T. McMahon, T. C. Südhof, *Journal of Biological Chemistry* **1995**, *270*, 2213-2217.
[104] C. Ungermann, K. Sato, W. T. Wickner, *Nature* **1998**, *396*, 543-548.
[105] H. Otto, P. I. Hanson, J. R., *Proc. Natl. Acad. Sci. USA* **1997**, *94*, 6197-6201.
[106] R. J. O. Barnard, A. Morgan, R. D. Burgoyne, *Journal of Cell Biology* **1997**, *139*, 875-883.
[107] J. Rizo, X. Chen, D. Arac, *Trends in Cell Biology* **2006**, *16*, 339-350.
[108] J. Tang, A. Maximov, O. H. Shin, H. Dai, J. Rizo, T. C. Südhof, *Cell* **2006**, *126*, 1175-1187.
[109] K. Reim, M. Mansour, F. Varoqueaux, H. T. McMahon, T. C. Südhof, N. Brose, C. Rosenmund, *Cell* **2001**, *104*, 71-81.
[110] D. H. Kweon, Y. Chen, F. Zhang, M. Poirier, C. S. Kim, Y. K. Shin, *Biochemistry* **2002**, *41*, 5449-5452.
[111] A. J. Morton, R. L. Faull, J. M. Edwardson, *Brain Research Bulletin* **2001**, *56*, 111-117.
[112] M. Basso, S. Giraudo, D. Corpillo, B. Bergamasco, L. Lopiano, F. M., *Proteomics* **2004**, *4*, 3943-3952.
[113] R. K. Tannenberg, H. L. Scott, A. E. Tannenberg, P. R. Dodd, *Neurochem Int* **2006**, *49*, 631-639.
[114] A. M. Barr, C. E. Hofmann, A. G. Phillips, J. Weinberg, W. G. Honer, *Alcohol Clin Exp Res* **2005**, *29*, 1915-1920.
[115] S. L. Eastwood, P. J. Harrison, *Brain Res Bull* **2001**, *55*, 569-578.
[116] K. Reim, H. Wegmeyer, J. H. Brandstätter, M. Xue, C. Rosenmund, T. Dresbach, K. Hofmann, N. Brose, *Journal of Cell Biology* **2005**, *169*, 669-680.

[117] D. A. Archer, M. E. Graham, R. D. Burgoyne, *Journal of Biological Chemistry* **2002**, *277*, 18249-18252.
[118] K. Hu, J. Caroll, C. Rickman, B. Davletov, *Journal of Biological Chemistry* **2002**, *277*, 41652-41656.
[119] H. Tokumaru, K. Umayahara, L. L. Pellegrini, T. Ishizuka, H. Saisu, H. Betz, G. J. Augustine, T. Abe, *Cell* **2001**, *104*, 421-432.
[120] A. Bracher, J. Kadlec, H. Betz, W. Weissenhorn, *Journal of Biological Chemistry* **2002**, *277*, 26517-26523.
[121] C. G. Giraudo, A. Garcia-Diaz, W. S. Eng, A. Yamamoto, T. J. Melia Jr., J. E. Rothman, *Journal of Biological Chemistry* **2008**, *283*, 21211-21219.
[122] J. R. Schaub, X. Lu, B. Doneske, Y. K. Shin, J. A. McNew, *Nature Structural & Molecular Biology* **2006**, *13*, 748-750.
[123] U. Arnold, M. P. Hinderaker, J. Koöditz, R. Golbik, R. Ulbrich-Hofmann, R. T. Raines, *J. Am. Chem. Soc.* **2003**, *125*, 7500-7501.
[124] N. H. Williams, *Annu. Rep. Prog. Chem.* **2004**, *100*, 407-434.
[125] S. H. Gellman, *Acc. Chem. Res.* **1998**, *31*, 173-180.
[126] P. E. Nielsen, *Acc. Chem. Res.* **1999**, *32*, 624-630.
[127] P. E. Nielsen, G. Haaima, *Chemical Society Reviews* **1997**, 73-78.
[128] P. E. Nielsen, M. Egholm, R. H. Berg, O. Buchhardt, *Science* **1991**, *254*, 1497-1500.
[129] U. Diederichsen, H. W. Schmitt, *Angew. Chem. Int. Ed.* **1998**, *37*, 302-305.
[130] E. Uhlmann, A. Peyman, G. Breipohl, D. W. Will, *Angew. Chem. Int. Ed.* **1998**, *37*, 2796-2823.
[131] A. Eschenmoser, E. Loewenthal, *Chem. Soc. Rev.* **1992**, *21*, 1-16.
[132] A. Eschenmoser, *Origins Life Evol Biosphere* **1994**, *24*, 389-423.
[133] A. Eschenmoser, *Science* **1999**, *284*, 2118-2124.
[134] W. F. DeGrado, J. P. Schneider, Y. J. Hamuro, *Journal of Peptide Research* **1999**, *54*, 206-217.
[135] D. Seebach, J. L. Matthews, *Chemical Communications* **1997**, 2015-2022.
[136] D. Seebach, S. Abele, K. Gademann, G. Guichard, T. Hintermann, B. Jaun, J. L. Matthews, J. V. Schreiber, L. Oberer, U. Hommel, H. Widmer, *Helvetica Chimica Acta* **1998**, *81*, 932-980.
[137] E. Juaristi, D. Quintana, J. Escalante, *Journal of Aldrichimica Acta* **1994**, *27*, 3-11.
[138] E. Juaristi, VCH, New York, **1997**.
[139] J. Podlech, D. Seebach, *Angew. Chem. Int. Ed.* **1995**, *34*, 471-472.
[140] S. A. Hart, A. B. F. Bahadoor, E. E. Matthews, Q. X. J., A. Schepartz, *J. Am. Chem. Soc.* **2003**, *125*, 4022-4023.
[141] T. L. Raguse, J. R. Lai, S. H. Gellman, *J. Am. Chem. Soc.* **2003**, *125*, 5592-5593.
[142] T. J. Peelen, y. Chi, E. P. English, S. H. Gellman, *Organic Letters* **2004**, *6*, 4411-4414.

[143] T. D. W. Claridge, J. M. Goodman, A. Moreno, D. Angus, S. F. Barker, C. Taillefumier, M. P. Watterson, G. W. J. Fleet, *Tetrahedron Letters* **2001**, *42*, 4251-4255.
[144] S. Hanessian, X. Luo, R. Schaum, S. Michnick, *J. Am. Chem. Soc.* **1998**, *120*, 8659-8570.
[145] K. Gademann, A. Häne, M. Rueping, B. Jaun, D. Seebach, *Angew. Chem. Int. Ed.* **2003**, *42*, 1543-1537.
[146] D. Seebach, D. F. Hook, A. Glättli, *Biopolymers (Peptide Science)* **2005**, *84*, 23-37.
[147] A. Kritzner, J. Tirado-Rives, S. A. Hart, J. D. Lear, W. L. Jorgensen, A. Schepartz, *J. Am. Chem. Soc.* **2005**, *127*, 167-178.
[148] R. L. Baldwin, G. D. Rose, *Trends in Biochemical Sciences* **1999**, *24*, 26-33.
[149] R. Aurora, G. D. Rose, *Protein Science* **1998**, *7*, 21-38.
[150] M. Schinnerl, J. K. Murray, J. M. Langenham, S. H. Gellman, *Eur. J. Org. Chem.* **2003**, 721-726.
[151] K. A. Bode, J. Applequist, *Macromolecules* **1997**, *30*, 2144-2150.
[152] J. Applequist, K. A. Bode, D. H. Appella, L. A. Christianson, S. H. Gellman, *J. Am. Chem. Soc.* **1998**, *120*, 4891-4892.
[153] R. I. Mathad, F. Gessier, D. Seebach, *Helvetica Chimica Acta* **2005**, *88*, 266-280.
[154] E. Vaz, L. Brunsveld, *Organic Letters* **2006**, *8*, 4199-4202.
[155] D. A. Guarracino, H. R. Chiang, T. N. Banks, J. D. Lear, M. E. Hodsdon, A. Schepartz, *Organic Letters* **2006**, *8*, 807-810.
[156] T. Hintermann, D. Seebach, *Chimia* **1997**, *51*, 244-247.
[157] J. Frackenpohl, P. I. Arvidsson, J. V. Schreiber, D. Seebach, *ChemBioChem* **2001**, *2*, 445-455.
[158] J. V. Schreiber, J. Frackenpohl, F. Moser, T. Fleischmann, H.-P. E. Kohler, D. Seebach, *ChemBioChem* **2002**, *3*, 424-432.
[159] D. Seebach, A. K. Beck, D. J. Bierbaum, *Chemistry & Biodiversity* **2004**, *1*, 1111-1239.
[160] D. Seebach, M. Overhand, F. N. M. Kühnle, B. Martinoni, L. Oberer, U. Hommel, H. Widmer, *Helvetica Chimica Acta* **1996**, *79*, 913-941.
[161] E. A. Porter, B. Weisblum, S. H. Gellman, *J. Am. Chem. Soc.* **2002**, *124*, 7324-7330.
[162] D. Seebach, M. Rueping, P. I. Arvidsson, T. Kimmerlin, P. Micuch, C. Noti, D. Langenegger, D. Hoyer, *Helvetica Chimica Acta* **2001**, *84*, 3503-3510.
[163] D. Liu, W. F. DeGrado, *J. Am. Chem. Soc.* **2001**, *123*, 7553-7559.
[164] K. Gademann, T. Kimmerlin, D. Hoyer, D. Seebach, *Journal of Mecinal Chemistry* **2001**, *44*, 2460-2468.
[165] D. Seebach, L. Schaeffer, M. Brenner, D. Hoyer, *Angew. Chem. Int. Ed.* **2003**, *42*, 776-778.
[166] A. R. Fersht, Freeman, New York, **1998**.
[167] E. Branden, J. Tooze, Garland Publishing, New York, **1999**.

[168] T. L. Religa, C. M. Johnson, D. M. Vu, S. H. Brewer, R. B. Dyer, A. R. Fersht, *Proc. Natl. Acad. Sci. USA* **2007**, *104*, 9272-9277.
[169] L. Aravind, V. Anantharaman, S. Balaji, M. M. Babu, L. M. Iyer, *FEMS Microbiological Reviews* **2005**, *29*, 231-262.
[170] J. N. Breg, J. H. J. Vanopheusden, M. J. M. Burgering, R. Boelens, R. Kaptein, *Nature* **1990**, *346*, 586-589.
[171] U. Mayor, C. M. Johnson, V. Daggett, A. R. Fersht, *Proc. Natl. Acad. Sci. USA* **2000**, *97*, 13518-13522.
[172] T. L. Religa, J. S. Markson, U. Mayor, S. M. Freund, A. R. Fersht, *Nature* **2005**, *437*, 1053-1056.
[173] P. Bork, M. Sudol, *Trends in Biochemical Sciences* **1994**, *19*, 531-533.
[174] M. J. Macias, V. Gervais, C. Civera, H. Oschkinat, *Nature Structural Biology* **2000**, *7*, 375-379.
[175] M. T. Bedford, D. Sarbassova, J. Xu, P. Leder, M. B. Yaffe, *Journal of Biological Chemistry* **2000**, *275*, 10359-10369.
[176] X. Michalet, S. Weiss, M. Jäger, *Chemical Reviews* **2006**, *106*, 1785-1813.
[177] B. Schuler, W. A. Eaton, *Current Opinion in Structural Biology* **2008**, *Current Opinion in Structural Biology* 16-26.
[178] J. Vogelsang, R. Kasper, C. Steinhauer, B. Person, M. Heilemann, M. Sauer, P. Tinnefeld, *Angew. Chem. Int. Ed.* **2008**, *47*, 5465-5469.
[179] E. Rhoades, E. Gussakovsky, G. Haran, *Proc. Natl. Acad. Sci. USA* **2003**, *100*, 3197-3202.
[180] L. D´Alfonso, M. Collini, F. Cannone, G. Chirico, B. Campanini, G. Cottone, L. Cordone, *Biophysical Journal* **2007**, *93*, 284-293.
[181] A. Mecke, C. Dittrich, W. Meier, *Soft Matter* **2006**, *2*, 751-759.
[182] T. Rosenkranz, A. Katranidis, D. Atta, I. Gregor, J. Enderlein, M. Grzelakowski, P. Rigler, W. Meier, J. Fitter, *ChemBioChem* **2009**, *10*, 702-709.
[183] P. Rigler, W. Meier, *J. Am. Chem. Soc.* **2006**, *128*, 367-373.
[184] K. A. Merchant, R. B. Best, J. M. Louis, I. V. Gopich, W. A. Eaton, *Proc. Natl. Acad. Sci. USA* **2007**, *104*, 1528-1533.
[185] M. Buscaglia, B. Schuler, L. J. Lapidus, W. A. Eaton, J. Hofrichter, *Journal of Molecular Biology* **2003**, *332*, 9-12.
[186] C. Wimmer, T. M. Hohl, C. A. Hughes, S. A. Müller, T. H. Söllner, A. Engel, J. E. Rothman, *Journal of Biological Chemistry* **2001**, *276*, 29091-29097.
[187] K. M. Fiebig, L. M. Rice, E. Pollock, A. T. Brunger, *Nature Structural Biology* **1999**, *6*, 117-123.
[188] L. M. Rice, P. Brennwald, A. T. Brunger, *FEBS Letters* **1997**, *415*, 49-55.
[189] U. Winter, *Biophysical Characterization of SNARE Complex Disassembly Catalyzed by NSF and α-SNAP*, Georg-August-Universität (Göttingen) **2006**.
[190] U. K. Laemmli, *Nature* **1970**, *227*, 680-685.
[191] S. J. Scales, B. Y. Yoo, R. H. Scheller, *Proc. Natl. Acad. Sci. USA* **2001**, *98*, 14262-14267.

[192] Y. Li, G. J. Augustine, K. Weninger, *Biophysical Journal* **2007**, *93*, 2178-2187.
[193] T. Ishizuka, H. Saisu, S. Odani, T. Abe, *Biochemical and Biophysical Research Communications* **1995**, *213*, 1107-1114.
[194] N. Brose, *Traffic* **2008**, *9*, 1403-1414.
[195] S. Pabst, J. W. Hazzard, W. Antonin, T. C. Südhof, R. Jahn, J. Rizo, D. Fasshauer, *Journal of Biological Chemistry* **2000**, *275*, 19808-19818.
[196] K. Weninger, M. E. Bowen, U. B. Choi, S. Chu, A. T. Brunger, *Structure* **2008**, *16*, 308-320.
[197] J. M. Edwardson, C.-T. Wang, B. Gong, A. Wyttenbach, J. Bai, M. B. Jackson, E. R. Chapman, A. J. Morton, *Journal of Biological Chemistry* **2003**, *278*, 30849-30853.
[198] J. Liu, T. Guo, J. Wu, X. Bai, Q. Zhu, S. M. Sui, *Biochemistry (Moscow)* **2007**, *72*, 439-444.
[199] H. Tokumaru, C. Shimizu-Okabe, T. Abe, *Brain Cell Biology* **2008**, *36*, 173-189.
[200] A. Stein, *Untersuchungen zur Rekonstitution der SNARE-vermittelten Membranfusion*, Freie Universität Berlin (Berlin) **2007**.
[201] A. Stein, R. Jahn, *Neuron* **2009**, *64*, 295-297.
[202] K. Kirshenbaum, R. N. Zuckermann, K. A. Dill, *Current Opinion in Structural Biology* **1999**, *9*, 530-535.
[203] R. P. Cheng, S. H. Gellman, W. F. DeGrado, *Chemical Reviews* **2001**, *101*, 3219-3232.
[204] F. Arndt, B. Eistert, W. Partale, *Berichte Deutsche Chemische Gesellschaft* **1927**, *60*, 1364-1368.
[205] D. C. Cole, *Tetrahedron* **1994**, *50*, 9517-9582.
[206] T. Kunieda, T. Nagamatau, T. Higuchi, M. Hirobe, *Tetrahedron Letters* **1988**, *29*, 2203-2206.
[207] D. Tanner, P. Somfai, *Tetrahedron* **1988**, *44*, 613-618.
[208] C. Gennari, I. Venturini, G. Gislon, G. Schimpema, *Tetrahedron Letters* **1987**, *28*, 227-230.
[209] S. G. Davies, I. Dordor-Hedgecock, K. H. Sutton, J. C. Walker, *Tetrahedron Letters* **1986**, *27*, 3787-3790.
[210] S. Kobayashi, T. Iimori, T. Izawa, M. Ohno, *J. Am. Chem. Soc.* **1981**, *103*, 2406-2408.
[211] N. Kawabata, Y. Inamoto, K. Sakane, T. Iwamoto, S. Hashimoto, *Journal of Antibiotics* **1992**, *45*, 513-517.
[212] J. Podlech, D. Seebach, *Liebigs Annalen der Chemie* **1995**, *1995*, 1217-1228.
[213] C. Guibourdenche, J. Podlech, D. Seebach, *Liebigs Annalen der Chemie* **1996**, *1996*, 1121-1129.
[214] M. Liu, M. P. Sibi, *Tetrahedron* **2002**, *58*, 7991-8035.
[215] M. Rueping, Y. R. Mahajan, B. Jaun, D. Seebach, *Chemistry - A European Journal* **2004**, *10*, 1607-1615.

[216] S. A. Palasek, Z. J. Cox, J. M. Collins, *Journal of Peptide Science* **2007**, *13*, 143-148.
[217] M. Cemazar, D. J. Craik, *Journal of Peptide Science* **2008**, *14*, 683-689.
[218] E. Kaiser, R. L. Colescott, C. D. Bossinger, P. I. Cook, *Analytical Biochemistry* **1970**, *34*, 595-598.
[219] A. Müller, C. Vogt, N. Sewald, *Synthesis* **1998**, 837-841.
[220] A. M. Brückner, *Synthese und Strukturuntersuchung von Nucleobasen-funktionalisierten ß-Peptiden*, Georg-August University (Göttingen) **2003**.
[221] A. M. Brückner, P. Chakraborty, S. H. Gellman, U. Diederichsen, *Angew. Chem. Int. Ed.* **2003**, *42*, 4395-4399.
[222] P. Chakraborty, A. M. Brückner, U. Diederichsen, *European Journal of Organic Chemistry* **2006**, 2410-2416.
[223] R. W. Woody, *Methods in Enzymology* **1995**, *246*, 34-71.
[224] A. Glättli, X. Daura, D. Seebach, W. F. van Gusteren, *J. Am. Chem. Soc.* **2002**, *124*, 12972.
[225] M. Schiffer, A. B. Edmundson, *Biophysical Journal* **1967**, *7*, 121-135.
[226] P. Y. Chou, G. D. Fasman, *Annu. Rev. Biochem.* **1978**, *47*, 251-176.
[227] P. Y. Chou, C. T. Zhang, G. M. Maggiora, *Proteins* **1997**, *28*, 99-108.
[228] C. N. Pace, J. M. Scholtz, *Biophysical Journal* **1998**, *75*, 422-427.
[229] N. Kurochkina, *Journal of Theoretical Biology* **2010**, *264*, 585-592.
[230] M. Xue, K. Reim, X. Chen, H. T. Chao, H. Deng, J. Rizo, N. Brose, C. Rosenmund, *Nature Structural & Molecular Biology* **2007**, *14*, 949-958.
[231] J. Liu, T. Guo, Y. Wei, M. Liu, S. M. Sui, *Biochemical and Biophysical Research Communications* **2006**, *347*, 413-419.
[232] J. W. Neidigh, R. M. Fesinmeyer, N. H. Anderson, *Nature Structural Biology* **2002**, *9*, 425-430.
[233] U. Mayor, J. G. Grossmann, N. W. Foster, S. M. Freund, A. R. Fersht, *Journal of Molecular Biology* **2003**, *333*, 977-991.
[234] M. L. DeMarco, D. O. Alonso, V. Daggett, *Journal of Molecular Biology* **2004**, *341*, 1109-1124.
[235] J. E. Berlier, A. Rothe, G. Buller, J. Bradford, D. R. Gray, B. J. Filanoski, W. G. Telford, S. Yue, J. Liu, C. Y. Cheung, W. Chang, J. D. Hirsch, J. M. Beechem, R. P. Haugland, R. P. Haugland, *Journal of Histochemistry and Cytochemistry* **2003**, *51*, 1699-1712.
[236] N. Panchuk-Voloshina, R. P. Haugland, J. Bishop-Stewart, M. K. Bhalgat, P. J. Millard, F. Mao, W.-Y. Leung, R. P. Haugland, *Journal of Histochemistry and Cytochemistry* **1999**, *47*, 1179-1188.
[237] J. Kovacs, G. L. Mayers, R. H. Johnson, R. E. Cover, U. R. Ghatak, *Journal of Organic Chemistry* **1970**, *35*, 1810-1815.
[238] P. Wang, L. P. Miranda, *International Journal of Peptide Research and Therapeutics* **2005**, *11*, 117-123.
[239] N. Ferguson, C. M. Johnson, M. Macias, H. Oschkinat, A. R. Fersht, *Proc. Natl. Acad. Sci. USA* **2001**, *98*, 13002-13007.

[240] T. Graen, *Dye´ing for FRET: The HTH motif in smFRET-MD Simulation*, Bachelor thesis thesis, Georg-August University (Göttingen) **2009**.
[241] D. Fasshauer, W. Antonin, M. Margittai, S. Pabst, R. Jahn, *Journal of Biological Chemistry* **1999**, *274*, 15440-15446.
[242] M. Margittai, H. Otto, R. Jahn, *FEBS Letters* **1999**, *446*, 40-44.
[243] C. G. Schuette, K. Hatsuzawa, M. Margittai, A. Stein, D. Riedel, P. Kuster, M. König, C. A. M. Seidel, R. Jahn, *Proc. Natl. Acad. Sci. USA* **2004**, *101*, 2858-2863.
[244] M. M. Bradford, *Analytical Biochemistry* **1976**, *72*, 248-254.
[245] K. Weber, M. Osborn, *Journal of Biological Chemistry* **1969**, *244*, 4406-4412.
[246] V. J. Nesatyy, A. Dacanay, J. F. Kelly, N. W. Ross, *Rapid Communications in Mass Spectrometry* **2002**, *16* 272-280.
[247] Invitrogen, in *Colloidal Blue staining kit - Instruction Manual, Vol. Version F*.
[248] Novabiochem, Darmstadt, **2009**.
[249] M. Gude, J. Ryf, P. D. White, *Letters of Peptide Science* **2002**, *9*, 203-206.
[250] Y. Han, F. Albericio, G. Barany, *Journal of Organic Chemistry* **1997**, *62*, 4307-4312.

Acknowledgements

Mein besonderer Dank gilt Prof. Dr. ULF DIEDERICHSEN für die interessante Themenstellung, die gewährte wissenschaftliche Freiheit, die gute Betreuung, die entspannte Arbeitsatmosphäre und die Unterstützung während der gesamten Zeit der Dissertation.

Ebenso danke ich den weiteren Mitgliedern meines 'Thesis Committee', Prof. Dr. REINHARD JAHN und Prof. Dr. CLAUDIA STEINEM für die Betreuung meiner Promotion und für die stetige Diskussionsbereitschaft.

Prof. Dr. REINHARD JAHN danke ich zudem für die Übernahme des Korreferats, ebenso für sein ständiges Interesse an meiner Arbeit und seine Diskussions- und Hilfsbereitschaft beim Erlernen der biologischen Fragestellungen rund um SNAREs.

Prof. Dr. JÖRG ENDERLEIN, Jun.-Prof. CHRISTIAN DUCHO und Prof. Dr. KAI TITTMANN danke für ihre Bereitschaft meiner Prüfungskommission anzugehören.

Der *Göttingen Graduate School of Neurosciences and Molecular Biosciences (GGNB)* und dem integrierten Promotionsprogramm, der *International Max-Planck Research School: Physics of Biological and Complex Systems (IMPRS-PBCS)* danke ich für ein vielseitiges und engagiertes Programm, sowie die vielen Möglichkeiten sich weiterzubilden. ANTJE ERDMANN danke ich für ihre unkomplizierten Hilfen, ihre Geduld und ihre vielen Antworten auf unzählige Fragen rund um die Promotionsordnung.

Meinen jetzigen und ehemaligen Kollegen in Labor 108 Dr. STEFAN CORTEKAR, Dr. ANDRÉ NADLER, Dr. STEPHANIE SCHOLZ, ANTONINA LYGINA, FRANK STEIN, TAHIR MEHMOOD, ULRIKE ROST, DR. TATJANA BARANOVA, ZEYHNEP KANLIDERE und ARNE SÖREN SUMFLETH danke ich für das immer lebendige Laborleben und das kreative Chaos. Die gemeinsame Suche nach unzähligen Filzstiften, Pipettenhütchen, Rührschweinen

und vor allem -Kolben!- die ständig im laboreigenen Bermudadreieck verschwanden, war selten langweilig. Allen übrigen Arbeitskreismitgliedern danke ich für ihre Hilfsbereitschaft, nette Kaffeerunden, abwechslungsreiche AK-Fahrten und die entspannte Arbeitsatmosphäre.

Für das gemeinsame Erlernen der vielen Tricks und Kniffe beim Arbeiten mit SNARE-Komplexen, ebenso wie für die vielen hilfreichen und konstruktiven Diskussionen bezüglich unseres gemeinsamen Themas und danke ich ANTONINA LYGINA und KARSTEN MEYENBERG. KARSTEN, dir danke ich auch für deinen unermüdlichen Einsatz bei der Bekämpfung der vielen Kinderkrankheiten des Peptidsynthesizers.

Für das unzählige Korrekturlesen meiner Arbeit und die konstruktive Kritik danke ich Dr. ANDRÉ NADLER, JULIANE GRÄFE, JULIAN STROHMEIER, ANTONINA LYGINA und EIKE SACHS.

Der NMR-Abteilung unter der Leitung von Herrn REINHARD MACHINEK sowie der Massenabteilung unter der Leitung von Herrn Dr. HOLM FRAUENDORF danke ich für die Messung der zahlreichen Spektren.

Dr. KATJA GLATZ (geb. BENSMANN) danke ich für die fürsorgliche Einarbeitung in die Tiefen der HPLC-Reparaturen sowie die unzähligen Stunden die wir gemeinsam bei Reparaturen an diesen verbracht haben. Ebenso danke ich JOHANNA LEBER, ANTONINA LYGINA und URSULA KOTYRBA für ihren Beistand und die gemeinsam erlebten Höhen und Tiefen bei dem regelmäßigen Kampf gegen immer neue kleine und große Probleme der HPLC-Geräte. Frau '*Jasco*', Dr. GABI SCHMIDT danke ich für ihre unendlich wertvollen Tipps bei der Bewältigung unzähliger mechanischer Probleme an den Geräten.

Dr. MATTHEW HOLT, Dr. SAHEEB AHMED und Dr. GEERT VAN DEN BOOGART vom Max-Planck-Institut für Biophysikalische Chemie in Göttingen danke ich sehr für ihre Hilfe beim Erlernen der verschiedenen biologischen Techniken, ihre vielen Tipps, ihre stetige Diskussionsbereitschaft, sowie die unzähligen SNARE Proteine die sie mir zur Verfügung gestellt haben. URSEL RIES danke ich für die Reinigung des NSF.

Dr. QUI VAN und PHILLIP KROEHN aus dem III. Physikalischen Institut in Göttingen danke ich für die gute Zusammenarbeit und ihre Hilfsbereitschaft.

Im Institut für Bioanalytik danke ich ASTRID SITTE, Dr. DANILO MEYER und STEFAN LÜDTKE für ihre Antworten auf meine unzähligen biologischen Fragen und ihre Hilfsbereitschaft beim Aufreinigen der SNARE Komplexe.

MEIKE QUAST danke ich für die gemeinsame Arbeit am Complexin-Projekt während ihrer Bachelorarbeit.

Ebenfalls möchte ich mich bei den Hausmeistern WOLFRAM MATTHIES und FRANK PETERS dafür bedanken, das sie immer sofort zur Stelle waren wenn handwerkliche oder andere Probleme zu bewältigen waren. Auch danke ich euch für die persönliche Zustellung meiner vielen Pakete. HOLGER TUCHOLLA aus der Chemikalienausgabe danke ich für seine Hilfsbereitschaft bei der täglichen Chemikalienbestellung, sowie seine aufmunternden Worte wenn es im Labor gerade nicht so gut lief. DANIEL FRANK danke ich sehr für seine vielen kleinen, aber wichtigen Verbesserungen der kleinen Dinge im Arbeitsalltag, auch wenn sie manchmal als selbstverständlich erscheinen.

Dem AK BOYSEN, besonders Dr. TOBIAS MINUTH, Dr. MUSTAFA IRMAK, TOBIAS LEHNERT, HOLGER GRUGEL und natürlich dir, MIKE danke ich dafür, dass ich in meinem alten Arbeitskreis immer mit offenen Armen empfangen wurde, auch wenn meine Besuche in letzter Zeit leider etwas selten geworden sind.

DR. STEFANIE SCHOLZ und Dr. SVEN STOLLER danke ich für die kurzen Pausen während des gemeinsamen Zusammenschreibens, in denen wir uns gegenseitig wieder etwas aufgebaut haben, um anschließend mit neuem Mut weiterzuschreiben.

JULIANE, du weißt, wenn ich könnte würde ich dir 38 Seiten des Dankes schreiben (ich glaub soviel hast du dir gewünscht), aber wer soll die denn alle Korrektur lesen? Darum mach ich es kurz und danke dir für deine Freundschaft, deine unendliche Hilfsbereitschaft in allen Lebenslagen, deine vielen aufmunternden Worte und dein offenes Ohr wenn ich mal wieder mein Herz ausschütten musste.

Besonders danken möchte ich JULIAN STROHMEIER, DR. SVEN STOLLER, Dr. DANIEL HEINRICH, Dr. STEFAN CORTEKAR, Dr. ANDRÉ NADLER, JULIANE GRÄFE und CARMEN SCHAFIE-NURMOHAMMADIE für die vielen 'nicht chemischen' Unternehmungen bei denen ich Göttingen kennenlernen konnte, auch wenn die Chemie dabei nie wirklich ganz vergessen werden konnte. ARNE, TIMO, FRANK, FELIX und JOHANNES, euch danke ich dafür, dass ihr mich so herzlich aufgenommen habt. Bei euch ist wirklich immer was los. Dr. KATJA GLATZ danke ich für ihre herzliche Art und ihre Freundschaft, die auch nach ihrer Zeit in Göttingen anhält. ULRIKE ROST danke ich für ihre fröhliche Art und ihren Humor, die besonders die letzten Monate im Labor wie im Flug vergehen ließen.

KAREEN und ANDREAS, euch danke ich für eure Freundschaft, eure aufmunternden Worte und eure vielen kleinen und großen Hilfen um mir den Rücken freizuhalten, wenn ich mal wieder ganz in meine Arbeit versunken war.

JULIAN, dir danke ich für deine Liebe, deine unvergleichliche Art und die schöne gemeinsame Zeit. Mit dir wird es wirklich nie langweilig.

Mein größter Dank gilt meinen Eltern, die nie aufhörten an mich zu glauben und ohne deren Liebe, Unterstützung und Verständnis in allen Lebenslagen dies alles nicht möglich gewesen wäre. Ihr habt es immer wieder geschafft mir neuen Mut zu geben.

Curriculum Vitae

Annika Groschner

Born July, 27th 1979 in Gardelegen (Germany)

Nationality: German

Education

11/2010	Doctoral exam for the award of the degree 'doctor rerum naturalium' at the Georg-August University of Göttingen
01/2007-11/2010	PhD thesis in the group of Prof. Dr. ULF DIEDERICHSEN, Georg-August-University Göttingen, Institute of Organic and Biomolecular Chemistry, with the topic: '*Synthesis of SNARE proteins with respect to the NSF/α-SNAP-mediated disassembly*' since 06/2009: Member of the Göttingen Graduate School for Neurosciences and Biomolecular Biosciences (GGNB) since 01/2009: Project staff of the Collaborative Research Centre 803: 'Functionality Controlled by Organisation in and between Membranes'
05/2006-11/2006	Diploma thesis in the group of Jun.-Prof. Mike M. K. BOYSEN, Leibniz University Hannover: *'Untersuchung der Wirkungsweise von Bis(oxazolin)-Liganden auf Kohlenhydratbasis an verschiedenen asymmetrischen Synthesen*'.

10/1998-04/2006	Studies of chemistry at the Leibniz-University Hannover (intermediate diploma: 01/2004)
07/1998	Final secondary school examination (Geschwister-Scholl Gymnasium, Gardelegen)

Teaching

02/2007-03/2007	Supervision of the practical course 'Organisch-Chemisches Grundpraktikum'
04/2007-07/2007	Supervision of the course 'Experimentalchemie'
10/2007-03/2009	Supervision of the practical course 'Organisch-Chemisches Fortgeschrittenenpraktikum'
04/2008-07/2008	Education practical course 'Chemisch Technischer Assistent'
10/2008-02/2009	Supervision of the course 'NMR-Spektroskopie'
04/2009-07/2009	Supervision of the course 'Experimentalchemie'
07/2009-08/2009	Supervison practical course high school student
11/2009-03/2010	Supervision Bachelorthesis
04/2010-07/2010	Supervision of the Seminar for the practical course 'Organische Chemie für Lehramtskandidaten'